

ULTRASTRUCTURE OF THE CAT INFERIOR OLIVE
An anatomical study using three
new combination techniques

Ultrastructuur van de oliva inferior in de kat
Een anatomische studie met drie
nieuwe combinatie technieken

PROEFSCHRIFT

Ter verkrijging van de graad van doctor
aan de Erasmus Universiteit Rotterdam
op gezag van de Rector Magnificus
Prof. Dr. C.J. Rijnvos
en volgens besluit van het College van Dekanen.
De openbare verdediging zal plaatsvinden op
woensdag 7 februari 1990 om 15.45 uur

door

CHRISTIAAN INNOCENTIUS DE ZEEUW

Geboren te Gouda

universiteits
Erasmus
DRUKKERIJ

1990

PROMOTIECOMMISSIE

PROMOTOR: Prof. Dr. J. Voogd

OVERIGE LEDEN: Prof. Dr. H. Collewijn
Prof. Dr. G.F.J.M. Vrensen
Dr. R.M. Buijs

COPROMOTOR: Dr. J.C. Holstege

cepi ipsi mihi cerebellum
(ik volg mijn eigen hoofd, Petr.)

OLIVA
VIOLA

Foto omslag: morfologisch model van de ultrastructuur van de oliva inferior (voor uitleg zie figuur 1, chapter V).

CONTENTS

Chapter I	General introduction	7
	a. Explanation of thesis subject	7
	b. Olivary subnuclei and their connections	8
	c. Cytology and ultrastructure of olivary cells and their afferent fibers	12
	d. Neurotransmitters involved in the olivary system	15
	e. Physiology of the inferior olive	17
	f. Different combinations of anterograde tracing, immunocytochemistry, and/or intracellular labeling of neurons at the ultrastructural level	32
Chapter II	Ultrastructure of the inferior olive studied by means of a combination of WGA-HRP anterograde tracing and postembedding GABA-immunocytochemistry	38
	a. A new combination of WGA-HRP anterograde tracing and GABA-immunocytochemistry applied to afferents of the cat inferior olive at the ultrastructural level. (1988) <i>Brain Res</i> 477:369-375.	38
	b. The cerebellar, mesodiencephalic and GABAergic innervation of the glomeruli in the cat inferior olive. A comparison at the ultrastructural level. (1989) In P. Strata (Ed.): <i>The Olivocerebellar System in Motor Control. Suppl. Exp. Brain Res.</i> 17:111-117.	44
	c. Ultrastructural study of the GABAergic, cerebellar and mesodiencephalic innervation of the cat medial accessory olive: Anterograde tracing combined with immunocytochemistry. (1989) <i>J. Comp. Neurol.</i> 284:12-35.	49
Chapter III	Mesodiencephalic and cerebellar terminals terminate upon the same dendritic spines in the glomeruli of the cat and rat inferior olive: An ultrastructural study using a combination of (3H)leucine anterograde tracing and WGA-HRP anterograde tracing. <i>Neuroscience</i> (in press).	81
Chapter IV	Intracellular labeling of neurons in the medial accessory olive of the cat:	92
	a. Physiology and light microscopy. <i>J. Comp. Neurol.</i> (submitted).	92
	b. Ultrastructure of dendritic spines and their GABAergic innervation. <i>J. Comp. Neurol.</i> (submitted).	109
	c. Ultrastructure of axon hillock and initial segment, and their GABAergic innervation. <i>J. Comp. Neurol.</i> (submitted).	129
Chapter V	General discussion	146
	a. Technical aspects	146
	b. Major results	149
	c. Functional implications	157
	d. General conclusions	161

References	162
Summary	188
Samenvatting	190
Dankwoord	193
Curriculum vitae	195
List of publications	196

CHAPTER I General introduction

- a. Explanation of thesis subject
- b. Olivary subnuclei and their connections
- c. Cytology and ultrastructure of olivary cells and their afferent fibers
- d. Neurotransmitters involved in the olivary system
- e. Physiology of the inferior olive
- f. Different combinations of anterograde tracing, immunocytochemistry, and/or intracellular labeling of neurons at the ultrastructural level

a. Explanation of thesis subject

The function of neurons is determined by their biochemical assets, the electrophysiological properties of their membrane and by their position in a neuronal network. Neuroanatomy studies the structure of these networks at different levels. Axonal tracing methods are used to chart the connections with the light microscope, but the detailed anatomy of the connectivity of individual nerve cells only can be visualized using electron microscopy. At higher magnifications, however, one tends to lose track of its traces and special methods are needed to trace and to identify structures in the jungle of the neuropil.

The inferior olive (IO) is a group of nerve cells, strongly related to the cerebellum. It has been the subject of several earlier studies of this laboratory (Groenewegen and Voogd,'77; Gerrits and Voogd,'82; Ruigrok and Voogd, submitted). The function of the olivary neurons is to a large degree determined by their outstanding synchronizing and oscillating firing properties, and by the afferent systems which modulate these properties. To find out which afferent systems may regulate these functions, the morphology of the major synaptic inputs of the IO was studied and quantified. In order to relate the different ultrastructural parameters to each other, three new combinations of electron microscopical methods were developed. The first one relates the origin of the synaptic inputs with their neurotransmitter (Chapter

II), a second one relates the different synaptic inputs to each other (Chapter III), and a third technique relates the synaptic input to the physiological and morphological characteristics of the postsynaptic olivary cell (Chapter IV).

The present ultrastructural study focuses on two of the subnuclei of the IO: The medial accessory olive (MAO) and the principal olive (PO). These subnuclei, which are predominantly innervated by descending systems and by a recurrent pathway from the central cerebellar nuclei, may be involved in the preparation and execution of movements. Accurate timing obviously is essential in these processes. The morphological observations of this study will be discussed in relation to the electrophysiological properties of the olivary neurons (Chapter V). It will be attempted to show that the specific formation of the dendritic elements of these cells together with their synaptic input are well suited to serve as a timing device.

In an ongoing study we are studying the reaction of the IO to massive trauma of the cerebellum (for preliminary results see Ruigrok et al., '89; de Zeeuw et al. '89c). This reaction, which consists of an hypertrophy of the olivary neurons, probably is unique for the CNS. It can be induced experimentally in the rostral MAO and dorsal lamella of the PO of the cat by contralateral hemicerebellectomy (Verhaart and Voogd,'62; Voogd and Boesten,'76; Boesten and Voogd,'85).

Olivary hypertrophy has also been found at autopsy of patients with lesions of the brainstem and/or deep cerebellar structures (Foix et al., '26; Guillain and Mollaret, '31; Trelles, '57). These patients often show a motor disorder of delayed onset, characterized by contractions of the soft palate (palatal myoclonus). Although such a clonus could be the result of an hypersynchronization of motoneurons due to a patho-

logically absent timing device, a direct correlation with olivary hypertrophy is still a matter of discussion (Robin and Alcala, '75; Kane and Thach, '89).

The subject of this thesis will be introduced (this chapter) by a survey of the anatomy of the IO and its connections (part b, c, and d), a synopsis of its physiology (part e), and a description of the methods used (part f).

b. Olivary subnuclei and their connections

The inferior olive (IO) is one of the precerebellar nuclei. The cerebellum receives information about peripheral events and central nervous processes through numerous precerebellar systems, which terminate in different layers of the cerebellar cortex as climbing and mossy fibers, and as multilayer afferents which include the monoaminergic afferents. The IO gives rise to the climbing fibers; mossy fibers have their origin from a number of centers in the spinal cord and the brain stem. The output signals of the cerebellum to the brain stem and spinal cord are mediated through the central cerebellar and vestibular nuclei.

The IO is located in the ventral part of the medulla oblongata and is composed of the principal olive and two accessory olives (Kooy, '16; Brodal, '40; Whitworth and Haines, '86; see Fig. 1A for reconstruction of the IO). 1) The principal olive (PO) consists of a folded sheet of grey matter. Rostrally a dorsal and a ventral lamella can be distinguished. Caudally the PO is continuous with the ventrolateral outgrowth and the dorsal cap of Kooy ('16). 2) The medial accessory olive (MAO) includes several subnuclei. The subnucleus beta and the dorsomedial cell column are located at its caudal and rostral medial side, respectively. 3) The dorsal accessory olive (DAO) is located dorsally from the PO. The projection from these subnuclei to the cerebellum has been studied mainly in the cat (for reviews see Brodal and Kawamura, '80; Voogd, '82)

but also in primates and subprimates (for reviews see Brodal, '81 and '82; Whitworth and Haines, '86), and rats (for reviews see Flumerfelt and Hrycyszyn, '85; Voogd, '82). The climbing fibers, which are all derived from the IO (Desclin, '74), innervate the Purkinje cells in the cerebellar cortex (Szentágothai and Rajkovits, '59; Eccles, '66; Murphy et al., '73). Each olivary subnucleus projects almost exclusively contralaterally to one or more longitudinal strips (which are about 1 mm wide in cat) of Purkinje cells and gives off primary collaterals to that part of the central cerebellar nuclei (Groenewegen et al., '79; Andersson et al., '87b), which receives its main input from the same zone (Voogd and Bigaré, '80), (Figure 1A). Since the cerebellar nuclei in return project to the olivary subnucleus from which they receive collaterals (Tolbert et al., '76; Dietrichs and Walberg, '85 and '86; Dietrichs et al., '85 and '86), the direct connections between them are reciprocally and topographically organized. The restiform body is the pathway of the olivo-cerebellar fibers, while the cerebello-olivary fibers are located in the brachium conjunctivum (Figure 1B). In short, the caudal parts of both accessory olives are connected with the vermis of the cerebellar cortex and the fastigial and Deiters' nuclei, while the rostral parts of the accessory olives and the PO are connected with the hemisphere and the anterior and posterior interposed nuclei and the dentate cerebellar nucleus (Figure 1A).

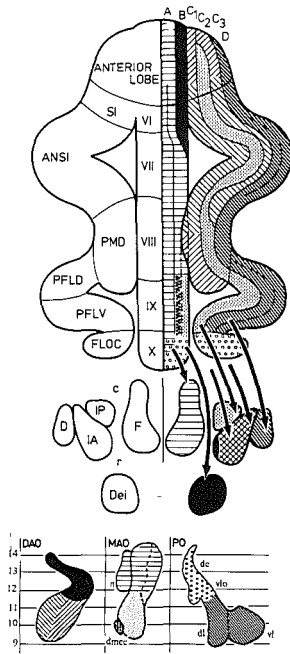


Fig. 1A. Diagram summarizing the projections of the IO to the cerebellum; by Groenewegen, Voogd and Freedman (1979). This Figure shows the longitudinal organization of the projection from the IO to the cerebellar cortex (top) and the cerebellar nuclei (middle). The cortico-nuclear interrelations are indicated with arrows. At the bottom unfolded reconstructions of the three subnuclei of the inferior olive are represented. The zone(s), central nucleus, and olivary subnucleus which are connected with each other are indicated by the same symbols. Abbreviations: ANSI, ansiform body; B, beta nucleus; D, dentate or lateral cerebellar nucleus; DAO, dorsal accessory olive; dc, dorsal cap of Kooy; Dei, Deiters' nucleus; dl, dorsal lamella of the principal olive; dmcc, dorsomedial cell column; F, fastigial nucleus; FLOC, flocculus; IA, anterior interposed nucleus; IP, posterior interposed nucleus; MAO, medial accessory olive; PFLD, dorsal paraflocculus; PFLV, ventral paraflocculus; PMD, paramedian lobule; PO, principal olive; SI, simple lobule; vl, ventral lamella of the principal olive; vlo, ventrolateral outgrowth.

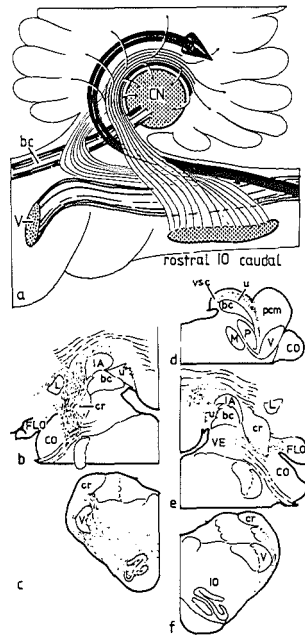


Fig. 1B. Lateral view of the localization of olivocerebellar fibers in the brain stem and the cerebellum (a). Fibers from the caudal half of the inferior olive (d-f) pass lateral to the spinal tract (V) and ascend in the restiform body to enter the cerebellum medial to the spino-, cuneo-, and reticulocerebellar components of the restiform body (thick arrow). Fibers from the rostral half of the inferior olive (b,c) enter the cerebellum lateral to these systems. In the cerebellum, olivocerebellar fibers become applied to the rostral and dorsal surface of the central nuclei and their efferent tracts. bc, Brachium conjunctivum; CN, central nuclei; CO, cochlear nuclei; cr, restiform body; FLO, flocculus; IA, anterior interposed nucleus; L, lateral cerebellar nucleus; M, motor nucleus of the trigeminal nerve; P, principal sensory nucleus of the trigeminal nerve; pcm, brachium pontis; u, uncinat tract; V, trigeminal nerve; VE, vestibular nuclei; vsc, ventral spinocerebellar tract. From Voogd and Bigaré ('80).

It was found in man, cat and rat that the number of Purkinje cells is about ten times as high as the number of olivary cells (Kreuzfuchs,'02; Braitenburg and Atwood,'58; Moatamed,'66; Armstrong and Schild,'70; Palkovits et al.,'71; Mlonyeni,'73), and that each Purkinje cell is provided with one climbing fiber (Eccles et al.,'66). One olivo-cerebellar axon fiber, therefore, should give rise to about ten climbing fibers. Branching of olivo-cerebellar fibers just below the cerebellar cortex was indeed demonstrated in Golgi studies (Estable,'23; Fox et al.,'69). Some of the climbing fibers of one olivary cell may be located in the same folium, but the others of the same cell may be located remotely within the same or even in a different cerebellar zone of other folia or lobules (Faber and Murphy,'69; Armstrong et al.,'71ab; Armstrong et al.,'73a,d; Rosina and Provini,'83,'85 and '87; Ekerot and Larson,'82; Andersson et al.,'87b). A climbing fiber terminates with multiple serial excitatory synapses on the proximal dendrites of one Purkinje cell (Palay and Chan-Palay,'74). In addition olivary fibers give off collaterals to the central nuclear neurons and to the Golgi, basket, stellate and granular cells in the cerebellar cortex (Palay and Chan-Palay,'74).

The afferent systems of the IO have been reviewed for cat (Brodal and Kawamura,'80), rat (Brown et al.,'77; Flumerfelt and Hrycyszyn,'85), and opossum (Martin et al.,'80). Apart from the cerebello-olivary projection mentioned above, three sets of afferent systems can be distinguished (Figure 2). The first one consists of the projections from the cerebral cortex most of which are interrupted in a set of nuclei at the mesodiencephalic border. The second group of afferent systems originate from centres in the spinal cord and the brain stem, relaying information about peripheral events and subcortical systems. The third group are the afferents from the reticular formation and raphe nuclei. The descending pathways from the mesodiencephalic junction to the olive are the medial and central tegmental tracts (Ogawa,'39; Mitomo,'42; Busch,'61). This region includes the nucleus of Darkschewitsch and the

parvocellular red nucleus, and nearby regions like the nucleus of Bechterew, the nucleus interstitialis of Cajal, the tegmental field of Forel, the zona incerta, the subparafascicularis nucleus, and the suprarubral reticular formation (Ogawa,'39; Walberg,'56; Brown et al.,'77; Linauts and Martin,'78; Leonard et al.,'78; Cintas et al.,'80; Saint-Cyr and Courville,'80 and '82; Kawamura and Onodera,'84; Ruigrok et al.,'88; Spence and Saint-Cyr,'88). These nuclei receive afferents from the motor- and premotorcortex and to a limited degree from the superior parietal lobule (Rinvik and Walberg,'63; Niimi et al.,'63; Mabuchi and Kusama,'66; Kuypers and Lawrence,'67; Hartmann-von Monakow et al.,'79; Nakamura et al.,'83; Saint-Cyr,'87), but also from the cerebellar nuclei (Voogd,'64; Kievit,'79; Courville,'66; Kawamura et al.,'82; Sugimoto et al.,'82). They project to the rostral MAO and PO, and to a lesser extent to the caudal MAO (Walberg,'74; Walberg,'82c; Swenson and Castro,'83; Onodera,'84; Holstege and Tan,'88). This projection is ipsilateral but some fibers cross (these contralateral fibers are increased in neonatal hemispheric-tomised rats; Swenson and Castro,'82). The anterior and posterior sigmoid gyrus of the cerebral cortex itself projects directly with an ipsilateral preponderance to the caudal MAO and the border region of the more rostrally located ventral lamella of the PO and the DAO (Sousa-Pinto and Brodal,'69; Bishop et al.,'76; Saint-cyr and Courville,'80; Saint-Cyr,'83; Swenson and Castro,'83). The second group of afferent pathways includes several sensory relay nuclei, which project predominantly contralaterally, like the dorsal horn of the spinal cord, the dorsal column nuclei and the spinal trigeminal nucleus (Brodal et al.,'50; Mizuno,'66; Boesten and Voogd,'75; Groenewegen and Voogd,'77; Berkley and Hand,'78; Armstrong et al.,'82; Swenson and Castro,'83; Gerrits et al.,'85a; Huerta et al.,'85). Spino-olivary fibers mainly originate from neurons in the intermediate zone (Armstrong et al., '82). The vestibular nuclei (with exception of the lateral vestibular nucleus), the medial and descending vestibular nuclei (Saint-cyr

and Courville,'79; Gerrits et al.,'85b), the parasolarius nucleus (Ebbeson,'68; Leowy and Burton,'78; Nelson and Mugnaini,'87), group Y (Gerrits et al.,'85b; McCrea and Baker,'85), and the superior colliculus (Hoddevik et al.,'76; Weber et al.,'78) give rise to projections to certain subdivisions of the MAO including the group Beta and the dorsal medial cell column. Visual centres with directional sensitivity involved in the optokinetic reflex, like the nucleus of the optic tract, the nuclei of the accessory optic tract and the nucleus prepositus hypoglossi project to the dorsal cap and the ventrolateral outgrowth (Mizuno et al.,'73; Walberg et al.,'81; Itoh et al.,'83; Gerrits et al.,'85b; McCrea and Baker,'85). These sensory associated areas, therefore, project primarily to the DAO, caudal MAO, subgroup beta, ventrolateral outgrowth and dorsal cap. Taken together, the cortical projections, most of which are relayed through nuclei at the mesodiencephalic border, and the bulbo-spinal afferents, which include several relay nuclei, remain separated at the level of the IO. So far, the only possible area of convergence of these inputs appears to be the caudal MAO (see also part e5.6).

In addition to the cerebellar input and the cortical and sensory associated afferents described above, the IO is innervated by fibers from different parts of the reticular formation and the raphe nuclei (Saint-cyr and Courville,'81; Walberg,'82ab; Walberg and Dietrichs,'82; Bishop and Ho,'86; Matsuyama et al.,'88). These fibers terminate more or less in each olivary subnucleus, and include the serotonergic innervation of the IO.

The rostral MAO and PO, which are innervated by the nuclei at the mesodiencephalic junction, project to zones in the hemisphere which intermingle with strips of Purkinje cells innervated by the rostral DAO (Groenewegen et al.,'79), which itself receives its inputs primarily from sensory relay nuclei. Parallel fibers, which are the T shaped axons of the granular cells of the cerebellar cortex, are oriented at right angles to these longitudinal strips. Parallel fibers may attain a

length of several millimeters (Mugnaini,'72; Brand et al.,'76; Mugnaini,'83; Kim et al.,'87), and thus may extend across several of these strips where they terminate on the distal, spiny branches of Purkinje cells.

The mossy fibers, which terminate on the granular cells, are the first link in the mossy fiber - parallel fiber pathway to the Purkinje cells (For review of mossy fiber paths, see Ito,'84; Voogd and Marani, in press). Some of the nuclei, which innervate the IO, also give rise to mossy fibers. This is the case with vestibular nuclei, the nucleus prepositus hypoglossi, the spinal nucleus of the trigeminal nerve, the dorsal column nuclei, certain reticular nuclei, and the spinal cord. The main cerebro-cerebellar mossy fiber pathway is relayed through the basal pontine nuclei and therefore remains separated from the cortico-olivary pathway, which passes through the nuclei of the mesodiencephalic junction. The terminations of mossy fibers in the granular layer are more diffuse and patchy than those of the climbing fibers, but most of them are still aggregated in illdefined sagittal zones. For some areas like the cuneate nucleus it has been shown that there is a high degree of overlap between the mossy and the related climbing fiber projections in the cerebellar cortex (Groenewegen and Voogd,'77; Groenewegen et al.,'79; Gerrits et al.,'85b; Gerrits,'87).

Both the climbing fibers and the mossy fibers give off collaterals to the central nuclei (van der Want et al.,'87; Gerrits and Voogd,'87; Wiklund et al.,'88; van der Want et al.,'88; van der Want et al.,'89). However, up to now, it has not been elucidated whether both afferents actually make synaptic contacts with both the inhibitory (Gabaergic) and excitatory cells in the cerebellar nuclei. The inhibitory cells innervate the IO (Nelson et al.,'84; see part d, this chapter) and possibly also the bulbar reticular formation (Buisseret-Delmas et al.,'89), and may give off some collaterals to the pons (Aas and Brodal,'89). The excitatory cells relay their information to areas in the thalamus, midbrain and brainstem without giving off collaterals to the IO (Bharos et al.,'81).

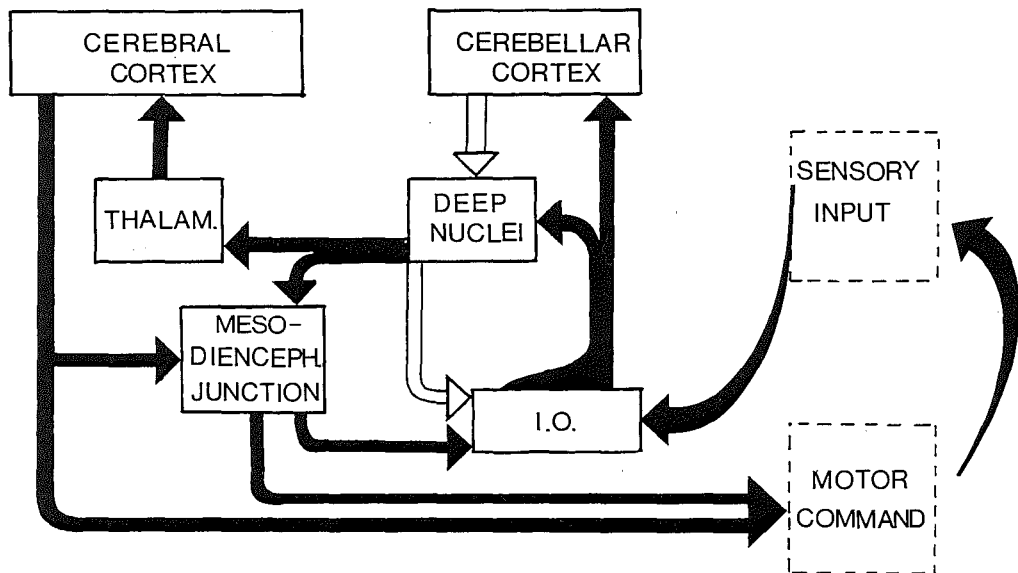


Fig.2. Graphic representation of the major afferent and efferent connections of the inferior olive. White arrows indicate inhibitory pathways and black arrows mark the excitatory systems. Note that the monoaminergic afferents of the inferior olive are not depicted.

c. Cytology and ultrastructure of olivary cells and their afferent fibers

The olivary neurons and their synaptic inputs show several characteristic features which will be shortly reviewed below, both at the light and electron microscopical level.

Although the corpora olivares (olivary bodies) were first identified and so named by Gabriel Fallopius near the middle of the sixteenth century (Willis, 1664), more than 300 years passed before Vicenzi (1886) characterized the inferior olive nerve cells and portrayed their unique highly ramified dendritic trees. Kölliker (1893) and van Gehuchten ('05) elaborated upon the cytological features of the IO, but it was Ramon y Cajal ('09) who most thoroughly described this brainstem area using the Golgi

method. From his lightmicroscopical studies and those performed by others, it became evident for various animals that several types of neurons and afferents exist in the IO (Ramon y Cajal,'09; Scheibel and Scheibel,'55; Scheibel et al.,'56; Bowman and King,'73; Gwyn et al.,'77; Sotelo et al.,'74; Rutherford and Gwyn,'80; Foster and Peterson,'86; Iwahori and Kiyota,'87; Szteyn,'88). Three types of afferent fibers were revealed by these studies: One type, which may preferentially innervate the somata of olivary neurons, was relatively smooth with conspicuous varicosities at regular intervals (heavy rosette-bearing type), another type gave off fine branches, each

branch ending in a small chalice (thin bouton-bearing type), and the last type of afferent did not give off branches in its trajectory across the subdivision until it ended in a terminal bush-like efflorescence (bushy terminal of Cajal). It has been suggested that some afferent systems may issue all three types of fibers, whereas others terminate with one type of fiber (Scheibel and Scheibel,'55; Scheibel et al.,'56).

The population of olivary neurons was not homogeneous either. Apart from a few interneurons, which may be GABAergic (Nelson et al.,'88; Walberg and Otterson,'89), it is composed of two main types of neurons. The first type (type I) is equipped with relatively long and diffuse, sparsely branched, spiny dendrites radiating away from the soma. The dendritic field of type I cells is large and it mainly occurs in the caudal parts of the accessory olives. The second type (type II) is a neuron with a spherical cell body with a diameter (15 to 30 μm) somewhat larger than of the first type (Ruigrok et al., submitted), and with an arbor of complex, spine-bearing dendrites which are highly branched and tend to turn back toward the soma, at times creating spirals. This type of neuron occupies a relatively small three dimensional area. It represents the predominant cell type in the PO and the rostral part of the MAO and the DAO. Both cell types are probably projecting neurons, i.e. give rise to the climbing fibers, since the axons of both types of cells leave the neuropil of the adult IO without giving off collaterals (Foster and Peterson,'86; Ruigrok et al., submitted). In the IO of young animals, however, recurrent collaterals are probably present (Ramon y Cajal,'09; King,'80; see also Ruigrok et al., submitted).

The ultrastructure of the IO has been described in many studies of various animals including the opossum (Bowman and King,'73; King,'80), rat (Gwyn et al.,'77), rabbit (Mizuno et al.,'74), cat (Walberg,'63; Walberg,'64; Walberg,'66; Sotelo et al.,'74; Bozhilova and Ovtcharoff,'79), and monkey (Rutherford and Gwyn,'80). In general, most neural elements in the olivary neuropil are enveloped in thin processes of fibrous as-

trocytes. The neuronal somata are oval or round in shape, and their cytoplasm contains subsurface cisterns of the endoplasmic reticulum, spherical inclusions that may be lipofuchsin deposits, and the complement of organelles characteristic of most neurons in the central nervous system. Somata sometimes are apposed to dendrites. These appositions are usually without any membrane specialization, but in the MAO of the cat submembraneous dense bodies have been found under one of the apposite membranes (Bozhilova and Ovtcharoff,'79). The segments of olivary dendrites bear simple, pedunculated club-shaped, and/or racemose spiny appendages (Sotelo et al.,'74; Gwyn et al.,'77), and they sometimes contain varicose dilatations packed with mitochondria.

The most characteristic features of the olivary neuropil are the glomeruli (Nemecek and Wolff,'69; Bowman and King,'73; Sotelo et al.,'74; King et al.,'75; King,'76; Gwyn et al.,'77; Rutherford and Gwyn,'77), and to less extent the dendritic thickets (Sotelo et al.,'74; Molinari,'87). The dendritic thickets are formed by several (up to four) serial dendrites in direct apposition with each other, but without any dendro-dendritic membrane specialization. The glomeruli contain a core of several dendritic appendages surrounded by terminals and glia. The spines in the centre of these complex synaptic structures are frequently linked by gap junctions. Benardo and Foster ('86) showed in slices of the guinea pig inferior olive that intracellular injected Lucifer yellow can pass from one cell to the other through the gap junctions. They were able to label aggregates containing up to six coupled olivary cells. Harmaline induced synchronous firing, which is probably also mediated through the gap junctions (see part e3), suggests that in the intact IO the coupled cellular aggregates can extend to a much larger size (Linás and Volkind,'73; Sjölund et al.,'80). So far gap junctions have been found in each olivary subnucleus except for the dorsal cap (Mizuno et al.,'74).

Terminals on neurons of the IO differ as to their morphology, localization, their membrane specializations, their neurotrans-

mitter and their origin. It was found in aldehyde fixed tissue postfixed in osmium that more than half of the terminals contained rounded vesicles (Bowman and King,'73; Mizuno et al.,'74; Sotelo et al.,'74; Gwyn et al.,'77; Rutherford and Gwyn,'80). These terminals usually are associated with asymmetric synapses (for definitions of morphology of synapses see Gray,'59 and Gray and Guillery,'66). The second largest group of terminals contains pleomorphic vesicles and is provided with symmetric synapses, they are roughly of the same size as the round vesicle containing terminals. A small minority of the terminals contains either dense core vesicles or only flattened vesicles (Bowman and King,'73; Gwyn et al.,'77). The large majority of the terminals contact the distal dendrites and/or their spines, whereas the somata receive relatively few terminals. The somatic terminals consist mainly of terminals with pleiomorphic vesicles. In the IO of the rat, somatic terminals are most frequently found on cells of the MAO (Gwyn et al.,'77). Special types of synapses, including synapses associated with subsynaptic densities as described by Taxi (Taxi,'61) and so-called crest synapses (Milhaud and Pappas,'66ab; Akert et al,'67) are present in the IO of several animals (Mizuno et al,'74; Gwyn et al,'77; Rutherford and Gwyn,'80; Cintas et al,'80; Sotelo et al,'86). Chemical dendrodendritic synapses in the IO have only been observed in the opossum (King,'80), while axo-axonal contacts have not been described.

Several methods have been used to further identify profiles of neurons and their processes, and afferent fibers in the neuropil of the IO. Neurons can be studied both at the light and electron microscopical level by adaptations of the Golgi method and by intracellular injection of horse radish peroxidase (HRP) which can be converted into an electron dense reaction product (for technical details see part f). Intracellular labeling of olivary neurons to study their ultrastructural morphology has thus far only been used by King ('80). One of his major observations was that several HRP labeled profiles (up to five) belonging to the same neuron may be en-

countered in a section through a glomerulus. The glomeruli were not reconstructed, however, and the question whether these profiles belong to a single or to multiple spines could not be resolved. Using the same technique to label neurons in the reticular formation dorsal to the IO, it was found that the dendrites of reticular cells may enter the IO to terminate in the olivary glomeruli (Bishop and King,'86; Foster and Peterson,'86).

Afferent fibers and their terminals can be identified by anterograde degeneration or tracing, and immunocytochemistry. In cat, rat and/or opossum anterograde degeneration and/or tracing have been used to study the afferent projections to the olive from the cerebellum (King et al.,'76; Mizuno et al.,'80; Angaut and Sotelo,'87), mesodiencephalic junction (Walberg,'65; King et al.,'78; Cintas et al.,'80), spinal cord (King et al.,'75; Mizuno et al.,'76; Gwyn et al.,'83; Molinari and Starr,'88; Molinari,'88), pretectum (Mizuno et al.,'74), and gracile nucleus (Molinari,'87; Molinari and Sluyters,'87). None or only a small minority of these afferent fibers were found to contact somata. Most terminals are apposed to distal dendrites or spines inside and outside the glomeruli and dendritic thickets, and contain rounded vesicles and asymmetric synapses. Terminals with pleiomorphic vesicles and symmetrical synapses were only found after 3H-leucine injections in the cerebellar nuclei of the rat (Angaut and Sotelo,'87). The cerebellar terminals have been associated with dendrites linked by gap junctions (King et al.,'76; Angaut and Sotelo,'87), whereas the afferents from the spinal cord and gracile nucleus have never been found in close proximity to gap junctions (Molinari and Starr,'88; Molinari,'88 and '87).

Immunocytochemical studies of the IO which identified the ultrastructural distribution and morphology of labeled terminals are relatively scarce. Up till now, immunocytochemical studies have been performed using antibodies against glutamic acid decarboxylase (Sotelo et al.,'86) and gamma-amino butyric acid (Angaut and Sotelo,'87), serotonin (Sjölund et al.,'80; Wiklund et al.,'81; King et al.,'84; Compoin et al.,'88), and

enkephaline (King et al., '87a; King et al., '89). The indolaminergic terminals were found to contain many dense core vesicles and tubulovesicular elements, and only rarely displayed a synapse. When they were present the synapses were of the asymmetric type. The GABAergic terminals usually contained pleomorphic vesicles and were provided with symmetric synapses. Enkephaline-like immunoreactivity was found in a group of large terminals which contain dense core vesicles, and in a group of terminals containing small clear vesicles (King et al., '89). In general, these cytochemically identified terminals were

distributed randomly over the olivary neuropil. However, King et al. ('84 and '89) observed in the opossum that enkephalinergic terminals do not end upon somata, and that serotonergic terminals are not present within glomeruli. Although it has been suggested that the serotonergic (Sjölund et al., '80) and enkephalinergic (King et al., '89) input to the IO are concerned with the regulation of electrotonic coupling, it has so far only been demonstrated for the GABA-ergic (Sotelo et al., '86; Angaut and Sotelo, '87) and cerebellar (see above) terminals that they are apposed to dendrites linked by gap junctions.

d. Neurotransmitters involved in the olivary system

The olivary neurons contain a variety of neurotransmitters and they are innervated by many afferent systems containing many different sorts of neurotransmitters.

Immunohistochemical data (Wiklund et al., '82ab; Wiklund et al., '84; Matute et al., '87; Campistron et al., '86; Walberg and Otterson, '89), and physiological and pharmacological studies (Crepel et al., '83; Toggenburger et al., '83; Kimura et al., '85; Cuénod et al., '88) strongly suggest that the climbing fibers, at least of the cerebellar hemisphere, use the amino acid aspartate as their neurotransmitter. Aspartate is known to be excitatory (Johnson, '78). Homocysteate and adenosine may be involved in climbing fiber synaptic transmission as well (Kostopoulos et al., '75; Cuénod et al., '88 and '89). In addition, the neuropeptides corticotropin releasing factor (CRF), (Young et al., '86; Mugnaini and Nelson, '87; Palkovits et al., '87; Powers et al., '87; van den Dungen et al., '88; Cummings et al., '88; Foote and Choong, '88), enkephaline (ENK), (King et al., '87a) and cholecystokinin (CCK), (King et al., '88) have been found in olivary neurons and/or climbing fibers. In some of these neurons and fibers CRF and ENK are co-localized (Cummings and King, '88; King et al., '88). CRF probably potentiates the actions of aspartate and glutamate in the cat's cerebellum (Bishop,

'89). It is interesting to note that the CRF content of the inferior olive is the highest of all extrahypothalamic brainstructures (Palkovits et al., '85). When the brain stem is transected in cats at the level of the pons the CRF content is increased in olivary cells (Kitahama et al., '88). Since this also occurs in the cat IO after cerebellectomy (Mugnaini and Nelson, '89) but not following hypophysectomy or adrenalectomy (Kitahama et al., '88), the increased CRF level in the olivary cells of pontine cats is probably due to an interruption of the cerebello-olivary connections and not to a disturbed regulation of extraolivary hormones. In addition, the CRF production of the olivary neurons can be increased in the dorsal cap after prolonged physiological optokinetic activation (Barmack and Young, '88). Other peptides found in olivary cells are vitamin D-dependent calcium-binding protein (Baimbridge and Miller, '82; Maler et al., '84; Fournet et al., '86), gamma-amino butyric acid transaminase (Nagai et al., '85), and somatostatin (Vincent et al., '85; Cotter and Laemle, '87). Somatostatin was only found to be present in the MAO, a property it may share with the receptors for nerve growth factor (Yan and Johnson, '88).

The olivary cells themselves are innervated by many afferent systems which contain different neurotransmitters or peptides. One

of the main transmitters is gamma-amino butyric acid (GABA). GABAergic boutons are widely distributed throughout the rat, cat and human IO (Nelson and Mugnaini,'85; Sotelo et al.,'86; Gotow and Sotelo,'87; Nelson and Mugnaini,'88 and '89; Nelson et al.,'89) and are probably derived mainly from the cerebellar nuclei (Nelson et al.,'84; Nelson and Mugnaini,'85; Buisseret-Delmas et al.,'87 and '89), but also from the lateral and descending vestibular nuclei, the parasolitary and cuneate nuclei (Nelson et al.,'86; Nelson and Mugnaini,'87; Nelson and Mugnaini,'89), and from GABAergic olivary interneurons (Nelson et al.,'88; Walberg and Otterson,'89; Nelson and Mugnaini,'89). Weber et al. ('89) found evidence that the IO in the monkey also receives a GABAergic input from the pretectum. However, this was neither found by Horn and Hoffman ('87) in monkey, cat and rat, nor by Nunes Cardozo and van der Want (in press) in rabbit. Like GABA, neuropeptide ENK is presumed to be inhibitory (Roberts,'74; Schulman,'81) and localized in terminal profiles throughout the IO (King et al.,'87a). CCK -and CRF immunoreactive terminal profiles are also present in each olivary subnucleus but they are more restricted in their distribution (King et al.,'87b). The same accounts for substance P (Ljungdahl et al.,'78; Bishop and Ho,'84) and serotonin (Fuxe,'65; Wiklund et al.,'77; Wiklund et al.,'81; Sladek and Hofman,'80; Takeuchi and Sano,'83; Bishop and Ho,'84; King et al.,'84; Compoin et al.,'88; Compoin and Buisseret-Delmas,'88). In some parts of the olive, like the DAO, Substance P and serotonin may coexist in the same terminals (Pare and Descarries,'85; Pare et al.,'87). Apart from an indolaminergic input, the IO is also innervated by catecholamines (Sladek and Bowman,'75; Sladek and Hoffman,'80; Kamei et al.,'81). The distribution of this catecholaminergic input is rather different for different species. Positive immunostaining in afferent fibers of the IO has furthermore been found for enkephaline-methionine (which was not, like normal enkephaline, present in olivary neurons; Conrath-Verrier et al.,'83), histamine (Airaksinen and Panula,

'88), glycine (Nelson and Mugnaini,'89), neurotensin (during development; Mailloux and Vanderhaeghen,'88), and galanin (Beal et al.,'88).

Muscarinic and nicotinic cholinergic receptors are present in respectively the human and zebra finch IO (Hyde et al.,'88; Watson et al.,'88), and acetylcholine esterase is differentially distributed in all olivary subnuclei (Marani et al.,'77). However, acetylcholine is probably not an operative excitatory neurotransmitter since the synthesizing enzyme choline acetyltransferase is not present in the IO (Tatehata et al.,'87). Aspartate does not act as an excitatory neurotransmitter in the IO either since no positively stained terminals could be found in the monkey IO (Walberg and Otterson,'89)*¹. The application of acetyl and l-glutamate probably increases the excitability of the cellmembrane of olivary neurons (Duggan et al.,'73), and receptors*² have been found for N-methyl-D-aspartate and L-glutamate in the IO (Monaghan and Cotman,'85). However, the evidence for glutamate as an excitatory transmitter in afferents of the IO is still far from complete. So far, immunocytochemical methods have not been used to clarify this. Another possible excitatory neurotransmitter in the IO is Di-homocysteic acid. When this excitant drugs is administered to olivary neurons the olivary firing rate accelerates.

*Note*¹. Because the presumed neurotransmitter of the climbing fibers is aspartate (see above), this observation also argues against the presence of recurrent collaterals of olivary neurons (see part c).*

*Note*². With regard to other receptors, it was found that olivary neurons contain binding sites for calcitonine gene-related peptide (Skofitsch and Jacobowitz,'85; Sexton et al.,'86), substance-P (Helke et al.,'84; Buck et al.,'86; Shigematsu et al.,'87) and tachykinin (Mantyh et al.,'89), D-2 dopamine and 5-HT₂ serotonin (Nakada et al.,'84), cholecystokinin (Diehl et al.,'87), neuropeptide y (Harfstrand et al.,'86), alpha 1-adrenaline (Jones et al.,'85) and alpha 2-adrenaline (Probst et al.,'84), dihydro-*

testosterone (Heritage et al., '81), glycine (de Montis et al., '82), and angiotensin II (Gehlert et al., '84; Mendelsohn et al., '84; Nazarali et al., '87; Walters and Speth, '88; Gutkind et al.,

'88). With respect to angiotensin, it is interesting to note that angiotensin converting enzyme has been found in the IO as well (Chai et al., '87).

e. Physiology of the inferior olive

- e1. Introduction
- e2. Electrophysiological characteristics of olivary neurons
- e3. Effects of olivary discharges on cerebellar neurons
- e4. Function of the olivo-cerebellar system
- e5. Physiology of olivary afferents

e1. Introduction

One of the aims of neurobiology is to relate the static images of morphology to the state of flux of the living brain. The physiological properties of olivary neurons, such as their propensity to oscillate, their slow firing rate, and their tendency to fire synchronously, are important in this respect. These dynamic properties are determined by the distribution of conductances and electrical synapses (gap junctions) over the cell membrane of the soma and the dendrites, and they can be influenced by the activity of neurotransmitters (e.g. GABA) or drugs (e.g. harmaline). The intrinsic properties of the olivary neurons and the way they are affected will be discussed in more detail below (part e2).

The two main afferent systems of the cerebellum, the climbing fibers from the IO and the mossy fiber - parallel fiber pathway, terminate at two levels. They have their main effects directly on the Purkinje cells, but they also give off collaterals to the neurons of the central cerebellar nuclei. Each olivary neuron exerts a strong, characteristic, excitatory action on the proximal dendritic tree of a small number of Purkinje cells, while the parallel fibers have a weak excitatory effect on the spiny branchlets of the distal dendrites

of numerous Purkinje cells. The impulse frequency of the climbing fibers is low and is a limiting factor in the transfer of information to the Purkinje cells. Climbing fiber activity induces, apart from a direct excitation of the Purkinje cells, a change in their response to the parallel fibers. These major effects of the olivo-cerebellar fibers both on the Purkinje cells and on the central nuclei cells will be considered more extensively in part e3.

Several theories have been developed to explain the function of the olivo-cerebellar system and the mossy fiber - parallel fiber pathway, taking the spatial organization of these systems into account. These theories view the olivocerebellar system as a gating or learning device influencing the transmission of information from the parallel fibers to the Purkinje cells. For an understanding of the function of the inferior olive it is essential to compare the individual actions of climbing and parallel fibers on Purkinje cells and to review the physiological basis for their interaction in more detail (part e4).

To understand the function of the inferior olive it is important to know what kind of information it receives and how it is processed and transmitted to the cerebellum. This problem has been studied for different afferent systems and for different parts of the

olive. The inhibitory effects from GABAergic nucleo-cerebellar pathways and the excitation by descending mesodiencephalic pathways are of special interest in the scope of this thesis. The transfer of information and the convergence of afferent pathways at pre-olivary levels have been studied in greater detail in paradigms involving other parts of the olive, which will also be shortly reviewed (part e5).

e2. Electrophysiological characteristics of olivary neurons

The intrinsic properties of the olivary neurons determine the nature of the response to their afferents, their unusual low maximum firing rate, and their tendency for rhythmic and synchronous firing. This synchronism is due to the fact that the neurons of the IO are electrotonically coupled (Llinás et al., '74; Llinás and Yarom, '81a) by gap junctions (see part c). The electrotonic coupling also explains why some olivary neurons discharge orthodromic impulses (the olivary reflex) after cerebellar stimulation even when they are not antidromically invaded (Eccles et al., '67; Armstrong et al., '74; Crill, '70; Llinás et al., '74; Andersson, '84). Compared to the other olivary subnuclei, the level of electrotonic coupling in the MAO is relatively high (Llinás and Yarom, '81a). Synchronous firing in the IO can be modulated (Bower and Llinás, '83) by GABA (Sasaki and Llinás, '85). The mechanism responsible for this modulation may be a similar one as found in Navanax buccal ganglia, where electrical coupling of motoneurons can be short-circuited (shunting) by presumed inhibitory terminals located near the gap junctions (Spira and Bennett, '72; Spira et al., '80).

The propensity of olivary neurons to oscillate is the result of the differential distribution of membrane conductances over the cell membrane. When activated antidromically or orthodromically, the IO cell at rest generates, in addition to the usual fast sodium action potential, a prolonged (about 15 ms) after-depolarizing potential (ADP) and a long-lasting (about 100 ms) large after-

hyperpolarizing potential (AHP), (Armstrong et al., '68; Crill, '70; Llinás and Yarom, '81ab; Pettigrew et al., '88). The dendritic high threshold calcium conductance responsible for the ADP can be triggered antidromically by the initial somatic sodium spike. Trains of secondary action potentials (spikelets) can occur in association with this prolonged depolarization (Ochi, '65; Sedgwick and Williams, '67; Armstrong and Harvey, '66; Armstrong et al., '68; Crill, '70). These ADP component spikes, with interspike intervals of approximately 2 ms, are especially prominent in the olivary reflex potential (Armstrong and Harvey, '66; Eccles et al., '67). The ADP activates a calcium-dependent potassium conductance^{*3}, which is responsible for the AHP. Following this hyperpolarization, a low threshold calcium-conductance (located in or near the soma) is activated, which in turn may generate again a new sodium spike. This low threshold calcium-conductance may cause the rebound potentials (see also part a, Chapter IV), and is inactivated at rest membrane potential (Llinás and Yarom, '81b).

The long lasting afterpotential (AHP) of the olivary cells is the main factor underlying their low maximum firing frequency of about 10 Hz (Armstrong et al., '68; Bell and Grimm, '69; Bell and Kawasaki, '72; Eccles et al., '72ab; Armstrong and Rawson, '79; Sasaki and Llinás, '85; Benardo and Foster, '86) and their tendency to oscillate and to fire rhythmically (Llinás and Yarom, '81ab; Benardo and Foster, '86; Llinás and Yarom, '86; Yarom and Adan, '88). Their firing rate depends on the state of depolarization of the cell. In fact, olivary neurons tend to fire rhythmically at two preferred frequencies: 3-6 Hz when the cells are actively depolarized and 9-12 Hz when they are actively hyperpolarized (Llinás and Yarom, '86). In depolarized cells the dendrites will be actively involved (high threshold dendritic calcium conductance), causing a long lasting and deep AHP, whereas hyperpolarized, the dendrites will not actively participate resulting in a shorter period. In addition to these basic features several conductances have been found which may modulate the electro-

responsive properties of the IO neurons in the long-term (Yarom and Llinás,'87).

At rest, olivary cells in vitro may display subthreshold oscillations synchronously in a group of these neurons (Benardo and Foster,'86; Llinás and Yarom,'86). After a small external input these subthreshold oscillations will become sustained oscillations provided that the electrotonic coupling between the cells is strong enough (Yarom and Adan,'87; Yarom,'89). In order to stop an oscillation in a cell ensemble some of the cell-units have to be disconnected from it. These findings show that the ability of olivary neurons to fire synchronously coincides nicely with their tendency to oscillate, and they offer the interesting possibility that the rhythmical firing frequency can be decreased by inhibitory afferents which are strategically located to reduce the level of electrotonic coupling !

Olivary neurons fire synchronously and rhythmically following stimulation of afferents (which will be discussed in part e5) but also after application of drugs like the indol alkaloid harmaline (Llinás and Volkind,'73; de Montigny and Lamarre,'73). Harmaline, increases the olivary cell excitability by hyperpolarizing the neurons and shifting the inactivation curve of the somatic Ca spike to a more positive membrane potential level (Llinás and Yarom,'86). By this mechanism probably, harmaline is capable to evoke spontaneous and regular bursts which last for long periods at frequencies around 8/s or higher. The bursts are evoked in the caudal MAO and the DAO (de Montigny and Lamarre,'73; Llinás and Volkind,'73; Sjölund et al.,'80). These subdivisions of the olive are most heavily innervated by serotonergic pathways (Wiklund et al.,'77). Moreover, it has been found that the oscillatory effect of harmaline in vitro is blocked by noradrenaline but increased by serotonin (Llinás and Yarom,'86) whereas destruction of the serotonergic innervation of the rat IO with specific neurotoxic drugs can markedly reduce the harmaline tremor (Sjölund et al.,'77 and '80). Thus, although serotonin exerts, in contrast to harmaline, a depolarizing effect on the membrane of

olivary neurons (Llinás and Yarom,'86), the induction of oscillation by harmaline may still depend on the presence of serotonin (see also Wiklund et al.,'81; Barragan et al.,'85). The olivary rhythm induced by harmaline coincides with a tremor at the same frequency (Llinás and Volkind,'73; see also Llinás,'84). Apparently, the rhythmic activity of the IO can be transmitted through the cerebellar nuclei to motoneurons. Similar tremorgenic effects follow the application of other unrelated alkaloids as dihydro-B-erythroidine, curare, strychnine, bicuculline (Biscoe et al.'73), and quipazine (Barragan et al.,'85). The tremor evoked by harmaline is markedly antagonized by ethanol (Sinclair et al.,'82; Sinton et al.,'87), which blocks the low threshold calcium conductance (Llinás and Yarom,'86), and it can be abolished by application of 3-acetyl-pyridine*⁴ (Bardin et al.,'83; Bernard et al.,'84).

*Note*³. These include probably a specific class of channels sensitive to apamin (Mourre et al.,'86).*

*Note*⁴. Three-acetyl-pyridine is a nicotinic acid antimetabolite (Gibson and Blass,'85) and probably interferes with the energy supply of the neurons in the IO (Montgomery,'80). The neurons in the caudal MAO are the last to be affected by this drug (Anderson and Flumerfelt,'84; Rossi, personal communication). Whether it affects primarily Type I neurons (see part d1), which are usually located in the caudal MAO, is unknown.*

e3. Effects of olivary discharges on cerebellar neurons

The mean conduction velocity of axons of olivary cells is rather low (5 m/s ranging from 3.7 to 23 m/s in cat; Eccles et al.,'67; Armstrong et al.,'74; Kitai et al.,'77). These axons innervate both cells in the cerebellar cortex and in the cerebellar central nuclei.

EFFECTS ON CORTICAL CELLS. In the cerebellar cortex, the climbing fibers exert effects not only on the Purkinje cells but also on the inhibitory interneurons. The primary effect of climbing fiber impulses is a powerful excitation of Purkinje cells which is termed climbing fiber response (Eccles et al., '66). When recorded intracellularly a climbing fiber response begins with a spike followed by a long-lasting depolarization with two to six superimposed wavelets which probably originate from the Purkinje cell dendrites (Martinez et al., '71; Llinás and Sugimori, '80; Ito, '84). The large depolarization underlying the climbing fiber response is generated by a unitary excitatory postsynaptic potential (EPSP) that behaves in an all-or-none fashion, indicating that it is produced by a single climbing fiber terminating on the Purkinje cell (Eccles et al., '66). This potential is so large that it is conspicuous even in extracellular recordings (Fujita, '68; Faber and Murphy, '69; Murphy and Sabah, '71). When recorded extracellularly from the Purkinje cell soma one can see the "complex spike" response (Thach, '68 and '70). It is composed of a short burst of up to 6 component action potentials with a frequency of about 500/s superimposed on a slow wave lasting about 10-15 ms. Corresponding with the number of component spikes, the response in a Purkinje cell axon to a single complex spike can consist of up to five impulses (Ito and Simpson, '71). Recordings from Purkinje cells and/or their axons showed that the number of component spikes varied from cell to cell and even from spike to spike within the same cell (Thach, '67; Ito and Simpson, '71; Armstrong and Rawson, '79b; Ito, '84). The number of component spikes in the complex spike can be reduced by inhibition of the Purkinje cell from the basket cells (Eccles et al., '67), and it may be increased when the climbing fiber response is preceded by a parallel fiber volley (cf. Mano, '70 and '74) or when it is followed immediately by another climbing fiber response (Campbell and Hesslow, '86). Parallel fiber activity is known to evoke simple spikes in the Purkinje cells (Eccles et al., '67). Climbing fibre responses can also be recorded

from the surface of the cortex as field potentials (eg. following A B and C-fibre activation, see Ekerot et al., '85ab). These field potentials probably indicate synchronous discharges in many climbing fibres (Andersson et al., '87b).

The EPSP's generated by the climbing fiber impulses do not only evoke complex spikes in the soma of the Purkinje cells but also prolonged plateau-like depolarizations in their dendrites (Ekerot and Oscarsson, '80 and '81; Campbell et al., '83b). The plateau potentials are generated by an increase of the calcium conductance at the climbing fiber synapses and spread actively to the distal dendrites (Llinás and Sugimori, '80 and '82; Tank et al., '88). The duration of the plateau potential in the proximal dendrites takes several tens of milliseconds, whereas in the distal dendrites it may last hundreds of milliseconds. The length of this plateau potential in the distal dendrites depends on the actual membrane potentials in the individual dendritic branches (Campbell et al., '83a). The membrane potential in the distal dendrites is probably determined by the preceding synaptic activity of parallel fibers and interneurons. Campbell and colleagues ('83b) actually showed that the plateau potential can be shortened or abolished by a superimposed IPSP from the stellate cells.

Many efforts have been made to study the possible heterosynaptic effect of climbing fiber responses on the simple spike activity. The plateau potential, which spreads towards the distal parallel fiber innervated spiny branchlets, may be involved in mediating this effect. So far, three possible heterosynaptic phenomena have been described. These are the climbing fiber pause, the long-lasting depression, and the short-lasting enhancement.

The climbing fiber pause is a silence of simple spikes which usually occurs directly after a climbing fiber response (Granit and Phillips, '56; Eccles et al., '67; Bell and Grimm, '69; Martinez et al., '71; Bloedel and Roberts, '71; Armstrong et al., '73c). The duration of the climbing fiber pause varies like the plateau potentials from ten to several hundreds of milliseconds, and may also

depend on the preceding membrane potential. In fact, it was found that the duration of the pause is related to the simple spike activity preceding the climbing fiber response (Latham and Paul,'71). However, Murphy and Sabah ('71) showed that the duration of the pauses is also related to the size of the stimulus to the IO itself and to the number of olivary neurons discharged. The suppression of simple spikes by a complex spike may be due to a direct heterosynaptic effect of the climbing fibers on the Purkinje cells or to the involvement of the inhibitory interneurons which are known to receive climbing fiber synapses and which in turn may modulate the Purkinje cell membrane potential (Eccles et al.'66c; Schulman and Bloom,'81). In behavioural experiments with awake monkeys it was found that the pauses which follow spontaneous climbing fiber responses are usually short (Thach,'68), whereas the pauses which occur after climbing fiber responses preceding the onset of movement (Thach,'70) or during arousal responses (Mortimer,'73), commonly last 100 ms or more. This suggests that the duration of the climbing fiber pause is an important factor in the coordination of motorbehaviour.

Ekerot ('85) proposed that the climbing fiber evoked plateau potentials could underlie the long-lasting (up to two hours) depression of parallel fiber responses. This heterosynaptic depression of simple spikes occurs after a short period (several minutes) of conjunctive electrical stimulation of climbing fibers and parallel fibers terminating on the same Purkinje cells (Ito et al.,'82; Ekerot and Kano,'83). When the parallel fiber response occurs within 20 ms after the climbing fiber response the depression can be found in the majority of the Purkinje cells tested, whereas after 400 ms it is only present in a minority of the cells (Ekerot and Oscarsson,'81). The occurrence of a long lasting depression also depends on the local membrane potential of the Purkinje cell dendrites. Synapses located on dendrites receiving a strong net excitatory input will be strongly affected, whereas synapses located on hyperpolarized dendrites will be little or not at all

influenced by a climbing fiber impulse (Campbell et al.,'83a). Kano and Kato ('88) found evidence that the occurrence of long term depression is strictly dependent on conjunction of climbing fiber activity with quisqualate receptor activation. The above findings suggest that individual synapses and dendrites of Purkinje cells have a learning capacity.

The third possible heterosynaptic effect is the opposite of the former one. When parallel fibers are activated by natural (Ebner and Bloedel,'81ab) or electrical (Ebner and Bloedel,'84) stimulation shortly after (20 ms or more; thus probably after the initial climbing fiber pause) a spontaneously occurring (Ebner and Bloedel,'81ab), somatosensory evoked (Ebner et al.,'83), or behaviorally evoked (Lou and Bloedel,'86; Mano et al., '86) climbing fiber input, the simple spike responses are enhanced for a short duration (about 100 ms). This suggests that the climbing fiber input may enhance the responsiveness of Purkinje cells in a real time operation.

It may be important to stress that the climbing fiber pause and short-lasting enhancement apparently occur following a normal activation of the climbing fibers. However, the long-lasting depression is produced only by long lasting (several minutes) electrical activation. This long tonic discharge has rarely been found in the IO following natural stimulation (see part d1).

EFFECTS ON CEREBELLAR NUCLEAR CELLS. Olivary discharges influence the central nuclei neurons directly via collaterals of olivocerebellar axons and indirectly via the climbing fiber input to the Purkinje cells, which monosynaptically inhibit the cells in the cerebellar nuclei (Ito and Yoshida,'66; Ito et al.,'70). Intra- and extracellular recordings from neurons in the deep cerebellar nuclei (Latham et al.,'70; Eccles et al.,'71 and '74ab; Kitai et al.,'77; Andersson and Oscarsson,'78; Armstrong et al.,'73e; Llinás and Mühlethaler,'88ab) or in Deiters' lateral vestibular nucleus (Ito and Yoshida,'66; Ito et al.,'66; Allen et al.,'72ab; Ten bruggencate et al.,'72) following direct or

indirect stimulation of the IO usually showed that the background frequency of about 50 spikes per second changed into the expected sequence of an early short-lasting excitatory postsynaptic potential (EPSP) followed by an inhibitory postsynaptic potential (IPSP), the latter lasting about 100 ms. The same sequence of potentials, although with somewhat shorter latencies, can be seen following mossy fiber stimulation (McCrea et al.,'77). The preceding EPSP is sometimes absent (Llinás and Mühlethaler,'88ab), suggesting that the climbing fiber collaterals are not innervating every central nuclei cell. This is in accordance with the observation that the decrease of the activity of the central neurons following destruction of the IO by 3-acetyl pyridine is due to an increased inhibitory effect of the Purkinje cells and not to a deafferentation of the central nuclei neurons from the olivary collaterals (Batini and Billard,'85). Together these data indicate that the olivo-cerebellar fibers mainly exert their effects on the central nuclei cells indirectly through the Purkinje cells (see also Andersson and Oscarsson,'78). The IPSP is often followed by a prolonged (approximately 60 ms) burst caused by disinhibition of the nuclear cells during the climbing fiber pause. The amplitude, latency, and duration of the prolonged depolarization is variable in any one cell, and the number of cells in which an acceleration of the resting discharge can be detected varies between different cerebellar nuclei (Armstrong et al.,'73e; Armstrong,'74; Kitai et al.,'77).

e4. Function of the olivo-cerebellar system

The cerebellum probably coordinates voluntary as well as reflex movements through coactivation of descending paths to alpha-motoneurons for the generation of muscle power, and to gamma-motoneurons for the adjustment of the sensors for muscular position and velocity (Brooks and Thach,'81). In this way, the cerebellum supports posture and motor control, through a tonic action on reflexes and the phasic

triggering of motor programs (Bloedel and Courville,'81).

The climbing fiber system is present in the cerebellum of all vertebrates (Llinás,'85), and cerebella deprived of the climbing fiber system retain only a rudimentary motor coordinator function (Llinás et al.,'75; Demer and Robinson,'82). Several investigators (Wilson and Magoun,'45; Carrea et al.,'47; King,'48; Dow and Moruzzi,'58; Passouant et al.,'65; Murphy and O'Leary,'71; Soechting et al.,'76; Kennedy et al.,'82) have found in cats, rabbits and monkeys that a lesion or destruction of the IO produces disturbances of motor control that closely resemble those produced by ablation of the cerebellum. The types of disorders can be more or less related to the location of the lesions. Apart from general disfunctions like ataxia and hypotonia, lesions of the vermis and the paravermal region produce an abnormality in the sequence of muscle contractions during rapid movements, and dysmetria and tremor during slow movements, whereas lesions of the hemispheres are characterized by delays in movement initiation and in coordination of distal limb movements. It is generally believed that whereas the execution of movements is more controlled by the spinocerebellum, the lateral cerebellum plays a prominent role in the preparation to move (Allen and Tsukahara,'74; Brooks and Thach,'81; Lamarre and Chapman,'86; Ivry et al.,'88).

The major function of the olivo-cerebellar system is probably to influence the transmission of information from the parallel fibers to the Purkinje cells. In several instances it has been found that peripheral or cortical stimulation evoked activity in mossy and climbing fiber pathways converges upon the same Purkinje cells (Provini et al.,'67 and '68; Ekerot and Larson,'80). This is in accordance with the anatomical findings (see part b) that the terminations of mossy fibers in the granular layer are, although less specific than the climbing fibers, also aggregated in sagittal zones, and that some nuclei like the dorsal column nuclei give rise to mossy fibers which project to the same

zones as their related climbing fiber projection. These data are also supported by studies which showed that mossy fibers preferentially excite the Purkinje cells which overlie their focal terminations in the granular layer (Ekerot and Larson,'73 and '80; Llinás,'82; Bower and Woolston,'83). This may be explained by presuming that the ascending parts of the T shaped parallel fibers exert a more important effect on the Purkinje cells than the transversal parts (Llinás,'82). Thus far, the assumption that the medio-lateral topical specificity in mossy fiber systems will be erased by the transversely oriented parallel fiber pathway has not been confirmed in experimental studies; mossy fibers evoked Purkinje cell activity rather follows the same zonal pattern as the climbing fibers.

The precise function of the IO in the cerebellar system remains a controversial issue. The theories on olivary function can be divided into three groups: Those which argue that complex spike discharges control tonic muscle activity (Marchesi and Strata,'71; Colin et al.,'80; Barmack and Simpson,'80; Montarolo et al.,'82; Benedetti et al.,'83; Strata,'85), those suggesting that the climbing fiber system is principally involved in phasic, real time processing in the cerebellar cortex (Llinás and Volkind,'73; Pellionisz and Llinás,'82; Bloedel and Ebner,'85; Pellionisz,'85; Llinás,'89; Bloedel and Zuo,'89), and those proposing that the climbing fiber system plays an important role in motor learning (Marr,'69; Albus,'71; Gilbert and Thach,'77; Ito,'82ab; Ito,'84).

The tonic theory has been promoted mainly by Strata and colleagues. This idea was based on experiments that showed a maintained higher average discharge frequency of complex spikes during non-REM sleep than during REM sleep with its phasic phenomena (Marchesi and Strata,'70 and '71). In further experiments using natural or electrophysiological stimulation of the IO it was shown that the complex spike frequency is, in the long term, inversely related to the following simple spike frequency (cf. the climbing fiber pause, see e3), (Ferini et al.,'70 and '71;

Ghelarducci et al.,'75; Gilbert and Thach,'75; Barmack,'79; Leonard and Simpson,'82; Rawson and Tilokskuchai,'81 and '82). This reciprocal behavior in the complex and simple spike activity was confirmed in other experiments which recorded Purkinje cell activity after irreversible (Colin et al.,'80) and reversible (Montarolo et al.,'81; '82) lesions of the IO. In addition, experimental evidence has become available showing that an altered olivary output actually may exert a tonic effect on muscle activity: 1) Barmack and Simpson ('80) observed a conjugate drift of the eyes toward the side contralateral to the lesion applied to the IO, 2) Boylly ('78;'80) found that repetitive stimulation in the caudal MAO (projecting to the A zone which is involved in posture) influences the tonic activity within the muscles, 3) Batini et al. ('83) found that lesions of the IO resulted in a decrease of the electromyographic activity of the triceps muscles, and 4) Strata et al. ('85) found that destruction of the IO by kainic lesion produced a clear-cut hypotonia. Therefore, it is now believed that the olivocerebellar pathway exerts a tonic enhancing effect on muscle tension (Strata,'85) through a tonic inhibitory effect on the Purkinje cells simple spike discharge.

The argument that the climbing fibre system may be involved in shorter-term processes important for real time processing in the cerebellar cortex has been mainly propagated by Llinás and Bloedel. Llinás proposed that the olive serves as a timing device in the execution of rapid movements. Here (Llinás,'85; Llinás and Yarom,'86; Llinás and Mühlethaler,'88ab), the climbing fiber input is seen as a "real" afferent input which forces the Purkinje cells directly to be active in a burst manner at particular moments in time, instead of having a mere modulatory role as proposed in the tonic or learning theory. Since human reaction-time movements have been reported to be paced by the normal human 10/s physiological tremor (Goodman and Kelso,'83), and since olive discharge has a periodicity at 10/s (Armstrong and Harvey,'66; Crill,'70) that, under harmaline, is dramatically increased

and can drive a 10/s body tremor (see part e2), the inferior olive may serve as the "clock" of the motor system, triggering the onset of rapid movements on the beat of its 10/s rhythm (Llinás and Volkind,'73; Llinás,'84). Bloedel and colleagues suggested that the IO is involved in time processing by exerting rapid short lasting effects on the responses of the Purkinje cells to the parallel fibers. They demonstrated that there is a short-lasting enhancement of Purkinje cell responses evoked by mossy fibre inputs following either spontaneously occurring or naturally activated climbing fibre inputs to the same neuron (see part e3; Ebner and Bloedel,'81ab; Ebner et al.,'83; Ebner and Bloedel,'84; Lou and Bloedel,'86). It was argued that the climbing fibre system regulates synchronously (due to the electrotonic coupling of the olivary cells and the branching of their axons) the gain of a selected group of Purkinje cells to mossy fibre inputs activated by peripheral or descending inputs. A short-term synchronized action of the climbing fibers would synchronize and steepen the onset of the simple spike frequency modulation in the Purkinje cells (Llinás,'89; Bloedel and Zuo,'89; Mano et al.,'89). This synchronization effect of the climbing fiber activation on the simple spike activity could occur when a motor command is required to be transmitted with precise timing as in externally triggered movements (Mano et al.,'89), at the onset of normal ballistic movements (Llinás,'70; de Montigny and Lamarre,'73; Llinás,'84), and possibly even of spontaneous movements (Fukuda et al.,'87). Since Gibson and Chen ('88) showed that direct electrical stimulation of the IO does not produce any movements (except for stimulation in the dorsal cap which evokes eye movements when visual feedback is prevented; see Barmack and Hess,'80b), the IO may rather accelerate a good start than initiate a movement (see also Brooks and Thach,'81).

One of the most widely held theories about olivary function is that the IO provides the cerebellum with an error signal that indicates inadequate motor performance and that this signal is used to correct motor

performance. It was suggested that the olive may be involved in the adaptation of repeated movement in motor learning itself (Marr,'69; Albus,'71; Ito,'72 and '84; Gilbert,'74). This idea is supported by four lines of evidence: (a) Ablation of portions of the cerebellum has eliminated various motor adaptations and has prevented further adaptation. These include adaptation of the vestibulo-ocular reflex (Ito et al.,'74; Robinson,'76), acquisition of the conditioned eye blink reflex (Yeo et al.,'84; McCormick and Thompson,'84; Lavond et al.,'84 and '85), conditioning of leg-flexion responses (Donegan et al.,'83), long-term habituation of the acoustic startle response (Leaton and Supple,'86), and conditioning of heart rate (Lavond et al.,'84). In the paradigm of the classically conditioned eyeblink response (McCormick et al.,'85) and skeletal muscle responses (Steinmetz et al.,'89) indirect evidence was found that the climbing fibre input operates as the unconditioned stimulus while the mossy fibers should transmit the conditioned stimulus. (b) By recording Purkinje cell discharge during adaptation of limb (Gilbert and Thach,'77) or eye (Watanabe,'84) movements in the awake animal it was shown that the olivary firing rate initially increases after applying a new external trigger (which probably results in a conjunction of climbing fiber and mossy fiber activity), but when the animal gradually learns to recognize the trigger and to react with a correct movement the same external trigger does not evoke complex spikes anymore. The Purkinje cell simple spike response appeared to be reduced after the triggering event and remained so even after the decrease of complex spikes. (c) Following the application of conjunctive stimulation of climbing and parallel fibers (see part e3) there is a long-term reduction in the amplitude of Purkinje cell responses evoked by the mossy fibres (Ito et al.,'82; Kano and Kato,'87) or the parallel fibers (Ito and Kano,'82; Rawson and Tilokskulchai,'82; Ekerot and Kano,'85). (d) Injections of B-noradrenergic substances in the flocculus of rabbits affect adaptation of the vestibulo-ocular reflex (VOR) gain (van Neerven et al., in press).

Although the three theories mentioned above are quite different, they are not mutually exclusive. In fact, it could be possible 1) that the low spontaneous olivary firing frequency at rest is part of a tonic control, 2) that this frequency increases synchronously in a specific group of olivary neurons when a particular rapid movement is required (this could be triggered by simple peripheral unexpected events and mediated through the ascending pathways or by more complicated indirectly related external or internal events and mediated through the descending pathways), and 3) that the quality and reaction time of these types of movements, which are correlated with olivary activity, gradually improve after heterosynaptic changes in the cerebellar cortex induced by repeated climbing fiber activity.

It can be concluded that there is agreement on a role of the climbing fiber system in the modification of the response characteristics of ensembles of Purkinje cells and through them, the activity of the central nuclear neurons. Whether these modifications hold for short or long periods of time is still a controversial matter.

e5. Physiology of olivary afferents

e5.1 Introduction

e5.2 Quality of information transmitted by the olivary neurons

e5.3 Inhibitory cerebellar afferents

e5.4 Excitatory descending afferents

e5.5 Somatosensory, teleceptive and vestibular afferents

e5.6 Convergence of inputs

e5.1 Introduction

Physiological studies demonstrated that many afferent systems exert effects on the IO. These effects have been studied mostly by recording climbing fiber responses at the cerebellar cortex but also directly by microelectrode recordings within the IO. Under natural circumstances olivary cells can be activated 1) after presenting the animal

unexpected sensory stimuli, 2) at the beginning of externally triggered voluntary movements which need to be performed under a strict time constraint, and 3) during the performance of novel motor tasks (see also part e.4). In addition, olivary cells are activated following electrical stimulation of peripheral and cranial nerves, the spinal funiculi, certain areas of the cerebral cortex, and several midbrain structures, while they can be inhibited by stimulation of afferents from the cerebellar nuclei, or by activation of specific somatosensory and vestibular afferents.

Below, it will be discussed how the olivary neurons transmit their information (part e5.2), what the effects are of an activation of the cerebellar (part e5.3) and descending (part e5.4), and somatosensory, teleceptive and vestibular (part e5.5) pathways, and whether these systems converge in the IO and/or at a preolivary level (part e5.6).

e5.2 Quality of information transmitted by the inferior olive

The firing frequency of an afferent system, is usually related to the strength of the stimulus (Gibson and Gellman,'87). However, following stimulation of their afferents the spontaneous and irregular firing rate of olivary neurons (approximately 1-2 Hz; Eccles et al.,'67), increases rhythmically and phasically*⁵ to a maximum of 10 Hz. Therefore, olivary neurons are not very potent to discharge parametrically as a continuous function of the input stimulus (Murphy et al.,'73; Rushmer et al.,'76; Gellman et al.,'83 and '85; Gibson and Gellman,'87; Mano et al.,'89). Weak correlations have so far only been described for neurons in the dorsal cap of which the activity was more or less related to the speed of the visual stimulation (Maekawa and Simpson,'73; Simpson and Alley,'74; Alley et al.,'75; Barmack and Hess,'80; Simpson et al.,'81), and for neurons in the beta nucleus which responded in phase with the position of the sinusoidal vestibular roll stimulus or with the velocity of this stimulus (Barmack et al.,'89).

An ensemble of olivary neurons seem to be more capable of mediating information. It has been observed that the firing of olivary cells is locked in time to the onset of a peripheral stimulus when the rising phase of such a stimulus is fast or to the onset of a descending command when performed under a strict time constraint. Gibson and Gellman ('87) showed that olivary cells fire directly after passive limb displacements of a high velocity whereas their moment of firing is variable following slowly induced changes. Similarly, a perturbation of locomotion, which means a rapid peripheral change evoking a fast reaction movement, has been found to increase the synchronicity of olivary firing (Bloedel and Zuo,'89). Furthermore, it was shown that olivary neurons of animals, which had been learned to make specific wrist movements following visual stimuli, respond synchronously at a moment related to the onset of movement, when these movements have to be made as quickly as possible after the visual stimulating event (Mano et al.,'89). Thus, it seems that the level of synchronicity in olivary firing (see also Sasaki and Llinás,'85) carries information about the velocity of peripheral changes or about the timing of movements, whereas the firing of individual olivary neurons indicate the presence but not the intensity of the afferent input. Whether the afferent systems modify the synchronism of the olivary discharge by increasing the electrotonic coupling or solely by simultaneous postsynaptic effects upon different olivary neurons, has not been elucidated yet.

*Note*². An exception to this general response behaviour of olivary neurons seems to be the tonic activity of olivary neurons which can be evoked by noxious stimulation in contrast to normal tactile stimulation (Ekerot et al.,'85b), or by displacing a limb in an unnatural upper static position (Kolb and Rubia,'80).*

e5.3 Inhibitory cerebellar afferents

Hesslow and Andersson found evidence that the cerebello-olivary projection in cat mediated via the brachium conjunctivum is inhibitory (Hesslow,'86; Andersson and Hesslow,'86 and '87abc; Andersson et al.,'88 and '89). Their studies were mainly restricted to the climbing fiber projections to the C1 and C3 zone which originate from the rostral DAO, but in some cases similar results were obtained for the climbing fiber projections from the rostral MAO (they did not obtain direct evidence for an inhibitory nucleo-olivary projection to the caudal DAO and MAO). When peripheral nerve or olive stimulation was preceded at long intervals (>35 ms) by weak electrical stimulation of an ipsilateral mesencephalic area close to the brachium conjunctivum, climbing fiber responses could be virtually abolished (Hesslow,'86). In addition, it was found that inhibition of climbing fiber activity after a conditioning stimulation of a peripheral nerve can no longer be produced after a lesion of the brachium conjunctivum (Andersson and Hesslow,'86; Andersson and Hesslow,'87a) while injections of the GABA-receptor blocker bicuculline methiodide into the IO reversibly blocked the post-conditioning inhibition (Andersson et al.,'88). Recently, it was suggested that the cerebellar nuclei exert their inhibition to the DAO through a relay nucleus rather than through the direct cerebello-olivary fibers (Andersson et al.,'89). Lesions of this relay nucleus, from which no antidromic responses could be recorded in the brachium conjunctivum, abolished the inhibition of climbing fiber responses by brachium conjunctivum stimulation.

The climbing fiber projections to the B, C1 and C3 zones can be subdivided in microzones (Andersson and Oscarsson,'78). These small subzones with a wide of about 200 μ m can not be identified anatomically but they are characterized by the set of limbs from which they can be activated, and by the latency of the corresponding climbing fiber responses. Adjacent cerebellar microzones

show mutual inhibition (with a short latency of about 15 ms) as it was demonstrated following subsequent stimulations of different peripheral nerves (Andersson,'84). This inhibition is strongest between olivary cells which project to an adjacent microzone, and it is probably due to post-synaptic inhibition within the IO itself. If this inhibition is derived from the cerebellar nuclei, this would mean that there is a subtle mismatch of the reciprocal connections between the olivary and central nuclei cells. However, according to the physiological results from Andersson ('84), the mutual inhibition could just as well be derived from inhibitory interneurons within or nearby the IO, or from inhibitory neurons of the dorsal column nuclei projecting to the IO, and/or from a neuronal interaction of coupled olivary cells.

According to Andersson et al. ('88) the inhibitory nucleo-olivary cells could serve several functions. The nucleo-olivary pathway may be part of a negative feedback system regulating the tonic inhibitory control which the climbing fibres are believed to exert on the simple spike firing rate (Colin et al.,'80; Montarolo et al.,'82; see part e4).

A second suggestion pertains to the possibility that the parallel fibre-Purkinje cell synapses are sites of motor learning (Albus,'71; Ito et al.,'82; Ekerot and Kano,'85; see part e4). It was demonstrated that the climbing fibre input tends to depress those parallel fibre synapses which have just been active (long lasting depression, see part e3). In order to ensure that the magnitude of this depression is appropriate, the inhibitory cerebello-olivary feedback loop might be important. Such a feed-back mechanism could explain the blocking phenomenon in classical conditioning (Kamin,'67). When a motor response has been firmly conditioned to one stimulus, for example a tone, and a second conditioned stimulus, for example a light, is then presented simultaneously with the tone, conditioning to the second stimulus is very inefficient. If instead, only the second conditioned stimulus is paired with the unconditioned stimulus, conditioning proceeds normally.

A third possibility, not incompatible with the previous suggestions, is that the nucleo-olivary pathway is involved in the gating of olivary transmission. According to the "error signal" hypothesis of Oscarsson ('80; see also Ito,'84), the climbing fibres signal to the cerebellar cortex that some movement has been or is being incorrectly performed. The empirical findings, that climbing fibres discharge in response to passive tactile stimulation of the paw, but not when such a stimulation results from an active movement (Armstrong et al.,'82; Gellman et al.,'85; Andersson and Armstrong,'87) lend support to this hypothesis. The nucleo-olivary projection might play a crucial role in deciding whether a movement was expected or not (cf. role rubro-spinal pathway, part e5.5).

A fourth hypothesis was provided by the studies of Llinás and Sotelo. As mentioned above (part e2) olivary cells are electrotonically coupled and this coupling can be modulated by GABA (Bower and Llinás,'83; Sasaki and Llinás,'85; Lang et al.,'89). The observations that cerebellar (King et al.,'76; Angaut and Sotelo,'87) and GAD-positive terminals (Sotelo et al.,'87) are associated with gap junctions in the inferior olive, suggest that the nucleo-olivary fibers are engaged in the modulation of electrotonic coupling of olivary neurons, rather than exerting a classical inhibitory effect. The results of Andersson and colleagues of a strong inhibition of the inferior olive, as described above, do not necessarily exclude such a mechanism. The high frequency climbing fibre activation employed in their experiments produced a very strong activation of the interposito - olivary cells (Andersson and Hesslow,'87b). It is possible, therefore, that these experiments were not well suited for revealing more subtle effects on the inferior olivary neurons.

e5.4 Excitatory descending afferents

Olivary neurons are probably not clearly activated during normal movements. Discharges from IO neurons have been recorded at preferred times during the step cycle of the

walking cat (McElligot,'76, Boylls,'80, and Udo et al.,'81), but other studies aimed at recording olivary discharges during normal locomotion failed to confirm these findings (Brooks and Thach,'81; Armstrong et al.,'82; Gellman et al.,'85). However, when the animal performs a voluntary movement under a strict time constraint olivary cells projecting to the intermediate and lateral hemisphere, and therefore most likely located in the PO and rostral MAO, can be activated (Mano et al.,'89). Several studies lend support to this hypothesis. A phasic increase in climbing fiber responses can be observed after a triggering stimulus and before the subsequent reaction movement in several paradigms: 1) Prompt arm movement triggered by a light signal (Thach,'70), 2) startle responses to loud acoustic or intense flash stimuli (Mortimer,'73 and '75), 3) moving back the handle displaced from a holding position by external load (Gilbert and Thach,'77), 4) adjusting movement during locomotion when it is mechanically disturbed (Matsukawa and Udo,'85; Gellman et al.,'85; Andersson and Armstrong,'86; Gibson and Gellman,'87; Bloedel and Lou,'87; Armstrong and Andersson,'87; Kim et al.,'87), and 5) following targets by wrist movements (Mano et al.,'86). In these experiments, animals were required to initiate the movement as soon as possible in response to an external trigger stimulus. According to the figures presented by Mano et al. ('86 and '89) olivary fibers were activated about 200 ms after the external trigger and about 125 ms before the actual movement, while Llinás ('87), even found positive correlations of climbing fiber activities 10-15 ms prior to phasic movements. On the other hand, phasic climbing fiber responses can not be observed during self paced movements (Mano et al.,'86), rapid alternating arm movements (Thach,'68), alternate pushing movements (Mano,'74), a precision grip by thumb and forefinger (Smith and Bourbonnais,'81), and non-disturbed locomotion (Armstrong et al.,'82; Gellman et al.,'85). In these later paradigms, the timing of the movement was not a prerequisite for the performance of the animal.

Most, if not all, of the olivary responses found prior to the reaction movements are probably mediated by the descending afferents from cortical areas since most of them were triggered by complex external events. Pathways of the cerebral cortex to the IO have been shown in many physiological studies (Jansen and Fangel,'61; Armstrong and Harvey,'66 and '68; Provini et al.,'68; Andersson et al.,'87b). The dominating cortical projection to the IO with probably the shortest latencies (Kato et al.,'88) originates in the pericruciate sensorimotor cortex (Armstrong,'67; Jansen,'57; Miller et al.,'69a), especially in the posterior but also in the anterior sigmoid gyri (motorcortex), (Andersson and Eriksson,'81; Andersson and Nyquist,'83; Andersson et al.,'87b; Kato et al.,'88). In addition, electrical stimulation of cerebral cortical areas like the orbital and anterior ectosylvian gyri (Jansen,'57; Kato et al.,'88), and auditory and visual receiving areas (Snider and Eldred,'51 and '52), the second somatosensory area (SII), and area 5 in the parietal cortex (Andersson and Eriksson,'81; Andersson and Nyquist,'83; Andersson et al.,'87b) were found to evoke climbing fiber responses. According to the termination zones of these climbing fiber responses, which were predominantly contralateral, the cerebral cortical input is present in all olivary subnuclei. Apart from the pericruciate projection, the PO/D and rostral MAO/C2 complex receive especially a powerful input from the parietal cortex and SII respectively (Andersson et al.,'87b). Convergence of pathways from different cerebral areas on to the same olivary cell has been found for several areas (Sedgwick and Williams,'67; Andersson et al.,'87b).

The cortical input to the IO is relayed partly through nuclei in the lower brainstem like the dorsal column nuclei (Oscarsson,'69b; Andersson,'84) but primarily through higher centres in the midbrain. Stimulation in the nucleus of Darkschewitsch and surrounding areas in the mesodiencephalic junction produced climbing fiber responses in the cortex of the paramedian lobule and the intermediate part of the anterior lobule (Miller et

al.,'69b; Appelberg,'67; Appelberg and Molander,'67; Appelberg and Jeneskog,'73; Jeneskog,'74, and '81; Jeneskog,'87; Oka,'88), the caudal vermis (Jeneskog,'81 and '83), or the flocculus (Maekawa and Simpson,'73). The mean latency from the Darkschewitsch region to the rostral MAO/C2 complex was 11 ms (Jeneskog,'87; see also Ruigrok et al., part a of Chapter IV). Stimulation of the caudate nucleus (Sedgwick and Williams,'67) was also found to evoke predominantly contralateral climbing fiber responses but has not been confirmed since.

No specific hypotheses have been proposed for the function of the descending olivary inputs. However, regarding the location of the cortical and midbrain areas which can evoke climbing fiber responses, and considering the events which evoke activity in the olivary subnuclei connected with these regions, the information mediated through this projection to the IO is probably involved in the processing of complex sensory stimuli and their related motor commands.

e5.5 Somatosensory, teleceptive and vestibular afferents

SOMATOSENSORY AFFERENTS. The effective stimuli of the olivary neurons include teleceptive and vestibular (see below), and autonomic (Widén,'55; Newman and Paul,'69), but primarily somatosensory activation (for reviews see Miller and Oscarsson,'70; Oscarsson,'67; Oscarsson,'73, Armstrong,'74; Ekerot et al.,'79; Andersson et al.,'87b). The studies using natural stimuli showed that olivary cells are activated after the onset, but also under specific conditions, at the offset of peripheral stimuli (Eccles et al.,'72ab; Rushmer et al.,'76; Gellman et al.,'83 and '85). The effective somatosensory stimuli, which excited primarily the cutaneous receptors, included pinching skin and deep tissues (Thach,'67; Oscarsson,'68 and '69a), taps against the footpads (Larson et al.,'69a), light puffs of air on hairy skin (Eccles et al.,'72ab), vibration, stroke, light touch and slip (Gellman et al.,'85), electric shocks (Gellman et al., '83), and differential sti-

mulation of cutaneous A B- and C-fibres (Ekerot et al.,'85ab). Proprioceptive effects were obtained following stimulation of muscle afferents (Armstrong et al.,'68; Ishikawa et al.,'72ab), dynamic stretch, isometric contraction or excitation of Golgi tendon receptors but not after isotonic contraction (Faber et al.,'71; Ishikawa et al.,'72ab; Murphy et al.,'73), or passive movement or rotation of a limb especially when performed with a change in acceleration (Rushmer et al.,'76; Kolb and Rubia,'80; Gellman et al.,'85).

One of the most comprehensive studies was performed by recording directly in the IO following somatosensory stimulation in the anaesthetized, decerebrated (Gellman et al.,'83) or awake (Gellman et al.,'85) cat. In these studies, it was found that the majority of the olivary cells responded to somatosensory stimuli. In all subnuclei a mediolateral somatotopy was observed with the face and forelimb represented medially and the hindlimb laterally.

In the DAO, all inspected neurons were responsive to somatosensory stimuli (with rather short latencies, 10 - 20 ms). Cells with cutaneous input predominated in the rostral part, whereas those with exclusively proprioceptive input were more common in the caudal region of this subnucleus. The receptive fields of the DAO cells were usually restricted to a small part of an ipsilateral limb, together revealing a refined map of the entire contralateral body surface.

In the MAO, 88% of the cells reacted to somatosensory stimulation (with long latencies 25 - 40 ms). The receptive fields of individual MAO neurons were more complicated and larger, sometimes including all four of the limbs (see also Leicht et al.,'72; Armstrong,'74). They were mostly affected by proprioceptive inputs only. These proprioceptive neurons were activated when a limb or set of limbs was unexpectedly displaced in a particular direction (see also Kolb and Rubia,'80). Different from the other subnuclei which had purely excitatory fields, the caudal MAO showed spatial patterns of excitation and inhibition on somatosensory

stimulation. This inhibition might be derived from GABAergic neurons in the cuneate nucleus (see part d, this Chapter).

Of the PO cells 74% were responsive at the onset of unexpected somatosensory stimuli (also with rather long latencies). The receptive fields of the PO were also rather large. Cells with cutaneous input predominated in the POvl, whereas those with exclusively proprioceptive input were more common in the POdl.

The somatosensory (but also some autonomic) input to the IO is mediated by cranial and spinal afferents. In various sorts of animals stimulation of several cranial nerves was found to produce climbing fiber responses. These include the lingual (Bowman and Combs,'69) and trigeminal nerve (V) (Baker et al.,'72), facial nerve (VII) (Widen,'55), the glossopharyngeal nerve (IX) (Hanamori et al.,'87), and the vagal nerve (N X), (Lam and Ogura,'52; Van Gilder and O'Leary,'71; Albert et al.,'86; Tong et al.,'89).

Most studies of the somatosensory inputs are concerned with the spinal afferents. There is a limited degree of modality specificity of the spino-olivary pathways (Eccles et al.,'68ab; Eccles et al.,'71; Armstrong,'74). Each funiculus in the spinal cord carries this information to specific olivary subnuclei and corresponding cerebellar termination zones (Oscarsson,'68; Oscarsson,'69ab; Armstrong et al.,'73b; Armstrong,'74; Oscarsson,'80; Andersson et al.,'87b). There are five of such spino-olivo-cerebellar paths. In agreement with the variability of the receptive fields of individual olivary neurons described above, each path deals with its own set of limbs or part of a limb, and some paths relay only ipsilateral, whereas others transmit bilateral information. The ventral funiculus spino-olivary pathway (VF-SOCP) provides a direct input to the IO whereas the others contain relays in other centres. This confirms the finding that the mean latencies are shortest in the DAO (Gellman et al.,'83), which is innervated by the VF-SOCP. The indirect somatosensory spinal pathways are probably relayed through

the dorsal column nuclei (Oscarsson,'69a; Andersson,'84) and other, as yet unidentified, higher brain areas (Larson et al.,'69ab; Armstrong,'74; Gellman et al.,'83 and '85).

The cerebellar termination zones of the SOCP's are longitudinally organized, most of them covering several of the anatomical zones (see Figure 1, part a) and overlapping with one or more of the other physiologically identified zones. This spatial overlap extends to the single unit level so that one olivary cell and one Purkinje cell can be excited via two distinct SOCP's. This shows that the different spino olivary paths converge onto the same olivary cells. According to their fine receptive fields, the major zones innervated by the olivary areas which receive rather direct peripheral inputs (i.e. the A, B, C1 and C3 zone innervated by the caudal MAO and DAO, see part b) can be subdivided into microzones with a width of 200 μ m or less (Andersson and Oscarsson,'78; Oscarsson,'79; Bower and Llinás,'83; Andersson et al.,'87b).

Several functions have been suggested for the spino-olivary system. Armstrong ('74) suggested that the spino-olivo-cerebellar paths from the limbs interact with mossy fiber paths to provide a predictive control system for gait. Others assumed that the IO monitors and compares the commands from higher motor commands mediated by the descending systems, the activity these commands evoke in the lower spinal center, and the resulting movement (Miller and Oscarsson,'70; Oscarsson,'73 and '80). By comparing these various pieces of information, the IO would detect perturbations of the commands introduced in the lower center by reflex activity, and perturbations of the evolving movement due to unexpected changes in load or resistance. However, the spino-olivary transmission of "expected information" (such as the end of a step when the animal touches the floor) is probably inhibited at a preolivary level by descending connections from the magnocellular red nucleus (Gibson and Gellman,'87; McCurdy et al.,'88; Houk et al.,'88) and/or the cerebral cortex (Leicht et al.,'72 and '73; McCurdy et al.,'88). Thus, it seems more likely that comparing processes

such as described above occur at a preolivary level (see also below, convergence of inputs), and that the IO relays information from the spinal cord which has already been "filtered" and recognized as unexpected information (cf. role cerebello-olivary afferents as suggested by Andersson, part e5.3).

TELECEPTIVE AND VESTIBULAR INPUT. Auditory, visual and vestibular stimulation are known to evoke olivary activity. Auditory stimulation produces responses in the medial MAO (Gellman et al., '83) and climbing fiber responses in the paraflocculus (Azizi et al., '81). Light flashes evoke responses in the dorsal cap (Barmack and Hess, '80; Gellman et al., '83) and large climbing fiber potentials on the vermis (Buchtel et al., '72) and flocculus (Maekawa and Simpson, '73). Floccular climbing fiber activity mediated through the dorsal cap can be modulated in relation to speed and direction of movement of large patterns over the visual field (Simpson and Alley, '74; Waespe and Henn, '81; Blanks and Precht, '83; Watanabe, '84; Stone and Lisberger, '86). In the dorsal cap three zones have been identified which respond differentially to optokinetic stimuli moving in particular planes of physical space (Simpson et al., '81; Leonard et al., '88; Simpson et al., '89; see also Graf et al., '88). The preferred axis of each of these three zones are closely aligned with those of the semicircular canals of the vestibular apparatus. However, the neurons in the dorsal cap are not sensitive to vestibular stimulation (Barmack et al., '89). Caloric, electrical and natural stimulation of the vestibular labyrinth itself evokes action potentials in and near the Beta nucleus (Robinson, '87) and gives rise to climbing fiber responses in the cerebellum (Ferin et al., '71; Precht et al., '76ab; '77; Ghelarducci et al., '75). The cells of the beta nucleus are very sensitive to low frequency yaw oscillations in a specific direction, but do not signal quantitatively the magnitude of movement, speed or acceleration (Robinson et al., '88). In indicating the presence but not the speed of movement, yaw-sensitive olivary cells resemble the somatosensory cells. Neurons in the nucleus

Beta, which are sensitive to vestibular stimulation about the longitudinal axis, are excited when the animal (rabbits) is rolled onto the side which is contralateral to the recording site, and inhibited when the rabbit is rolled ipsilaterally (Barmack et al., '89). The vestibular receptive cells in the IO are not responsive to somatosensory or visual stimuli (Gibson and Gellman, '87; Barmack et al., '89) indicating that these afferent systems do not converge onto the same olivary cells.

e5.6 Convergence of inputs

Different spinal pathways or pathways from different cerebral areas converge on to the same olivary cell (see above). More important is the finding that the olivary neurons in each subnucleus receive a convergent input from spino-olivary pathways on one hand, and cortico-olivary pathways on the other (Sedgwick and Williams, '67; Miller et al., '69ab; Crill, '70; Leicht et al., '73; Andersson and Eriksson, '81; Andersson and Nyquist, '83; Andersson et al., '87b). The laterality of these connections is in agreement with this general pattern: The olivary neurons in the rostral MAO and caudal DAO, which receive a bilateral peripheral input also receive a bilateral cortical input, and neurons in the other subnuclei, which receive only an ipsilateral peripheral input, receive a strictly contralateral cortical input (Andersson et al., '87b).

With respect to the convergence of descending and ascending afferents there is a discrepancy between the anatomical results, which suggest that the descending cortical and ascending sensory input to the olive are largely segregated (see part b), and the physiological results which indicate that each olivary subdivision receives both. The conclusion should be that most of the convergence of descending and ascending afferents occurs at a preolivary level. For the DAO, which receives a direct input from the periphery, this convergence occurs at the level of the dorsal column nuclei, which receive both peripheral and cortical afferents (Andersson, '88). The cortical input to the PO and MAO apparently is mediated by the midbrain. The

precise pathway of the indirect peripheral input to the PO and rostral MAO is presently unknown, but this information could be mediated through midbrain areas as well, since the spinal cord (Björkelund and Boivie,'84ab; Yezielski,'88) and the dorsal column nuclei (Wiberg and Blomqvist,'84ab) are known to project to the midbrain including the nucleus of Darkschewitsch (see also Larson et al.,'69ab).

Besides the preolivary convergence of the descending and ascending inputs, it should be stressed that the entire IO receives a strong GABAergic innervation from the cerebellar nuclei and to less extent from other hind-

brain areas (see Figure 2 part b, and see part d). Therefore, the excitatory inputs converge entirely with these inhibitory inputs in the IO. In this respect, it may be relevant to point out that in addition the cerebellar nuclei project to the midbrain and thalamus. The first area provides in its turn an input to the olive, whereas the thalamus may be able to induce olivary responses through the cortical connections, which again may involve the midbrain. In conclusion, it would appear that olivary responses are governing and are being governed by many neural loops, which all play a specific role in olivary functioning.

f. Methods combining anterograde tracing, immunocytochemistry, and/or intracellular labeling at the ultrastructural level

- f1. Introduction
- f2. Individual methods
- f3. Combination methods

f1. Introduction

In the past decades many new techniques have been introduced to the study of the anatomy of the brain at the ultrastructural level. These include different axonal tracing methods, immunocytochemical techniques to identify certain substances in histological sections, and staining methods for entire neurons. Most of these methods have also been applied to study the afferent systems, the neurotransmitters, and cellular morphology of the IO (see part c).

In the present study an attempt was made to combine different methods in the same animal. These special combinations have not been used before, neither in any ultrastructural study of the IO nor for the study of other regions of the CNS. WGA-HRP anterograde tracing was combined with postembedding GABA-immunocytochemistry (Chapter II), WGA-HRP anterograde tracing with (3H)leucine anterograde tracing (Chapter III), and intracellular HRP labeling with postembedding GABA-immunocyto-

chemistry (Chapter IV). Below, different methods for identifying structures at the electron microscopical level will shortly be reviewed (for details see Holstege,'89). The three combination techniques will be compared to other, currently available combinations.

f2. Individual methods

TRACING METHODS. Up to the seventies the axonal degeneration was the most important tool for tracing connections in light and electron microscopical studies (Nauta and Gyax,'57; Gray and Hamlyn,'62; Colonier,'64; Fink and Heimer,'67; Lieberman,'71). Modern axonal tracing methods make use of the naturally occurring transport mechanisms in the nerve cell and therefore respect its integrity. The most widely used substances for ultrastructural anterograde and retrograde axonal tracing are the enzyme horseradish peroxidase (HRP) often conjugated to wheat germ agglutinin (WGA), and the tritiated amino acids like 3Hleucine

(Holstege and Dekker,'79; Holstege and Vrensen,'88; Holstege,'89). Other substances used for retrograde tracing at the EM level are tritiated monoamines and proteins (for review Cuénod and Streit,'83), gold particles coupled to WGA-HRP (Menetrey and Lee,'85), and bacterial toxins like Tetanus and Cholera Toxin (Schwab and Thoenen,'76; for review Trojanowski,'83; Sawchenko and Gelfen,'85). Plant lectins like phaseolus vulgaris leucoagglutinin (Pha-L), (Wouterlood and Groenewegen,'85; van der Want et al.,'89; Rossi et al.,'89) can also be identified at the ultrastructural level. Because Pha-L is taken up by a limited number of cells which become completely stained including their spines, dendrites, soma, axon and terminals, this lectin can be used for anterograde tracing but also for intracellular labeling.

IDENTIFICATION OF NEUROTRANSMITTERS. The first neurotransmitters were chemically identified at the light microscopical level by means of the histofluorescence method for monoamines (Falck et al.,'62). Identification of neurotransmitters at the ultrastructural level became possible after the development of immunocytochemical methods. These transmitters, their synthesizing enzymes or their receptors were identified by means of labeled antibodies (Coons,'58; Gelfen et al.,'69). The antibodies can be directly or indirectly coupled to HRP or gold-substituted silver peroxidase (Liposits et al.,'85; van den Pol and Gorcs,'86), gold particles with various diameters (Varndell and Polak,'84), silver-intensified gold (van den Pol,'85), Uranium (Sternberger et al.,'65), ferritin (Morris and Saelinger,'82), or radioactive molecules (Larsson and Schwartz,'77; Cuello et al.,'82; Alonso,'86; for review see Polak and Varndell,'84; Bosler et al.,'86). The tissue is exposed to these labeled antibodies before (pre-embedding) or after (post-embedding) it is embedded in plastic, or even as frozen (non-embedded) ultrathin sections (for review see Pelletier and Morel,'84). Neurotransmitters can also be identified at the ultrastructural level by a non-immunocytochemical method which is based upon the presence of a high affinity uptake mechanism

in certain terminals. This mechanism only occurs for particular neurotransmitters like the monoamines and certain amino acids. When tritiated neurotransmitters are applied to the brain either in vivo or in vitro, the structures which are provided with such an uptake mechanism can be labeled by autoradiographical methods (for review see Descarries and Beaudet,'83; Bosler et al.'86). For the identification of catecholaminergic terminals it is also possible to inject 5-hydroxydopamine (Ajika and Hökfelt,'73). This substance is taken up by neurons with an uptake mechanism for these neurotransmitters and precipitates within the cell, resulting in an ultrastructural visualization without any necessary intermittent labeling step.

INTRANEURONAL LABELING. The morphology of light microscopically identified neurons including all their processes can be studied in the electron microscope (EM), following silver impregnation according to Golgi (Somogyi et al.,'79) and after impregnation with Pha-L (Wouterlood,'86). The most complete staining of neurons is obtained by intracellular injection of different substances such as cobalt (Pitman et al.,'72; Gillette and Pomeranz,'73), Procion brown (Christensen,'73), HRP (Muller and McMahon,'76; Snow et al.,'76; Hanker et al.,'77; Gilbert and Wiesel,'79), or Lucifer yellow (Maranto,'82). This latter dye can be visualized in the EM by means of a photo-oxidation reaction (Maranto,'82; Sandel and Masland,'88) or an immuno reaction (Taghert et al.,'82; Einstein,'88).

f3. Combination methods

Most of the ultrastructural methods mentioned above have been combined with one another to label multiple profiles of a different identity in the same ultrathin section (for summary, see Table 1, p.37).

TRACING-TRACING. In some ultrastructural studies different tracers were combined in the same animal. Multiple retrograde labeling at the EM level is possible by using gold particles (coupled to a WGA-

HRP conjugate) with different sizes (Menetrey and Lee,'85). This method can be used to label different types of neurons but also for demonstrating collateralization of a single type of neuron. In order to determine the presence of contacts between identified terminals and neurons, retrograde tracing of HRP can be combined with anterograde axonal degeneration (Somogyi et al.,'79; Nakamura et al.,'83) or with anterograde axonal tracing of 3Hleucine (Dekker,'81; Holstege and Kuypers,'87ab). Similarly to the latter combination two methods of anterograde tracing can be combined: Anterograde tracing of WGA-HRP with that of 3Hleucine in (Chapter III).

TRACING-TRANSMITTER. The combination of immunocytochemistry with an axonal tracing method at the ultrastructural level has been used in several studies (see Table 1). Immunocytochemistry can be combined with retrograde tracing of HRP (Ruda,'82; Nunes Cardozo and van der Want, in press), WGA (Luppi et al.,'86) and tritiated serotonin (Araneda et al.,'86). The combination of immunocytochemistry with anterograde axonal tracing by means of degeneration (Somogyi et al.,'79), autoradiography (Sumal et al.,'83) or Phaseolus (Freund and Antal,'88; van der Want et al., personal communication) has also been used. However, none of these methods seems very potent to determine both the origin and neurotransmitter of the same terminals in single ultrathin sections. In Chapter II, such a single section technique will be presented. It consists of a combination of WGA-HRP anterograde tracing with postembedding GABA-immunocytochemistry.

TRACING-CELL. In order to study specific synaptic inputs on cells with identified morphological and possibly also physiological characteristics, anterograde degeneration has been combined with intracellular labeling of HRP (Maxwell et al.,'84), Phaseolus (Wouterlood,'86), or Golgi-silver material (Somogyi et al.,'79; Cipolloni and Keller,'89). Somogyi and colleagues ('79) and Cipolloni and Keller ('89) even succeeded in obtaining a triple labeling by

adding respectively retrograde tracing of HRP and postembedding immunocytochemistry to the above combinations. Intracellular labeling of HRP combined with retrograde tracing of HRP has also been achieved (Maxwell et al.,'85; Maxwell and Koerber,'86).

TRANSMITTER-TRANSMITTER. In many ultrastructural studies two different neurotransmitters have been identified in the same neuronal structure or in different pre- and postsynaptic structures. Most of the various combinations of two immunocytochemical techniques performed so far, suggest that intraneuronal double labeling for identifying the coexistence of two neurotransmitters is difficult or even impossible to obtain when one of the methods is an HRP preembedding technique and the other uses labeling with ferritin (Roth and Binder,'78), postembedding gold or a silver intensification (van den Pol,'85; van den Pol and Gorcs,'86). This incompatibility is probably due to a masking effect by the HRP reaction product. However, when the preembedding HRP/DAB incubation is preceded by immunocytochemical labeling with small gold particles of a diameter of 5 nm, double labeling is possible (Triller et al.,'85). Another method for obtaining intraneuronal double labeling of two different transmitters is provided by the combination of the HRP preembedding immuno technique with uptake autoradiography (Pelletier,'83; Descarries and Beaudet,'83; Weiler and Ball,'84; Priestly,'84; Pickel and Beaudet,'84; Bosler et al.,'86) or by labeling each neurotransmitter with gold particles of a specific size (Bendayan,'82; Tapia et al.,'83; Varndell and Polak,'84).

All these combinations allow the combined labeling of different pre- and postsynaptic structures of different chemical identities. This also holds true for the combination of uptake of 5-hydroxydopamine with uptake autoradiography or immuno-HRP (Nakada and Nakai,'85).

TRANSMITTER-CELL. Studies combining cellular labeling with immunocytochemistry are relatively scarce. Somogyi combined Golgi impregnation with three

different techniques of neurotransmitter identification: 1) uptake of tritiated GABA (Somogyi et al., '81), 2) preembedding peroxidase (HRP) immunocytochemistry using an antibody directed against the GABA synthesizing enzyme glutamic acid decarboxylase (GAD) (Somogyi et al., '83), and 3) postembedding GABA-immunocytochemistry using gold particles (Somogyi et al., '85; Somogyi and Hodgson, '85). The first combination procedure, however, is not reliable since it was found in the monkey visual cortex that not all of the neurons accumulating (3H)GABA were immunoreactive to GABA (Kisvárdy et al., '84). Freund and colleagues ('85) combined postembedding GABA-immunocytochemistry with intracellular labeling of HRP. In this study the immunocytochemistry was performed on

semithin sections by means of the peroxidase method. This scarcely allows a continuous serial analysis through large parts of the labeled cell. Therefore, intracellular injection of HRP was combined with postembedding immuno gold staining of the GABAergic molecules allowing both physiological, morphological, and immunocytochemical identification and serial analysis (Chapter IV).

CELL-CELL. This technique allows the separate identification of two differently labeled individual neurons in the same section. For this purpose intracellular HRP labeling of a single identified neuron can be combined with intracellular injections of Lucifer Yellow (Maranto, '82), with Golgi staining (Freund et al., '85), and probably with cellular degeneration (Chapter IV).

Table 1 (on page 37). Summary of different ultrastructural combination techniques performed in the CNS providing multiple visualization in one ultrathin section (numbers refer to references).

References represented in the Table (* indicate techniques which are presented in this thesis)

- | | |
|--|----------------------------------|
| 1. de Zeeuw et al., in press | 17. Triller et al., '85 |
| 2. de Zeeuw et al., '88 | 18. van den Pol, '85 |
| 3. Dekker, '81 | 19. Descarries and Beaudet, '83 |
| Holstege and Kuypers, '87 | Weiler and Ball, '84 |
| 4. Sumal et al., '83 | Priestly, '84 |
| 5. Somogyi et al., '79 | Bosler et al., '86 |
| Nakamura et al., '83 | 20. Somogyi et al., '83 |
| 6. Hunt et al., '80 | 21. Doerr-Schott and Lichte, '84 |
| Leranath and Frotscher, '83 | Beauvillain et al., '84 |
| 7. Maxwell et al., '84 | 22. Bosler et al., '86 |
| 8. Wouterlood, '86 | 23. Freund et al., '85 |
| 9. Somogyi et al., '79 | 24. Morris and Saelinger, '82 |
| 10. Freund and Antal, '88 | Doerr-Schott and Lichte, '84 |
| van der Want et al., personal | 25. Bendayan, '82 |
| communication | Tapia et al., '83 |
| 11. Ruda, '82 | Varndell and Polak, '84 |
| Luppi et al., '86 | 26. de Zeeuw et al., submitted |
| 12. Nunes Cardozo and van der Want, in | 27. Maranto, '82 |
| press | 28. Nakada and Nakai, '85 |
| 13. Maxwell et al., '85 | 29. Menetrey and Lee, '85 |
| Maxwell and Koerber, '86 | 30. Cipolloni and Keller, '89 |
| 14. Araneda et al., '86 | 31. Somogyi and Hodgson, '85 |
| 15. van den Pol, '85 | 32. Somogyi et al., '81 |
| van den Pol and Gorcs, '86 | |
| 16. Alonso, '86 | |
| Cuello et al., '82 and '83 | |

Aim	Techniques	Code	C1a	C1b	C1c	C1d	C2a	C2b	C2c	N1a	N1b	N1c	N1d	N2a	N2b	N2c	N3a	N3b	M1a	M1b	M1c	M2a	M2b		
Connection	Anterograde tracing	WGA/HRP (C1a)		1*												2*									
		Autoradiogr. (C1b)	1*			3			4																
		Degeneration (C1c)					5			6										7			8	9	
	Phaseolus (C1d)															10									
	Retrograde tracing	WGA/HRP (C2a)	3	5						11						12			13					9	
		Autoradiogr. (C2b)									14														
		Goldpt. (C2c)							29																
Transmitter	Immuno-preembed.	HRP (N1a)	4	6		11	14			15	16	17				18	19	28						20	
		Silver int. (N1b)								15							18								
		Autoradiogr. (N1c)								16															
		Goldpt. (N1d)								17															
	Immuno-postembed.	HRP (N2a)														21	22		23					31	
		Ferritin (N2b)															24								
		Goldpt. (N2c)	2*		10	12				18	18			21	24	25	22			26*		26*			30
Uptake	Autoradiogr. (N3a)								19					22	22									32	
	SOH-dopamine (N3b)								28																
Cellmorph.	Injection	HRP (M1a)		7		13								23		26*				27	26*			23	
		Lucifer Vel. (M1b)																			27				
		degeneration (M1c)															26*				26*				
	Uptake	Phaseolus (M2a)		8																					
		Golgi (M2b)		9		9			20					31	30	32			23						

CHAPTER II Ultrastructure of the inferior olive studied by means of a combination of WGA-HRP anterograde tracing and postembedding GABA-immunocytochemistry

- a. A new combination of WGA-HRP anterograde tracing and GABA-immunocytochemistry applied to afferents of the cat inferior olive at the ultrastructural level. (1988) *Brain Res* 477:369-375.
- b. The cerebellar, mesodiencephalic, and GABAergic innervation of the glomeruli in the cat inferior olive. A comparison at the ultrastructural level. (1989) In P. Strata (Ed.): *The Olivocerebellar System in Motor Control*. Suppl. Exp. Brain Res. 17:111-117.
- c. Ultrastructural study of the GABAergic, cerebellar, and mesodiencephalic innervation of the cat medial accessory olive: Anterograde tracing combined with immunocytochemistry. (1989) *J. Comp. Neurol.* 284:12-35.

a. A new combination of WGA-HRP anterograde tracing and GABA-immunocytochemistry applied to afferents of the cat inferior olive at the ultrastructural level.

Abstract

In order to identify cerebellar terminals in the cat inferior olive which contain gamma-aminobutyric acid (GABA), a technique was developed combining anterograde transport of wheatgerm agglutinine-conjugated horseradish peroxidase (WGA-HRP) with gold-immunocytochemistry. With this technique both the HRP reaction product and the immunogold labeling can be visualized in a single ultrathin section. Our results suggest that most, if not all of the WGA-HRP labeled cerebellar terminals in the rostral medial accessory olive (MAO) and the rostral principal olive (PO) are GABAergic. In an additional experiment the GABAergic innervation of the rostral MAO was studied in combination with WGA-HRP anterograde tracing from the rostral mesencephalon. In this case the WGA-HRP labeled terminals were never found to be GABA-positive.

Introduction

There exists a reciprocal connection between the inferior olive and the cerebellar nuclei, which is topographically organized (Tolbert et al., '76; Voogd and Bigaré, '80). The cerebellar innervation of the inferior olive is largely GABA-ergic as demonstrated lightmicroscopically in the rat by means of retrograde transport of HRP combined with glutamatedecarboxylase (GAD) immunohistochemistry (Nelson et al., '84). We studied the cerebellar GABAergic innervation of the cat inferior olive at the ultrastructural level to answer the question whether all cerebello-olivary terminals are GABAergic. For this purpose a technique was developed combining postembedding GABA-immunogold staining with anterograde transport of WGA-HRP. For HRP histochemistry tetramethyl benzidine (TMB) was used as a chromogen. The incubation in TMB was followed by a

stabilization procedure with diaminobenzidine-cobalt (DAB-Co), (Lemann et al., '85). In order to determine whether the stabilization procedure could induce false positive labeling with GABA, the same technique was applied to another, presumably non-GABA-ergic system. In this additional experiment WGA-HRP was injected in the nucleus of Darkschewitsch which is known to project to the MAO (Onodera, '84).

Material and methods

In two cats 0.5 ul. WGA-HRP (7% in saline) was injected bilaterally in the interposed and lateral nuclei of the cerebellum under Nembutal anaesthesia (Fig. 1A). In another cat a similar injection was made in the rostral part of the nucleus of Darkschewitsch and its surrounding area (Fig. 1B). After a survival time of 3 days the cats were deeply anaesthetized with Nembutal and perfused transcardially with 100 ml. 0.9% saline in 0.1 M phosphate buffer (PB)(pH 7.3) under artificial respiration, followed by 2 l. 5% glutaraldehyde in 0.1 M PB(pH 7.3). The brainstem was removed and a block containing the inferior olive was dissected and left in the fixative for one hour. Subsequently the inferior olive was cut transversely into slices of 80 um. on a vibratome. The vibratome sections were incubated with TMB in 0.05 M acetate buffer (AB)(pH 4.8), rinsed twice in 0.05 M AB(pH 4.8) and once in 0.1 M PB(pH 7.3), and then stabilized with DAB-Co (Lemann et al., '85). All sections were osmicated with 1.5% osmiumtetroxide in 0.1 M PB(pH 7.3) during 40 min. at 45 C (the use of 1.5% KFe(CN)₆ during the osmication results in a better ultrastructural preservation but it decreases the immunolabeling and the use of 8% D(+)-glucose during the osmication worsens the preservation but it improves the immunolabeling). Subsequently all sections were rinsed in distilled water (4 times), blockstained in 2% aqueous uranylacetate for 30. min at room temperature, directly dehydrated in dimethoxypropane (Truter et al., '80) and embedded in Araldite. Some sections of the

cats with the cerebellar injections were processed for HRP histochemistry without the stabilization step (Holstege, '87). Areas of the rostral inferior olive containing only anterograde labeling or both anterograde and retrograde labeling were selected in semithin sections and separated. Ultrathin sections with a silver interference colour were cut from the selected tissue blocks, mounted on formvar coated nickel grids and processed for GABA-immunocytochemistry. The grids were rinsed in a solution of 0.05 M Trisbuffer(pH 7.6) containing 0.9 % NaCl and 0.1% Triton X-100 (TBS-Triton) and left overnight in a droplet of GABA-antibody diluted 1:1000 in TBS-Triton. The GABA-antibody, which was thoroughly tested on its specificity (Seguela et al., '84; Buijs et al., '87), was kindly provided by dr. Buijs of The Netherlands Institute for Brainresearch. The next morning the grids were rinsed in TBS-Triton (2 times), stored in the same solution for half an hour, rinsed in TBS-Triton(pH 8.2) and incubated for one hour in a droplet of goat anti-rabbit IgG labeled with gold particles (diameter 15 nm; Janssen Pharmaceuticals), diluted 1:40 in TBS-Triton(pH 8,2). After this final incubation the grids were rinsed in TBS-Triton (2 times) and in distilled water (2 times), and contrasted with uranylacetate and leadcitrate. The rostral MAO was studied both in the cats with the cerebellar injections and in the cat with the mesencephalic injection; the lateral bend of the rostral PO was only studied in the cats with injections in the cerebellum. For each subnucleus of each cat seven stabilized vibratome sections were processed for electron microscopy. From each of these tissue-blocks at least one ultrathin section was processed for GABA immunocytochemistry and analyzed in the electron microscope (Philips 300). In this analysis a terminal was considered to be GABA-positive if the number of gold particles overlying it was at least ten times higher than the number of particles over the postsynaptic structures (with approximately the same area). If the number of particles was between three and ten times higher it was considered as doubtfully positive and if it was less, the

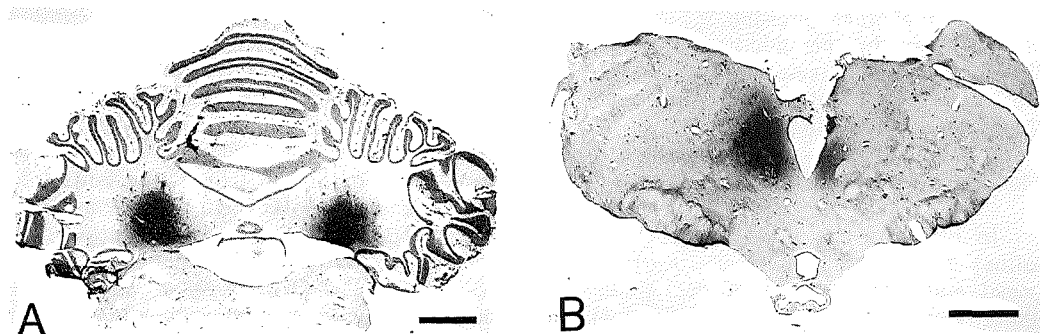


Fig 1. Light microscopical photographs of the WGA-HRP injection areas in the lateral and posterior interposed nuclei of the cerebellum (A) and in the rostral part of the nucleus of Darkschewitsch and its surrounding area (B). DAB was used as a chromogen for HRP histochemistry. Scale bar = 3 mm.

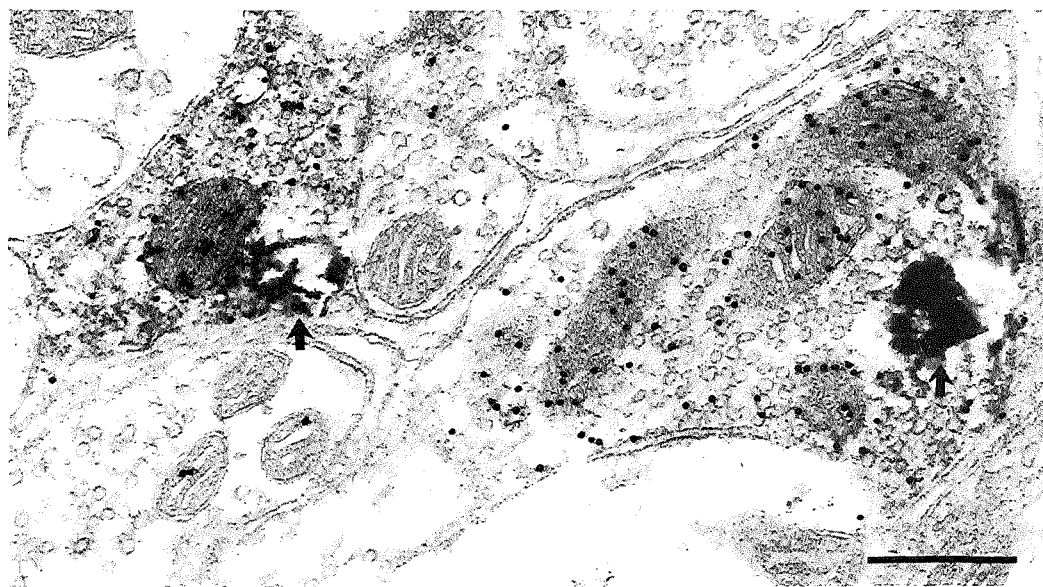


Fig 2. An electron micrograph of two double-labeled terminals in the PO following injection of WGA-HRP in the cerebellar nuclei. Scale bar = 0,4 μ m.

profile was considered to be GABA-negative. For each section the percentages of WGA-HRP labeled terminals which were GABA-positive, doubtfully positive or GABA-negative, were determined. For each subnucleus these data were averaged and the standard error of the mean (SEM) was determined. It was possible to base the SEM on the overall data because a variance analysis (Snedecor and Cochran,'80) performed on the different percentages obtained in each ultrathin section did not show any statistically significant difference.

Results

Ultrathin sections from the stabilized tissue blocks of the cats with the cerebellar injections, contained several retrogradely labeled perikarya and proximal dendrites. Between these structures numerous GABA labeled terminals were observed. Many of these terminals were found to be double-labeled with HRP reaction product and gold particles (Fig. 2). Both in the rostral MAO and in the rostral PO, 85% of the WGA-HRP labeled terminals was GABA-positive, 13% was of a doubtful nature and 2% was GABA-negative (Figs. 3 I-MAO and 3 I-PO). The percentages obtained in areas with only labeling of terminals were similar to those obtained in areas where, both anterograde labeling of terminals and retrograde labeling of perikarya was present. In the case with an injection in the mesencephalon only single GABA- or WGA-HRP labeled terminals were observed (Fig. 3 II-MAO, Fig. 5). Ultrathin sections from the non-stabilized tissue blocks, which were not processed for GABA-immunocytochemistry contained many WGA-HRP labeled structures. However, in sections from the same material, which were processed for immunocytochemistry, most of the WGA-HRP labeling had disappeared (Figs. 4A and 4B) and double-labeled terminals were only seldom observed.

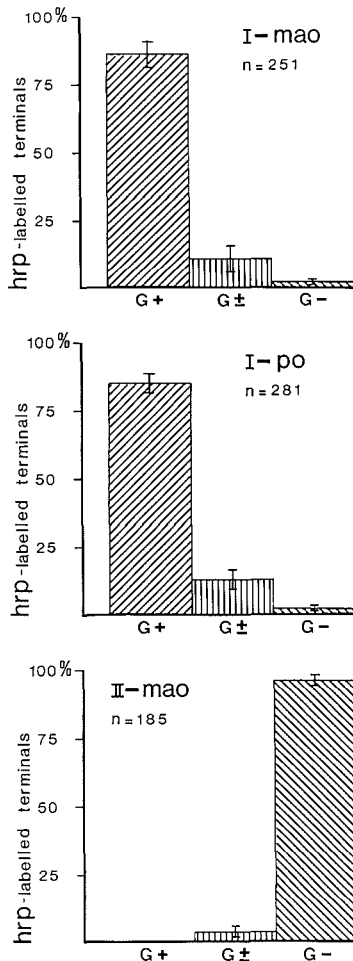


Fig 3. Distributions of the WGA-HRP labeled terminals in the rostral MAO and PO, which were GABA positive (G+), doubtfully GABA-positive (G±) or GABA-negative (G-) following injection of WGA-HRP in the cerebellar nuclei (I-MAO and I-PO) or the mesodiencephalon (II-MAO). Values indicated are mean percentages (\pm S.E.M.) and total numbers of WGA-HRP terminals (n).

Discussion

These results show that the GABAergic nature of a terminal and its origin can be determined in a single ultrathin section using a combination of postembedding GABA-immunogold staining with anterograde transport of WGA-HRP. It is demonstrated that the sensitive chromogen TMB (Mesulam, '78) can be used for HRP histo-chemistry in combination with immunocyto-chemistry at the ultrastructural level provided that the TMB crystals are stabilized with DAB-Co. This stabilization is essential because the non-stabilized TMB crystals disappear during the immunostaining (Fig. 4A and 4B). In this respect there seems to be no difference between the stability of TMB-crystals embedded in araldite and the stability of TMB-crystals in lightmicroscopical tissue (Rye et al., '84). The high ratio of double-labeled terminals which was found in the ultrathin sections from the stabilized tissue blocks of the cats with injections in the cerebellar nuclei, suggests that all the nucleo-olivary fibers, which terminate in the rostral MAO and the rostral PO, are GABAergic. Since GABA is known as an inhibiting neurotransmitter (Roberts, '74), these findings are in agreement with the physiological finding in the cat that the cerebello-olivary projection is inhibitory (Hesslow, '86). The high percentage of double-labeled terminals may indicate that

the sensitivity of the GABA-antibody is high enough to detect nearly all the GABAergic nucleo-olivary terminals. Since the olivo-cerebellar fibers give off collaterals to the cerebellar nuclei (Groenewegen et al., '79; Voogd and Bigaré, '80), the present data may be influenced by retrograde transneuronal transport of WGA-HRP (Harrison et al., '84). The percentages found in areas with only anterograde labeling were similar to those found in areas with both anterograde and retrograde labeling. Therefore, it is unlikely that the results were affected by retrograde transneuronal labeling. In the cat injected in the mesencephalon WGA-HRP labeled terminals were never found to be GABA-positive. This demonstrates that the WGA-HRP reaction product does not directly induce false positive GABA-labeling. It is interesting to note that the majority of neurons in the nucleus of Darkschewitsch of the rat is GABAergic (Mugnaini and Oertel, '85). Our data show that in the cat there are no GABAergic projections from the nucleus of Darkschewitsch to the inferior olive.

It may be concluded that the combination of anterograde transport of WGA-HRP with GABA immunocytochemistry is a useful technique for identifying both the origin and the GABAergic nature of a terminal and for quantifying the GABAergic proportion of terminals of which the origin is known.

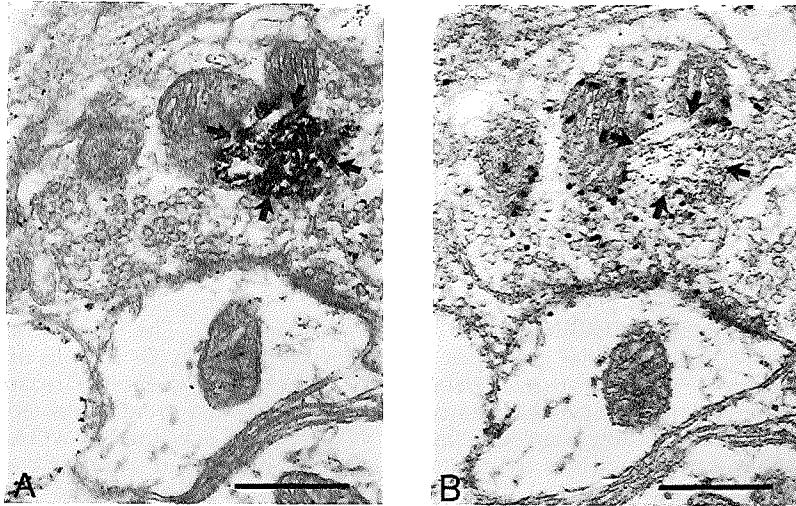


Fig 4. Two electron micrographs of the same terminal from two serial sections of a non-stabilized tissue block. Note the WGA-HRP reaction product in the section, which has not been processed for immunocytochemistry (A, arrows) and its disappearance in the adjacent serial section, which has been processed for GABA-immunocytochemistry (B, arrows). Scale bar = 0,4 μ m.



Fig 5. Electron micrograph of two single labeled terminals in the rostral MAO after injection of WGA-HRP in the rostral mesencephalon combined with GABA-immunocytochemistry: A non-GABA-ergic WGA-HRP labeled (black arrows) terminal on the left side and a single GABA labeled terminal on the right side. Scale bar = 0,4 μ m.

b. The cerebellar, mesodiencephalic, and GABAergic innervation of the glomeruli in the cat inferior olive. A comparison at the ultrastructural level.

Introduction

Using lightmicroscopical methods, Nelson et al. ('84) demonstrated the GABAergic nature of the cerebello-olivary projection. These observations were confirmed and extended by de Zeeuw et al. ('88a) who showed in an electronmicroscopical study in the cat that virtually all cerebellar terminals in the rostral inferior olive (IO) are GABAergic. It has been demonstrated that neurons in the IO are electrotonically coupled (Llinas et al.'74; Llinas and Yarom,'81) by dendrodendritic gap junctions in the IO glomeruli (Sotelo et al.,'74) and that GABA may modulate this coupling (Sasaki and Llinas,'85). This is in agreement with the presence of GAD positive terminals in close proximity of gap junctions within the glomeruli (Sotelo et al.,'86). The origin of these GABAergic terminals are likely to be the cerebellar nuclei since terminals of cerebello-olivary fibres have been shown presynaptic to dendrites engaged in gap junctions (Angaut and Sotelo,'87). The possible role of non-GABAergic terminals in regulating electrotonic coupling has not yet been elucidated. In this study we shall compare the distribution over glomeruli and non-glomerular neuropil of the two main afferent systems of the rostral medial accessory olive (MAO) of the cat, i.e. the GABAergic projection from the posterior interposed nucleus of the cerebellum and the non-GABAergic projection from the mesodiencephalic junction (de Zeeuw et al.,'88a). For this purpose the following values were determined: 1) What percentage of the cerebellar, GABAergic and mesodiencephalic terminals were located within glomeruli, 2) What percentage of the total number of terminals located within the glomeruli were cerebellar, GABAergic, and mesodiencephalic terminals, and 3) What percentage of the glomeruli contained both GABAergic and mesodiencephalic terminals.

Material and methods

The measurements were made in the rostral part of the MAO in two groups of experiments, using a combination of antero-grade tracing with WGA-HRP and postembedding immunogold labeling of the GABAergic terminals. The GABA antibody was kindly provided by Dr R Buijs of the Netherlands Institute for Brain Research (Buijs et al.,'87). The first group consisted of two cats with bilateral injections of WGA-HRP in the posterior interposed nuclei of the cerebellum. The two cats of the second group received similar injections in the mesodiencephalon including the nucleus of Darkschewitsch, which is known to project to the rostral MAO (Onodera,'84). After a survival time of 3 days the cats were perfused with glutaraldehyde. The IO was cut transversely on a vibratome and processed according to the technique combining WGA-HRP histochemistry with GABA-immunocytochemistry at the electron-microscopical level. Details of the procedure have been published (de Zeeuw et al.,'88a). From each cat at least two blocks were used for analysis. In the ultrathin sections of these blocks two populations of terminals were studied. The first population of terminals was randomly collected from the entire rostral MAO neuropil i.e. from the glomeruli and from the neuropil in between these glomeruli. Each category of terminals (see below) was collected separately. The second population of terminals consisted of all the terminals present in a random population of glomeruli (defined as a core of at least three dendritic structures, surrounded by at least two terminals and some glia). In these two populations four categories of terminals were present: non-labeled (N), single GABA labeled (G), single WGA-HRP labeled (H) and double GABA/WGA-HRP labeled (G+H) terminals.

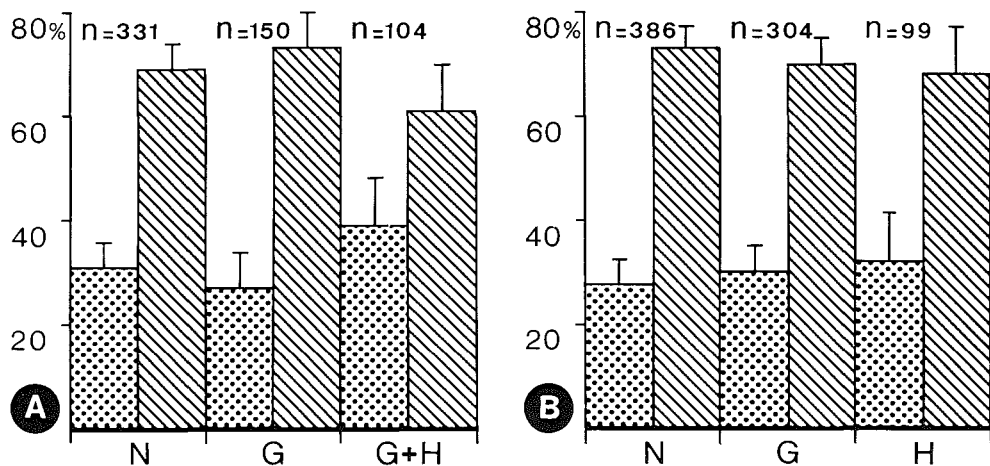


Fig. 1. Histograms showing the proportions of the non-labeled (N), single GABA labeled (G), single WGA-HRP labeled (H) and double GABA/WGA-HRP labeled (G+H) terminals which are located in a glomerulus (dots) and outside a glomerulus (oblique lines) for the cerebellar (A) and the mesodiencephalic (B) experiments. Indicated values are mean percentages (+SD) and the total number (n) of each terminal category. It should be noted that the different total numbers of the various terminal categories do not indicate a specific relation.

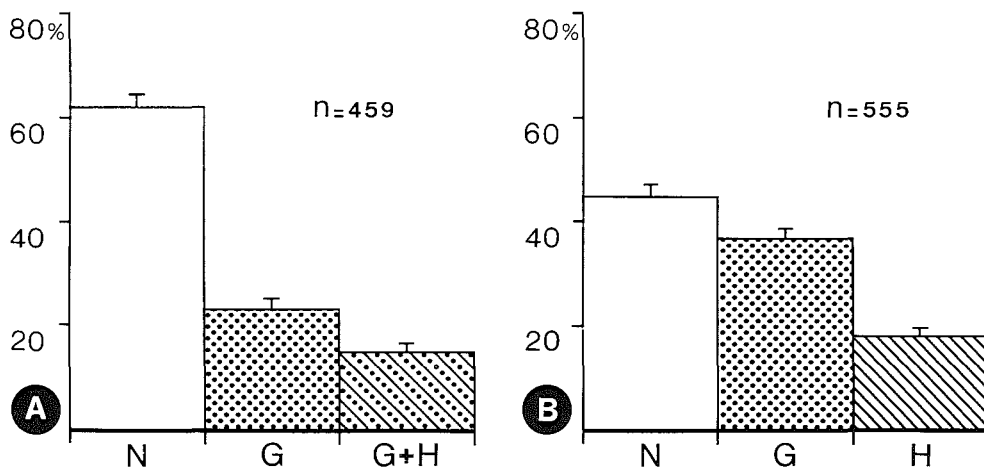


Fig. 2. Histograms showing what percentage of the terminals within the glomeruli are cerebellar, mesodiencephalic, and/or GABAergic terminals (for symbols see Fig. 1) following injections in the cerebellum (A) and the mesodiencephalon (B). values indicated are mean percentages (+SD) and total numbers (n).

Results

The ultrathin sections from the cats with an injection of WGA-HRP in the cerebellum contained numerous N-, G- and (G+H) labeled terminals (Fig. 3A) and only a few H labeled terminals (about 2% of all the WGA-HRP labeled terminals). Most of the labeled terminals contained pleiomorphic vesicles and showed a symmetrical synapse. From the random sample of 585 terminals from the entire neuropil an average of 31% of the N-, 27% of the G- and 39% of the (G+H) labeled terminals was located within glomeruli (Fig. 1A). These percentages increased from about 20% in the caudal part of the rostral MAO to about 45% for its rostral part. This increase was approximately equal for each category of terminals and due to an increase in the number and the size of the glomeruli. The second population consisted of 459 terminals collected from 103 glomeruli and contained an average of 62% N-, 23% G- and 15% (G+H) labeled terminals (Fig. 2A). In the cases with an injection in the mesodiencephalic junction only N-, G- and H labeled terminals were observed (Fig. 3B). Most of the mesodiencephalic terminals contained rounded vesicles and showed an asymmetrical synapse. In the population of 789 terminals randomly collected from the entire neuropil an average of 27% of the N-, 30% of the G- and 32% of the H labeled terminals was located within glomeruli (Fig. 1B). These cases revealed a similar caudo-rostrally increase in the proportion of the terminals located within a glomerulus. The second population consisted of 555 terminals collected in 126 glomeruli and contained an average of 45% N-, 37% G- and 18% H labeled terminals (Fig. 2B). It was found that 50% of these glomeruli contained both G- and H labeled terminals (Fig. 3B).

Discussion

The percentages of the different categories of terminals from the general samples (Figs. 1A and 1B) were not significantly different ($p < 0.05$), neither between different categories of terminals from the same experimental group nor between any of the categories from the cerebellar experiments and any of the mesodiencephalic experiments. These data indicate that in the rostral MAO an average of about one third of the terminals of each category is located within glomeruli. Thus the proportions of the GABAergic cerebellar terminals and of the mesodiencephalic terminals which are located within glomeruli, are similar. The percentages from the second sample of terminals from the cerebellar and the mesodiencephalic experiments (Figs. 3A and 3B) show that the total GABAergic input to the glomeruli is about 37% (for the cerebellar experiment, Fig. 3A: $G + (G+H) = 38\%$ and for the mesodiencephalic experiment, Fig. 3B: $G = 37\%$) and that the cerebellar GABAergic input (15%) to the glomeruli is not more extensive than the mesodiencephalic input (18%). The finding that 50% of the glomeruli in the mesodiencephalic experiments contained one or more GABAergic terminals as well as one or more WGA-HRP labeled terminals is in agreement with the percentage which can be obtained by calculations of probabilities presuming that there is a random distribution of all the categories of terminals over the glomeruli *. This would mean that there is no obvious separation or coexistence of the GABAergic and mesodiencephalic terminals in I.O. glomeruli. It may be concluded with respect to the innervation of the glomerulus in the rostral MAO that both the GABAergic cerebellar and the non-GABAergic mesodiencephalic afferent system have a random and an equal input.

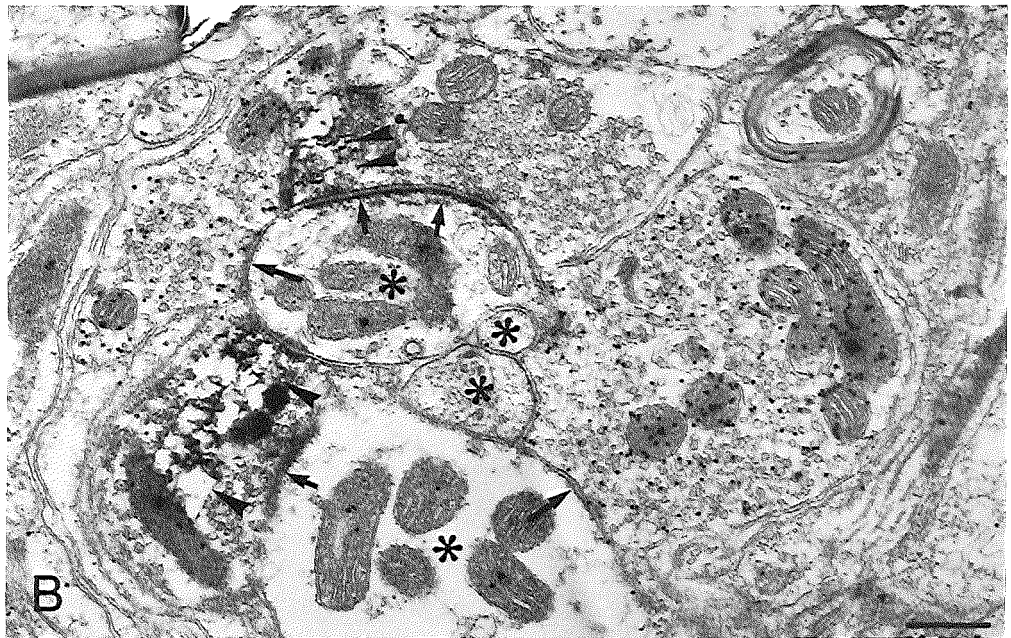
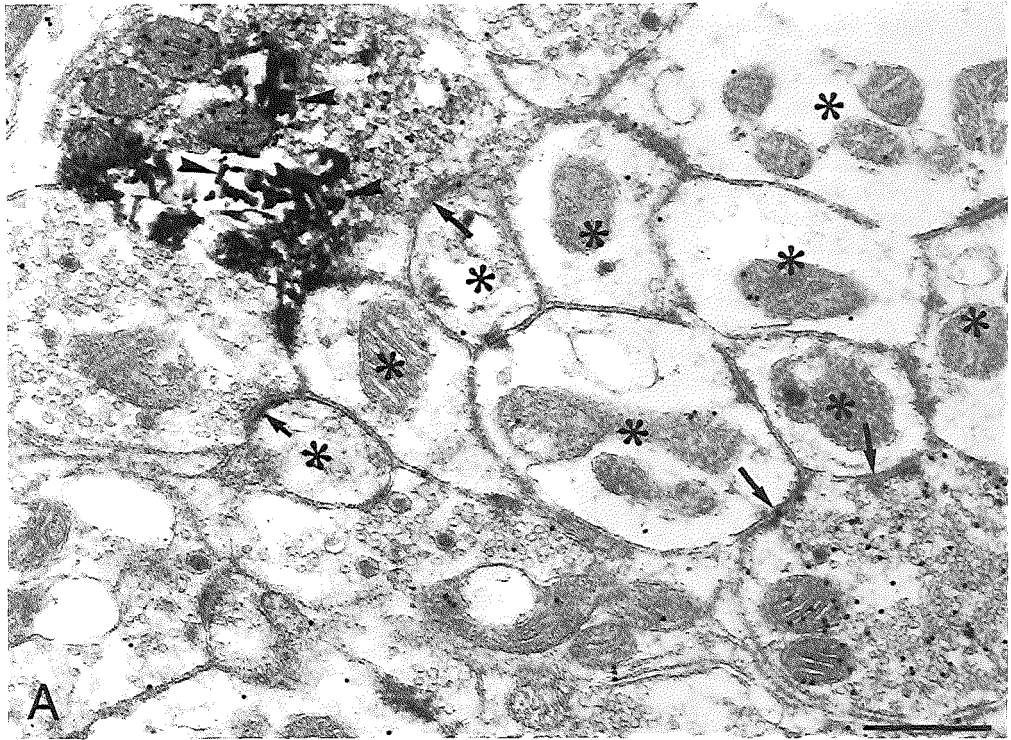
Note *. Using the percentages for the 3 categories of terminals (G, H and N) of the second sample in the mesodiencephalic experiment (i.e. 45%, 37% and 18%) and the mean number of terminals/glomerulus (T/G) and presuming that there is a random innervation of glomeruli, the probability (P) that there is at least one G and at least one H can be calculated as follows.

If $T/G = 4$, there are 6 possible combinations in which there is at least one G and at least one H: (G,H,N,N), (G,H,H,N), (G,H,H,H), (G,G,H,N), (G,G,H,H) and (G,G,G,H). The P for each combination is:

$$P(G^a, H^b, N^c) = \frac{P(G)^a \times P(H)^b \times P(N)^c}{(a+b+c)! / a!b!c!}$$
in which a is the total number of G-, b the total number of H- and c the total number of N labeled terminals.
 $P(\text{total}) = P(G,H,N,N) + P(G,H,H,N) + P(G,H,H,H) + P(G,G,H,N) + P(G,G,H,H) + P(G,G,G,H) = 0.162 + 0.065 + 0.009 + 0.133 + 0.027 + 0.036 = 0.432$. This indicates that the probability that G and H will be located together is 43% in a glomerulus of 4 terminals. However in the rostral MAO neuropil the observed T/G was $555/126 = 4.4$ instead of 4.0. If the P is calculated for $T/G = 3$ and for $T/G = 5$, and if a fluent curve is drawn through $P(T/G = 3)$, $P(T/G = 4)$ and $P(T/G = 5)$ it is found that $p(T/G = 4.4)$ is approximately 48%.

The 95% confidence interval of $p(T/G = 4.4)$ is approximately 39%-57%. Thus the observed 50% lies within the expected interval which is based upon the assumption that there exists a random GABAergic and mesodiencephalic innervation of the glomerulus in the rostral MAO. If there were more separate glomeruli for the GABAergic and/or the mesodiencephalic terminals the observed $p(T/G = 4.4)$ would be $< 39\%$ and if there was a significant coexistence of the GABAergic and the mesodiencephalic terminals the observed $p(4.4)$ would be $> 57\%$.

Fig. 3 (next page). Electronmicrographs of two glomeruli in the rostral MAO following injection of WGA-HRP in the cerebellar nuclei (A) and the mesodiencephalon (B). The glomerulus in A shows nine dendritic structures (stars) surrounded by three non-labeled and two gold-labeled GABAergic terminals, one of which contains WGA-HRP reaction product (arrowheads) indicating a cerebellar origin. The glomerulus in B shows four dendritic structures (stars) surrounded by two gold-labeled terminals and two single WGA-HRP labeled terminals (arrowheads) indicating a mesodiencephalic origin. Large arrows indicate symmetrical synapses, small arrows indicate asymmetrical synapses. Scale bar=0.5 μm .



c. Ultrastructural study of the GABAergic, cerebellar, and mesodiencephalic innervation of the cat medial accessory olive combining anterograde tracing with immunocytochemistry.

Abstract

The rostral medial accessory olive (MAO) of the cat was studied by using an ultrastructural technique combining wheat germ agglutinin coupled horseradish peroxidase (WGA-HRP) anterograde tracing and postembedding GABA-immunocytochemistry. One group of cats received a WGA-HRP injection in the posterior interposed nucleus of the cerebellum and another group received an injection in the nucleus of Darkschewitsch.

Based on differences in their morphology three types of GABAergic and three types of non-GABAergic terminals were observed. One type of the GABAergic terminals was often GABA/WGA-HRP double labeled in the cerebellar experiments, and one type of the non-GABAergic terminals was often WGA-HRP labeled in the mesodiencephalic experiments.

Following injections of WGA-HRP in the cerebellar nuclei virtually all WGA-HRP labeled terminals were GABA positive. Quantification of these GABA/WGA-HRP double labeled terminals showed that 1) 30% of the GABAergic terminals randomly selected from the entire neuropil were double labeled, 2) 13% of the GABAergic terminals adjacent to perikarya were double labeled, and 3) 34% of the GABAergic terminals strategically located next to both of the dendritic elements linked by a gap junction were double labeled. Statistical analysis of the above data showed that significantly fewer GABAergic terminals adjacent to perikarya were double labeled ($p < 0.001$) than would be expected from the double labeled proportion of the randomly selected GABAergic terminals.

Following injection of WGA-HRP in the nucleus of Darkschewitsch, all WGA-HRP labeled terminals were GABA-negative. Quantification of these terminals showed that 1) 26% of the randomly selected non-

GABAergic terminals were WGA-HRP labeled, 2) 20% of the non-GABAergic terminals adjacent to perikarya were WGA-HRP labeled, and 3) 23% of the non-GABAergic terminals strategically located next to a gap junction were WGA-HRP labeled. No significant differences were found among these populations.

Quantification of terminals of both groups of experiments mentioned above, showed that GABAergic terminals comprised 1) 38% of the randomly selected terminals, 2) 64% of the terminals apposed to perikarya, and 3) 53% of the terminals strategically located next to gap junctions. Statistical analysis of the above data showed that significantly more GABAergic terminals were located adjacent to perikarya ($p < 0.001$) and strategically next to a gap junction ($p < 0.05$) than would be expected from the random GABAergic innervation.

The above findings of the GABAergic, cerebellar and mesodiencephalic input are discussed with regard to their functional role in the neuronal circuitry of the rostral MAO. In addition, the possible non-cerebellar origins of the GABAergic inputs to the IO are discussed.

Introduction

The inferior olive (IO) is the source of the climbing fibres innervating the Purkinje cells of the cerebellum (Szentágothai and Rajkó, '59; Eccles, '66; Murphy et al., '73; Desclin, '74). The three main subnuclei of the IO are the principal olive (PO), the dorsal accessory olive (DAO) and the medial accessory olive (MAO). The present ultrastructural study of the cat IO is focussed on the rostral MAO. The rostral MAO projects to a longitudinal strip of Purkinje cells (C2 zone) in the cerebellar hemisphere and to the posterior interposed nucleus (Groenewegen et al., '79), a central cerebellar nucleus, which receives its main input from the Purkinje

cells of the same zone (Voogd and Bigaré, '80). Since the posterior interposed nucleus projects to the rostral MAO (Tolbert et al., '76), the direct connections between these two nuclei are reciprocally organized. The projection from the central cerebellar nuclei to the IO is GABA (gamma-amino butyric acid) -ergic (Nelson et al., '84; de Zeeuw et al., '88a) and originates from a subset of small neurons (Nelson and Mugnaini, '87), which probably do not send collaterals to the thalamus (Bharos et al., '81). An indirect projection from the central nuclei to the rostral MAO is relayed through the nucleus of Darkschewitsch (Ogawa, '39; Voogd, '64; Kievit, '79). Although the connections of the posterior interposed nucleus with the nucleus of Darkschewitsch seem to be rather specific, they are part of the more widespread projection to other parts of the mesodiencephalon (Ruigrok et al. in press). The projection from the nucleus of Darkschewitsch to the olive (Onodera, '84; Holstege and Tan, '88) is non-GABAergic (de Zeeuw et al., '88a).

The firing pattern of the IO neurons is determined by their afferent systems and intrinsic properties. Two of the salient electrophysiological features of olivary neurons are their propensity to oscillate (Armstrong et al., '68; Llinas and Yarom, '86; Benardo and Foster, '86) and to discharge synchronously (Llinas et al., '74; Llinas and Yarom, '81a). The oscillating property of IO neurons is due to specific conductances, which are distributed differentially over the cell membrane of the soma and the dendrites (Llinas and Yarom, '81a and '81b). Synchronous firing of IO neurons is a result of electrotonic coupling (Llinas et al., '74; Llinas and Yarom, '81a) by dendro-dendritic gap junctions, which are located primarily in the IO glomeruli (Sotelo et al., '74; King, '76; Gwyn et al., '77; Rutherford and Gwyn, '77). There is physiological (Sasaki and Llinas, '85) and morphological (Sotelo et al., '86) evidence that GABA modulates this coupling in the IO.

In order to relate further the interaction between afferent inputs and intrinsic properties of IO neurons, we studied the

morphology and distribution of the GABAergic, cerebellar and mesodiencephalic terminals on the rostral MAO neurons in the cat by means of a technique combining anterograde transport of wheat germ agglutinin coupled horseradish peroxidase (WGA-HRP) with GABA immunocytochemistry. Special emphasis was put on the terminals apposed to perikarya and on the terminals associated with dendrites coupled by gap junctions. We determined quantitatively the proportions of the GABAergic, cerebellar and mesodiencephalic terminals on these structures, and compared them with their overall distribution in the neuropil and with each other.

Material and methods

In one group of four cats 0.5 ul WGA-HRP (7% in saline) was injected bilaterally in the posterior interposed nuclei of the cerebellum under pentobarbital anaesthesia. In another group of three cats injections were made in the nucleus of Darkschewitsch and surrounding mesodiencephalic area. After a survival time of 3 days the cats were anaesthetised with pentobarbital and perfused transcardially with 100 ml. 0.9% saline in 0.18 M (pH 7.3) cacodylate buffer (for one cat in each group 0.1 M phosphate buffer was used instead) under artificial respiration, followed by 2 liters 5% glutaraldehyde in the same buffer. The cerebellum and mesodiencephalon were cut in 40 um sections and incubated with diaminobenzidine (DAB) according to Graham and Karnovsky ('66). The IO was left for two hours in the fixative and cut transversely on a vibratome. Subsequently, the sections were processed according to a technique combining WGA-HRP histochemistry with postembedding GABA-immunostaining. Details of the procedure were published elsewhere (de Zeeuw et al., '88a). Briefly, it consisted of the following steps. Vibratome sections were incubated with tetramethylbenzidine and stabilized with DAB-cobalt (Rye et al., '84; Lemann et al., '85), osmicated (in 8% glucose solution), blockstained with uranyl acetate (UA), without rinsing directly dehydrated in

dimethoxypropane (Truter et al., '80) and embedded in Araldite. Guided by the findings in the semithin sections, we made pyramids of the rostral MAO from the plastic embedded vibratome sections. From these tissue blocks serial and non-serial ultrathin sections were mounted on formvar coated nickel grids (200 mesh) and processed for GABA-immunocytochemistry. The polyclonal GABA antibody was raised in rabbit (for details about the specificity of the antibody, see Seguela et al., '84 and Buijs et al., '87). The goat anti-rabbit (GAR) antibody (Janssen, Belgium) was labeled with 15 nm gold particles. The sections were counterstained with UA and leadcitrate and examined in a Philips (300) Electron Microscope.

Collection and analysis of the data

From the four cats with injections of WGA-HRP in the cerebellar nuclei and from the three cats with injections of WGA-HRP in the nucleus of Darkschewitsch, the three and two cats respectively, with the largest number of labeled terminals were used for quantitative analysis. Four non-serial ultrathin sections obtained from two embedded tissue blocks of each of these cats, were examined. In these sections three populations of terminals were selected. The first population consisted of a random sample of all terminals present in the olivary neuropil. The second population consisted of terminals located adjacent to somata, and the third of terminals associated with gap junctions. The first population was obtained by scrutinizing a small but equal area of each gridsquare, which contained tissue of the rostral MAO. Since relatively few of the terminals were apposed to perikarya and located next to dendrites coupled by gap junctions, the second population was selected from a large sample area of each gridsquare and the third population was selected from the entire tissue area in the gridsquares. All three populations were obtained from the same gridsquares of the same sections.

The first population of terminals was studied as follows. It was determined for the total sample area of each ultrathin section of both experimental groups 1) what percentage of all terminals were GABAergic and non-GABAergic (first column, Table 1A and B), 2) what percentage of the GABAergic and non-GABAergic terminals were or were not WGA-HRP labeled (second column, Table 1A, B), 3) what percentage of the terminals mentioned at point two, were located inside or outside a glomerulus (third column, Table 1A, B), 4) what percentage of the intra- and extraglomerular terminals exhibited a synapse (fourth column, Table 1A, B), and 5) what percentage of the synapse containing terminals, established an asymmetric or a symmetric synapse (fifth and sixth column, Table 1A, B). In this analysis a terminal was considered 1) GABA positive, when the number of gold particles overlying it was at least eight times higher than the number of particles overlying surrounding non-GABAergic structures, 2) WGA-HRP labeled, when crystalline electrondense deposits were observed, 3) located inside a glomerulus, when it was one of two or more terminals, which surrounded a core of at least three small dendritic elements, and when some glia surrounded this synaptic complex (de Zeeuw et al., '89b), 4) to exhibit a synaptic complex, when membrane specializations contained a synaptic cleft, a post synaptic density and a cluster of presynaptic vesicles adjacent to the presynaptic membrane (Gray and Guillery, '66), and 5) to establish an asymmetric (Gray's type I) or a symmetric (Gray's type II) synapse, when the width of the synaptic cleft was about 30 nm, or 20 nm respectively and when the thickness of the postsynaptic density was about 40 nm, or 20 nm respectively (Gray, '59). Terminals, which displayed more than one synaptic junction in the same electron micrograph were counted as a single terminal. The percentages of all the morphological features mentioned above, were averaged for all ultrathin sections and the standard errors of the means (SEM) were calculated.

TABLE 1A. Population of Terminals (n = 912) Randomly Selected From the Entire Neuropil, Following Injection of WGA-HRP in the Posterior Interposed Nucleus of the Cerebellum Combined With GABA Immunocytochemistry (Values Indicated Are Mean Percentages [\pm SEM] of Data Obtained in the Ultrathin Sections [N = 12]; for Details See Materials and Methods)

Terminal subgroup		Glomerular location		Terminals with synaptic junctions	Type I	Type II
GABA 37 \pm 1.5	Single GABA 70 \pm 3.3	{Extra	71 \pm 1	48 \pm 6	13 \pm 3	87 \pm 3
		{Intra	29 \pm 1	88 \pm 1	11 \pm 4	89 \pm 4
	Double GABA/WGA-HRP 30 \pm 3.3	{Extra	63 \pm 5	37 \pm 3	7 \pm 4	93 \pm 4
		{Intra	37 \pm 5	90 \pm 4	6 \pm 2	94 \pm 2
Non-GABA 63 \pm 1.5		{Extra	67 \pm 5	49 \pm 2	92 \pm 5	8 \pm 5
		{Intra	33 \pm 5	80 \pm 3	94 \pm 1	6 \pm 1

TABLE 1B. Population of Terminals (n = 721) Randomly Selected From the Entire Neuropil, Following Injection of WGA-HRP in the Mesodiencephalic Junction Combined With GABA Immunocytochemistry (Values Indicated Are Mean Percentages [\pm SEM] of Data Obtained in the Ultrathin Sections [N = 8], for Details See Materials and Methods)

Terminal subgroup		Glomerular location		Terminals with synaptic junctions	Type I	Type II
GABA 38 \pm 2.7		{Extra	70 \pm 2	39 \pm 4	16 \pm 2	84 \pm 2
		{Intra	30 \pm 2	85 \pm 3	9 \pm 6	91 \pm 6
Non-GABA 62 \pm 2.7	Non-labeled 74 \pm 2.7	{Extra	72 \pm 5	42 \pm 4	90 \pm 4	10 \pm 4
		{Intra	28 \pm 5	68 \pm 8	96 \pm 2	4 \pm 2
	Single WGA-HRP 26 \pm 2.7	{Extra	69 \pm 6	46 \pm 2	92 \pm 6	8 \pm 6
		{Intra	31 \pm 6	87 \pm 2	97 \pm 3	3 \pm 3

TABLE 2A. Population of Terminals (n = 278) Located Adjacent to Perikarya, Following Injection of WGA-HRP in the Posterior Interposed Nucleus of the Cerebellum Combined With GABA Immunocytochemistry (Values Indicated Are Mean Percentages [\pm SEM] of Data Obtained in the Ultrathin Sections [N = 12]; for Details See Materials and Methods)

Terminal subgroup		Terminals with synaptic junctions	Type I	Type II
GABA 62 \pm 2.1	Single GABA 87 \pm 0.9	63 \pm 4	3 \pm 2	97 \pm 2
	Double GABA/WGA-HRP 13 \pm 0.9	74 \pm 12	8 \pm 6	92 \pm 6
Non-GABA 38 \pm 2.1		40 \pm 4	53 \pm 4	47 \pm 4

TABLE 2B. Population of Terminals (n = 216) Located Adjacent to Perikarya, Following Injection of WGA-HRP in the Mesodiencephalic Junction Combined With GABA Immunocytochemistry (Values Indicated Are Mean Percentages [\pm SEM] of Data Obtained in the Ultrathin Sections [N = 8]; for Details See Materials and Methods)

Terminal subgroup		Terminals with synaptic junctions	Type I	Type II
GABA 66 \pm 2.1		70 \pm 5	7 \pm 3	93 \pm 3
Non-GABA 34 \pm 2.1	Non-labeled 80 \pm 2.5	44 \pm 4	52 \pm 10	48 \pm 10
	Single WGA-HRP 20 \pm 2.5	38 \pm 13	60 \pm 22	40 \pm 22

TABLE 3A. Population of Terminals (n = 127) Associated With Gap Junctions, Following Injection of WGA-HRP in the Posterior Interposed Nucleus of the Cerebellum Combined with GABA Immunocytochemistry (Values Indicated Are Mean Percentages [\pm SEM] of Data Obtained in the Ultrathin Sections [N = 9]; for Details See Materials and Methods)

Terminal subgroup			Glomerular location		Terminals with synaptic junctions		Type I	Type II
			Extra	Intra	Extra	Intra		
Strategic 33 \pm 8.5	GABA 55 \pm 4.1	Single GABA 66 \pm 10.2	Extra	18 \pm 9	100	0	100	
			Intra	82 \pm 9	86 \pm 9	8 \pm 8	92 \pm 8	
	Non-GABA 45 \pm 4.1	Double GABA/WGA-HRP 34 \pm 10.2	Extra	10 \pm 10	100	0	100	
			Intra	90 \pm 10	90 \pm 10	0	100	
				Extra	30 \pm 8	60 \pm 24	100	0
				Intra	70 \pm 8	72 \pm 11	89 \pm 7	11 \pm 7
Non-strategic 67 \pm 8.5	GABA 36 \pm 9.2	Single GABA 70 \pm 15.3	Extra	17 \pm 5	83 \pm 17	0	100	
			Intra	83 \pm 5	79 \pm 10	15 \pm 10	85 \pm 10	
	Non-GABA 64 \pm 9.2	Double GABA/WGA-HRP 30 \pm 15.3	Extra	13 \pm 13	0	—	—	
			Intra	87 \pm 13	92 \pm 8	13 \pm 13	87 \pm 13	
				Extra	21 \pm 5	57 \pm 17	80 \pm 12	20 \pm 12
				Intra	79 \pm 5	66 \pm 6	93 \pm 4	7 \pm 4

TABLE 3B. Population of Terminals (n = 129) Associated With Gap Junctions, Following Injection of WGA-HRP in the Mesodiencephalic Junction Combined with GABA Immunocytochemistry (Values Indicated Are Mean Percentages [\pm SEM] of Data Obtained in the Ultrathin Sections [N = 7]; for Details See Materials and Methods)

Terminal subgroup			Glomerular location		Terminals with synaptic junctions		Type I	Type II
			Extra	Intra	Extra	Intra		
Strategic 30 \pm 8.8	GABA 50 \pm 11.2		Extra	13 \pm 6	67 \pm 33	0	100	
			Intra	87 \pm 6	83 \pm 9	4 \pm 4	96 \pm 4	
	Non-GABA 50 \pm 11.2	non-labeled 77 \pm 10.5	Extra	24 \pm 8	50 \pm 29	100	0	
			Intra	76 \pm 8	77 \pm 10	90 \pm 10	10 \pm 10	
			Single WGA-HRP 23 \pm 10.5	Extra	0	—	—	—
				Intra	100	78 \pm 22	100	0
Non-strategic 70 \pm 8.8	GABA 34 \pm 9.9		Extra	18 \pm 3	40 \pm 24	0	100	
			Intra	82 \pm 3	75 \pm 7	5 \pm 5	95 \pm 5	
	Non-GABA 66 \pm 9.9	non-labeled 74 \pm 6.0	Extra	23 \pm 6	53 \pm 18	88 \pm 3	12 \pm 3	
			Intra	77 \pm 6	69 \pm 10	83 \pm 7	17 \pm 7	
			Single WGA-HRP 26 \pm 6.0	Extra	10 \pm 6	50 \pm 50	100	0
				Intra	90 \pm 6	70 \pm 10	95 \pm 5	5 \pm 5

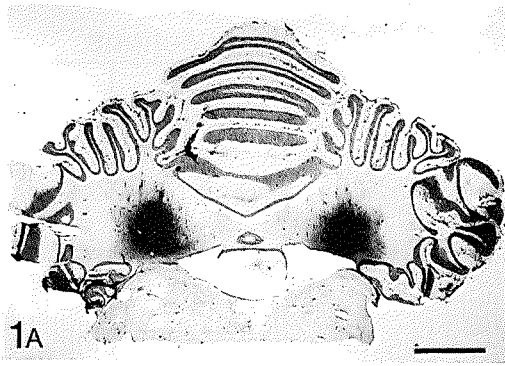


Fig. 1. Photomicrographs from one of the cerebellar experiments. A. The areas of the WGA-HRP injections bilaterally in the posterior interposed nuclei of the cerebellum. Scale bar = 3.6 mm. B. Semithin section of the rostral MAO following injection of WGA-HRP as in A. Note the retrogradely labeled perikarya and the anterograde labeling in between. Scale bar = 20 μ m.

The second population consisted of terminals located adjacent to perikarya or their spines. The cell bodies were identified and distinguished from large dendrites by their nuclei, organelles and size. These terminals were analyzed in a manner similar to that of the terminals of the first population, except that it was not determined whether they were located in a glomerulus (Table 2A, B).

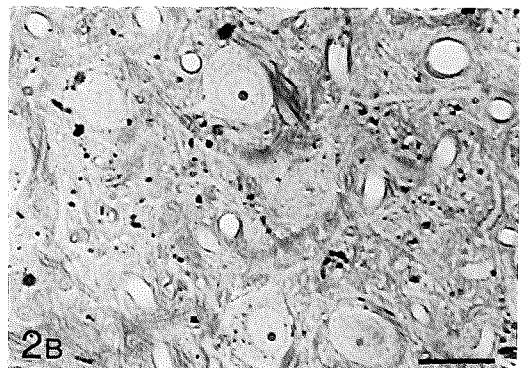
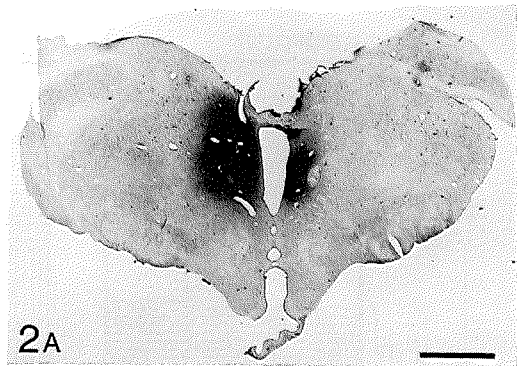
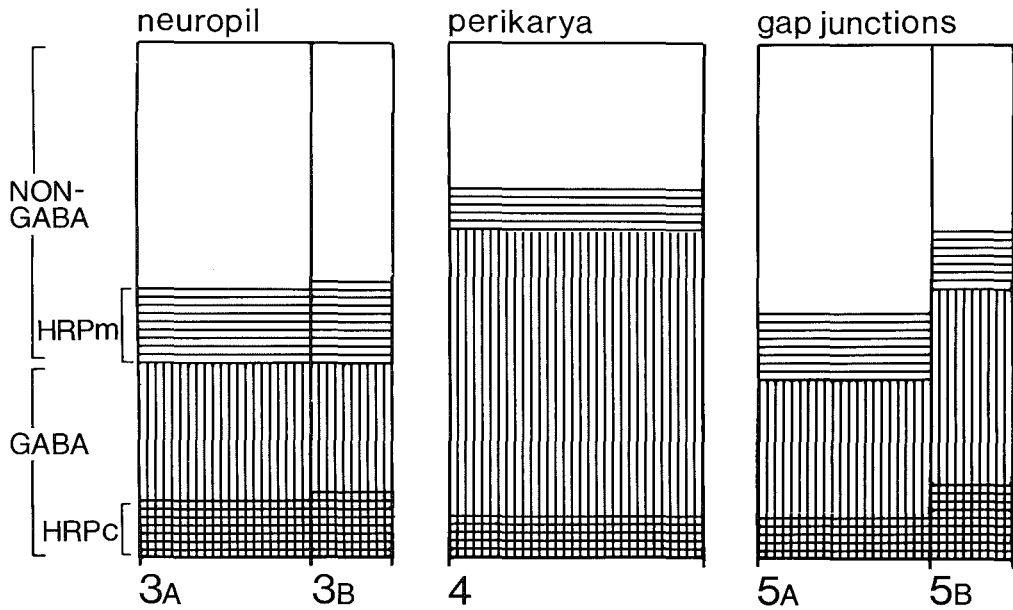


Fig. 2. Photomicrographs from one of the mesodiencephalic experiments. A. The areas of the WGA-HRP injections bilaterally in the nucleus of Darkschewitsch and the surrounding mesodiencephalic area. Scale bar = 3.2 mm. B. Semithin section of the rostral MAO following injection of WGA-HRP as in A. Note the anterograde labeling and the absence of the retrogradely labeled perikarya. Scale bar = 22 μ m.

The third population consisted of terminals apposed to dendritic structures coupled by a gap junction. A junctional zone was considered to be a gap junction when it showed a heptalaminar structure with and intercellular gap of approximately 2 nm and when it revealed patches of electrondense material apposed to both cytoplasmic sides of the junctional membrane (Sotelo et al., '74). In this population it was determined what



Figs. 3-5. Graphic representations showing the proportions of the terminals, which are WGA-HRP labeled (horizontal lines) in the cerebellar (HRPc) and mesodiencephalic (HRPm) experiments, and the proportions of the GABAergic (vertical lines) and non-GABAergic (absence of vertical lines) terminals obtained from both groups of experiments. The surface areas of the different terminal subgroups in each figure represent their averaged proportions. It should be noticed that the proportions of WGA-HRP labeled terminals only reveal a minority (probably about one third) of the actual number of terminals, whereas the proportions of the GABAergic terminals probably represent the actual proportions. Figure 3 shows the population of terminals selected randomly from the entire extraglomerular (A) and intraglomerular (B) neuropil, Figure 4 the population of terminals apposed to perikarya, and Figure 5 the population of terminals non-strategically (A) and strategically (B) located next to dendrites coupled by gap junctions. Note that the different surface areas of A and B in Figures 3 and 5 represent their relative shares.

percentage of the terminals were located strategically or non-strategically next to the dendrites coupled by gap junctions (first column, Table 3A, B). A terminal was considered to be strategically located, when it was apposed to both dendritic structures, which were linked by a gap junction, and non-strategically, when it was adjacent to only one of the two dendrites. In addition, percentages (\pm SEM) of morphological features were

determined as in the first population (Table 3A, B).

Statistical analysis was performed using the Student's t test. If the general assumptions of the Student's t test were not fulfilled, the results were verified using the Wilcoxon test (Glantz, '81). Differences were considered as non-significant, when the significance level was larger than five percent ($p > 0.05$).

Results

The injection sites of the cerebellar experiments all included the posterior interposed nucleus (Fig. 1A), while the injection sites of the mesodiencephalic experiments, all included the nucleus of Darkschewitsch (Fig. 2A). Semithin sections of the rostral MAO from the cats injected with WGA-HRP in the cerebellar nuclei contained retrogradely labeled perikarya and proximal dendrites, and anterogradely labeled fibers in between (Fig. 1B). The labeling was ubiquitous with a slight increase in density towards the periphery of the MAO. In semithin sections of the cats with WGA-HRP injections in the nucleus of Darkschewitsch only anterograde labeling was observed (Fig. 2B). This labeling showed the same distribution.

The immunostained ultrathin sections of the cats injected with WGA-HRP in the cerebellar nuclei contained, apart from the WGA-HRP labeled perikarya, proximal dendrites and myelinated axons, numerous non-labeled, GABA (single) labeled and (GABA/WGA-HRP) double labeled preterminal segments and terminals (Figs. 6-10, 20-26) and rarely, a WGA-HRP (single) labeled terminal. The ultrathin sections of the cats with WGA-HRP injections at the mesodiencephalic junction contained WGA-HRP labeled myelinated axons (Fig. 16) and numerous non-labeled, GABA labeled and WGA-HRP labeled preterminal segments (Figs. 11, 29) and terminals (Figs. 11-19, 27-29). Almost none of the profiles was double labeled. Following examination of serial sections it was found that the WGA-HRP labeled terminals of the mesodiencephalic experiments did not differ obviously in spatial orientation from the double labeled terminals of the cerebellar experiments. GABAergic cell bodies were not observed in any of the experiments.

The four subgroups, i.e. the non-labeled, GABA labeled, double labeled and WGA-HRP labeled terminals, which were present in the population obtained from the entire

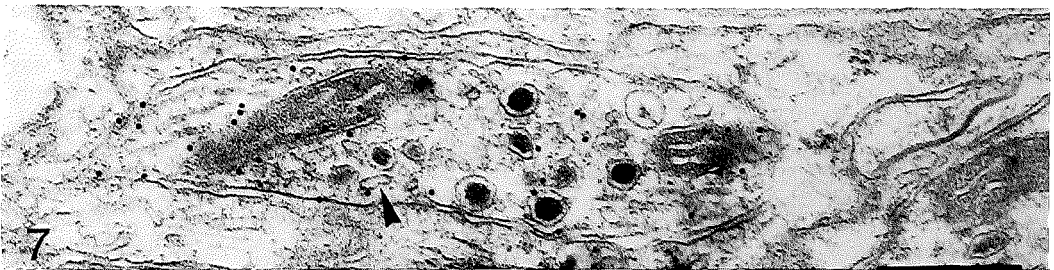
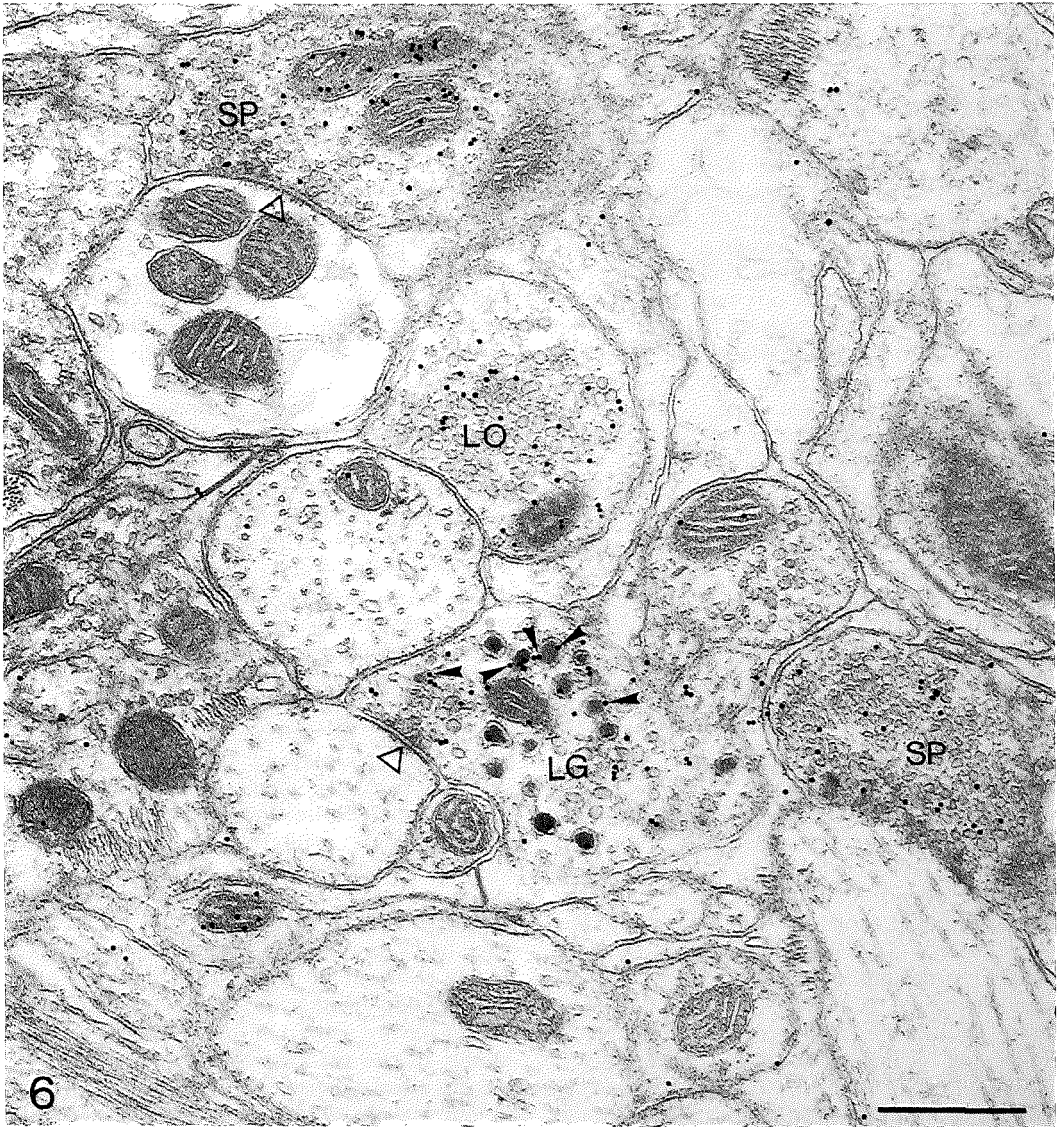
neuropil (Figs. 6-15), were observed also among the terminals apposed to perikarya (Figs. 16-20), and among the terminals associated with gap junctions (Figs. 21-29).

Terminals selected from the entire neuropil.

MORPHOLOGY. Based on differences in vesicle shape as observed in the sections of the animals perfused with the cacodylate buffered fixative, three types of GABAergic terminals (Fig. 6) and three types of non-GABAergic terminals (Figs. 12, 15) were observed.

The first and most numerous GABAergic type contained mainly small pleomorphic vesicles of 20x40 nm (Fig. 6). These terminals were often double labeled in the cerebellar experiments. They ranged in diameter from 0.5 μ m to 3.5 μ m with an average of 1.8 μ m, and often included mitochondria and a few dense core vesicles. They established primarily, but not invariably (84%-94%), synapses corresponding to Gray's type II (Figs. 6, 9, 11; Tables 1A, B). The larger terminals of this type frequently showed more than one synapse (Fig. 9). Infrequently, these GABAergic terminals showed single rows of subsynaptic densities which were located in a constricted dendrite and interposed between two terminals exhibiting clear asymmetric synapses (Figs. 13, 14). These structures, which resemble the so-called crest synapses (Milhaud and Pappas,'66; Akert et al.,'67), have been described for the dorsal cap of the rabbit (Mizuno et al.,'74), for the MAO of the monkey (Rutherford and Gwyn,'80), and for an olivary spine and two GABAergic terminals of the rat (Sotelo et al.,'86). Five of the six crest synapses observed, were formed by one or two GABAergic terminals, indicating that most crest synapses in the rostral MAO may be associated with GABAergic terminals.

The second GABAergic type, which was less frequently observed, contained mainly large oval vesicles of 40x65 nm (Fig. 6). Apart from the shape and size of the vesicles, these terminals resembled morphologically the first type.



The third GABAergic type, the large granular type, contained a large number of dense core vesicles of 90 nm, interspersed between clear oval vesicles and tubulovesicular elements (Fig. 6, 7). All types of vesicles in these terminals appeared irregularly shaped. The terminals were more or less elongated and ranged in diameter from 0.4 to 1.5 μm with an average of 0.8 μm . They rarely exhibited a synapse. None of them were ever found to be WGA-HRP labeled in the cerebellar experiments.

The first non-GABAergic type, which accounted for about 95% of the non-GABAergic terminals, contained primarily large, round and oval vesicles of 40x50 nm. It was the only type, which was WGA-HRP labeled in the mesodiencephalic experiments. These terminals ranged in diameter from 0.5 μm to 4.1 μm with an average of 1.9 μm , and usually contained mitochondria and sometimes a few dense core vesicles. The vast majority (90%-97%) of them formed synapses corresponding to Gray's type I (Figs. 12, 15, 18; Tables 1A, B), sometimes with an intermediate band in the synaptic cleft (Fig. 18). They frequently made more than one synapse (Fig. 15), some of which established both an asymmetric and a more symmetric synapse. Taxi bodies (Taxi,'61) were observed much

Fig. 6. Electron micrograph showing the three types of GABAergic terminals (black dots): two terminals contain small clear pleomorphic vesicles (SP), one terminal contains large clear oval vesicles (LO) and another one contains a high number of large granular vesicles (LG). Note that some dense core vesicles contain one or more gold particles in their clear peripheral part (arrow heads). Two of the GABAergic terminals establish a symmetric synapse (triangle). Scale bar = 0.51 μm .

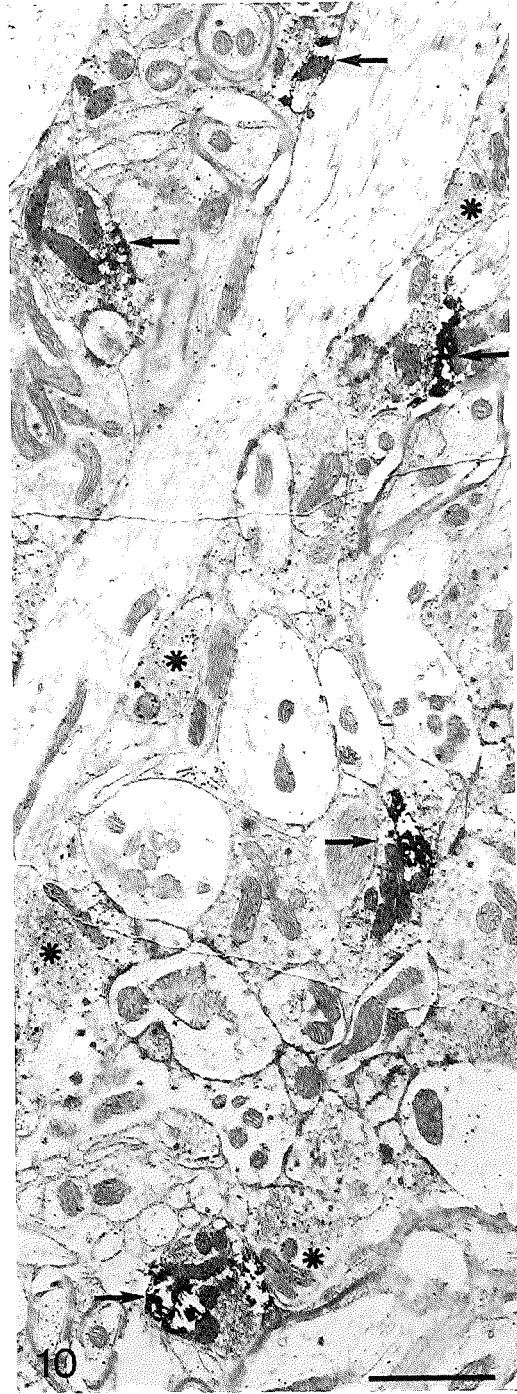
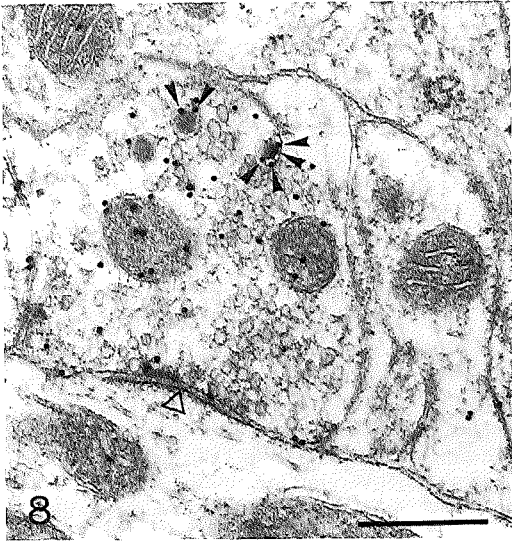
Fig. 7. Electron micrograph of a GABAergic large granular terminal-profile with an elongated shape, which contains a variety of large granular vesicles and tubulovesicular elements (arrow head). Scale bar = 0.42 μm .

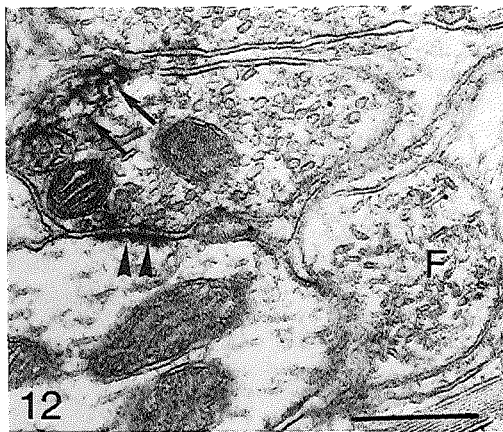
more frequently subsynaptic to these WGA-HRP labeled and non-labeled terminals (Figs. 19, 27) than to GABAergic terminals.

The second non-GABAergic type, contained a large number of dense core vesicles and was morphologically similar to the GABAergic, large granular type. This type of non-GABAergic terminals accounted for approximately 85% of the total number of large granular terminals.

The third non-GABAergic type, which was only rarely observed, contained only flattened vesicles of 15x50 nm (Fig. 12). These terminals, which were observed before in the IO of the opossum by Bowman and King ('73), ranged in diameter from 0.4 μm to 1.2 μm with an average of 0.7 μm . The last two types of non-GABAergic terminals, which were never WGA-HRP labeled in the mesodiencephalic experiments, rarely established a synaptic contact.

Considering the labeling at the subcellular level it was found in most of the GABAergic profiles that the gold particles were concentrated over the matrices of the mitochondria (Figs. 11, 28), while fewer were located in the vesicles and the axoplasm in between. When dense core vesicles were labeled, the gold particles were primarily located in their clear peripheral part. This was observed both, in large granular terminals (Fig. 6) and in clear vesicle terminals, which contained only a few dense core vesicles (Figs. 8, 9). With regard to the TMB/DAB-Co reactionproducts of the WGA-HRP labeled profiles, it was observed that they appeared as electrondense deposits, which showed the dense outline of the original crystalline TMB reactionproduct. Sometimes, the centers of these products contained electron lucent spaces (Figs. 9, 10, 15). In most cases, the reaction products were located in the periphery of the labeled profile (Fig. 10) and occasionally it pierced through the membrane. The WGA-HRP labeled profiles often displayed a slight increase in density of their axoplasm (Fig. 16) and vesicle membranes (Figs. 15, 18). Infrequently smaller and more diffuse reaction products were observed (Fig. 9).





Figs. 8-10. Electron micrographs of labeled profiles following injection of WGA-HRP in the cerebellar nuclei combined with GABA immunocytochemistry.

Fig. 8. A GABA labeled terminal showing a synapse with a rather wide synaptic cleft (triangle). Note that the terminal with predominantly clear vesicles contains a few dense core vesicles which are labeled with gold particles in their clear peripheral part (arrow heads). Scale bar = 0.37 μ m.

Fig. 9. A GABA/WGA-HRP double labeled terminal, which establishes symmetric synapses with several dendritic elements (triangles). The TMB/DAB-Co reaction product appears as electron dense deposits along the outline of the original crystalline TMB reaction product (large arrows), which is electron lucent in the center and contains almost no gold particles. Some smaller and more diffuse reaction products are present in the upper part of the terminal (small arrows). The terminal contains a few dense core vesicles, which contain gold particles in their clear peripheral part (arrow heads). Scale bar = 0.70 μ m.

Fig. 10. Example of an area, in which the majority of the GABAergic terminals is GABA/WGA-HRP double labeled. The GABA single labeled terminals are indicated by the asterisks and the GABA/WGA-HRP double labeled terminals by the arrows. Note that the dense TMB/DAB-Co reaction products of the double labeled terminals appear in most cases along the membrane of the terminal. Scale bar = 2.3 μ m.

Figs. 11-14. Electron micrographs of labeled profiles, following injection of WGA-HRP in the mesodiencephalic junction combined with GABA immunocytochemistry.

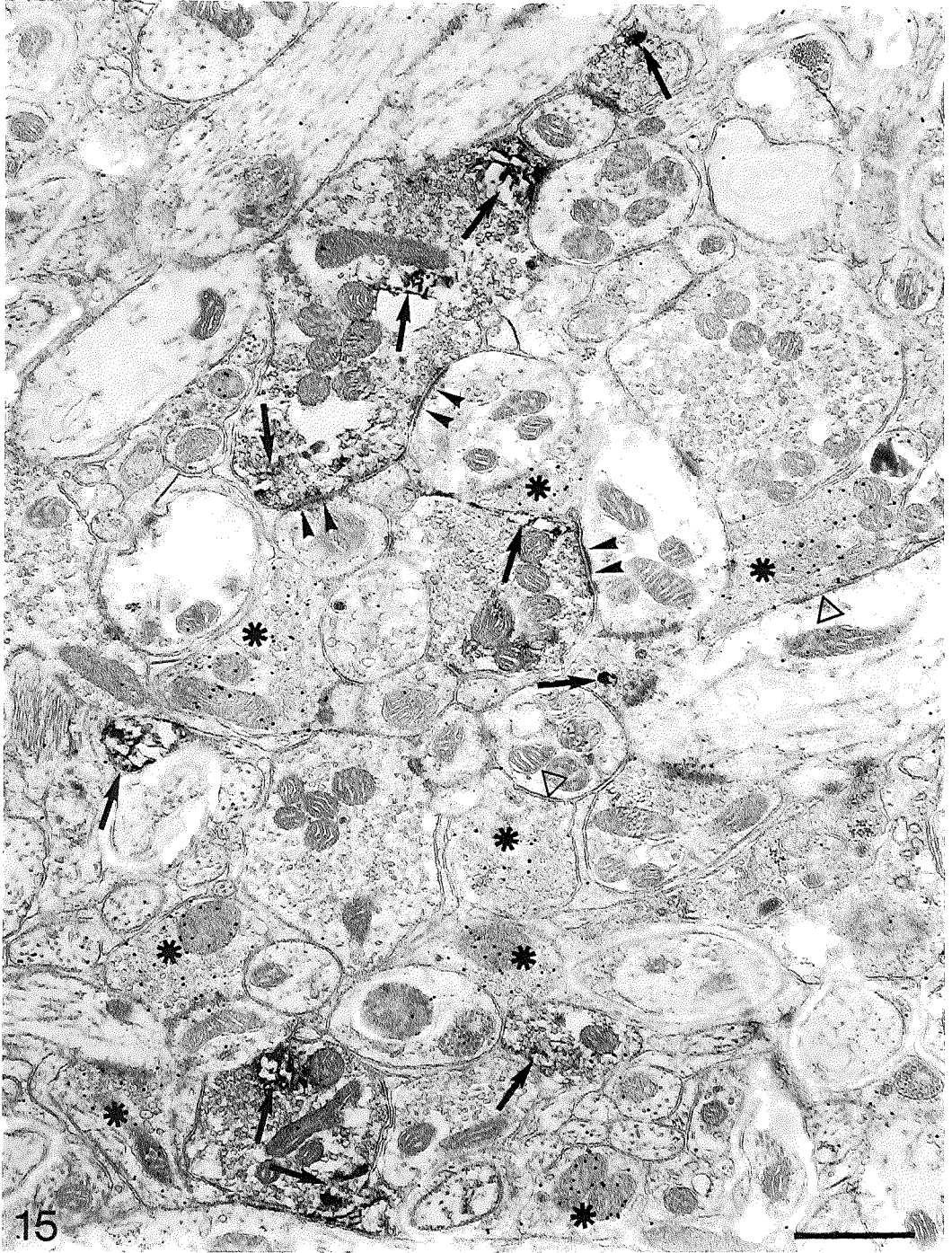
Fig. 11. A GABA labeled terminal and its preterminal axon, which is cut longitudinally and two WGA-HRP labeled preterminal axon segments (arrows), which are cut transversally. The GABAergic terminal establishes a symmetric synapse (triangle). Note that the mitochondria of the GABAergic bouton and its preterminal segment, are densely labeled. Scale bar = 0.9 μ m.

Fig. 12. Two non-GABAergic terminals, of which one contains only flattened vesicles (F), while the other one contains primarily oval vesicles. This latter terminal is WGA-HRP labeled (arrows) and establishes an asymmetric synapse (arrow heads). Scale bar = 0.37 μ m.

Fig. 13. A crest synapse between two GABAergic terminals. Note that the upper GABAergic terminal does not only establish a crest synapse with the narrow dendritic element, but also a symmetric synapse (triangle) with the dendrite on the right. Scale bar = 0.57 μ m.

Fig. 14. A narrow dendritic element of a crest synapse running parallel to the dendrite from which it arises (two open arrows). Note that the GABAergic terminal on the right contacts the narrow dendritic element involved in the crest synapse with an asymmetric synapse and the larger part of the same dendritic structure with a symmetric synapse (triangle). Scale bar = 0.62 μ m.

Fig. 15. Electron micrograph of an area, in which the majority of the non-GABAergic terminals is WGA-HRP labeled, following injection of WGA-HRP in the mesodiencephalic junction combined with GABA immunocytochemistry. The WGA-HRP labeled profiles are indicated by the arrows and the GABA labeled terminals by the asterisks. The WGA-HRP labeled terminals establish asymmetric synaptic contacts (arrow heads) and the GABAergic terminals symmetric synapses (triangles). Scale bar = 1.3 μ m.



QUANTIFICATION. The populations randomly selected from the entire neuropil in sections of cats with injections of WGA-HRP in the cerebellum (n=912) and with injections at the mesodiencephalic junction (n=721) consisted for respectively 37% and 38% of GABAergic terminals *1, (first columns Tables 1A, B). Double labeling from the cerebellum in the first experimental group was found in 30% of the GABAergic terminals (second column Table 1A). Conversely only 1% of the non-GABAergic terminals in this group was WGA-HRP labeled (not represented in the Table). Of the non-GABAergic terminals in the mesodiencephalic experiments 26% were WGA-HRP labeled (second column Table 1B), and only one GABAergic terminal was found to be double labeled.

Labeling with WGA-HRP was restricted to a minority of the GABAergic and non-GABAergic terminals. However, these percentages represent averages over a large number of areas. When areas containing the largest numbers of WGA-HRP labeled terminals were considered, it was obvious that the majority of the GABAergic terminals obtained from the cerebellar experiments (Fig.10), and the majority of the non-GABAergic terminals obtained from the mesodiencephalic experiments (Fig. 15) were WGA-HRP labeled.

LOCATION. Two thirds (63%-72%) of the terminals of each subgroup of both experimental groups, were located outside a glomerulus (Figs. 3A, B; Tables 1A, B). Half or less (37%-49%) of these terminals established one or more synapses, mostly with intermediate and small dendrites and sometimes with proximal dendrites. For the intraglomerular terminals (28%-37%), it was found that the majority (68%-90%) exhibited a synapse, most often with a small dendrite.

Among the 1633 terminals selected randomly from the entire neuropil of both experimental groups only 39 (2.4%) were located adjacent to perikarya or perikaryal spines and only 20 (1.2%) were apposed to dendrites linked by gap junctions.

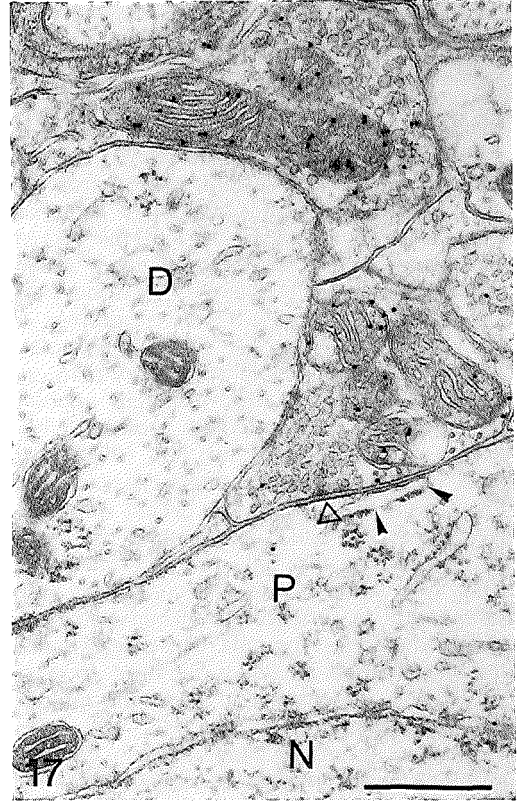
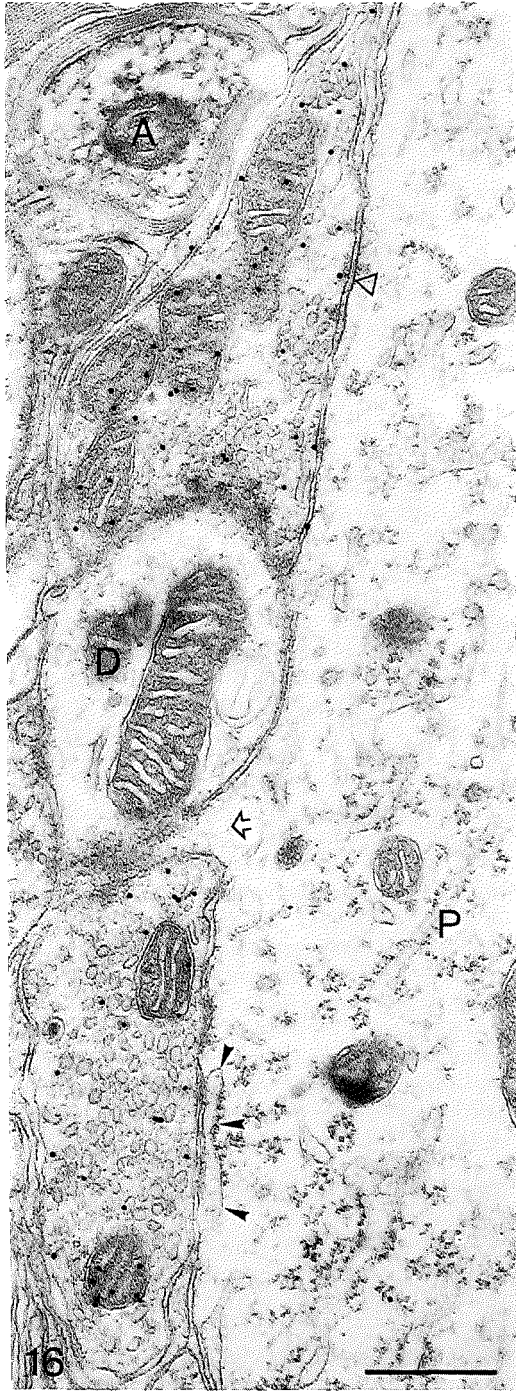
Figs. 16-18. Electron micrographs of labeled profiles apposed to perikarya, following injection of WGA-HRP in mesodiencephalic junction combined with GABA immunocytochemistry.

Fig. 16. Two GABAergic terminals apposed to a perikaryon (P). The upper one establishes a symmetric contact (triangle) with the perikaryon and is located adjacent to a dendrite (D), which is itself apposed to the same soma. The other one shows a subsurface cistern (arrow heads) and is apposed to a protrusion (open arrow) of the perikaryon. In the upper left corner a myelinated axon (A) is sparsely labeled with WGA-HRP. Scale bar = 0.35 μ m.

Fig. 17. Two GABAergic terminals of which one is apposed to a perikaryon (P), while the other one is apposed to a nearby dendrite (D). Note that the GABAergic terminal adjacent to the cell body shows both a symmetric contact (triangle) and a subsurface cistern (arrow heads). The nucleus (N) of this olivary cell is located in close proximity to this terminal. Scale bar = 0.50 μ m.

Fig. 18. A WGA-HRP labeled terminal (arrows) is apposed to a perikaryon (P) without a synapse but contacts a dendrite (D) with an asymmetric synapse (arrow heads), which shows an intermediate band in its cleft. A GABA labeled terminal is also present. This terminal is neither apposed to the perikaryon nor to the dendrite. Note that the membranes of the vesicles of the WGA-HRP labeled terminal appear denser stained than those of the GABAergic terminal. Scale bar = 0.54 μ m.

*Note *1. The cumulative average (38% \pm 0.8) of the proportions of GABAergic terminals obtained from both experimental groups was significantly lower (Student's t test, $p < 0.001$) than the one of the non-GABAergic terminals (62% \pm 0.8).*



Terminals apposed to perikarya.

MORPHOLOGY. The three types of GABAergic terminals (see above), including those which were double labeled in the cerebellar experiments, were all present among the terminals adjacent to perikarya. With an average diameter of 1.3 μm , ranging from 0.5 μm to 2.5 μm , these GABAergic terminals were somewhat smaller than in the rest of the neuropil. The majority of them (63%-74%) established a synapse with the perikaryon, mostly (92%-97%) according to Gray's Type II (Figs. 16, 17, 20; Tables 2A, B). A few of them established more than one synapse. The GABAergic terminals apposed to a perikaryon frequently showed subsynaptic cisterns (Rosenbluth, '62), which were most often present as a single cistern with a few ribosomes (Figs. 16, 17). These subsurface structures, which were found previously in the IO of the opossum (Bowman and King, '73), were observed more frequently subsynaptic to GABAergic terminals than to non-GABAergic terminals. This suggests that the GABAergic terminals apposed to perikarya may be associated with the protein synthesizing apparatus.

Apart from a few large granular terminals, all non-GABAergic terminals apposed to perikarya contained round and oval vesicles. Some of them were WGA-HRP labeled in the mesodiencephalic experiments (Figs. 18, 19). The diameter of these terminals ranged from 0.5 μm to 2.7 μm , with an average of 1.4 μm . Compared with the randomly selected terminals in the neuropil relatively few of these somatic terminals (38%-44%) made synaptic contacts, and only about half of these synapses (52%-60%) were according to Gray's Type I (Tables 2A, B). The post-synaptic densities of the asymmetric synapses were less distinct than usual, and Taxi bodies were observed once (Fig. 19).

QUANTIFICATION. Among the populations of somatic terminals selected from cats with injections in the cerebellar nuclei ($n=278$) and from cats with mesodiencephalic injections ($n=216$) GABAergic terminals accounted for respectively 62% and 66% (Tables 2A, B). Therefore, GABAergic terminals

constitute the majority of the somatic terminals, and were observed more frequently than would be expected from the overall GABAergic innervation in the neuropil*2. The proportion of GABAergic terminals, which was double labeled from the cerebellum was significantly lower (Student's T-Test, $p<0.001$) among the terminals located adjacent to perikarya ($13\% \pm 0.9$) than among the terminals selected randomly from the neuropil ($38\% \pm 0.8$), (compare Figs. 3 and 4). For the non-GABAergic terminals, none was labeled from the cerebellum, whereas from the mesodiencephalic junction an average of 20% was found to be labeled. This percentage ($20\% \pm 2.5$) did not differ significantly from the percentage ($26\% \pm 2.7$) of the non-GABAergic, WGA-HRP labeled terminals selected randomly from the neuropil.

LOCATION. Most of the terminals contacting perikarya, were arranged in clusters of two or three terminals. These somatic terminals often were apposed to single dendrites located adjacent to the perikaryon (Figs. 16, 17), sometimes making synaptic contacts with both. Less frequently terminals were apposed to perikaryal spines (Figs. 16, 19). Some of the GABAergic terminals, which were not arranged in a cluster but present as single terminals on the perikarya, were found to be of the en passant type.

*note*2. The cumulative average ($64\% \pm 1.5$) of the proportions of GABAergic terminals adjacent to perikarya obtained from both the cerebellar and mesodiencephalic experiments was significantly higher (Student's t test, $p<0.001$) than the one of the non-GABAergic terminals adjacent to perikarya ($36\% \pm 1.5$), and than the one of the GABAergic terminals selected randomly in the entire neuropil ($38\% \pm 0.8$).*

Terminals next to dendrites coupled by a gap junction.

MORPHOLOGY. The GABAergic terminals associated with gap junctions, including the terminals which were double labeled in the cerebellar experiments, contained mostly small pleomorphic vesicles. None of them

was of the large granular type. With an average diameter of 1.5 μ m, ranging from 0.8 to 3.1 μ m, these terminals were somewhat smaller than those sampled from the entire neuropil. Frequently, they contained mitochondria and a few dense core vesicles. The majority of them (85%-100%) established synapses according to Gray's Type II (Figs. 23, 24; Tables 3A, B).

The mesodiencephalic experiments showed that all WGA-HRP labeled and non-labeled terminals associated with gap junctions, contained round or oval vesicles. These non-GABAergic terminals with an average diameter of 1.5 μ m ranging from 0.6 to 3.3 μ m, frequently contained mitochondria and a few dense core vesicles, and the majority of them (80%-100%) exhibited a synapse according to Gray's type I (Figs. 28, 29; Tables 3A, B).

QUANTIFICATION. Among the terminals sampled from the cerebellar group (n=127) and the mesodiencephalic group of experiments (n=129) respectively 33% and 30% were located strategically with respect to a gap junction (i.e., apposed to both dendrites coupled by a gap junction), (tables 3A, B). Half of the strategically located terminals was GABAergic (55% in the cerebellar group; 50% in the mesodiencephalic group). When both groups of experiments were combined the cumulative average of the GABAergic terminals was significantly higher (Wilcoxon test, $p < 0.05$) for this group of strategically located terminals ($53\% \pm 5.3$) than among the terminals randomly selected from the entire neuropil ($38\% \pm 0.8$). This indicates that there are more GABAergic terminals contacting both dendrites coupled by a gap junction than would be expected from a random GABAergic input (Compare Fig. 3 and 5B). GABAergic terminals occurred less frequently among the non-strategically located terminals (36% in the cerebellar group, 34% in the mesodiencephalic group), (Tables 3A, B). The cumulative average of the GABAergic, non-strategically located terminals in the combined experimental groups ($34\% \pm 6.7$) did not differ significantly from the

population of GABAergic terminals from the entire neuropil ($38\% \pm 0.8$). With regard to the WGA-HRP labeled terminals, it appeared that their proportions among the strategically and non-strategically located, GABAergic and non-GABAergic terminals in the two experimental groups did not differ significantly from the percentages obtained from the entire neuropil (compare second columns Table 1A, B and 3A, B).

LOCATION. The majority (70%-100%) of the non-labeled, GABA labeled, double labeled and WGA-HRP labeled terminals associated with gap junctions was located within a glomerulus, most frequently contacting small dendritic elements (Figs. 21-29; Tables 3A, B). Most of the intra- and extraglomerular located terminals established synapses. The strategically located, GABAergic, glomerular terminals relatively often exhibited a synapse (83%-90%), whereas, the non-strategically located, non-GABAergic, extraglomerular terminals exhibited relatively few synapses (50%-57%). Gap junctions between cell bodies were never observed. Only in one case, a junctional zone of a perikaryal spine was observed with some characteristics of a gap junction (Fig. 20).

PERCENTAGES OF GAP JUNCTIONS. In the analyzed, non-serial ultrathin sections 94 gap junctions were observed (49 from the cerebellar and 45 from the mesodiencephalic experiments). Of these gap junctions 70 were associated with at least one GABAergic terminal and 80 with at least one non-GABAergic terminal. The total number of terminals apposed to the electro-tonically coupled dendrites was 256, indicating that in this two-dimensional analysis, on the average 2.7 (256/94) terminals were apposed to two dendrites linked by a gap junction.

Discussion

The rostral MAO receives a projection from the posterior interposed nucleus of the cerebellum (Tolbert et al., '76) and the nucleus of Darkschewitsch (Onodera, '84). In the present study, we looked at the morphology and distribution of these afferents in relation

to the GABAergic input. Special emphasis was put on terminals apposed to perikarya and located next to dendrites coupled by gap junctions.

General morphology of the terminals.

As described in cat (Walberg,'66; Sotelo et al.,'74), opossum (Bowman and King,'73), rat (Gwyn et al.,'77) and monkey (Rutherford and Gwyn,'80), it was observed in the present study that the majority of olivary boutons contained either round and/or oval vesicles and asymmetric synapses or pleomorphic vesicles and symmetric synapses.

With regard to the GABAergic terminals, we distinguished three different types. The most frequent type, which was often double labeled in the cerebellar experiments, contained pleomorphic vesicles and exhibited primarily, but not exclusively, symmetric synapses. Our findings are largely in agreement with recent studies of the GABAergic and cerebellar innervation of the rat IO (Sotelo et al.,'86; Angaut and Sotelo,'87). However, in previous studies of the IO of the opossum and the cat it was found that cerebellar terminals contained spherical vesicles (King et al.,'76; Mizuno et al.,'80) and exhibited asymmetric synapses (Mizuno et al.,'80). The difference in shape of the vesicles may be due to a different type and osmolarity of the buffer used for the fixative (Valdivia,'71) and/or to a different duration of exposure of the tissue to aldehydes (Paula-Barbosa,'75).

Concerning the mesodiencephalic terminals, which were all non-GABAergic (cf. De Zeeuw et al.,'88a), our results were in agreement with studies of King et al. ('78) and Cintas et al. ('80), which showed respectively in opossum and rat, that most of the mesodiencephalic terminals had round vesicles and asymmetric synapses. Taxi bodies were much more associated with mesodiencephalic terminals than with GABAergic terminals. Similar structures have also been observed subsynaptic to asymmetric synapses of round vesicle containing terminals in the IO of the opossum (Bowman and King,'73), and the squirrel monkey (Rutherford and

Gwyn,'80). Although these subsynaptic densities are apparently primarily associated with excitatory synapses, their precise functional significance remains unclear.

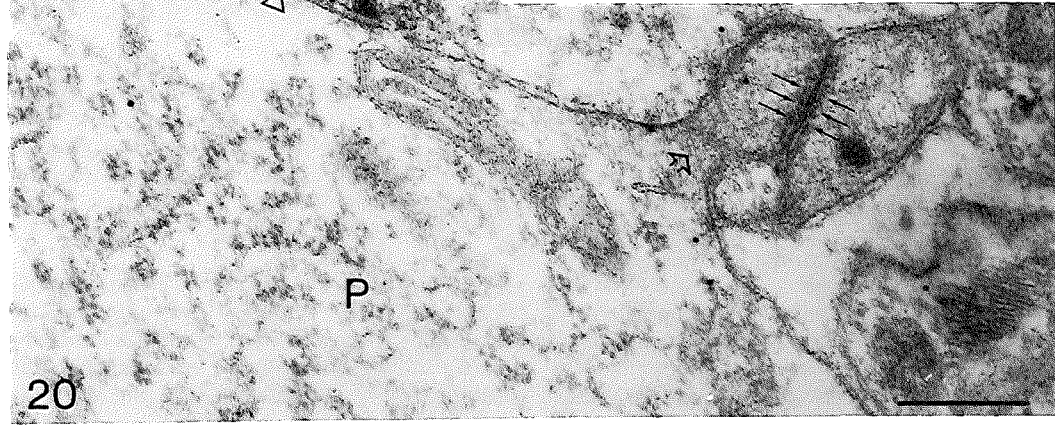
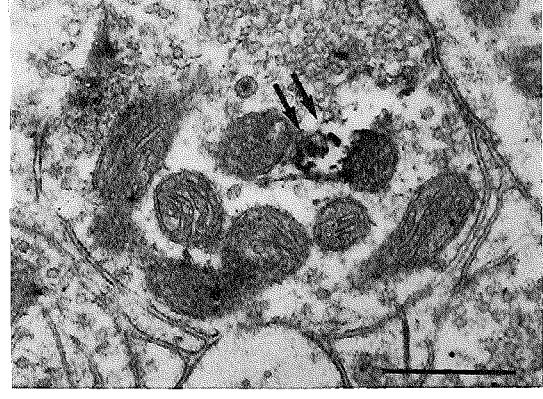
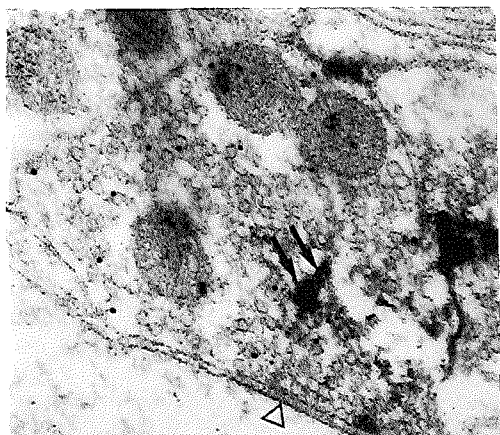
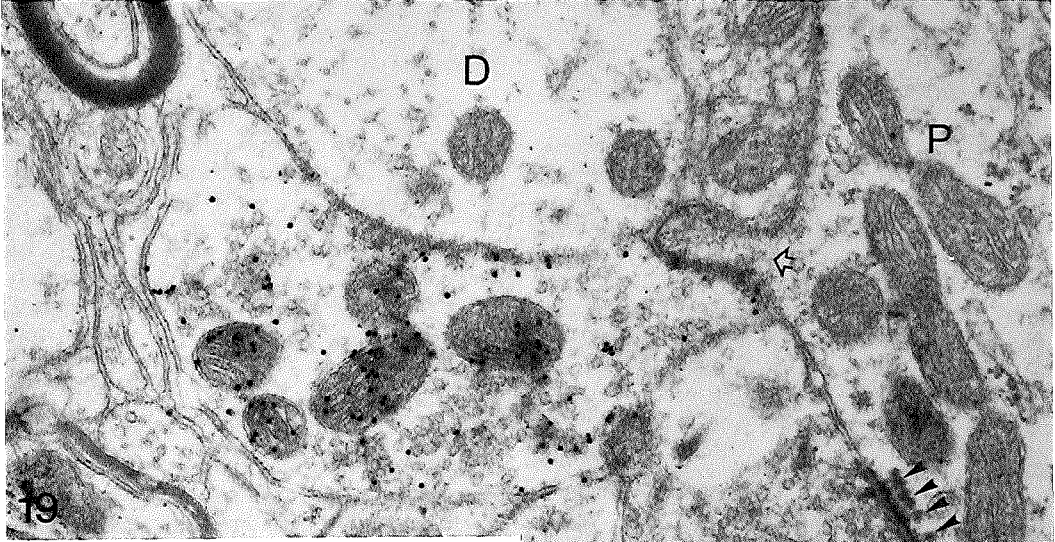
General observations at the subcellular level.

GABA immunostaining generally resulted in dense labeling of the matrices of mitochondria. This finding, which was also reported in a study by Buijs et al. ('87), suggests that GABA is primarily produced in mitochondria. This is in line with the fact that the key reaction of GABA formation in the CNS is a decarboxylation of L-glutamate (Seiler and Lajtha,'87), which is for the greater part synthesized from an intermediate of the citric acid cycle in the mitochondrial matrix (Stryer,'81).

GABA immunolabeling was also found within dense core vesicles. This suggests a coexistence of GABA with one or more neuropeptides, which are presumably located in the dense core of these vesicles (for review, see Hokfelt et al.,'86). The relatively

Fig. 19. Electron micrograph of labeled profiles following injection of WGA-HRP in the mesodiencephalic junction combined with GABA immunocytochemistry. A GABA labeled terminal is apposed to a perikaryal spine (open arrow) and a dendrite (D). A WGA-HRP labeled terminal (arrows) contacts the perikaryon (P) with an asymmetric synapse, which shows a row of subsynaptic densities (arrow heads). Scale bar = 0.40 μ m.

Fig. 20. Electron micrograph of a GABA/WGA-HRP double labeled terminal (arrows) following injection of WGA-HRP in the cerebellar nuclei combined with GABA immunocytochemistry. This terminal establishes a symmetric synapse (triangle) with a perikaryon (P). Nearby a spine (open arrow) with a junctional zone (small arrows) emerges from the perikaryon. The membranes of this zone are closer to each other than usual and at both sides of it there is a deposit of dense cytoplasmic material, suggesting the presence of a gap junction. Scale bar = 0.34 μ m.



high number of gold particles in the clear periphery of these vesicles suggest that the GABA molecules may be located primarily in this area.

With regard to the WGA-HRP labeled profiles, the TMB/DAB-Co reaction products appeared as electron dense deposits often showing the dense outline of the original crystalline TMB reaction product with in the center electron lucent spaces. These holes were probably due to the DAB-Co stabilization procedure, since they did not appear in non-stabilized material (Mesulam, '78; Holstege and Kuypers, '87; De Zeeuw et al., '88a) and since they appeared as well in stabilized material, which was not processed for immunocytochemistry (Lemann et al., '85).

Quantification of terminals.

The percentages of the GABAergic, cerebellar and mesodiencephalic terminals in the rostral MAO were determined by counting terminals present in a randomly selected area of ultrathin sections (see collection and analysis of the data). Differences in size and possible differences in orientation between the different subgroups appeared to be small, according to the present results and those earlier described for opossum (King et al., '76; King et al., '78), rat (Gwyn et al., '77) and monkey (Rutherford and Gwyn, '80). Therefore this quantification of the percentages in the two dimensional plane may provide a reliable estimate of the actual distributions.

WGA-HRP tracing studies only label a minority of the actual number of terminals. Since injections of WGA-HRP at different locations in different animals may yield a different proportion of labeling, direct quantitative comparisons between proportions of WGA-HRP labeled terminals from the cerebellar and the mesodiencephalic experimental group were avoided. Comparisons were only made between different populations obtained from the same group of experiments. On the other hand, we felt confident in comparing the proportions of GABAergic and non-GABAergic terminals because the present GABA-immunocytochemical procedure was found to detect

consistently almost all GABAergic terminals (de Zeeuw et al., '88a).

Terminals selected from the entire neuropil.

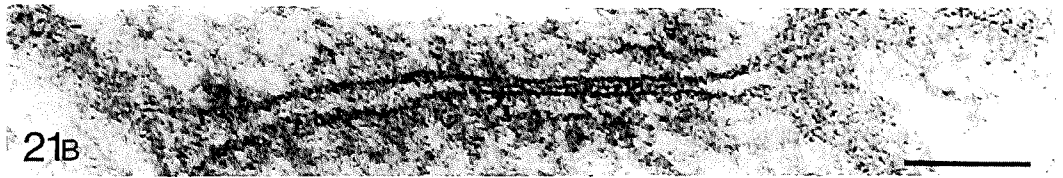
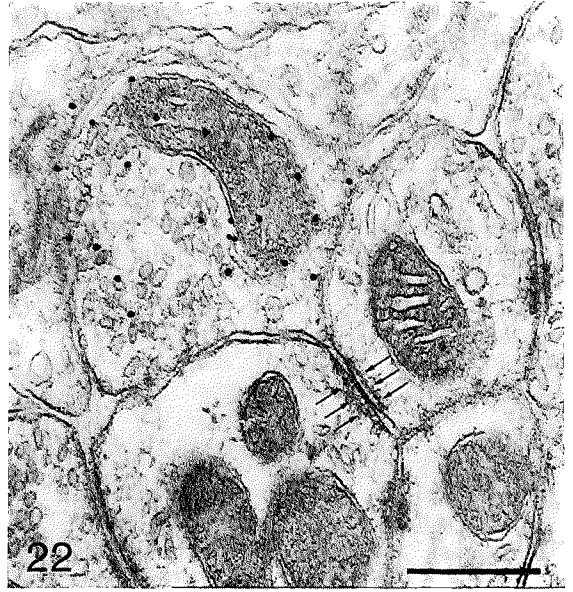
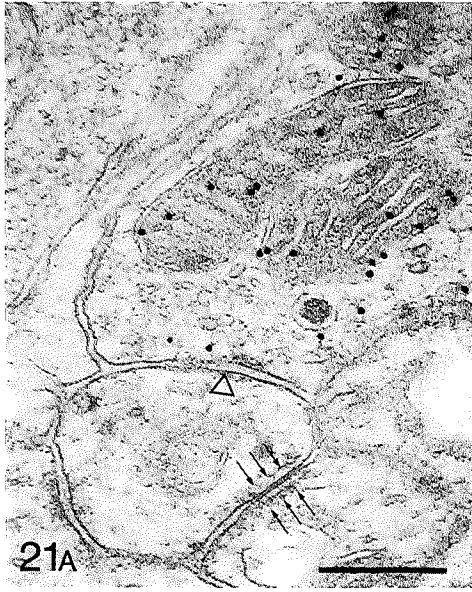
It was found in the cerebellar experiments that the majority of the GABAergic terminals was double labeled in sample areas with relatively large numbers of WGA-HRP labeled terminals (Fig. 10). Moreover, most of the GABA single and double labeled terminals showed the same morphological characteristics. Together with the finding of Nelson and Mugnaini ('87), that more than 90% of GABAergic fibers in the rostral MAO disappear following cerebellectomy, these data indicate that the large majority of these GABAergic fibers are derived from the cerebellar nuclei. Our quantitative analysis, in which the data of all sample areas were averaged, showed that 30% of the GABAergic terminals were double labeled. This indicates that our WGA-HRP anterograde tracing technique as applied to the cerebello-olivary projection, may detect on average one third of the actual number of terminals.

The quantitative analysis of the mesodiencephalic experiments, showed that 26% of the non-GABAergic terminals were

Fig. 21. Electron micrograph of a non-strategically located GABAergic terminal making a synaptic contact (triangle) with one of the dendritic structures coupled by a gap junction (small arrows in A; higher magnification in B). Scale bar in A = 0.28 μ m, in B = 0.07 μ m.

Fig. 22. Electron micrograph of a strategically located GABAergic terminal apposed to both dendritic elements coupled by a gap junction (small arrows). Note that the terminal does not make any synaptic contact with any of the dendritic elements. Scale bar = 0.29 μ m.

Fig. 23. Electron micrograph of two strategically located GABA labeled terminals making symmetric synaptic contacts (triangles) with the dendritic elements coupled by a gap junction (small arrows). Scale bar = 0.23 μ m.



labeled with WGA-HRP. Provided the efficacy of anterograde transport in this pathway is the same as in the nucleo-olivary projection, this means that the majority (78%) of the non-GABAergic terminals originates in the mesodiencephalic junction. This agrees with the observations that the majority of non-labeled and WGA-HRP labeled terminals showed the same morphological features, and that the majority of the non-GABAergic terminals was WGA-HRP labeled in the areas with the highest number of WGA-HRP labeled terminals (Fig. 15). The cumulative average of the non-GABAergic terminals (62%) selected randomly in the neuropil of both the cerebellar and mesodiencephalic experiments was significantly higher than that of the GABAergic terminals. Thus, the terminals, which probably originate for a large part in the mesodiencephalon, predominate the innervation of the rostral MAO neuropil. These results are in agreement with studies in monkey (Rutherford and Gwyn,'80), cat (Mizuno et al.,'76) and rabbit (Mizuno et al.,'74), which found respectively that about 56%, 60% and 60% of randomly selected olivary terminals had round and oval vesicles and asymmetric synapses.

The above findings strongly suggest that the bulk of the innervation of the rostral MAO is derived from the posterior interposed nucleus of the cerebellum and the mesodiencephalic junction. This is in line with lightmicroscopic studies of the afferents of the IO, which did not describe any other substantial projection to the rostral MAO (Tolbert et al.,'76; Onodera,'84; Swenson and Castro,'83).

With respect to their location, it appeared that the proportions of GABAergic and non-GABAergic terminals and the relative frequency of their labeling with WGA-HRP were the same in the extra- and intraglomerular neuropil (Table 1A, B; Figs. 3A, B). This reemphasizes the hypothesis that the cerebellar and mesodiencephalic innervation of the glomeruli in the rostral MAO is random (de Zeeuw et al.,'89b).

Terminals apposed to perikarya.

In our study, a small number (2.4%) of the randomly selected terminals (first population) was located adjacent to perikarya or their spines. A higher percentage (9.7%) was found for the opossum (Bowman and King,'73). Ultrastructural studies of the IO in monkey (Rutherford and Gwyn,'80), cat (Sotelo et al.,'74), and rat (Gwyn et al.,'77) mentioned that the perikarya receive relatively few terminals but did not provide quantitative data.

In the population of terminals adjacent to perikarya (second population) 64% of the terminals were GABAergic. This was significantly higher than the proportion of 1) non-GABAergic terminals apposed to perikarya, and 2) GABAergic terminals selected randomly in the entire neuropil (compare Fig. 3 and 4). Because more GABAergic terminals exhibited synapses on the somata than non-GABAergic terminals (Table 2A, B), the proportion of GABAergic terminals would be even higher when only terminals with synaptic junctions were considered. These findings generally agree with previous studies of the IO of several species, which described that most or all of the terminals contacting the IO somata contained pleomorphic vesicles and established Gray's type II synapses (Walberg,'63; Bowman and King,'73; Gwyn et al.,'77; Rutherford and Gwyn,'80).

The proportion of the GABAergic terminals, which was labeled with WGA-HRP in the cerebellar experiments was significantly lower among the somatic terminals than among the terminals selected randomly from the entire neuropil (compare Fig. 3 and 4). This suggests that a relatively small proportion of the GABAergic input to olivary somata is derived from the cerebellum. Cerebellar axosomatic terminals were not observed in the IO of the opossum (King et al,'76) and the cat (Mizuno et al,'80). In the rat IO, however, axosomatic terminals account for 6% of terminals, which can be labeled from the cerebellum (Angaut and Sotelo,'87) and for the same percentage of GAD-positive terminals (Sotelo et al,'86). This suggests that most of the axosomatic GABAergic terminals

in the rat IO are of a cerebellar origin.

Several non-GABAergic terminals, some of which were WGA-HRP labeled in the mesodiencephalic experiments, were located adjacent to perikarya. Our data are in agreement with the study of the mesodiencephaloolivary projection in rat by Cintas et al. ('80) and with the general study of the rat IO by Gwyn et al. ('77). However, in the study of the mesodiencephalic projection to the rat IO by King et al. ('78), and in studies of the IO in cat (Walberg,'63) and monkey (Rutherford and Gwyn,'80) no mesodiencephalic terminals apposed to perikarya were observed, and no somatic terminals were provided with asymmetric synapses, respectively.

Terminals next to dendrites coupled by a gap junction.

It was first demonstrated in rat by Sotelo et al. ('86) that olivary dendrites coupled by gap junctions were contacted by GAD-positive terminals. The present study of the cat IO confirmed and extended these findings. It was observed that virtually all GABAergic terminals associated with gap junctions established symmetric synapses. The quantitative analysis showed that of the terminals strategically located next to both dendritic elements coupled by a gap junction significantly more terminals were GABAergic than would be expected from the distribution of GABAergic terminals over the entire neuropil. Significant differences were found only for the strategically located terminals, indicating the importance of the exact localization of terminals next to the gap junctions. Since it has been shown that the ingrowth of GABAergic fibers precedes the development of gap junctions (Gotow and Sotelo,'87), this suggests that gap junctions may preferentially develop between two dendritic elements, which are both innervated by a GABAergic bouton.

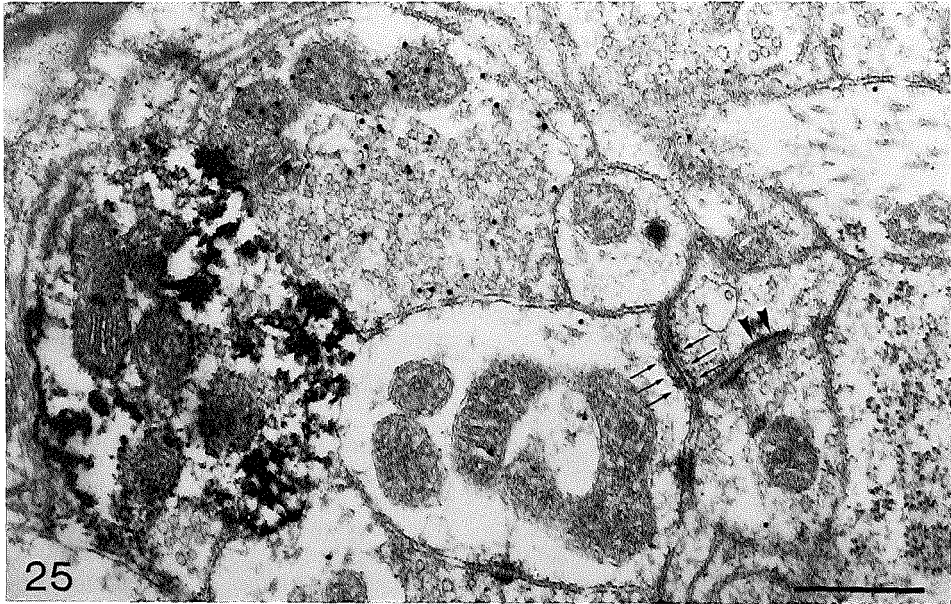
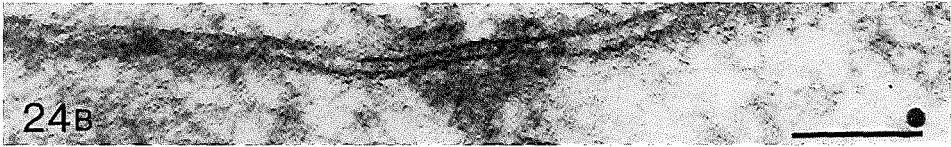
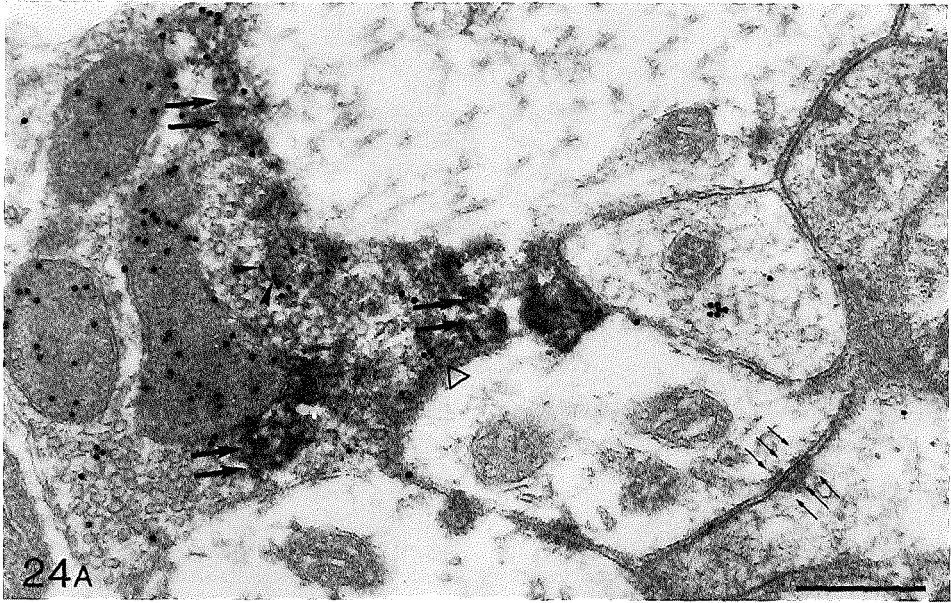
About one third of the strategically and non-strategically located GABAergic terminals were double labeled, following injection of WGA-HRP in the cerebellar nuclei. Since the present technique of WGA-HRP tracing may detect at most about one third of the actual number of terminals (see above), this

indicates that most if not all GABAergic terminals associated with gap junctions originate from the cerebellum. Our findings, which provide the first direct evidence for the cerebellar origin of the GABAergic terminals associated with gap junctions, agree with previous ultrastructural studies of the cerebellar innervation of the IO, which showed the presence of cerebellar terminals in close proximity to gap junctions (King et al., '76; Angaut and Sotelo,'87).

Non-GABAergic terminals, several of which originated from the mesodiencephalic junction, were also found to be strategically or non-strategically located next to dendrites coupled by gap junctions. Almost all these terminals, which exhibited synapses somewhat less frequently than the GABAergic terminals, established asymmetric synapses (Table 3A, B). This is in agreement with the original study of gap junctions in the cat IO by Sotelo et al. ('74), in which terminals with a similar morphology were observed next to the electrotonically coupled dendrites.

The existence and origin of a non-cerebellar GABAergic projection to the IO.

The study of Nelson and Mugnaini ('85) revealed that total cerebellectomy does not cause a complete disappearance of GAD positive terminals in the rat IO, including the rostral MAO, indicating that not all GABAergic terminals in the olive are derived from the cerebellum. Two findings of the present study confirmed this. Firstly, a substantial part of the GABAergic terminals adjacent to perikarya may be derived from a non-cerebellar source (see above). Secondly, a minority of the GABAergic terminals could be classified as large granular terminals. Large granular terminals were never, neither in the present nor in a previous study (King et al., '76; Mizuno et al., '80; Angaut and Sotelo,'87), found to originate from the cerebellum. Some GABAergic large granular terminals were apposed to somata, but they do not predominate the GABAergic axosomatic projection. The non-cerebellar GABAergic projection to the IO therefore appears to be heterogeneous. There are indications in the literature



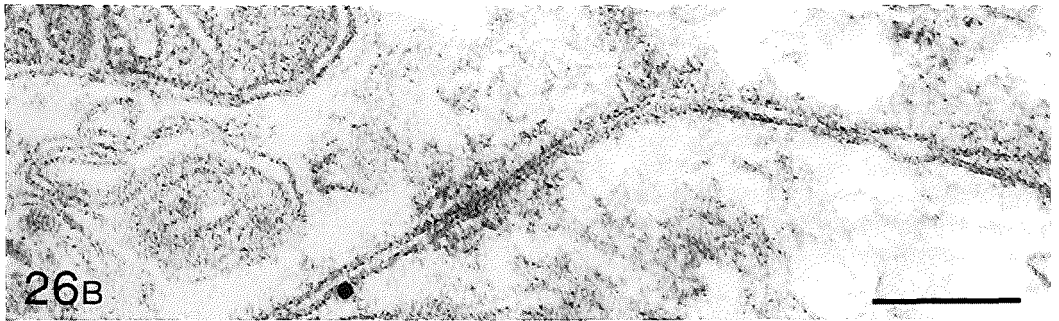
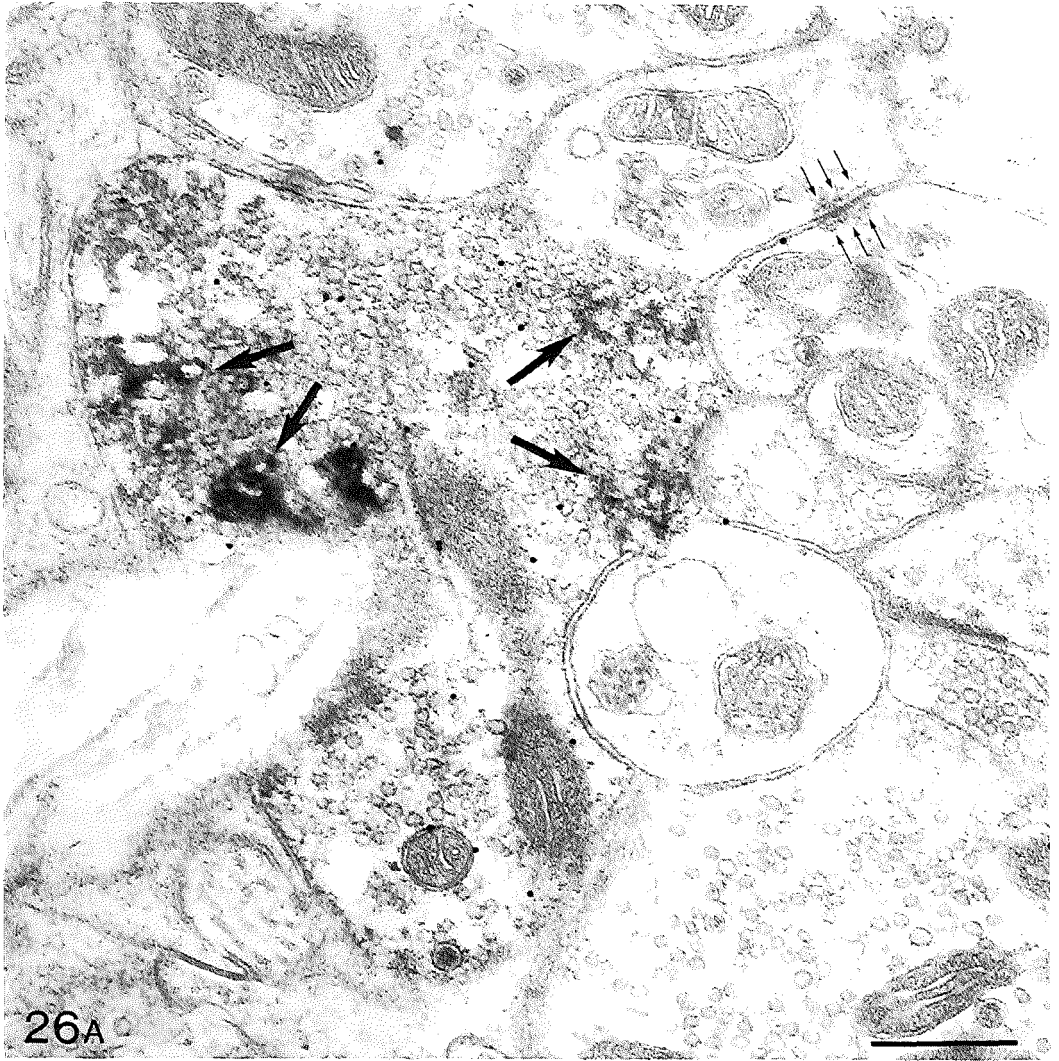


Fig. 24-26. Electron micrographs of terminals following injection of WGA-HRP in the cerebellar nuclei combined with GABA immunocytochemistry.

Fig. 24. A non-strategically located GABA/WGA-HRP double labeled terminal (arrows) establishes a synaptic contact (triangle) with one of the dendritic structures coupled by a gap junction (small arrows in A; higher magnification in B). Note that the indicated dense core vesicle (arrow heads) contains two gold particles in its clear peripheral part. Scale bar in A = 0.30 μm , in B = 0.08 μm .

Fig. 25. On the left, a non-strategically located GABA/WGA-HRP double labeled and GABA single labeled terminal do not establish synaptic contacts with one of the dendrites coupled by a gap junction (small arrows). Note that the GABA labeling of the double labeled terminal is almost restricted to the mitochondria, due to the abundant TMB/DAB-Co reaction product in the rest of the terminal. On the right, a strategically located non-labeled profile establishes an asymmetric synaptic contact (arrow heads) with the other coupled dendritic element. Scale bar = 0.41 μm .

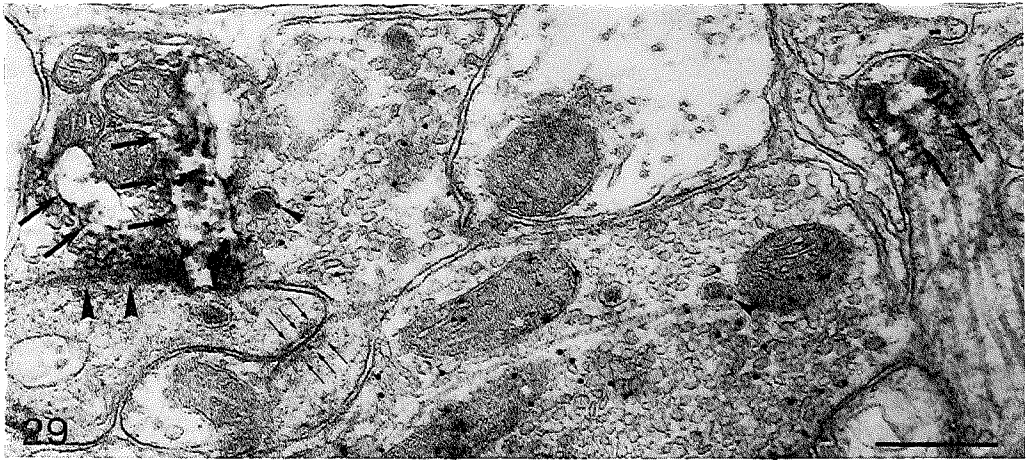
Fig. 26. A strategically located GABA/WGA-HRP double labeled terminal (arrows) is apposed to two dendritic structures coupled by a gap junction (small arrows in A; higher magnification in B). Note that the GABA labeling of this cerebellar terminal is rather sparse but that it stands out against the background labeling. Scale bar in A = 0.37 μm , in B = 0.15 μm .

Figs. 27-29. Electron micrographs of terminals, following injection of WGA-HRP in the mesodiencephalic junction combined with GABA immunocytochemistry.

Fig. 27. A non-strategically located WGA-HRP labeled terminal (arrows) and a non-strategically located GABAergic terminal, which are each apposed to one of the dendrites coupled by a gap junction (small arrows). Note that the WGA-HRP labeled terminal contacts a nearby dendrite with an asymmetric synapse with subsynaptically a small row of dense bodies (arrow heads). Scale bar = 0.58 μm .

Fig. 28. A glomerular gap junction (small arrows) between two spines, which are surrounded by four terminals. Two terminals, which are WGA-HRP labeled (arrows), a GABAergic terminal, which has a symmetric synapse (triangle) in the upper part of the picture and a non-labeled terminal, which makes an asymmetric synapse (arrow heads) with one of the electrotonically coupled spines. Scale bar = 0.49 μm .

Fig. 29. A WGA-HRP labeled terminal (arrows on the left side) and two GABAergic terminals apposed to two dendritic structures coupled by a gap junction (small arrows). The WGA-HRP labeled terminal contacts the dendritic element with an asymmetric synapse (large arrow heads). The small arrow heads in the GABAergic terminals indicate gold particles, which are located in the clear peripheral parts of the dense core vesicles. On the right side a WGA-HRP labeled preterminal axon segment can be seen (arrows). Scale bar = 0.35 μm .



however, which favour a common origin.

Part of the somatic GABAergic terminals may originate from a non-cerebellar source. Combined with the finding that the vast majority of the GABAergic axodendritic terminals originate from the cerebellar nuclei, this implies that these non-cerebellar GABAergic fibers project for a relatively large part to the olivary perikarya. Scheibel and Scheibel ('55) indeed demonstrated in their Golgi studies of the IO of various species the existence of fibers projecting mainly to somata and nearby dendrites. These fibers were found to enter the IO from the dorsomedial side and the adjoining reticular formation.

The non-cerebellar GABAergic large granular terminals resembled morphologically olivary serotonergic terminals as described by Wiklund et al. ('81) and by King et al. ('84), possibly indicating a coexistence of GABA and serotonin. Light microscopic studies of the rat, cat and monkey by Takeuchi and Sano ('83) showed that serotonin is indeed present in the rostral MAO. It seems likely that this projection originates in the nucleus reticularis paragigantocellularis (NPGC) and/or the nucleus raphe pallidus (NRP), which are both regions known to show coexistence of GABA and serotonin (Belin et al., '83; Mugnaini and Oertel, '85; Millhorn et al., '87; Harandi et al., '87) and to project to the IO (Walberg and Dietrichs, '82; Bishop and Ho, '86).

Taken together the above data suggest the existence of a non-cerebellar GABAergic projection to the IO, which may contact primarily the perikarya and/or which may show a coexistence with serotonin and originate in the NPGC or NRP.

Functional significances of the GABAergic, cerebellar and mesodiencephalic input to the rostral MAO of the cat.

The IO is probably involved in the onset of movement by modulating the synchronicity of motoneuronal firing (Llinas, '87). Two salient electrophysiological features of the olivary neurons are their tendency to oscillate (Armstrong et al., '68; Llinas and Yarom, '86;

Benardo and Foster, '86) and to fire in synchrony (Llinas et al., '74; Llinas and Yarom, '81a). Structures, which are most probably actively involved in these two processes are respectively the cell body and nearby regions, and the glomerular gap junctions. Below, the significance of the synaptic inputs to these structures is discussed, and in addition, we will discuss the most prominent input to the rostral MAO neuropil.

SOMATA. The present data indicated that the olivary somata receive a relatively small number of terminals. Still, they may be relatively important since these neurons show somatic rebound action potentials, which react in an all or none response to a small difference in the membrane potential (Llinas and Yarom, '81a and '81b). The majority of these olivary somatic terminals were found to be GABAergic. A relatively strong inhibitory input to somata is seen in many projecting neurons (Walberg, '63; Eccles, '64; Freund et al., '85; Oertel et al., '81) and may serve to inhibit impulse generation (Eccles, '64). The prominent GABAergic input to the olivary somata could just as well have an important impact on the excitability, but probably in a specific way. The tendency of these neurons to fire rhythmically is due to specific conductances, which are differentially distributed over the membrane of the soma and the dendrites (Llinas and Yarom, '81a and '81b). Recent studies (Llinas and Yarom, '86; Benardo and Foster, '86) suggested that the neuronal firing frequency of hyperpolarized cells will be dominated by a de-inactivation of the somatic Calcium conductance and that this frequency may be dependant on the level of hyperpolarization. GABA is known to have an inhibitory effect (Krnjevic and Schwartz, '66; Roberts, '74). Therefore, the main function of the prominent GABAergic input to the olivary somata, may be to regulate the somatic hyperpolarization level, and in this way, the excitability and the oscillatory firing rate.

It is interesting to note that the present study provided indirect evidence that the GABAergic somatic terminals may be derived for a substantial part from a non-cerebellar origin. This would mean that there are two

different GABAergic inputs, a non-cerebellar input regulating the excitability and a cerebellar input, which may modulate synchronous firing (to be considered next).

GAP JUNCTIONS. The present quantitative data indicated that significantly more of the terminals strategically located next to gap junctions were GABAergic than would be expected from the overall GABAergic input of the rostral MAO. Therefore, this projection may be specifically involved in the regulation of electrotonic coupling. Particular sets of parasagittal oriented Purkinje cells in the cerebellar cortex may be synchronously activated by groups of IO neurons, which are dynamically electrotonically coupled (Bower and Llinas,'83) by gap junctions in the olivary glomeruli (Sotelo et al.,'74). Physiological evidence was found that GABA may modulate this electrotonic coupling (Sasaki and Llinas,'85). Resulting conductance changes of activated GABAergic terminals are presumed to produce a shunt at the postsynaptic membrane, and in this way to reduce the coupling coefficient between the cells (Llinas,'74). The present results indicated that these more peripherally located GABAergic terminals, which have a desynchronizing effect, probably all originate from the cerebellar nuclei.

Our quantification also showed that still half of the terminals located strategically next to gap junctions were non-GABAergic, several of which originated from the mesodiencephalic junction. So far, no electrophysiological evidence has been found that these terminals may increase the electrotonic coupling of olivary neurons.

NEUROPIIL. The majority of the input to the rostral MAO neuropil was found to be non-GABAergic. Most of this input probably derives from the mesodiencephalic junction. Based on the following physiological, morphological and topographical findings, it is most likely that this non-GABAergic mesodiencephalic innervation is the major excitatory drive of the rostral MAO. Low intensity stimulation in the area of the nucleus of Darkschewitsch produces climbing fiber responses in the cerebellar C2 zone of the

cat (Jeneskog,'87), which is known to receive climbing fibers from the rostral MAO (Groenewegen et al.,'79). Since Golgi studies (Ramon y Cajal,'09; Scheibel and Scheibel,'55) and GAD immuno-staining studies (Sotelo et al.,'86; Nelson and Mugnaini,'87) showed that interneurons and GAD positive neurons are almost or totally absent in the IO, it may be assumed that the stimulation mentioned above had a direct excitatory effect in the rostral MAO. Recently, it was indeed demonstrated that stimulation in the nucleus of Darkschewitsch evoked monosynaptically action potentials in intracellularly penetrated IO cells (Ruigrok et al.,'88). The morphological finding that most of the mesodiencephalic terminals contained primarily rounded vesicles and synapses according to Gray's type I, also suggest that these terminals are excitatory (Uchizono,'65). Finally, the topographical finding that relatively few mesodiencephalic terminals made synaptic contacts with the somata, but that most of them were contacting peripheral dendrites, are in line with the idea that excitatory synapses are generally located at the periphery of a neuron (Eccles,'64).

Conclusion

The present study of afferents of the rostral MAO confirmed our previous findings (de Zeeuw et al.,'88a), which indicated that cerebello-olivary fibers were GABAergic, whereas fibres from the nucleus of Darkschewitsch were non-GABAergic. The GABAergic, cerebellar and mesodiencephalic terminals make synaptic contacts with all elements of olivary neurons, including the cell bodies and electrotonically coupled dendrites. The non-GABAergic input, originating primarily in the mesodiencephalon, predominates the innervation of the rostral MAO. The GABAergic input is prominently present on the cell bodies and strategically apposed to the dendrites coupled by gap junctions. At both neuronal structures the GABAergic input is more extensive than would be expected from the general GABAergic input to the neuropil. Part of the

somatic GABAergic innervation may originate from a non-cerebellar source and regulate the excitability and the oscillatory firing rate. The GABAergic input to the

dendrites linked by gap junctions derives from the cerebellar nuclei and may modulate the electrotonic coupling between olivary neurons.

CHAPTER III Mesodiencephalic and cerebellar terminals terminate upon the same dendritic spines in the glomeruli of the cat and rat inferior olive: An ultrastructural study using a combination of (3H)leucine and WGA-HRP anterograde tracing

Abstract

The mesodiencephalic and cerebellar afferents in the rostral medial accessory and principal olive of the cat and rat were studied following anterograde transport of tritiated leucine combined with anterograde transport of wheat germ agglutinin coupled horseradish peroxidase in the same animals. In all studied areas at least one third of the labeled glomeruli appeared to contain both mesodiencephalic and cerebellar terminals. In many of these cases it was found that the terminals from both afferent systems contacted the same dendritic spines. Therefore, these olivary spines may be, as will be discussed, well suited for being involved in a timing process.

Introduction

The inferior olive (IO) is the source of the climbing fibres innervating the Purkinje cells of the cerebellum (Szentágothai and Rajkovits,'59; Eccles,'66; Desclin,'74). Two of the main olivary subnuclei are the medial accessory olive (MAO) and the principal olive (PO). The rostral parts of these subnuclei project respectively to the C2 and D zones of Purkinje cells in the cerebellar hemisphere and give off collaterals to the posterior interposed and dentate nucleus (Groenewegen et al.,'79; van der Want et al.,'88; Wiklund et al.,'88). These cerebellar nuclei receive their main input from the Purkinje cells of the same zones (Voogd and Bigaré,'80). Since the posterior interposed nucleus and the dentate nucleus project respectively to the rostral MAO and PO (Tolbert et al.,'76; Dietrichs et al.,'85; Dietrichs and Walberg,'86), the direct

connections between the cerebellar and olivary nuclei are reciprocally organized. The projection fibers from the central cerebellar nuclei to the IO contain gamma-amino butyric acid (GABA), (Nelson et al.,'84; de Zeeuw et al.,'88a), and are therefore presumed to be inhibitory (Roberts,'74). An indirect projection from the central nuclei to the rostral MAO and PO is relayed through the mesodiencephalic junction which includes the nucleus of Darkschewitsch and the nucleus of Bechterew (Ogawa,'39; Voogd,'64; Kievit,'79; Swenson and Castro,'83; Onodera,'84; Ruigrok and Voogd,'88). The mesodiencephaloolivary projection is non-GABAergic (de Zeeuw et al.,'88a). This is in agreement with physiological studies which have shown that this afferent system is excitatory (Jeneskog,'87; Ruigrok et al.,'88).

The olivary neurons have a propensity to oscillate (Armstrong et al.,'68; Benardo and Foster,'86; Llinas and Yarom,'86) and to fire in synchrony (Llinas et al.,'74; Llinas and Yarom,'81a). The synchronizing property is a result of electrotonic coupling by dendrodendritic gap junctions, which are located primarily in the IO glomeruli (Sotelo et al.,'74; Gwyn et al.,'77). There is physiological (Sasaki and Llinas,'85) and morphological (Sotelo et al.,'86) evidence that the GABAergic terminals can modulate this coupling. In an anterograde tracing study combined with immunocytochemistry it was shown in cat (de Zeeuw et al.,'88b and 89a) but also in rat (Angaut and Sotelo,'89) that the GABAergic terminals associated with gap junctions are derived from the cerebellum. The non-GABAergic terminals from the mesodiencephalon also account for a substantial part of the glomerular terminals and are also directly apposed to dendrites linked by gap junctions

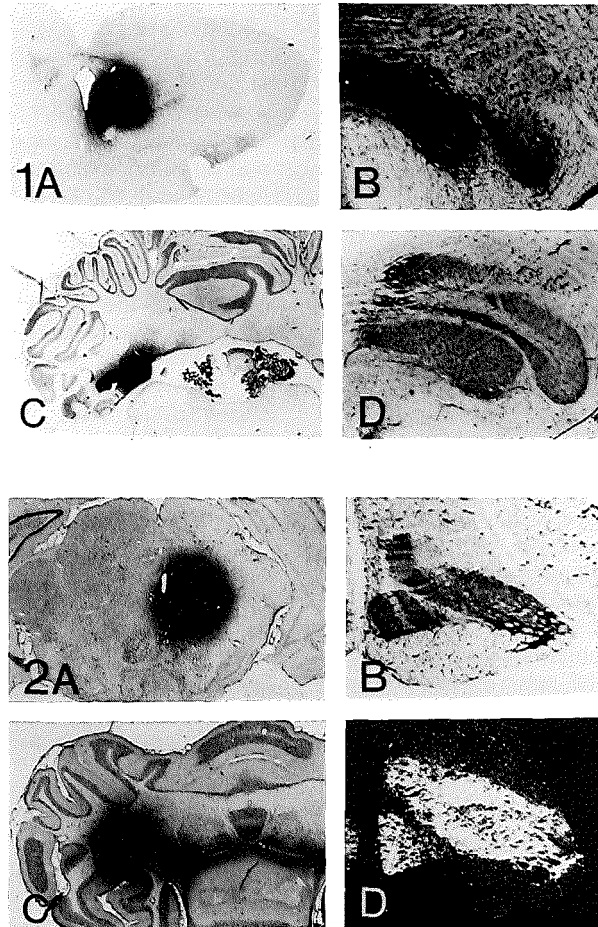


Fig. 1. Photomicrographs of the injection -and projection sites of one of the cats. The (3H)leucine injected at the mesodiencephalic junction included the nucleus of Darkschewitsch and part of the nucleus of Bechterew (A) and was transported ipsilaterally to the MAO and the ventral lamella and lateral bend of the PO but not to the dorsal accessory olive (DAO), (B). The WGA-HRP injected in the cerebellum included both the posterior and anterior interposed nuclei, and the lateral nucleus (C), and was transported to the MAO, PO and DAO of the contralateral IO (D). WGA-HRP reaction products were observed in the somata and in between.

Fig. 2. Photomicrographs of the injection -and projection sites of one of the rats. The WGA-HRP injected in the mesodiencephalic junction included the nucleus of Darkschewitsch and its surrounding areas (A) and was transported to the entire ipsilateral rostral MAO and PO but not to the DAO (B). The (3H)leucine injected in the cerebellum included all cerebellar nuclei (C), and was transported to the MAO, PO and DAO of the contralateral IO (D). Figure 1D is a dark-field micrograph of a 1.5- μ m-thick semithin section.

(de Zeeuw et al., '89a). Whether and how these terminals interact with the cerebellar terminals has not yet been elucidated.

The present study was undertaken to obtain direct evidence that the mesodiencephalic and cerebellar terminals coexist within the same glomeruli and innervate the same dendritic spines. Therefore, we studied these terminals in the rostral MAO and PO of the cat and the rat following anterograde transport of tritiated(3H) leucine combined with anterograde transport of wheat germ agglutinin coupled horseradish peroxidase (WGA-HRP) in the same animal.

Material and methods

Two pentobarbital anaesthetised cats received an injection of 0.4 ul (40 uCi) (3H)leucine (in saline) in the nucleus of Darkschewitsch and the nucleus of Bechterew and surrounding mesodiencephalic areas, and 1 week later an injection of 0.5 ul WGA-HRP (7% in saline) contralaterally in the posterior interposed and lateral nucleus of the cerebellum. In addition, reversed injections were made in four anaesthetised rats. They received an injection of 0.2 ul (20 uCi) (3H)leucine in the cerebellar nuclei and an injection of 0.3 ul WGA-HRP in the mesodiencephalic junction. The animals were anaesthetised 3 days after the injection with WGA-HRP and perfused transcardially with 100 ml. 0.9% saline in 0.18 M (pH 7.3) cacodylate buffer (cats) or in 0.1 M (pH 7.3) phosphate buffer (rats) followed by 2 liters of 5% glutaraldehyde in cacodylate buffer (cats) or 1 liter of 3% glutaraldehyde and 1% paraformaldehyde in phosphate buffer (rats). After perfusion, the (3H)Leucine and WGA-HRP injection sites were prepared for light microscopic autoradiography with a 1-month exposure time (Rogers, '79) or incubated with diaminobenzidine (DAB), (Graham and Karnovsky, '66), respectively. The IO was left for two hours in the fixative and cut transversely on a vibratome. Subsequently, the sections of the cats were incubated with tetramethylbenzidine (TMB) in acetate buffer (0.01 M, pH 4.8) followed by a stabilization with DAB-

cobalt (Rye et al., '84; Lemann et al., '85; de Zeeuw et al., '88a), whereas those of the rats were only incubated with TMB (pH 3.3). Part of the slabs were postfixed with 1.5% osmium tetroxide in phosphate buffer (pH 7.3 for the cats, pH 6.0 for the rats) during 45 min at 45 C, thoroughly rinsed in distilled water, block stained in uranyl acetate (only the cats), dehydrated in dimethoxypropane (Muller and Jacks, '75; Holstege, '87) and embedded in Araldite. Incubated vibratome sections which were not embedded and semithin sections made from the plastic tissue blocks were examined for WGA-HRP labeling and some of them were processed for light microscopic autoradiography (Rogers, '79).

Those blocks of the IO, from which the light microscopic sections showed both WGA-HRP labeling and a large number of silver grains, were processed for electron microscopic autoradiography as described earlier (Holstege and Vrensen, '88). In short the following steps were carried out: Silver non-serial ultrathin sections were cut from the pyramids of the rostral MAO and/or PO, placed on formvar- or collodion-coated slides and stained with uranyl acetate and lead citrate. A layer of carbon was evaporated on these slides which were then dipped in an Ilford L4 emulsion. The thickness of the emulsion was checked macroscopically by inspecting the interference colour (purple-blue) and in the electron microscope by examining the monolayer of silver-bromide crystals (slightly overlapping), (Rogers, '79). The slides carrying the ultrathin sections were kept for 3 months in the dark at 4 C and then developed with Kodak D19 and fixed with 28% sodium thiosulphate. The formvar or collodion films were floated off the slides on water and 200 mesh grids were placed on the ultrathin sections.

Collection and analysis of the data

From each cat and rat respectively two and one block(s), were used for analysis. In the ultrathin sections of these blocks the labeled glomeruli, i.e. those glomeruli which contained one or more (3H)leucine labeled

Table 1A. Distribution of the labeled glomeruli in the cat MAO (n=207) and PO (n=175) following combined injections of (3H)leucine at the mesodiencephalic junction and WGA-HRP in the cerebellar nuclei. Values indicated are mean percentages (\pm SEM) of data obtained in the ultrathin sections (N=8). The left column shows the percentages of the labeled glomeruli which contained only WGA-HRP labeled terminals, the right column presents the percentages of the labeled glomeruli which contained only (3H)leucine labeled terminals, and the middle column gives the percentages of the labeled glomeruli which contained both types of terminals. The values between parenthesis with a superscribed star (*) indicate percentages which were calculated with the presumption that terminals labeled with less than 4 grains also contained anterogradely transported (3H)leucine.

	WGA-HRP	WGA-HRP + (3H)leucine	(3H)leucine
Cat MAO	45(19*) \pm 2.8	29(55*) \pm 1.4	26 \pm 1.9
Cat PO	39(16*) \pm 3.2	32(55*) \pm 2.9	29 \pm 1.0

Table 1B. Distribution of the labeled glomeruli in the rat MAO (n=129) and PO (n=124) following combined injections of WGA-HRP at the mesodiencephalic junction and (3H)leucine in the cerebellar nuclei. For values indicated see Table 1A.

	WGA-HRP	WGA-HRP + (3H)leucine	(3H)leucine
Rat MAO	35(15*) \pm 4.4	32(52*) \pm 2.9	33 \pm 4.6
Rat PO	28(13*) \pm 3.4	34(49*) \pm 2.7	38 \pm 4.1

and/or one or more WGA-HRP labeled terminals, were studied. A glomerulus was defined as a core of at least three dendritic structures, surrounded by at least two terminals and some glia. A profile was considered to be labeled with (3H)leucine when a cluster of at least 4 silver grains was centered on it, while a terminal profile was considered to be labeled with WGA-HRP when one or more crystals were present. For each ultrathin section it was determined what percentage of the labeled glomeruli contained only one or more (3H)leucine labeled terminals, what percentage contained only WGA-HRP labeled terminals and what percentage was double labeled containing both (3H)leucine labeled terminals and WGA-HRP labeled terminals (Fig. 3; Table 1). In addition, it was determined what percentage of the WGA-HRP labeled glomeruli contained terminals with 1, 2 or 3 silver grain(s) but no cluster

labeled terminals. The percentages of all examined ultrathin sections were averaged and the standard errors of the means (SEM's) were determined (Table 1).

In order to find out whether the criterion (4 or more silver grains) for (3H)leucine labeling was reliable, we also determined the percentage (\pm SEM) of cluster labeled profiles which were non-axonal, i.e. glia, dendrites, cell bodies or blood vessels. In addition, the autoradiographic background activity was estimated by counting the silver grains which were present on the film next to the section. An average background activity of 15 grains per 10,000 μ m² was found, which is comparable to findings in other studies (Schonbach et al., '71; Holstege and Kuypers, '87). Background crystals as a result of the TMB incubation were not taken into account, since it has been shown that such crystals are virtually absent (Holstege, '87).

Results

LIGHTMICROSCOPY. The (3H)leucine and WGA-HRP injection sites in the mesodiencephalon included the nucleus of Darkschewitsch and the nucleus Bechterew and their surrounding areas (Figs. 1A and 2A), while those in the cerebellum (Figs. 1C and 2C) always included the posterior interposed and dentate nucleus and sometimes the anterior interposed nucleus. Examination of the light microscopic sections of the IO showed that the entire or large parts of the rostral MAO and PO contained both a dense accumulation of silver grains as well as a condensation of WGA-HRP reaction products (Figs. 1B,D and 2B,D).

ELECTRONMICROSCOPY. The ultrathin sections from both the cats (Figs. 4 and 5) and the rats (Fig. 6) contained numerous (3H)leucine labeled and WGA-HRP labeled profiles. In all examined ultrathin sections of both animals most of the clusters of more than 3 grains were located over terminals or myelinated axons. Only $0.8\% \pm 0.3$ of the clusters were associated with somata, dendrites or glia. Usually the grains of the clusters were randomly distributed within and on the membranes of the labeled profile. On few occasions tracks of grains (Rogers, '79) were observed. The profiles containing these tracks were not considered for cluster labeling except for one case in which a short track of only 5 grains was located over a terminal which contained some other grains beside it (Fig. 5A). The WGA-HRP labeling was also mainly restricted to axon terminals. Retrogradely WGA-HRP labeled perikarya and proximal dendrites were observed sometimes in the sections of the cat. The WGA-HRP/TMB reaction products, which were in the cat stabilized with DAB-cobalt, appeared as dense outlines of the original TMB crystals with electron lucent spaces in their centre and these products often were located at the periphery of the terminals (Figs. 4 and 5). On the contrary, the unstabilized reaction products in the rat appeared as entirely electron dense crystals usually located in the centre of the labeled profile (Fig. 6).

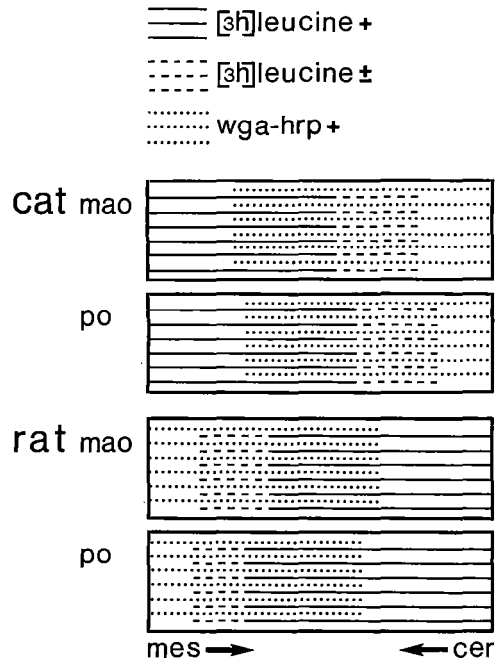


Fig. 3. Distribution of the labeled glomeruli in the MAO and PO of the cat and the rat following an injection of (3H)leucine (cats) or WGA-HRP (rats) in the mesodiencephalic junction (indicated from the left side) combined with an injection of WGA-HRP (cats) and (3H)leucine (rats) in the cerebellar nuclei (indicated from the right side). The continuous lines indicate the percentage of the labeled glomeruli which contained one or more terminals labeled with more than 3 grains ((3H)leucine +), the interrupted lines indicate the percentage of the labeled glomeruli which contained one or more terminals with less than 4 grains ((3H)leucine ±), and the dotted lines indicate the percentage of the labeled glomeruli which contained one or more WGA-HRP labeled terminals (WGA-HRP +). Note that in both olivary subnuclei of both animals at least one third of the labeled glomeruli shows a coexistence of mesodiencephalic and cerebellar terminals (for exact data, see Table 1).



Despite of the inferior morphology of the stabilized reaction products, the general ultrastructural preservation of the cats was better than the one of the rats (compare Figs. 4 and 5 with 6). The terminals labeled from the cerebellum with WGA-HRP reaction products (cats) or with autoradiographic clusters (rats) contained primarily pleiomorphic vesicles and symmetric synapses, whereas most of the mesodiencephalic (3H)leucine labeled (cats) and WGA-HRP labeled (rats) terminals had rounded vesicles and asymmetric synapses (Figs. 4, 5 and 6). The vast majority of the terminals labeled with 1, 2 or 3 silver grains showed the same morphological characteristics as the terminals labeled with clusters of more than three grains (compare Figs. 4B,C with Figs. 4A and 5). Both terminals labeled from the meso-

Fig. 4. Three electronmicrographs of profiles of the rostral MAO of the cat following injection of WGA-HRP in the cerebellar nuclei and (3H)leucine in the mesodiencephalic junction. The two spines in A (asterisks) are, as far as the present two-dimensional analysis revealed, not located in a glomerulus. Both of them are contacted by a mesodiencephalic terminal labeled with a cluster of more than three grains as well as by a cerebellar WGA-HRP labeled terminal (large arrows). The spines in B and C are located in glomeruli, which contain a WGA-HRP labeled terminal (large arrows) and one or two terminals labeled with less than 4 silver grains. Note that these terminals sparsely labeled with grains also exhibit asymmetric synapses (open arrows), which is one of the characteristic morphological features of the mesodiencephalic terminals. The asterisks in A and B demarkate the dendritic spines which are contacted by both mesodiencephalic and cerebellar terminals. In the centre of the glomerulus in C a gapjunction (small black arrows) connects two dendritic spines of which one is contacted by a presumptive mesodiencephalic terminal (grains) and the other one by a cerebellar terminal (large black arrows). Arrowheads indicate symmetric synapses. Scale bar = 0.4 μ m.

diencephalic junction and from the cerebellar nuclei were located inside and outside the glomeruli, and in both positions they were found apposed to dendrites linked by a gap junction (Figs. 4C and 6). Sometimes, they were found to establish synaptic contacts with somata. The cerebellar and mesodiencephalic labeled terminals were often found to be located in the same glomeruli (Figs. 4B,C and 5A,B) and/or to contact the same dendritic spines (Figs. 4A,B and 5A,B). Generally, the glomeruli of the rat were found to be smaller than those of the cat. This was mainly due to the fact that less spiny profiles were incorporated in the rat glomeruli.

QUANTIFICATION. In the cat rostral MAO an average of 26% of all the labeled glomeruli contained only one or more (3H)leucine labeled mesodiencephalic terminals, 45% contained only one or more WGA-HRP labeled cerebellar terminals, and 29% contained both autoradiographically labeled and histochemically labeled terminals (Table 1, Fig. 3). If the terminals, which were not cluster labeled but carried 1, 2 or 3 silver grains, were also considered as (3H)leucine labeled, the percentage of double labeled glomeruli containing both types of terminals would increase to 55%. For the PO of the cat these percentages were as follows: Of the labeled glomeruli 29% contained only one or more (3H)leucine labeled terminals, 39% included WGA-HRP labeled terminals, while the percentage of double labeled glomeruli would increase from 32% to 55% when all grain labeled terminals were considered as (3H)leucine labeled. For the rostral MAO of the rat these percentages were respectively 33%, 35%, 32% and 52%, and for the PO of the rat respectively 38%, 28%, 34% and 49% (Fig. 3; Table 1).

Discussion

TECHNICAL AND ANALYTICAL ASPECTS. Autoradiography and HRP/DAB (Dekker,'81) or WGA-HRP/TMB (Holstege and Kuypers,'87) histochemistry were used before at the ultrastructural level for the combination of anterograde with retrograde

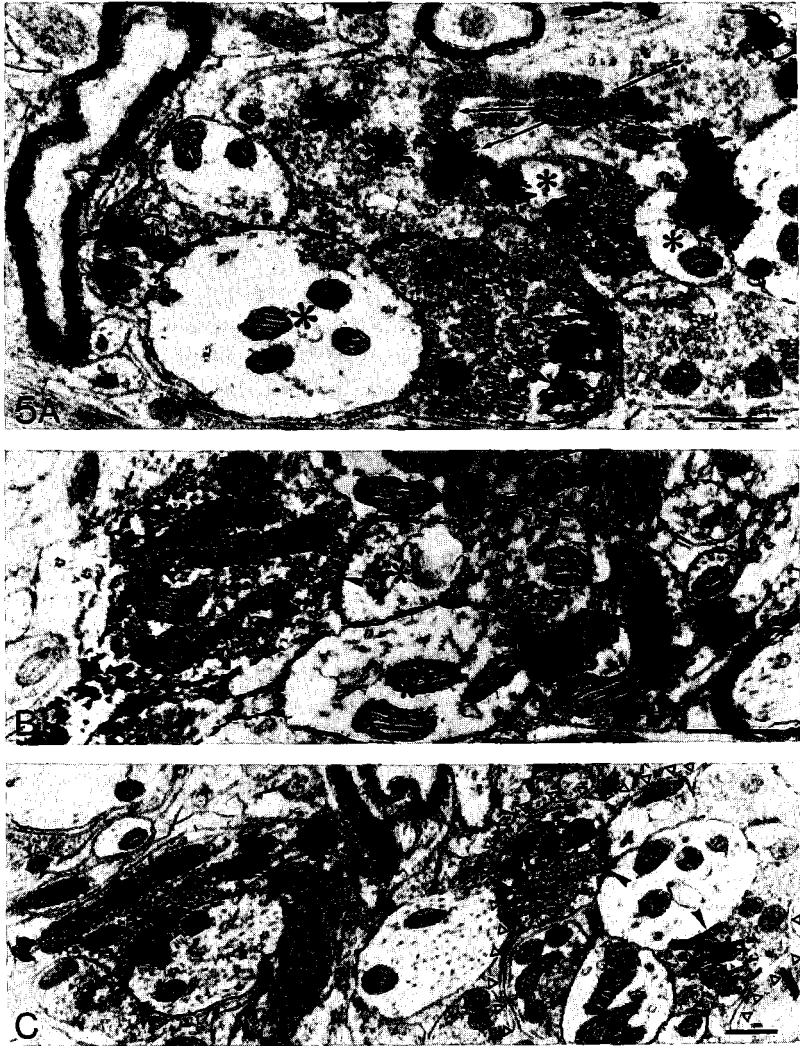


Fig. 5. Three electronmicrographs of glomeruli in the PO of the cat following injection of WGA-HRP in the cerebellar nuclei and (3H)leucine in the mesodiencephalic junction. The glomeruli in A and B contain one or more WGA-HRP labeled terminals (black arrows) as well as one or two grain labeled terminals, whereas the WGA-HRP labeled terminals and cluster labeled terminal in C are not located in the same glomerulus (the outline of the glomerulus with the WGA-HRP labeled terminals is indicated by triangles). Note that the grain labeled terminals in A are both doubtfully positively labeled: Number 1 because it contains less than 4 silver grains and number 2 because its grains on the left side seemed to form a short track. On the contrast, the cluster labeled terminals in B and C were regarded as clearly positively labeled for (3H)leucine. The dendritic structures contacted by both grain labeled and WGA-HRP labeled terminals are indicated by asterisks. Arrowheads indicate symmetric synapses and open arrows asymmetric ones. Scale bar = 0.4 μ m

tracing. However, to our knowledge the present ultrastructural study is the first in which (3H)leucine and WGA-HRP anterograde tracing were combined. It is evident that one can combine these anterograde tracing methods independent from the fact whether the WGA-HRP histochemistry was performed with (cats) or without (rats) a DAB-cobalt stabilization procedure. In this respect it differs from the combination technique of WGA-HRP anterograde tracing with postembedding immunocytochemistry, which requires a stabilization for double labeling (de Zeeuw et al., '88a). Because the percentage of double labeled glomeruli did not differ obviously between the cats and the rats, it seems that the efficiency of WGA-HRP anterograde tracing is not influenced by the stabilization. This is in agreement with a previous tracing study by Molinari (Molinari, '87) in which the stabilization and normal WGA-HRP histochemistry were compared for one afferent system in one type of animal. However, with respect to the ultrastructural preservation the stabilization has advantages. Using this procedure one can use a relatively high pH-level of 4.8 for the acetate buffer during the TMB incubation whereas with the normal procedure one needs to use a damaging pH-level of 3.3 in order to obtain sufficient anterograde labeling. In addition, it appears to be possible to stain the tissue en block in uranyl acetate once the WGA-HRP reaction products are stabilized, whereas unstabilized reaction products were found to be solved in the aqueous uranyl solution.

WGA-HRP/TMB reaction products are not formed in the absence of WGA-HRP and they are usually confined to the structure which contains the WGA-HRP (Holstege, '87). However, for the analysis of EM autoradiographs it must be taken into account that silver grains may be located above structures which do not contain (3H)leucine (for details see, Williams, '77). In order to circumvent this problem of autoradiographic cross-fire and autoradiographic background we used the cluster analysis (Holstege and Vrensen, '88). In the present study a profile was considered to be labeled when a cluster of at

least four grains was located above it. Although this number was arbitrary, it appeared to be a reliable criterion because almost none of these clusters of more than three grains were located above non-axonal structures.

MORPHOLOGY AND QUANTIFICATION. As observed before in cat (de Zeeuw et al. '88a) and rat (Angaut and Sotelo, '87 and '89; Cintas et al., '80) it was found that most cerebellar terminals contained pleiomorphic vesicles and symmetric synapses whereas most of the mesodiencephalic terminals had rounded vesicles and asymmetric synapses. The present study presents direct anatomical evidence that cerebellar and mesodiencephalic terminals are often located in the same glomeruli and often terminate upon the same dendritic spine heads. This is in agreement with previous observations in the rostral MAO of the cat that mesodiencephalic and GABAergic terminals innervate the same glomeruli and that the same is true for cerebellar and non-GABAergic terminals (de Zeeuw et al., '89b). With respect to the quantitative data, no obvious differences were found. In both the rostral MAO and PO of both animals about one third of the labeled glomeruli was found to contain both cerebellar and mesodiencephalic terminals (Fig. 3). However, the actual number of glomeruli which contain both cerebellar and mesodiencephalic terminals must be higher because of the following reasons: Firstly, the vast majority of the terminals labeled with 1, 2 or 3 grains showed the same morphological characteristics as the terminals with more than three grains, suggesting that most of them belonged to the same group of afferents. If we assumed that all grain labeled terminals originated from the same source, the percentage of double labeled glomeruli would be somewhat higher than 50% (Table 1). Secondly, part of the glomerular labeled terminals were missed because the glomeruli were studied in a single two-dimensional cross section. Thirdly, probably only about one third of the actual number of terminals from fibers originating from a given injection site can be labeled with WGA-HRP antero-

grade tracing (de Zeeuw et al., '89a). Since the efficiency of EM autoradiography using the cluster analysis may be only about twice as high as the WGA-HRP technique (Holstege and Vrensen, '88), it probably also accounts for the autoradiographic technique that only part of the actual terminals can be detected. Fourthly, at least half of all the glomeruli in the rostral MAO contain both mesodiencephalic and GABAergic terminals (de Zeeuw et al., '89b). Taken together, the present results strongly suggest that a majority of the glomeruli in the rostral MAO and PO contain both mesodiencephalic and cerebellar terminals and that a substantial part of the glomerular spines are innervated by both of these inputs.

FUNCTIONAL IMPLICATIONS. On the basis of physiological and morphological findings, the mesodiencephalic input to the rostral MAO and PO may be regarded as their major excitatory drive (Ruigrok et al., '88; de Zeeuw et al., '89a), while the cerebellar GABAergic input may function as a modulator of the electrotonic coupling within the glomeruli (Llinas, '74; Llinas et al., '74; Sotelo et al., '74; Llinas and Yarom, '81a; Bower and Llinas, '83; Sasaki and Llinas, '85; Sotelo et al., '86; de Zeeuw et al., '88b and '89a; Angaut and Sotelo, '87 and '89). However, because the present study of the rostral MAO and PO indicates that mesodiencephalic and cerebellar terminals extensively coexist in the glomeruli and synaps upon the same spines, it seems likely that the mesodiencephalic terminals directly interact with the cerebellar terminals in regulating the firing behaviour of the olivary neurons.

It has been shown for various regions in the central nervous system that the vast majority of dendritic spines are contacted primarily by asymmetric synapses (Kemp and Powell, '71; Palay and Chan-Palay, '74; Wilson and Grove, '80; Wilson et al., '83; Muller et al., '84), which are believed to be excitatory (Uchizono, '65). Therefore, the present finding that most spines are heavily innervated by both an excitatory (non-GABAergic mesodiencephalic) and an inhibitory (GABA-



Fig. 6. Electronmicrograph of a profile in the PO of the rat following injection of WGA-HRP in the mesodiencephalic junction. It shows two extraglomerular dendrites (D) linked by a gap junction (small arrows) and a small attachment plate (black triangles). One of these dendrites is contacted by a WGA-HRP labeled mesodiencephalic terminal (large arrows). Scale bar = 0.4 μ m.

ergic cerebellar) input, is highly unusual and may have specific functional implications. Recently, Segev and Rall (Segev and Rall, '88) showed in a computational study based upon the Hodgkin and Huxley equations of excitable membranes that the effect of synaptic inhibition can be enhanced especially in excitable dendritic spines that are contacted by both excitatory and inhibitory synapses, and that this enhanced inhibitory effect can be extremely sensitive to the timing between both types of inputs, with a temporal resolution well below 100 μ s. At present, it is not known whether the olivary dendritic spines contain excitable channels. However, since it has been shown by Llinas and Yarom (Llinas and Yarom, '81a, '81b and '86; Yarom and Llinas, '87) that inferior olivary neurons possess a variety of complex and interacting conductances, some of which may occur solely within the dendrites (high threshold non-inactivating Ca^{2+} -channels), it seems an attractive and likely working hypothesis that the spines of olivary dendrites indeed carry excitable channels. Moreover, the observation that olivary spines are extremely long and complex looking (Sotelo et al., '74; Gwyn et al., '77; Ruigrok et al., '88) are thought to be favourable assets of excitable spines (Segev and Rall, '88), (high input resistance combined with sufficiently available synaptic current). Thus, the model of Segev and Rall may very well be applicable to the olivary spines. If we do so, this may have two implications. Firstly, this could mean that the inhibitory cerebellar terminals, which contact the same spines as the excitatory mesodiencephalic terminals, are extremely well positioned to block the olivary firing induced by the mesodiencephalic input. Thus, the cerebellar GABAergic input to the olive is not only strategically located next to the dendritic spines linked by gapjunctions (as also shown before de Zeeuw et al., '88b and '89a; Angaut and Sotelo, '89) but in the same position also strategically terminating upon the same dendritic spines as the non-GABAergic mesodiencephalic terminals,

meaning that the same afferent system is well suited for uncoupling the olivary cells and in the same time for reducing their firing frequency. This is in line with a recent study by Yarom and Adan (Yarom and Adan, '88) which showed by interconnecting an analog simulator with an olivary neuron that once induced but intrinsically maintained oscillations of electrotonically coupled olivary neurons can be stopped more easily when they are disconnected from each other. Secondly, this could mean that the excitation of olivary cells can only be stopped when the inhibitory cerebellar terminals are firing at a specific moment related to the activity of the excitatory mesodiencephalic terminals. Several recent reports demonstrated that the olivo-cerebellar system may indeed function as a timing device (Llinas, '89). It was found that the IO is activated at the onset of movements which must be performed under a strict time constraint (Mano et al., '89), that the climbing fiber activity exerts a short lasting enhancement of the simple spike activity (Bloedel and Zuo, '89), and that lesions of the lateral cerebellum disturbs accurate timing of motor-activity (Ivry et al., '88). Therefore, the present results suggest that the timing between the cerebellar and mesodiencephalic afferents in the glomeruli of the rostral MAO and PO can be one of the main elements of the function of the olivo-cerebellar system.

Conclusion

It may be concluded that the cerebellar and mesodiencephalic input to the glomeruli and their dendritic spines in the rostral MAO and PO of the cat and the rat seemed to be well designed not only for modulating the electrotonic coupling of the olivary cells but also for regulating their firing frequency in a timing sensitive way.

CHAPTER IV Intracellular labeling of neurons in the medial accessory olive of the cat

- a. Intracellular labeling of neurons in the medial accessory olive of the cat: I. Physiology and light microscopy
- b. Intracellular labeling of neurons in the medial accessory olive of the cat: II. Ultrastructure of dendritic spines and their GABAergic innervation
- c. Intracellular labeling of neurons in the medial accessory olive of the cat: III. Ultrastructure of axon hillock and initial segment, and their GABAergic innervation

a. Intracellular labeling of neurons in the medial accessory olive of the cat: I. Physiology and light microscopy (Ruigrok et al., submitted)

Abstract

This study is the first of three reports on the detailed morphology of horseradish peroxidase injected neurons in the medial accessory olive of the cat.

Intracellular, *in vivo*, recordings of olivary cells were made and their response to mesodiencephalic stimulation was tested. In 44 units a short latency action potential could be recorded, which was very suggestive for a monosynaptic excitatory pathway. The short latency response was frequently followed by a long latency (mean 188 msec) or rebound action potential. Recordings were followed by intracellular iontophoresis of horseradish peroxidase.

A total of 21 neurons, all located within the medial accessory olive were chosen for morphological analysis. Cells could be divided into two categories on the basis of their overall morphological appearance. Type I cells (n=5) had sparsely branching dendrites that radiated away from the soma and were usually found in the caudal part of the medial accessory olive. The axon usually originated from the soma. Type II cells (n=16) were located more rostrally. They had larger cell bodies with dendrites that

ramified extensively, forming a globular structure (mean diam. 338 micron). The axon usually originated from a first order dendrite. No recurrent axon collaterals were observed on either type I and II cells. Both cell types carried long and complex spiny appendages, however, they were most numerous on the second and higher order dendrites of type II cells. Since the soma of these cells is usually not found in the centre of its dendritic field, even if the cell is located in the center area of the neuropil, it is suggested that the dendritic trees of up to 100 neurons may be intricately interwoven, establishing clusters with intensive intercommunication by means of dendritic gap junctions. The abundance, length and complexity of the spiny appendages suggest an important role in this process, but may also be relevant instruments in enhancing the computational capabilities of these neurons, especially in timing sensitive processes.

When relating the physiological and the morphological results, it was noted that both type I and type II cells could respond to mesodiencephalic stimulation and were both able to trigger a rebound action potential. No significant correlations were found between cell size and the latency of the rebound.

Introduction

The inferior olive is the source of the climbing fibers to the cerebellum and can be subdivided in three subnuclei. These subnuclei, termed dorsal accessory olive (DAO), principal olive (PO) and medial accessory olive (MAO) can be recognized in all mammalian species studied so far (see Withworth and Haines,'86 for review) and demonstrate a highly organized projection pattern to the cerebellum that appears to be preserved throughout phylogeny (Brodal and Kawamura,'80).

The present set of investigations focusses on the MAO of the cat. The caudal part of the MAO gives rise to climbing fibers to the A zone of the cerebellar vermis, whereas its rostral part projects to the C2 zone (Groenewegen and Voogd,'77; Groenewegen et al., '79). The input to the MAO also appears to recognize these subdivisions. E.g. the rostral part of the MAO receives non-GABAergic afferents from the nucleus of Darkschewitsch and surrounding areas (Ogawa,'39; Onodera,'84; de Zeeuw et al. '89a,b) and GABAergic fibers from the posterior interposed nucleus of the cerebellum (Tolbert et al.,'76; Nelson and Mugnaini,'85; '89; de Zeeuw et al.,'88a and '89a,b). The caudal MAO receives its main input from the spinal cord, dorsal column nuclei, trigeminal spinal nucleus and vestibular nuclear complex (Mizuno,'66; Boesten and Voogd,'75; Walberg,'82; Gerrits et al.,'85 a,b). However, also in this part of the olive projections from the mesodiencephalic junction (especially from the interstitial nucleus of Cajal: Onodera,'84) and the cerebellar nuclei (fastigial nucleus: Sugimoto et al.,'80; Dietrichs and Walberg,'85) have been demonstrated.

It was already noted by Scheibel and Scheibel ('55; Scheibel et al.,'56), and later confirmed by others (Ramon-Moliner,'62; Sotelo et al.,'74; Gwyn et al.,'77; Rutherford and Gwyn,'80; Foster and Peterson,'86), that two, morphologically distinct types of olivary cells can be recognized. The most characteristic and wellknown type (type II) is the one with the highly ramifying dendrites that

curl back towards the soma, as already described by Cajal ('09). However, especially in the caudal half of the accessory olives, neurons are found with rather long, poorly branched dendrites that radiate away from the soma (type I). Also, a transitional type has been described (Scheibel et al.,'56; Foster and Peterson,'86).

In order to study the functional implications of the relation between the incoming afferent input and the cellular morphology of the inferior olivary neurones, the following set of experiments was performed. Intracellular recordings of olivary neurons in the MAO were made in vivo and their response to mesodiencephalic stimulation was tested. This was followed by intracellular injection of horseradish peroxidase (HRP). This material was prepared for light microscopical examination. Ultrastructural studies of some of these HRP labeled neurons combined with postembedding GABA immunocytochemistry will be reported in two companion papers (De Zeeuw et al., submitted a,b).

Material and methods

The present experiments were performed on a total of 10 adult cats of both sexes.

STIMULATION ELECTRODES. In order to further identify the impaled inferior olivary neurons and to study their responses to afferent input, we implanted monopolar Tungsten stimulation electrodes (impedance appr. 100 k Ω) at the mesodiencephalic junction in 8 animals, 5 to 8 days prior to the experiment. After anaesthetizing the animals with sodium pentobarbital (35-40 mg/kg) a parietal bone flap was removed and two stimulation electrodes were implanted. As a landmark, the position of the red nucleus was established by the vigorous and large action-potentials that could be recorded upon advancing through this nucleus. As a second landmark, low intensity (< 20 μ A) stimulation of the oculomotor nucleus and/or its fibers was used to establish the approximate position of the nucleus of Darkschewitsch, prerubral field and the interstitial nucleus of Cajal (all areas known to project to the



Fig. 1. Macrophotograph of a cresylviolet stained section through the midbrain of cat 1903, indicating the location of the lesion as the result of a 15 sec, 1 mA negative current through the monopolar stimulation electrode. Approximate center of stimulation area was judged to be within the nucleus of Darkschewitsch and interstitial nucleus of Cajal. Bar equals 1 mm. Abbreviations: CM: corpus mamillare; D: nucleus of Darkschewitsch; ICA: interstitial nucleus of Cajal; PAG: periaqueductal grey; PC: posterior commissure; RF: retroflex bundle.

inferior olive; Onodera,'84). Typically, one electrode was placed at AP 5.0 and a laterality of 1.5 (N. of Darkschewitsch), the other at AP 7.0 and a laterality of 1.8 (prerubral field and/or interstitial nucleus of Cajal: stereotactic atlas of Berman,'68, was used). After placement, the electrodes were cemented to the skull with acrylic denture cement. Connectors were placed in silicone tubing and sutured to connectivity tissue. Finally, the wound was sutured and the animal allowed to recover. No obvious behavioral effects were observed due to the electrode placements.

EXPERIMENTAL PROCEDURE. After anaesthetizing the animal with sodium pentobarbital, an i.v. cannula was inserted for administration of drugs. Heart rate, temperature and CO₂ level were constantly monitored throughout the experiment and kept within physiological boundaries. When implanted, the connectors of the stimulating electrodes were retrieved, followed by a ventral, retropharyngeal approach of the brainstem. After dissection of the deep prevertebral muscles, the basilar part of the occipital bone was removed between the tympanic bullae, extending rostrally to the pontine level while caudally, a small rim of bone, directly rostral to the foramen magnum, was left intact. The dura mater and arachnoid were carefully reflected. For reference purposes, a glass micropipette was placed stereotactically at P 7.0 and 1.0 mm lateral to the basilar artery. This way the rostral-most 3 to 4 mm of the inferior olive (P 8.0 - P 9.0 to P 11.0 - P 12.0; atlas of Berman,'68) was available for penetration with micro-electrodes. The ventral surface of the brainstem was stabilized with a 2 % agar solution in physiological saline. In some instances, animals received Flaxedil as a muscle relaxant and were ventilated artificially in order to minimize brain movements.

Intracellular recordings were obtained with glass micro-pipettes, filled with 5% horseradish peroxidase (HRP; Boehringer) in 0.05 M Tris/HCl buffer (pH 7.6) with 0.2 M KCl. These pipettes, whose tips had been broken against a glass rod, had a DC resistance between 40 and 60 M Ω . Recordings were digitized and stored on a VHS tape recorder.

Penetrated olivary neurons could be easily recognized by their characteristic action potential (Crill,'70; Llinas and Yarom,'81a) that can be triggered by passing direct depolarizing current pulses (0.5 nA) through the recording pipette. Subsequently, the reaction to mesodiencephalic stimulation was recorded using a small burst of three pulses (660 hz, Jeneskog,'87) through either of the stimulation electrodes, with a period of

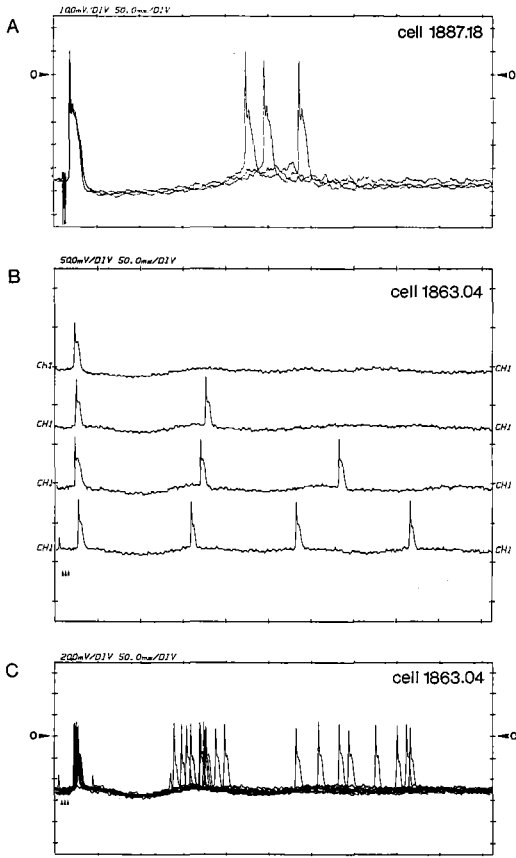


Fig. 2. Intracellular responses of inferior olivary neurons to mesodiencephalic stimulation. A: Response of cell 1887.18, 3 superposed traces. A brief train of three stimulation pulses evokes a short latency action potential followed by a long latency, rebound, action potential. The reconstruction of this cell is shown in Fig. 8 D. B: Responses of cell 1863.04, 4 traces with increasing stimulation strength. Note that initially only a short latency action potential is triggered, that, after enhancing the stimulation strength may be followed by up to three rebounds. C: Recordings from the same cell (1863.04), 7 superposed traces. Note that the variance in latency of the first and especially of the second rebound increases dramatically. The reconstruction of this cell is shown in Fig. 8 A.

1.5 sec. The stimulation threshold was established (usually between 100 - 250 μ A) and a number of recordings was made at approximately 2 to 3 times threshold. Finally, HRP was injected iontophoretically (4 nA for a period of 3 to 6 min, pulsed 0.2 sec on, 0.2 sec off, anode in pipette) in cells that still demonstrated a stable resting potential of at least -30 mV and discharging clearly recognizable olivary spikes. This way, a total of 10 to 15 neurons was injected on one side of the brain at intervals of at least 500 microns. The position of the injection sites was marked with respect to the reference pipette.

To indicate the stimulation sites, lesions were made at the end of the experiment by passing a negative current of 1 mA for 10 to 20 sec through the stimulation electrodes.

One to 16 hours after injection of the neurons the animal was perfused under deep sodium pentobarbital anaesthesia, using a protocol suited to perform GABA-postembedding immunocytochemistry (de Zeeuw et al., '89b). In short, after clamping the descending aorta, the cats were perfused transcardially with 100 ml physiological saline in 0.18 M cacodylate buffer (pH 7.3) under artificial respiration, followed by 2 l of 5% glutaraldehyde in the same cacodylate buffer.

The midbrain was, after immersion in 30% sucrose in 0.1 M phosphate buffer (pH 7.3) for at least 24 hours, serially sectioned on a freezing microscope (40 μ m). Sections were mounted on glass slides and Nissl stained in order to evaluate the location of the stimulation electrodes.

The brainstem containing the inferior olive was left in fixative for 1 to 2 hours, cut transversally on a vibratome in 70 μ m sections and incubated with diaminobenzidine (DAB, Sigma) according to Graham and Karnovsky ('66) for 1 hour. Most incubated vibratome sections were rinsed in 8% (D+) glucose dissolved in 0.1 M phosphate buffer (pH 7.3) and osmicated for 40 min at 45 $^{\circ}$ C with 1.5% osmiumtetroxide in the same phosphate buffer. Some sections were rinsed and osmicated without glucose, or not osmicated but, after mounting on glass slides, drying and counterstaining with cresylviolet,

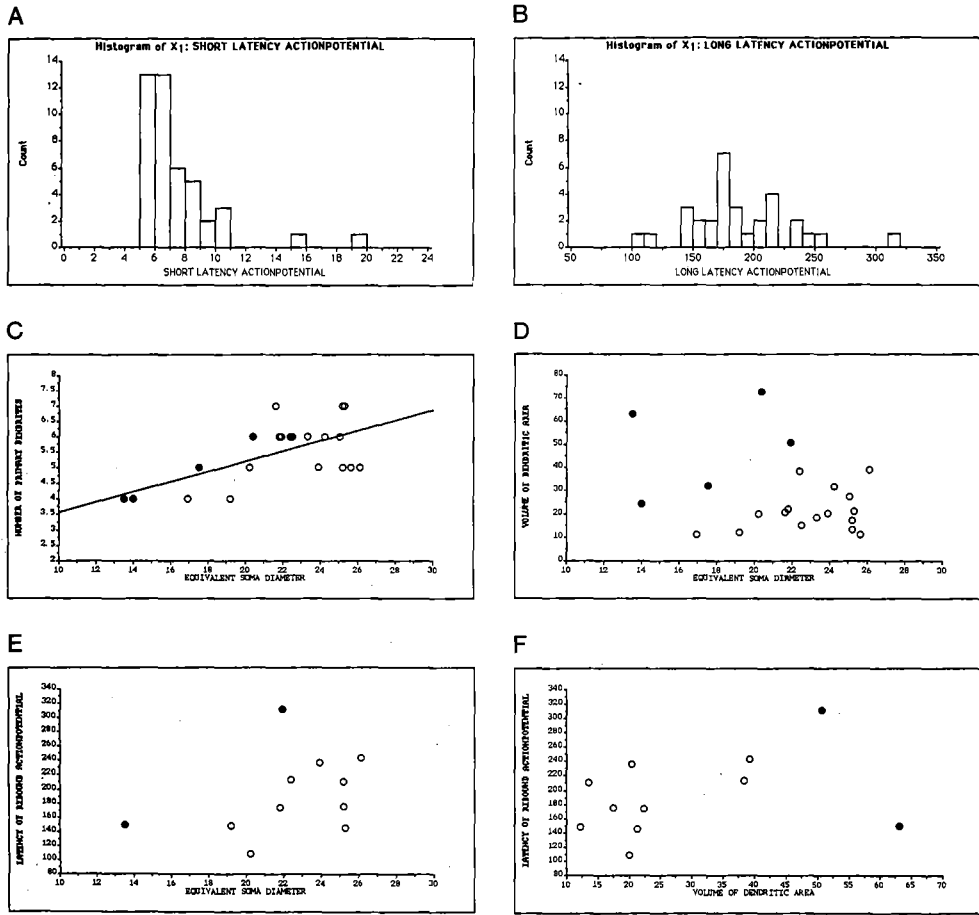


Fig. 3. A: Frequency histogram of the mean latencies of 44 cells for the short latency actionpotential upon mesodiencephalic stimulation. B: Histogram of the mean latencies for the rebound actionpotential of 31 units. Abscis in A and B in msec. C: Scattergram illustrating the relation between the equivalent soma diameter and the number of primary dendrites. Linear correlation coefficient: 0.62, $P < 0.001$, $n = 21$. Filled circles denote the type I cells, whereas the type II cells are represented by open circles (also in D,E,F). Soma diameter in μm . D: Scattergram illustrating the relation between the equivalent soma diameter and the neuropil area enveloped by its dendritic tree. Note that the type I cells are spatially separated from the type II cells. Soma diam. in μm ; volume of dendritic area in $10^6 \mu\text{m}^2$. E, F: Scattergrams illustrating the relation between both the equivalent soma diameter (E) and the volume of the dendritic area (F) and the latency of the rebound action potential. No significant correlations were observed. Scales as in A and D.

dehydrated in graded series of ethanol and xylene and, finally, coverslipped in Permount. The osmicated sections were rinsed in distilled water (4x), blockstained in uranyl acetate for 60 min at 4 °C, and, without rinsing, directly dehydrated in dimethoxypropane (DMP, Muller and Jacks,'75; Truter et al.,'80) and flat embedded in Araldite between teflon coated glass coverslips (Bishop and King,'82). This way the injected neurons could be studied with the light microscope prior to electron microscopical investigation (de Zeeuw et al., submitted a,b).

ANALYSIS. Well stained neurons were studied with a Wild light microscope equipped with Wild objectives and a Zeiss 100x (n.a. 1.25) oil objective. Camera lucida drawings were made with the aid of a drawing apparatus attachment.

As a measure for the soma size, an equivalent soma diameter was determined using a drawing of the soma's contour (using the 100x objective) on a piece of cardboard. Its cut out weight represented a measure for its surface area. From this, and assuming a circle to be an approximation of the soma contour, the equivalent soma diameter was calculated (see also Foster and Peterson,'86).

In a similar way, an estimate was calculated for the volume of neuropil enveloped by the dendritic tree of a neuron. The cross-sectional area of the entire dendritic tree in the transverse plane was determined using the card board technique, and the number of sections containing dendrites of the neuron was established. These values were entered in the equation for the volume of an ellipsoid*.

All cells were classified subjectively into either the type I or type II category on basis of the overall morphology of their dendritic tree (Foster and Peterson, 1986). Two cells

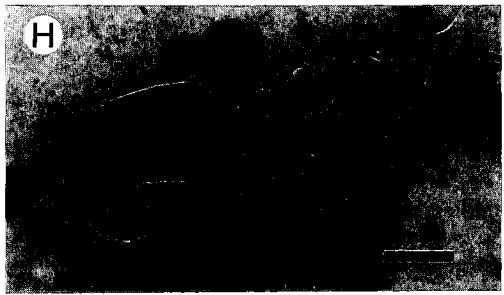
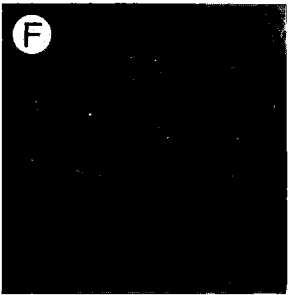
Note. The equation for the volume of an ellipsoid is: $V=4/3 \pi abc$, where a,b,c , are the radii in the three dimensions; πab was determined with the cardboard technique, c was calculated from the number (n) of 70 micron sections in which elements of the dendritic tree could be found: $c = 70(n-1)/2 \mu\text{m}$.*

of each category (type I: cells 1863.04 and 1868.05; type II: cells 1886.15 and 1887.18) were chosen for serial reconstruction on tracing paper (using the Zeiss 100x objective) and the drawing apparatus attachment. Sectioned dendrites were indicated and aligned with the cut dendrites of adjacent sections. These four reconstructed cells formed the basis for the ultrastructural studies presented in the companion papers (de Zeeuw et al., submitted a,b).

Results

PHYSIOLOGY. In 6 cats, with stimulating electrodes in the mesodiencephalic junction (Fig. 1), a total of 44 neurons were impaled that reacted to stimulation. A typical response pattern is shown in Fig. 2A. A short burst (at 660 Hz) of three stimulation pulses triggered a characteristic olivary action-potential, consisting of a fast initial part followed by an after-depolarizing potential that lasted for 10 to 15 msec on which one to several spikelets could be seen (Crill,'70; Llinas and Yarom,'81a). The afterdepolarisation was terminated by a large and long-lasting (at least 100 msec) afterhyperpolarization. In 70 % of the cases (31 neurons) this response was followed by a long latency (or rebound) actionpotential after 115 to 300 msec (mean: 188 ± 42 msec). Occasionally, especially with higher stimulation strength, a second or even third rebound actionpotential was triggered (Fig. 2B,C). The mean latencies of the short and long latency (when present) actionpotentials were determined at approximately 2 to 3 times stimulation threshold from at least three consecutive stimulations. The frequency distribution of these mean responses from the 44 neurons is presented in Fig. 3A, B.

The shortest latency found was about 5 msec (mean 7.2 ± 2.6). Since one or two stimulation pulses were not as effective in triggering olivary actionpotentials, it will be obvious that the time elapsing between the onset of the first pulse and the rising phase of the action potential may be overestimated by 1.5 or 3.0 msec. Therefore, the short latency



actionpotential is most likely monosynaptically triggered from the mesodiencephalon which leaves, after an additional extraction of approximately 1.0 msec for synaptic transmission (Eccles, '64), an actual conduction time in the order of 1 to 3 msec for an estimated pathway length of 14 to 18 mm.

MORPHOLOGY. The Araldite embedded tissue sections which were osmicated in the glucose solution had a light, golden brown colour. The HRP labeled cells appeared as black structures and could be easily recognized and followed in the 70 μm thick sections (Fig. 4A,B). Injected cells, located in sections that were osmicated without the use of glucose were evaluated with much more difficulty, while the small spiny appendages could hardly be identified. The labeled neurons in non-osmicated and ethanol dehydrated sections, could also easily be evaluated, however, the dendrites appeared rather wrinkled, indicating severe shrinkage of the tissue (Fig. 4H).

In 8 cats, 21 olivary neurons located within the MAO were judged to be sufficiently well labeled to warrant further research. All 21 neurons were grouped into either type I (n=5) or type II (n=16) neurons. The approximate position of these neurons was plotted on a series of transverse diagrams of the cat inferior olive (Fig. 5). Most of the type I cells (4 out of 5) were situated in the caudal half of the MAO,

Fig. 4. A,B: Photomicrographs of an intracellularly injected olivary neuron (cell 1886.16, type II). Two adjacent 70 μm sections. C: Detail of soma and proximal dendrites of the same cell. Note the sparse distribution of simple spiny appendages (arrow heads). D, E, F, G: Photomicrographs of various spiny appendages on second and higher order dendrites. Note their thin stalks, frequently carrying clusters of spine heads. H: Part of dendrite with spiny appendages (arrowheads) of an injected neuron that was dehydrated in a graded ethanol series. Note the convoluted course of the dendrite indicating severe shrinkage. Bars equal 50 μm in A,B; 10 μm in C, D, E, F, G, and 25 μm in H.

whereas the type II cells were all located in its rostral half.

The equivalent soma diameter was calculated from the surface area in the transverse plane (see Material and Methods). The mean values are depicted in Table 1. Between 4 and 7 primary dendrites were found to originate from the soma. Some of them divided almost immediately (within 10 μm) into second order branches. The number of primary dendrites correlated well with the soma size (Fig. 3C).

In most cases, it could be established whether the axon originated from the soma or from a dendrite. Some doubtful cases could be verified electron microscopically (de Zeeuw et al, submitted b). All but two of the type II cells had its axon originating from a first order dendrite. One stemmed from a second order dendrite while the last one was derived directly from the soma (Fig. 6: cell 1886.20 and 1903.18, respectively). The axons of four of the type I neurons also stemmed directly from the soma, while one was derived from a primary dendrite (Fig. 6: cell 1858.02). No collaterals could be observed on any of the axons, though all could be followed until they left the neuropil of the MAO and, frequently, even to the contralateral side of the brain. The cone shaped, axon hillock usually carried one or several spinelike appendages (see de Zeeuw et al., submitted b).

An estimate of the volume of neuropil enveloped by the dendritic tree was based on its transverse surface area and the number of sections containing elements of the dendritic tree of a given cell. The resulting volume is plotted against the equivalent soma diameter in Fig. 3D. From this plot it can be deduced that the type I cells usually, but not always, have smaller soma sizes correlated with larger dendritic trees. The position of the soma and the transverse extent of its dendritic tree is depicted in Fig. 7. Note that in most cases the soma is positioned eccentrically. Since the inferior olive is a closed nucleus (Cajal, '09), such an eccentric position is rather obvious for the somata located along the border of the neuropil (e.g. cells 1858.02, 1863.04,

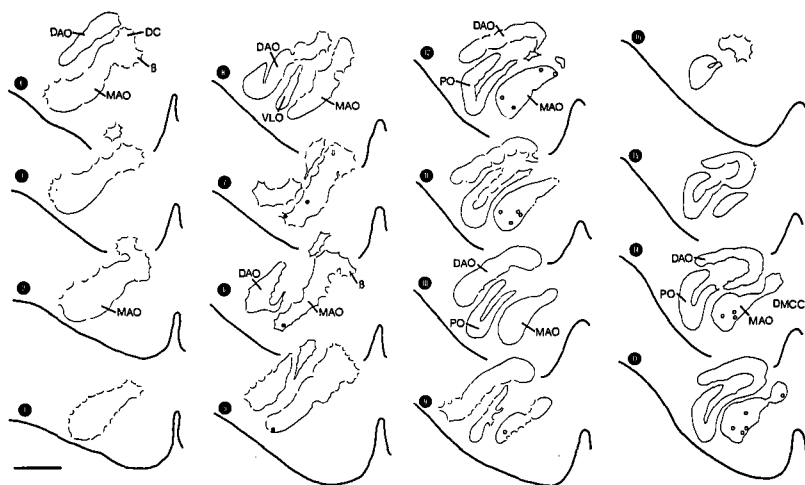


Fig. 5. Series of standardized transverse diagrams of the cat inferior olive, spaced 280 μ m. The approximate location of all 21, morphologically studied, neurons are indicated by filled (type I) and open (type II) circles. Abbreviations: B: 'beta' nucleus; DAO: dorsal accessory olive; DC: dorsal cap; DMCC: dorsomedial cell column; MAO: medial accessory olive; PO: principal olive; VLO: ventrolateral outgrowth. Bar equals 1 mm.

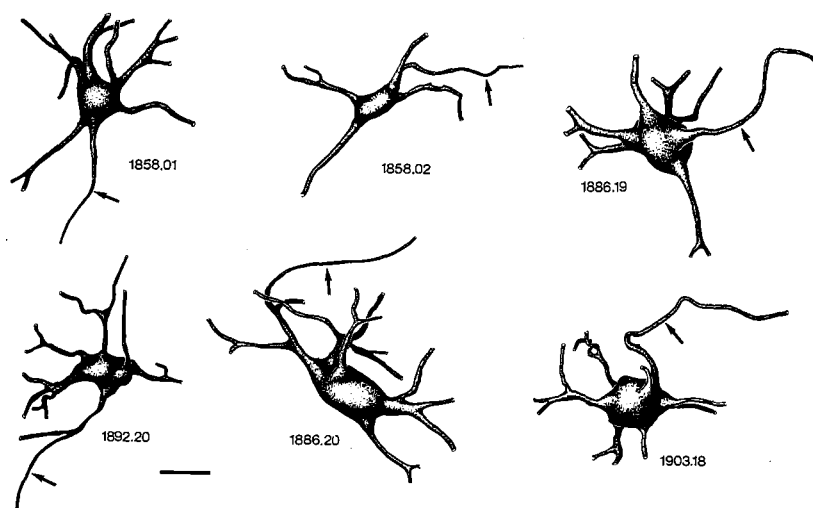


Fig. 6. Reconstructions of three type I (1858.01, 1858.02 and 1886.19) and three type II (1892.20; 1886.20 and 1903.18) cell bodies with their proximal dendrites. The axons are indicated with arrows. Note that the axons of cells 1858.01 and 1892.20 are derived from a first order dendrite, whereas the axon of cell 1886.20 originated from a second order dendrite. The spiny appendages were not indicated in these reconstructions. Bar equals 20 μ m.

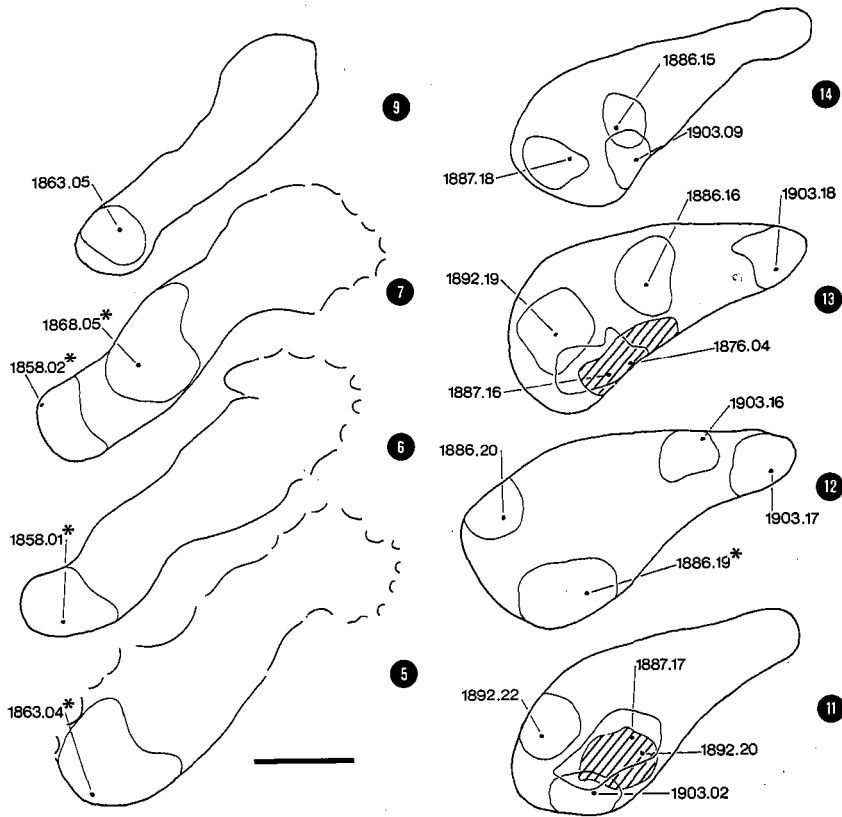


Fig. 7. Series of transverse diagrams depicting the medial accessory olive. Numericals on the right hand side of each level correspond to levels in Fig. 5. The approximate positions of the examined somata are indicated along with the transverse extent of their dendritic tree. Type I cells are marked with an asterisk. Cells 1892.20 and 1876.04 are hatched for clarity. See text for further explanation. Bar equals 500 μ m.

1887.16, 1903.16). However, also more centrally located neurons (e.g. 1868.04, 1886.20, 1887.18, 1892.20) may show a dendritic tree that is not symmetrically distributed around its soma.

Four neurons, two of each type, were reconstructed and are shown in Fig. 8. Cells 1863.04 and 1868.05 were classified as type I neurons and were positioned rather caudally within the MAO. Cells 1886.15 and 1887.18 belonged to the type II group and were found more rostrally (see Fig. 5). The most striking

differences between both cell types (besides the obviously larger area of neuropil enveloped by the dendritic tree) are the higher branching incidence and the abundance of very complex spiny appendages on especially the more distal parts of the dendrites of the type II neurons. The spiny appendages of both cell types showed one to numerous swellings, termed spine heads, and could attain a length of several tens of microns (Fig. 4D,E,F,G). Usually, the dendrites terminated as long, thin, threadlike fibers

carrying several swellings and thus appeared reminiscent of the spiny appendages. Occasionally, a dendrite terminated as a cluster of swellings (Fig. 8A). The somata of both cell types only gave rise to some, simple spiny appendages (Fig. 4C).

CORRELATION PHYSIOLOGICAL AND MORPHOLOGICAL DATA. An attempt was made to correlate physiological and morphological data. Of the 21 neurons examined morphologically, 6 neurons, located in three animals could not be investigated with respect to their responses to mesodiencephalic stimulation, since no stimulation electrodes had been placed (cat 1858) or due to misplacement of the stimulation electrodes (cats 1876 and 1892). Two additional neurons did not respond to mesodiencephalic stimulation, although a third cell from the same cat (1886.19) did. The remaining 13 neurons all reacted with a short latency action-potential and, in 11 cases, also with a long latency action-potential. Their mean values were well within the range of the 44 recorded cells described earlier. The responses of cell 1863.04 (type I, Fig. 8A) and cell 1887.18 (type II, Fig. 8C) are shown in Fig. 2B,C and 2A, respectively.

Since it has been speculated that the neuronal morphology of olivary cells may influence the frequency of the intrinsic oscillatory tendencies (Llinas,'84), we plotted both the equivalent soma and volume of the dendritic area, against the latency of the rebound spike (Fig. 3E,F). However, at this level of analysis, no significant correlation could be established.

Discussion

The present study was designed to study the morphology of olivary neurons in the medial accessory olive (MAO) of the cat and their response to mesodiencephalic stimulation. Responses of 44 inferior olivary neurons were recorded, while the morphology of 21 neurons located in the MAO was studied. The material comprises 13 neurons, located within the MAO that also reacted to mesodiencephalic stimulation.

PHYSIOLOGY. The mesodiencephalic area has been shown to be a major source of afferents to the inferior olive. More specifically, olivary afferents have been described to take their origin from the nucleus of Darkschewitsch, the interstitial nucleus of Cajal, the parvocellular red nucleus, the prerubral field and the fields of Forel (Onodera,'84; Saint-Cyr and Courville,'80; '81; '82; Spence and Saint-Cyr,'88). Most, if not all of these afferents are non-GABAergic (de Zeeuw et al.,'89a,b). Therefore, it was attractive to stimulate this area to study the olivary responses. Indeed, it was shown that 1) the olivary cells (located in either MAO or principal olive: PO) could be activated by stimulation of the mesodiencephalic junction and 2) the observed latencies (mean 7.2 ± 2.6 msec, measured to the onset of the rising phase of the action-potential) were very suggestive for a monosynaptic excitatory pathway. A similar conclusion was reached by Jeneskog ('87) using a similar stimulation paradigm but recording climbing fiber responses from the cerebellar surface.

Crill ('70) was the first to record from cat olivary neurons *in vivo*. When stimulating the cerebral cortex, he obtained similar responses as presented here, although the latencies of the triggered action-potentials were slightly higher (at least 7 msec with a mean of 9.5 ± 2.1 msec, measured to the onset of the synaptic potential). The difference in latencies with our studies can be explained by the fact that a longer pathway was stimulated, or more likely, that the pathway was not monosynaptic. Indeed, it was demonstrated anatomically by Saint-Cyr ('83) that cortico-olivary projections are only found in the medial part of the caudal MAO, an area that can only partly, and with difficulty (due to the thickness of the pyramidal tract) be reached in the experimental approach used by Crill ('70) which was the same as in our study. Therefore, it seems likely that the cortical stimulation excites other areas, presumably at the mesodiencephalic junction (Saint-Cyr and Courville,'80; Saint-Cyr,'87), which in turn excite the olivary cells in MAO and PO

monosynaptically.

An interesting and characteristic phenomenon of the olivary response to mesodiencephalic stimulation is the triggering of a long latency or rebound response. Usually, only one rebound action potential was observed, however, occasionally up to 3 rebounds could be recorded after a single stimulation burst. Working with the guinea pig slice preparation Llinas and Yarom ('81a,b; '86; Yarom and Llinas, '87) have demonstrated that the olivary neurons are equipped with a number of specific membrane conductances that may explain their propensity to discharge rhythmically (e.g. Sasaki and Llinas, '85). The preferred firing frequency appears to be different for either actively depolarized (3 - 6 Hz) or hyperpolarized cells (9 - 12 Hz; Llinas and Yarom, '86). In our material we found a mean latency of the first rebound spike of 188 msec, when adjusted for the latency of the fast response (mean 7.2 msec), a frequency of 5.5 Hz can be deduced, which fits well within the range of preferred frequencies for depolarized guinea pig olivary cells *in vitro*. Therefore, especially in this pentobarbital anaesthetized preparation, it is highly unlikely that the rebound action potential may be synaptically activated due to long reverberating loops (Tsukahara et al., '83). Also, chronic ablation of the (hemi-) cerebellum, including the deep cerebellar nuclei, did not abolish the rebound action potential, but rather facilitated it (Ruigrok et al., '89).

Apparently, it is important to trigger an ensemble of olivary cells in order to induce this rebound spike. At lower stimulation thresholds, the rebound was less frequently recorded, whereas at higher stimulation strengths, sometimes, a second and third one could be recorded. So, it would appear that an ensemble of simultaneously triggered neurons may give rise to the slow membrane potential changes that, synchronized and strengthened by the electrotonic coupling between cells (Llinas et al., '74; Sotelo et al., '74; Llinas and Yarom, '81a; Benardo and Foster, '86; Ruigrok et al. '89), are necessary to evoke the rebound action potential. Due to the fact that the time of onset of the rebound

showed quite some variability (e.g. Fig. 2A), this may contribute to the fact that the likelihood of triggering a second rebound is quite small, thus damping the response.

Although the rebound action potential is not always triggered by mesodiencephalic stimulation, the neurons may be highly receptive for incoming information between approx. 150 and 200 msec after discharging. In this respect, it is relevant to point out, that the cerebellar nuclei, which are under direct and indirect influence of climbing fibers (e.g. Voogd and Bigaré, '80; Llinas and Mühlethaler, '88 a,b; van der Want et al., '89), besides giving rise to a massive GABAergic pathway to the inferior olive (Nelson and Mugnaini, '85; '89; de Zeeuw et al., '89 a,b; de Zeeuw et al., *in press*) also give rise to an extensive projection to the mesodiencephalon and thalamus (Voogd, '64). Indeed, olivary neurons in the MAO can be orthodromically activated by stimulating the cerebellar nuclei, presumably through a cerebello-mesodiencephalo-olivary pathway (Ruigrok et al., unpublished results). The cerebello-mesodiencephalic, mesodiencephalic-olivary and cerebello-olivary interactions are presently being studied in our laboratory (Ruigrok and Voogd, '88; '90; de Zeeuw et al., '89a,b; de Zeeuw et al., *in press*).

MORPHOLOGY. Two distinct types of olivary neurons could be readily identified in the intracellularly labeled material. Neurons in, especially, the caudal part of the MAO, displayed long, relatively sparsely ramifying dendrites, that radiated away from the soma, but remained within the boundaries of the MAO neuropil (Type I). Type II neurons (terminology from Foster and Peterson, '86), possessed dendrites that branched frequently at short distances from the soma. These dendrites were curved and remained within 100 to 200 microns from the soma, forming a ball-like structure. These different types of olivary cells have been recognized and described in various mammalian species using Golgi techniques (e.g. opossum: Bowman and King, '73; rat: Gwyn et al., '77; guinea pig: Foster and Peterson, '86; cat: Scheibel and Scheibel, '55; Sotelo et al., '74; monkey:

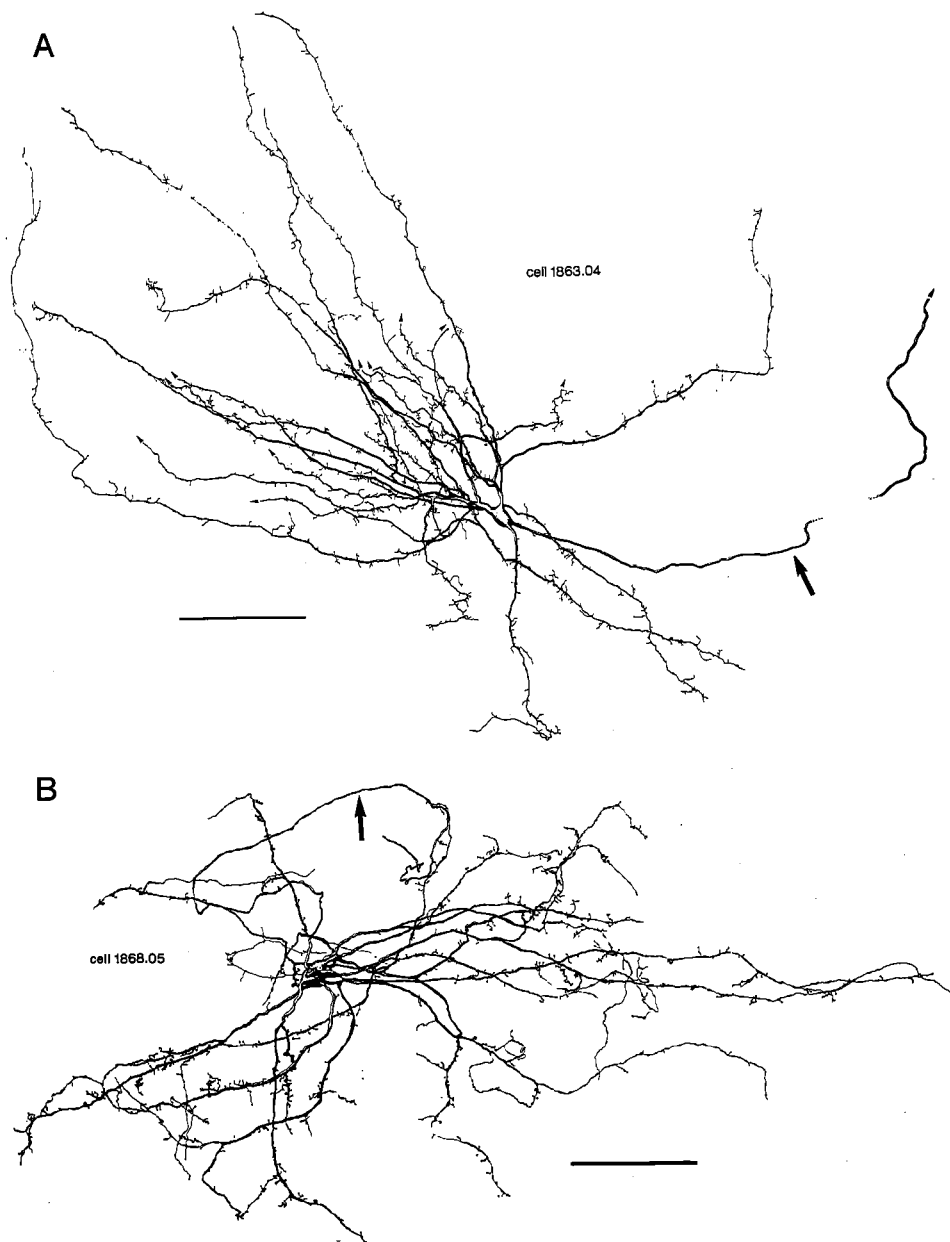
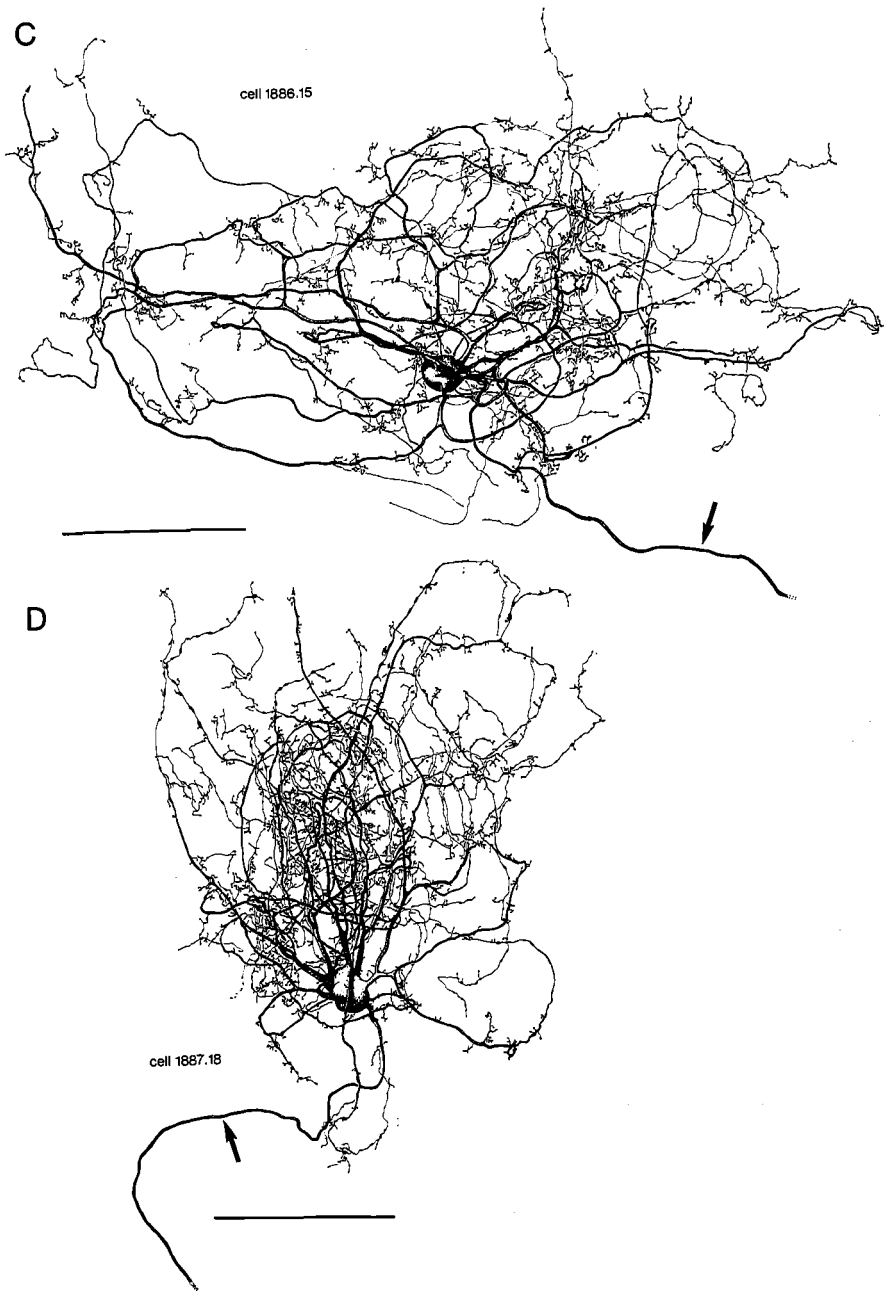


Fig. 8. Reconstructions of two type I olivary neurons: cell 1863.04 (A: see also Fig. 2 B,C) and cell 1868.05 (B) and two type II neurons: cell 1886.15 (C) and cell 1887.18 (D: see also Fig. 2A). These cells were also used for the ultrastructural analysis as reported in both companion



papers (de Zeeuw et al., submitted a,b). Axons are indicated by arrows. Arrowheads denote dendrites that were not fully reconstructed. Bar equals 100 μm . Note that magnification for C,D, is higher than for A,B.

Scheibel and Scheibel,'55; Rutherford and Gwyn,'80; man: Scheibel and Scheibel,'55).

The Scheibels ('55) noted that the extent of the dendritic tree of the type II neurons decreased in conjunction with a diminution of the 'packing' density of the olivary neurons when advancing in the phylogenetic scale from cat, to monkey, to man, indicating that the amount of overlap between the individual dendritic trees would become less in this order. However, their conclusions were doubted by Foster and Peterson ('86), who indicated that the dendritic tree of the type II guinea pig inferior olivary neurons was at least as compact as that of the cat dendritic tree. We tend to support this notion, with the following annotations. The type II neurons in the cat olive, although equipped with a larger dendritic tree than the guinea pig olivary neurons, also displayed a much more complex dendroarchitecture (cf. Fig. 8C,D with Fig. 4 of Foster and Peterson,'86). Also, spiralling dendrites did not occur in our material of the cat although we could confirm the existence of spiralling dendrites (the spirals having appr. the size of a cell body) in our own material of intracellularly injected guinea pig and rat olivary cells (unpublished observations). Finally, although we did not determine the packing density in the guinea pig inferior olive, it is much higher as compared to cat. It seems more likely, therefore, that the morphology of inferior olivary neurons is adapted to the functional demands of different animals, rather than obeying a specific evolutionary trend.

As Foster and Peterson ('86) demonstrated, the spatial extent of the dendritic tree can best be described as an ellipsoid. However, in literature usually only the diameter of the dendritic tree is given. Scheibel and Scheibel ('55) determined a mean diameter for cat olivary cells (presumably only type II neurons) of $211 \pm 48 \mu\text{m}$. When we consider our volumetric data (based on an ellipsoid) as a measure for a globular dendritic tree, we come to a mean diameter of $364 \pm 67 \mu\text{m}$ ($n=21$) for both cell types, and of $338 \pm 45 \mu\text{m}$ ($n=16$) for the type II cells only. There may be several reasons for this discrepancy.

Firstly, the dendrites illustrated by the Scheibels did not take a straight course but appeared rather 'wrinkled', suggesting a certain amount of shrinkage of their material. Indeed, it was recently indicated by Uylings et al. ('86) that linear tissue shrinkage of various Golgi techniques may be as high as 10 - 20%. In our material, using a 5% glutaraldehyde perfusion fixation, followed by an additional osmiumtetroxide fixation, chemical dehydration and Araldite embedding, shrinkage did not appear to be severe, as judged from the course of the dendrites (Figs 4A,B; 8). Secondly, the Golgi technique requires the use of young animals (the Scheibels used kittens of one to several weeks of age). Therefore, the olivary neurons may not have matured by then. Thirdly, the olivary cells may have a preference for a longitudinal organization, since, in our material, the mean diameter of the dendritic tree, solely based on their covered surface area in the transverse plane ($331 + 49 \mu\text{m}$), was slightly less, than when calculated from the volumetric area. Finally, and possibly more important, may be the fact that it is difficult to obtain correct values for the entire extent of the dendritic tree in Golgi material, since many neighbouring cells may obscure the course of certain dendrites. Also, incomplete Golgi impregnation (especially of rather thin dendritic elements) may bias the measurements. Such a bias was demonstrated for spinal motoneurons, where the dendritic extent of intracellularly HRP labeled cells was found to be significantly larger compared to Golgi stained material, (Brown,'81). From Fig. 8 C,D it can be seen that within the entire dendritic tree, a more or less spherical concentration of dendrites can be distinguished. When the diameter of this sphere is determined for the type II cells, the mean value of $248 \pm 36 \mu\text{m}$ is close to the value given by the Scheibels ('55). This diameter represents a globular neuropil volume of $8.0 * 10^6 \mu\text{m}^3$. The Scheibels ('55) estimated a mean packing density of appr. 23 neurons per $1.6 * 10^6 \mu\text{m}^3$, indicating that an average of approximately 115 neurons would be positioned within the dense globular part of the

TABLE 1. Some morphological data on HRP injected MAO neurons (- indicates if type I neurons differ significantly from type II neurons ($p < 0.05$)).

	equivalent soma diameter (mean \pm s.d.) in μm	number of first-order dendrites (mean \pm s.d.)	number of cells with axon originating from a dendrite	vol. of neuropil enveloped by dendritic tree (mean \pm s.d.) in $10^6 \mu\text{m}^3$
Type I (n=5)	17.5 \pm 3.7*	5.0 \pm 1.0	1*	48.7 \pm 20.3*
Type II (n=16)	23.0 \pm 2.6	5.6 \pm 1.0	15	21.4 \pm 8.8
Total (n=21)	21.7 \pm 3.7	5.4 \pm 1.0	16	27.9 \pm 16.8

dendritic tree. Much higher numbers will be involved when the entire dendritic tree is taken into account (appr. 290).

Most somata are not positioned in the center of their dendritic tree, but rather slightly to extremely eccentrically. This is obviously the case for neurons bordering the nucleus, however, also within the nucleus it can be seen that some cells display a clearly preferred direction of their olivary tree (see e.g. cell 1887.18, Fig. 8D). This could be in accordance with the suggestion made by Sotelo et al. ('74) that neurons within the olivary neuropil are located in clusters. The dendrites of a number of cells may seek each other out to become intricately interwoven. From our calculations, outlined above, we suggest that such a cluster may contain up to 100 neurons.

Besides the differences in dendritic architecture of the type I and II neurons, it was noted that the type I neurons generally had a smaller cell soma that carried less primary dendrites compared to the type II cells. Furthermore, axons of the type I cells

were usually derived from the soma, whereas they originated from a first, and in one case even a second, order dendrite in case of the Type II cells. Presently, we do not know whether these differences may have functional implications (see also de Zeeuw et al., submitted b).

From Golgi studies of various animals, reviewed by King ('80), it would appear that about 20 % of the olivary neurons carries recurrent axon collaterals. However, although in our material of the cat all axons could be followed outside of the MAO neuropil and frequently could be observed to cross the midline of the brain, no axon collaterals could be found, as was also reported for the 6 intracellularly HRP labeled cat olivary neurons by King ('80). To explain the discrepancy between the Golgi and the HRP studies, it should again be stressed that the Golgi techniques usually require the use of newborn animals or even fetuses (see King, '80, for review). Therefore, it seems possible that olivary axons of immature animals may be equipped with recurrent collaterals, which

disappear later.

One of the most striking features of the intracellularly injected cells were their spiny appendages. Especially the second and higher order dendrites carried an abundance of long and frequently very complex spines. Although the abundance of a variety of spines have been noted in Golgi studies of various animals (e.g. Scheibel and Scheibel,'55; Gwyn et al.,'77; Rutherford and Gwyn,'80; Foster and Peterson,'86), they were not described as very long (in our material frequently measuring up to tens of microns), possibly because of a failure to impregnate these very delicate structures. Most spiny appendages started as a thread-like protrusion from the dendrite and after or before branching displayed one up to numerous swellings (spine heads). As will be shown in the companion paper (de Zeeuw et al., submitted a), the spines are involved in glomeruli, which form a characteristic feature of the neuropil in the MAO (Sotelo et al.,'74; de Zeeuw et al.,'89 a,b; de Zeeuw et al., submitted a,b). Furthermore, theoretical studies have indicated the enormous importance of spines for the computational capabilities of neurons (Pongracz,'85; Segev and Rall,'88; see also de Zeeuw et al '89b; de Zeeuw et al., in press), while, in addition, they also may play a role in neuronal plasticity (e.g. Fifkova and Harrevel'd,'77; Lee et al.,'80; Crick,'82; Caceres et al,'83).

Conclusions

Olivary cells in the medial accessory olive can be activated monosynaptically from the mesodiencephalic junction. When an ensemble of olivary neurons is triggered simultaneously, a rebound actionpotential may be recorded with an interspike frequency of appr. 5.5 Hz.

Lightmicroscopical analysis of intracellularly labeled cells reveals two types of neurons. Type I has sparsely branched neurons that stream away from a usually small cell body that also gives rise to the axon. Type II cells are located more rostrally in the MAO, possess dendrites that branch frequently, forming a ball-like structure around a frequently eccentrically placed soma. The axon is usually derived from a first order dendrite. The extent and morphology of the dendritic tree of the type II cells suggest that they are intensively overlapping the dendritic field of approximately 100 other olivary neurons.

The abundance, length, and complexity of the spiny appendages suggest important roles in: 1) connecting individual olivary cells (through gap junctions, located in glomeruli), 2) the computational capabilities of the neurons (especially in time sensitive processes), 3) neuronal plasticity.

b. Intracellular labeling of neurons in the medial accessory olive of the cat: II. Ultrastructure of dendritic spines and their GABAergic innervation

Abstract

In order to describe the morphology of dendritic spines of identified neurons in the cat inferior olive together with their gamma-aminobutyric acid (GABA) synaptic input, a technique was used combining intracellular labeling of horseradish peroxidase with post-embedding gold-immunocytochemistry. With this technique physiologically identified olivary cells were reconstructed with the light microscope, and the horseradish peroxidase reaction product and immunogold labeling were subsequently examined in serial sections at the ultrastructural level. In addition, a degenerating neuron was observed resulting in a triple labeling in single ultrathin sections.

Quantitative and three-dimensional analysis showed that the dendritic spines were composed of long, thin stalks ending in one or more spine heads. The spines of cells located in the caudal half of the medial accessory olive (type I cells, characterized by dendrites which run away from the soma) were found to be less complex than those of cells located rostrally in this olivary subnucleus (type II cells, characterized by dendrites which tend to turn back towards the soma). Most, if not all, of the spines of both cell types were located within glomeruli. On average, the spines within individual glomeruli originated from 6 different dendrites (with a maximum of 8). Different spines within the same glomerulus were never derived from different dendrites of the same olivary neuron but single spines frequently gave rise to several spine heads which could be located either within different glomeruli or inside a single glomerulus. The glomerular spine heads originating from the same spine were rarely located near one another. All spines and most of the spine heads were contacted by both GABAergic and non-GABAergic terminals. Most of the GABAergic terminals contained pleio-

morphical vesicles and displayed symmetric synapses whereas the non-GABAergic terminals showed usually round to oval vesicles and asymmetric synapses.

Introduction

Most, if not all, of the cells of the inferior olive (IO) give rise to the olivo-cerebellar fibers which terminate as climbing fibers innervating the Purkinje cells of the cerebellar cortex (Szentágothai and Rajkovits,'59; Eccles,'66; Desclin,'74). Short axon cells seem to be absent in the olive, with the possible exception of a few GABAergic interneurons (Nelson et al.,'88; Walberg and Otterson,'89). The light microscopical morphology of olivary neurons was described for humans (Vincenzi, 1886; von Kölliker, 1893; van Gehuchten,'05; Ramon y Cajal,'09) and for various animals (Ramon y Cajal,'09; Scheibel and Scheibel,'55; Scheibel et al.,'56; Ramon-Moliner,'62; Bowman and King,'73; Gwyn et al.,'77; Sotelo et al.,'74; Rutherford and Gwyn,'80; Foster and Peterson,'86; Iwahori and Kiyota,'87; Sztajn,'88). Scheibel and Scheibel ('55) were the first to show that two basic types of neurons can be distinguished in Golgi material of the IO of various animal species. Later, these findings were confirmed in experimental studies of the guinea pig (Foster and Peterson,'86) and the cat (Ruigrok et al., submitted) in which olivary cells were intracellularly injected with horseradish peroxidase (HRP). Both cell types have a relatively small cell body and contain dendrites with spiny appendages, but the morphology of their dendritic tree is different. The first cell type (type I) is mainly present in the caudal medial and dorsal accessory olive. Its dendrites are relatively long, running away from the soma. They are sparsely branched and cover a large receptive field. The dendritic tree of the second type (type II) is more complex. The dendrites are highly branched and tend



to turn back towards the soma. This type of neuron predominates the rostral olivary subnuclei but is also present in the caudal parts (Scheibel and Scheibel,'55; Scheibel et al.,'56; Foster and Peterson,'86). It occupies a more limited area of the three dimensional space than the type I cells (see also Ruigrok et al., submitted).

Two of the major afferent systems of the medial accessory olive (MAO) and principal olive (PO) are a GABAergic input (Nelson et al.,'84; de Zeeuw et al.,'88a) derived from the cerebellar nuclei (Tolbert et al.,'76) and a non-GABAergic innervation (de Zeeuw et al.,'88a) from the mesodiencephalic junction (Ogawa,'39; Onodera,'84). The cerebellar and mesodiencephalic terminals are widely distributed over the extraglomerular and glomerular neuropil (de Zeeuw et al.,'89a). Frequently, the boutons of both inputs establish synaptic contacts with the same glomerular spines, some of which are electrotonically coupled by gap junctions (de Zeeuw et al., '88b; de Zeeuw et al., in press).

Fig. 1. Electron micrographs showing GABAergic terminals (white arrows) apposed to a cell body of an HRP labeled olivary neuron. The rectangular area indicated in B is magnified in A. Note that all GABAergic terminals are directly apposed to the soma and not to somatic spines. Scale bar in A = 0.9 μ m, in B = 3.2 μ m.

Fig. 2. Electron micrograph of an HRP labeled olivary neuron. Note the unstained inclusion of the cell membrane (arrow head) suggesting endo- or exocytotic processes to or from the nearby located Golgi apparatus. The nucleus (N) is labeled with HRP reaction products but not as heavily as the perikaryon. Scale bar = 1.2 μ m.

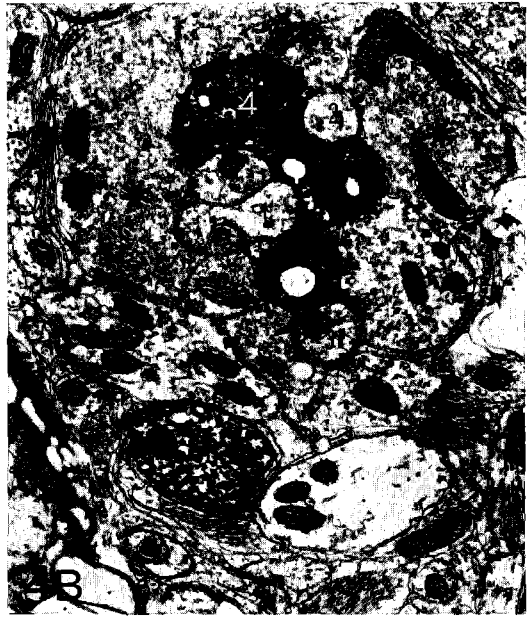
Fig. 3. Electron micrograph of two HRP labeled dendrites located near one another. Note that the dendrite indicated by the asterisk is much weaker labeled than the other one. Scale bar = 1.1 μ m.

Presently, it is not known whether the two cell types differ with respect to the morphology of their spines and whether they have a different synaptic input. Therefore, an attempt was made to study both types of cells in the MAO of the cat at the ultrastructural level by means of a combination of intracellular labeling of HRP with postembedding GABA-immunocytochemistry. The dendritic spines were analysed quantitatively in single and serial ultrathin sections in order to find out 1) whether all spines are located in glomeruli, 2) how many spines of how many different neurons are involved in a single glomerulus, and 3) whether all spines are contacted by both GABAergic and non-GABAergic terminals.

The physiological and most of the light microscopical data (Ruigrok et al., submitted) and the electron microscopical results of the olivary axons and their input (de Zeeuw et al., submitted) are published in both companion papers.

Material and methods

Details on the experimental procedure used to obtain intracellular recordings from olivary neurons and the subsequent iontophoretic injection of HRP are reported in a companion paper (Ruigrok et al., submitted). Briefly, cats were anaesthetized with pentobarbital and in each cat it was attempted to penetrate at least 10 olivary cells, to identify them physiologically and to inject them with HRP (5% in saline). The injected cells were spaced at least 500 μ m. After 1 to 16 hours the cats were deeply anaesthetized with pentobarbital and perfused transcardially with 100 ml. 0.9% saline in 0.18 M cacodylate buffer (pH 7.3) under artificial respiration, followed by 2 liters of 5% glutaraldehyde in the same buffer. The brainstem containing the IO was left in the fixative for 1 to 2 hours, cut transversely on a vibratome in 70 μ m sections and incubated with diaminobenzidine (DAB) according to Graham and Karnovsky ('66). Most of the incubated vibratome sections were rinsed in 8% (D+) glucose dissolved in 0.1 M phosphate buffer (pH



7.3), osmicated during 40 min at 45 °C with 1.5% osmiumtetroxide in the same solution, rinsed in distilled water (4 times), block-stained in 2% aqueous uranyl acetate for 60 min at 4 °C, without rinsing directly dehydrated in dimethoxypropane (DMP), (Muller and Jacks,'75; Truter et al.,'80), and flat embedded in Araldite between teflon coated glass slides (Bishop and King,'82). Some vibratome sections were rinsed and osmicated without glucose. After polymerization of the embedded sections, the intracellularly labeled neurons were studied in the light microscope (LM). A total of 21 intracellularly labeled neurons were located in the MAO and suited for light microscopical study. The neurons were classified according to the morphology of their dendritic tree as either type I or type

Fig. 4. Electron micrographs of a simple looking glomerulus containing four different spines (1, 2, 3, and 4). Most of the spines can be seen two or three times within the plane of a single section. The parent dendrite of the HRP labeled spine (4) is present at the bottom of the micrograph. Note that the GABA labeling (terminals indicated by the stars) is consistent in both serial sections A and B. Scale bar = 1.2 µm.

Fig. 5. Electron micrographs of a complex glomerulus (surrounded by small arrow heads). The parent dendrite in the right upper corner gives rise (follow the open arrows in A) to a spine (no. 1 in B) which branches in other spiny appendages (no. 2 and 3). Note that the secondary spiny appendages are located in "subglomeruli" which are more or less separated from the main glomerulus by invaginations of the glial sheath (follow small arrow heads). In A two spiny profiles of the same HRP labeled spine are located directly near one another (large arrow heads). However, following the serial sections it was evident that this only happened immediately after a branching point (compare A and B). In B a club pedunculated spine (arrow) is derived from the soma. Scale bar = 1.3 µm.

II neurons. Two type I neurons of the caudal MAO and two type II neurons of the rostral MAO were selected for electron microscopical examination (these cells, which were reconstructed in the preceding companion paper (Fig. 8 of Ruigrok et al., submitted) and were numbered as 1868.05, 1863.04, 1887.18, and 1886.15, will be referred to as cell A, B, C, and D, respectively). Serial photographs were made with an interval of 5 µm throughout the 70 µm thick embedded tissue sections. The tissue blocks containing the soma of these neurons were glued on plastic capsules. Pyramids were made (with a surface area of approximately 600 µm x 300 µm) from which about 1000 ultrathin sections with a silver interference colour were cut with a Diatome diamond knife on a Reichert ultratome (Ultracut). The ultrathin sections were mounted on formvar coated nickel slot grids and processed for postembedding GABA-immunocytochemistry. The grids were rinsed in a solution of 0.05 M Trisbuffer (pH 7.6) containing 0.9 % NaCl and 0.1% Triton X-100 (TBS-Triton) and left overnight in a droplet of GABA-antibody diluted 1:1000 in TBS-Triton. The GABA-antibody, which was raised in rabbit, had been tested on its specificity (Buijs et al.,'87; Seguela et al.,'84). The next morning the grids were rinsed in TBS-Triton (2 times), stored in the same solution for half an hour, rinsed in TBS-Triton (pH 8.2) and incubated for one hour in a droplet of goat anti-rabbit IgG labeled with gold particles (diameter 15 nm; Janssen Pharmaceuticals), diluted 1:40 in TBS-Triton (pH 8.2). After this final incubation the grids were rinsed in TBS-Triton (2 times) and in distilled water (2 times). The sections were counterstained with uranyl acetate and lead citrate, and examined and photographed in a Philips (300) Electron Microscope (EM).

Analysis

In the present study the HRP labeled dendritic spines and their GABAergic input were analysed both in non-serial and serial sections. From each of the 4 HRP injected cells 1 tissue block was selected.

SINGLE SECTION ANALYSIS.

Numerous HRP labeled spines were randomly selected and photographed by screening the surface area of non-serial ultrathin sections at regular distances. It was determined for each tissue block 1) what percentage of the HRP labeled spines were contacted by both a GABAergic and/or a non-GABAergic terminal, 2) what percentage of the HRP labeled spines were located within a glomerulus, 3) how many HRP labeled spiny profiles were located on average within the glomeruli which contained HRP labeled spiny appendages, and 4) what the average ratio was between the number of HRP labeled spines and the total number of spines in these glomeruli. In this analysis a profile was supposed to be HRP labeled when a dark granular HRP/DAB reaction product was equally distributed over the cytoplasm. The HRP labeled spines were distinguished from HRP labeled dendrites by their thin diameter (0.5 to 1.0 μm), the presence of several deformed vesicles including large granulated vesicles, coated vesicles, tubules of smooth endoplasmic reticulum, and multivesicular bodies, and by the absence of regularly interspaced microtubuli. A terminal was considered to be GABA-positive when the number of gold particles overlying it was at least 8 times higher than the number of particles over the surrounding non-labeled structures (De Zeeuw et al., '89a). A complex synaptic arrangement was supposed to be a glomerulus when it was composed of a central core of at least 3 dendritic elements surrounded by at least 2 axon terminals, and enwrapped in an astrocytic sheath (Sotelo et al., '74; de Zeeuw et al., '89b). The data of the 4 cells were averaged and the standard deviations (SD) were calculated (Table 1).

SERIAL SECTION ANALYSIS. A total of 67 HRP labeled spines obtained from all 4 selected neurons were followed through serial sections (up to 74 ultrathin sections). From each of the 4 studied cells a single spine and the glomerulus, in which the spine was located, were selected for a computer reconstruction. The outlines of all HRP labeled and

non-labeled spines, and GABAergic and non-GABAergic terminals located within the glomerulus were drawn, marked and made into a three dimensional reconstruction by means of a 3-D program (Macreco 3.2 by E. Otten, R.U. Groningen, the Netherlands). For each glomerulus it was determined 1) how many spines were incorporated and from how many different dendrites these spines emerged, 2) whether all the spines were contacted by both a GABAergic and non-GABAergic terminal, 3) how many spine heads were present, 4) whether all these spine heads were contacted by both a GABAergic and non-GABAergic terminal, and 5) how many GABAergic and non-GABAergic terminals were located within the glomerulus. A spine was defined as the whole of branching appendages and spine heads which originated from one single stalk (i.e. spine stem) arising from its parent dendrite. A spine head was distinguished from a spiny stalk by its relatively thick diameter ($>0.5 \mu\text{m}$) and the accumulation of deformed vesicles (see above), granular material and mitochondria. The data were averaged and the SD's were calculated (Table 2).

Results

LIGHT MICROSCOPY. Prior to ultrastructural investigation, the injected cells were investigated using the light microscope. The addition of glucose during the osmication appeared to be important for an optimal evaluation of these osmicated sections, since they turned out to be less darkly stained, revealing beautifully the finest dendritic ramifications and spiny appendages of the injected cell (see also Ruigrok et al., submitted). Light microscopical data on 21 injected olivary cells, all located within the MAO were published in the companion paper (Ruigrok et al., submitted). Five cells, 4 of which were located in the caudal half of the MAO, displayed the characteristics of type I neurons, whereas 16 cells were classified as type II neurons and were all positioned in its rostral half.

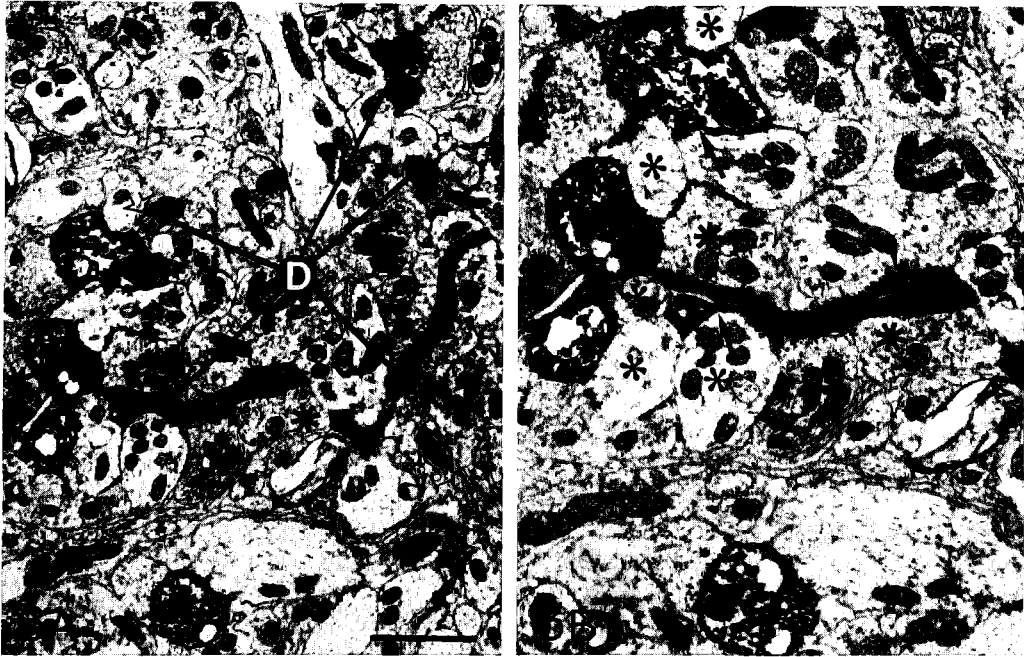


Fig. 6. Electron micrographs showing triple labeling: Intracellular labeling of HRP (of a type II neuron) combined with postembedding GABA-immunocytochemistry (stars) and cellular degeneration (D). The parent dendrites of the HRP labeled and degenerated spines are present respectively at the bottom and top of the Figure (A). The degenerated spiny profiles are somewhat shrunken, they contain multivesicular bodies (open arrow in A), they receive misshapen synaptic contacts (arrow heads), and at several locations they are apposed to HRP labeled (arrows in B) or non-labeled spiny profiles (asterisks in B). Scale bar = 1.9 μm .

GENERAL ELECTRON MICROSCOPICAL OBSERVATIONS. In the electron microscope we found numerous HRP labeled and GABAergic structures, and in addition some degenerating profiles. The HRP labeled structures included the cell body, axon, dendrites and spines. Most of these structures could be traced back in the LM photomicrographs and the LM reconstructions. The HRP reaction product appeared as granular densities ubiquitously distributed throughout the cytoplasm. Generally, multivesicular bodies and microtubuli could still be identified in the HRP labeled cells. Intraneuronal structures like mitochondria and the Golgi apparatus were mostly spared and sometimes unstained inclu-

sions were observed in or near the cellular membrane of the soma or proximal dendrites suggesting the presence of endo- and/or exocytotic processes (Fig. 2). The accumulation of reaction products in the nuclei of the olivary cells made it clear that HRP had penetrated through the nuclear pores. However, the nuclei were never stained as heavily as the perikaryon.

Different dendrites from the same HRP labeled olivary cell always remained apart. In only two cases of all studied ultrathin sections two HRP labeled dendrites were touching one another. In both cases one of the dendrites of both pairs was much weaker labeled than the other one (Fig. 3), and than could be expected from the staining intensity

Table 1. Quantification of HRP labeled spiny profiles (SP's) selected randomly in single sections.

	CELL A	CELL B	CELL C	CELL D	$\bar{X} \pm SD$
Cell type	Type I	Type I	Type II	Type II	
Number of examined SP's	41	45	179	110	94 \pm 66
SP's contacted by GABAergic and non-GABAergic terminals	22 (54%)	29 (64%)	86 (58%)	65 (59%)	59% \pm 4
SP's located within glomeruli	34 (83%)	33 (73%)	144(80%)	90 (82%)	80% \pm 5
Average number of HRP labeled SP's in a glomerulus	1.3	1.3	1.6	2.0	1.6 \pm 0.3
Ratio of HRP labeled SP's to total number of SP's in glomeruli	0.24	0.22	0.25	0.25	0.24 \pm 0.0

Table 2. Quantification of four reconstructed HRP labeled spines and their glomeruli.

	GLOM A	GLOM B	GLOM C	GLOM D	$\bar{X} \pm SD$
Cell type	Type I	Type I	Type II	Type II	
Number of spines	6	5	8	6	6 \pm 1
Spines contacted by GABAergic and non-GABAergic terminals	6 (100%)	5 (100%)	8 (100%)	6 (100%)	100%
Number of spine heads	15	18	19	23	19 \pm 3
Spine heads contacted by GABAergic and non-GABAergic terminals	11 (73%)	12 (67%)	15 (79%)	14 (61%)	70% \pm 8
Number of GABAergic terminals	6	5	3	5	5 \pm 1
Number of non-GABAergic terminals	6	5	5	7	6 \pm 1

of all other labeled profiles of the same cell. This might indicate that HRP leaked from one dendrite into the other.

While the somata only rarely gave rise to spiny appendages (Fig. 1), the proximal dendrites contained usually two or three spines. These centrally located appendages were relatively simple, resembling pedunculated club shaped spines (cf. Gwyn et al., '77). The distal dendrites, however, gave off most

of the spines. These spines often branched in different parts like racemose appendages with a complex appearance (Figs 5 and 7). These differences between the centrally and peripherally located spines were found for both type I and type II neurons. In some fortuitous sections, it was seen that many spines belonging to the same HRP labeled olivary cell were observed to contact the same unlabeled cell at various (up to 6) locations.

The HRP labeled spines were never found to be linked by gap junctions with non-labeled dendritic elements, whereas gap junctions between different non-labeled dendritic elements were frequently observed in the same material.

Concerning the GABAergic labeling we observed that gold labeled structures were present throughout the neuropil. In the serial analysis it was found that the profiles of the same GABAergic structures were consistently stained. These GABAergic structures were mainly terminals but labeled preterminal profiles and myelinated axons were observed as well. We did not find GABAergic somata or proximal dendrites. The presence of a few GABAergic neurons in the IO (Nelson et al., '88; Walberg and Otterson, '89) could therefore not be confirmed. As described previously (de Zeeuw et al., '89a), the GABAergic terminals usually contained pleiomorphic vesicles and symmetric synapses, whereas the non-GABAergic terminals showed mainly round to oval vesicles and asymmetric synapses. Occasionally, the non-GABAergic (Figs 8E and F) but also the GABAergic terminals showed subsynaptic densities as described by Taxi ('61). The densities subsynaptic to GABAergic terminals were much more frequently observed in the caudal MAO than in the rostral MAO. The GABAergic and non-GABAergic terminals were apposed to HRP labeled somata, proximal and distal dendrites, and axons (de Zeeuw et al., submitted). While the terminals apposed to the soma usually contacted directly the perikaryon (Fig. 1; cf. de Zeeuw et al., '89a), the terminals at the dendritic level mostly contacted the HRP labeled spines which arose from the dendritic shafts (Figs 4 to 10). In most cases the GABAergic and non-GABAergic terminals established synaptic contacts. When individual HRP labeled dendrites and their branching points were cut longitudinally, it could be observed that they received both GABAergic and non-GABAergic terminals, although the major part of their shafts was covered by glial sheaths.

Electron dense, shrunken profiles of structures incorporating cellular organelles

like mitochondria and multivesicular bodies were detected in the tissue block containing one of the HRP labeled cells in the rostral MAO (Fig 6). These structures resembled the profiles of degenerating neurons (for a review of the ultrastructural morphology of neuronal degeneration, see Lieberman, '71), and they could be distinguished from the HRP labeled structures, which appeared much darker and contained a more granular reaction product. Their restricted distribution in the glomeruli and the extraglomerular neuropil would be comparable with the location of dendrites and spines of an olivary neuron. The GABAergic and non-GABAergic terminals apposed to these degenerating spines frequently displayed an accumulation of presynaptic vesicles but the synaptic clefts seemed to be narrowed by the degeneration. In some cases the degenerating profiles were located together with HRP labeled and non-labeled spiny profiles in the same glomerulus (Fig. 6B), providing direct evidence that these synaptic clusters contained dendritic elements of at least three neurons. At several locations in these glomeruli, the degenerating profiles were apposed to the non-degenerating structures. Gap junctions, however, were never found between these degenerated and non-degenerated dendritic elements.

SINGLE SECTION ANALYSIS. In the ultrathin sections 41 and 45 HRP labeled spiny profiles were obtained from non-serial sections of cell A and B, respectively (both belonging to type I; see Table 1). From cell C and D (type II) 179 and 110 HRP labeled spines were selected using the same sampling procedures. Analysis of the spines of all four cells showed that an average of 59% received both a GABAergic and a non-GABAergic terminal, and that an average of 80% of these spines was located in a glomerulus. Type I and type II neurons did not differ in this respect (see Table 1). Regarding the glomeruli which contained one or more of the selected HRP labeled spiny profiles it was found that an average of 1.3 (SEM 0.01) HRP labeled spiny profiles (varying between 1 and 4) were located within a single glomerulus of neurons A and B (type I), whereas

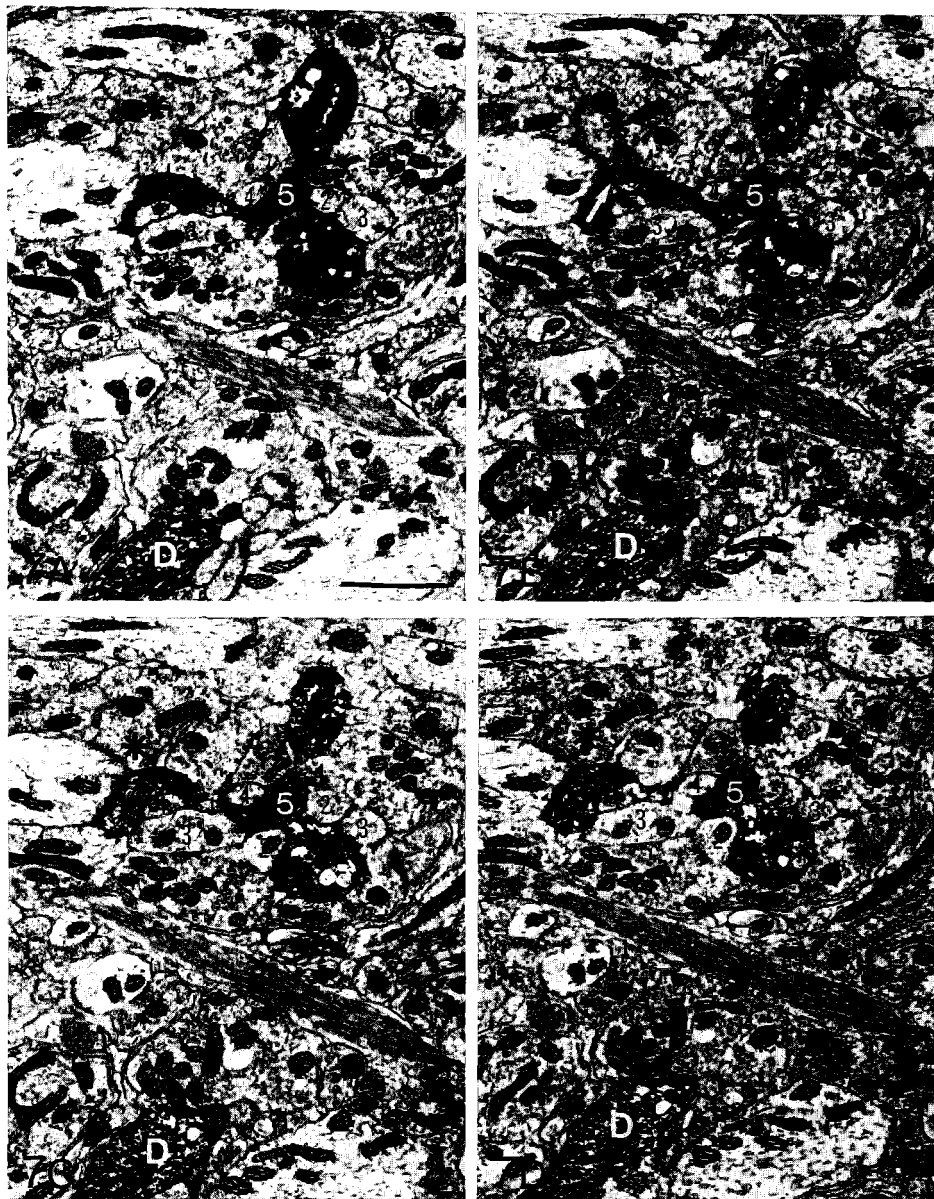


Fig. 7. Electron micrographs of a parent HRP labeled dendrite (white D) and one of its spines (white 5). Note that both a presumably GABAergic terminal (star) and a non-GABAergic terminal is apposed to the stalk (white arrow in B) of the HRP labeled spine but that a synaptic membrane specialization can not be observed at this location. The glomerulus containing five (1, 2, 3, 4, and 5) different spines can be followed through four serial sections (A, B, C, and D). Scale bar = 1.6 μ m.

the glomeruli from neurons C and D (type II) contained on average 1.8 (SEM 0.2) HRP labeled spiny profiles (with a maximum of 6; cf. King, '80). This difference was significant (Student T-test; $p < 0.05$). However, the ratio of the number of HRP labeled spines to the total number of spines in the glomeruli containing these labeled spines was almost the same for both cell types (Table 1). For all cells, approximately one out of four spiny profiles located within a glomerulus was HRP labeled. Together these data indicated that glomeruli with an HRP labeled spine from cell A or B contained fewer spiny profiles in the plane of a single section than those of cell C or D.

SERIAL SECTION ANALYSIS. Almost all HRP labeled spines which were followed through serial sections appeared to be located within glomeruli (65 out of 67), and most of them were composed of long stalks (varying from 0.5 to 6 μm) and one or more spine heads (up to 9). The three-dimensional analysis showed that when different HRP labeled spiny profiles (mostly spine heads) were located within an individual glomerulus, they were nearly always derived from a common spine. Only in one case (of type I neuron A) it was found that different HRP labeled spine heads located in the same glomerulus were derived from two different spines (Fig. 8B). These spines arose near one another from the same dendrite (Fig. 8A). It was seldomly found that two different spines or their spine heads belonging to the same HRP labeled cell were apposed to each other. When this occurred (Fig. 5A), the apposition was located just after a branching point of the spine (Fig. 5B). Spines which were intermingled with each other and which had large contact areas, usually entered the glomerulus from different directions (Figs 6 and 10).

Different dendrites from the same HRP labeled neuron never emitted different spines to the same glomerulus, but different spine heads of the same HRP labeled spine were frequently located within different glomeruli. This holds true for spine heads which originated after a bi- or trifurcation of a spine

but also for different spine heads of a non-branching spine chain. Sometimes, the stalks of peripheral spines were very long resembling small distal dendrites. Especially these long spines ran from one glomerulus to the other giving off one or more spine heads at each glomerulus.

The four glomeruli which were reconstructed by means of the Macreco program contained an average of six different spines (varying from 5 to 8) and nineteen different spine heads (varying from 15 to 23). Glomeruli C and D, which belonged to the two type II neurons, contained slightly more spines and spine heads than glomeruli A and B of the type I neurons (Table 2). All spines (100%) and most of the spine heads (70%) of these four glomeruli were contacted by one or more GABAergic as well as one or more non-GABAergic terminals. On average there were five GABAergic and six non-GABAergic terminals in each glomerulus (different types of neurons did not differ in this respect). The GABAergic and non-GABAergic afferents entered the glomeruli, like the spines themselves, from different directions. They made synaptic contacts primarily with the spine heads but frequently they were apposed to the spiny stalks as well (Fig. 7). In the center of one of the four reconstructed glomeruli (C) a gap junction was present between the stalks of two non-labeled spines (Figure 9A and C). In this case a non-GABAergic terminal established an asymmetric synaptic contact with both coupled dendritic elements (a so-called strategically located terminal; Sotelo et al., '86; de Zeeuw et al., '89a).

Discussion

TECHNICAL ASPECTS. Our technique of intracellular labeling of HRP combined with GABA postembedding immunocytochemistry allows physiological and light microscopical identification, and a simultaneous visualization of the HRP reaction product and the gold particles of the immunocytochemical reaction at the ultrastructural level. When light microscopic examination of

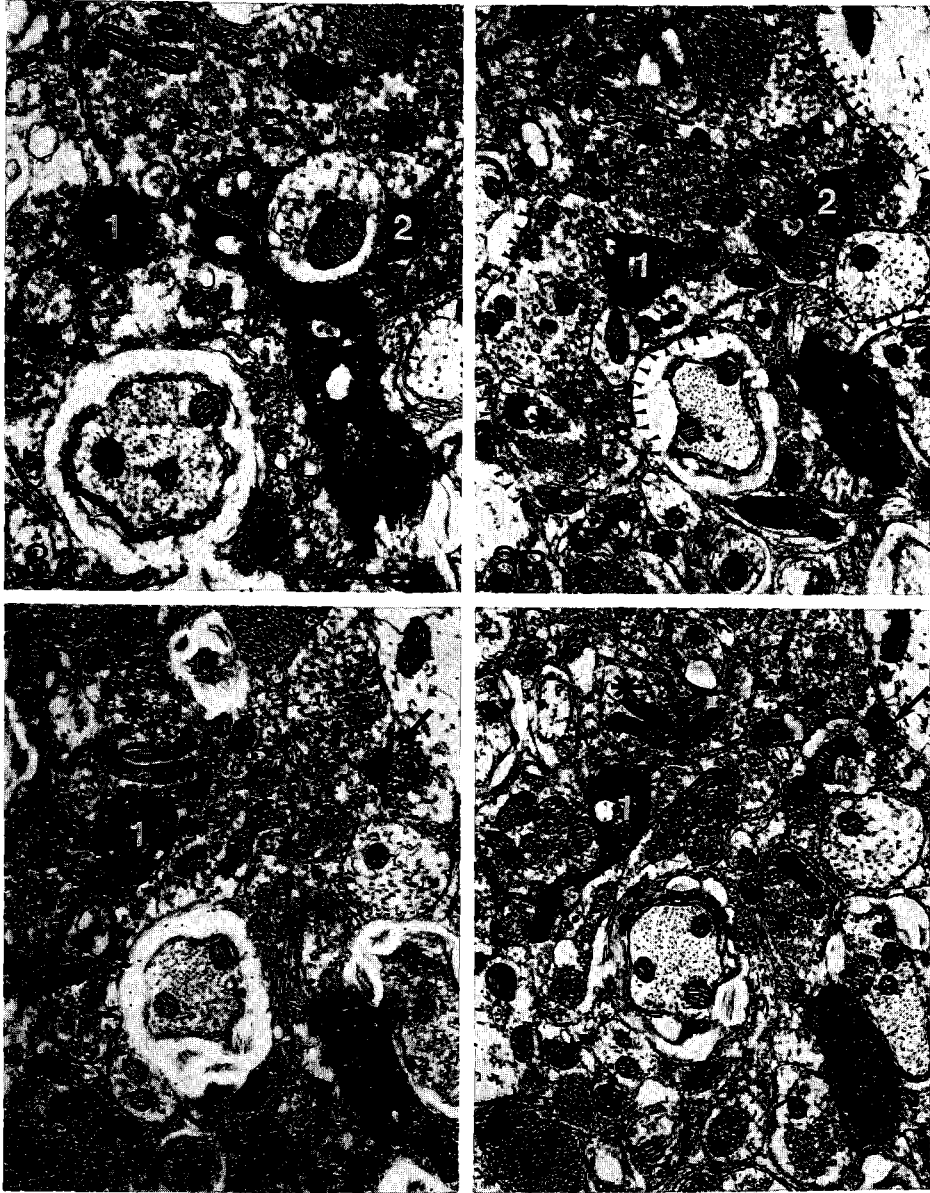
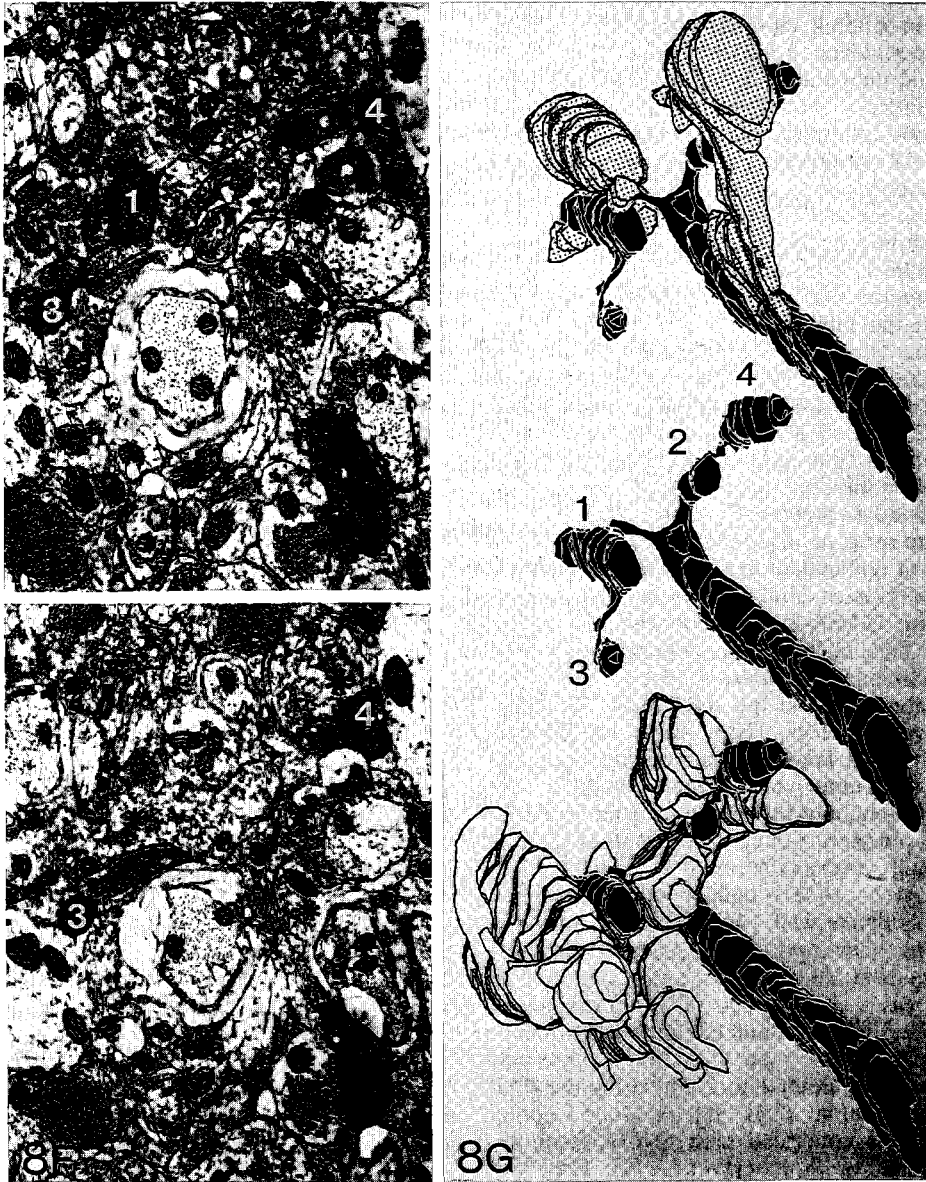


Fig. 8. Electron micrographs (A to F) and reconstruction (G) of two HRP labeled spines together with their GABAergic input (indicated by stars in electron micrographs, and represented by white profiles filled with black dots in reconstruction) and non-GABAergic input (not indicated in electron micrographs, and represented by empty white profiles in reconstruction). Both spines give rise to two spine heads (1 and 3, and 2 and 4) which are linked by thin stalks (note stalk between spine head 1 and 3 in Fig. 8D, and stalk (arrow) between spine head 2 and 4 in Figs. 8C and D),



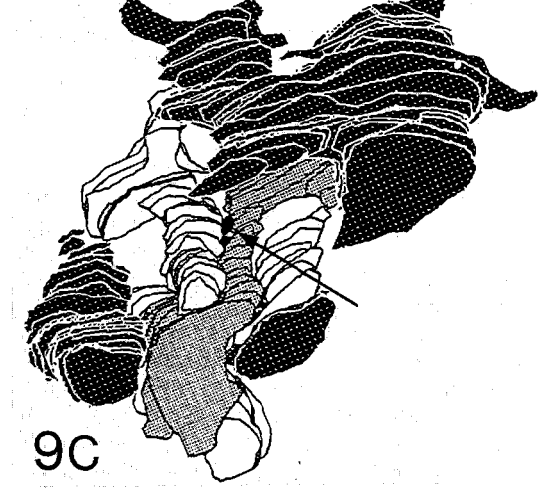
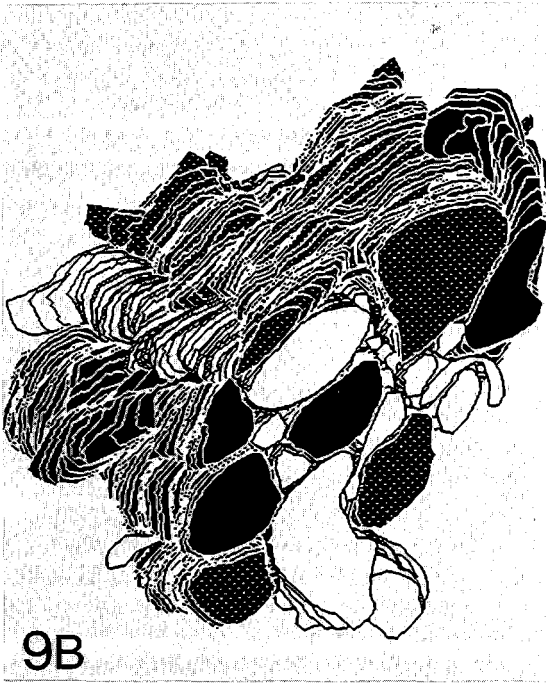
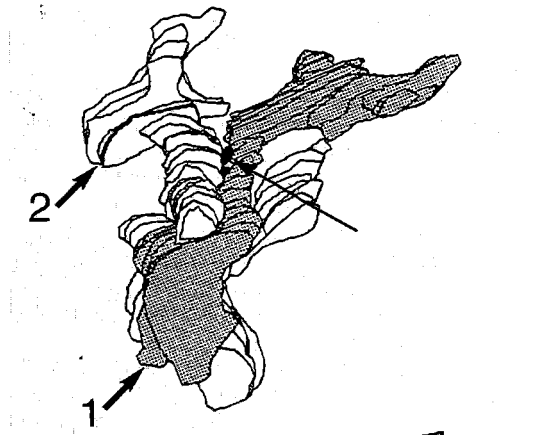
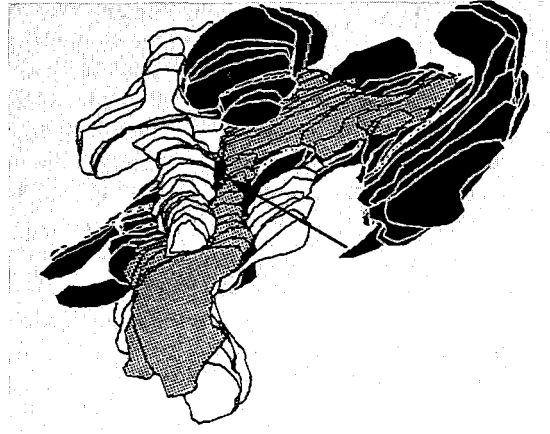
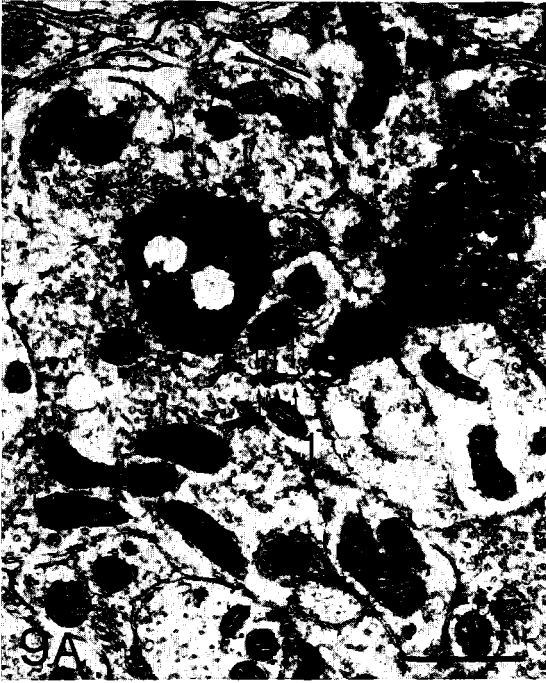
and both spines are contacted by at least one GABAergic and one non-GABAergic terminal. The first two spine heads (1 and 2) of both spines are located together in the same glomerulus (surrounded by small arrow heads in 8B) while spine heads 3 and 4 are located separately each with their own group of spiny neighbours (8E and F). Arrow heads in 8E and F indicate asymmetric synapse of non-GABAergic terminal with subsynaptic densities in the HRP labeled dendrite. The HRP labeled spines and dendrite originate from type I neuron A. Scale bar (8a) = 0.9 μm .

cells in a thick vibratome section is needed 1) the sections preferably should be osmicated and dehydrated in DMP because a dehydration by a graded ethanol series results in excessive shrinkage (wrinkling of the dendrites: Ruigrok et al., submitted), and 2) the osmication should be performed in a glucose solution since otherwise the sections will be stained too darkly, masking the fine dendritic branchlets. Apparently, the use of glucose counteracts the osmication without compromising the ultrastructural preservation. Since osmium is generally known to have a negative effect on the identification of antigens by antibodies (Priestly, '84), this may also explain why the use of glucose enhances the GABA immunogold staining (de Zeeuw et al., '88a).

An additional advantage of the present combination technique is the fact that an endless series of ultrathin sections can be cut from an embedded vibratome section (70 μm in the present study) prior to the postembedding GABA-immunocytochemistry procedure. This makes it possible to reconstruct long structures, like axons (see de Zeeuw et al., submitted), of physiologically identified neurons together with their GABAergic input. Other known ultrastructural combination techniques of cellular labeling with GABA-immunocytochemistry do not allow to make complete reconstructions through long neuronal structures (Freund et al., '83 and '85; Somogyi et al., '83) and/or to combine this with physiological identification of the neurons (Somogyi et al., '81, '83 and '85; Freund et al., '83; Cipolloni and Keller, '89). In these cases intracellular HRP labeling was combined with postembedding GABA-immunocytochemistry on semithin sections (thickness of about 1 to 2 μm) using the PAP method (Freund et al., '85), or Golgi impregnation was combined with GABA immunogold labeling (Somogyi et al., '85; Cipolloni and Keller, '89), with glutamic acid decarboxylase(GAD)- or GABA-immunocytochemistry using the PAP method (Freund et al., '83; Somogyi et al., '83; Somogyi et al., '85), or with high affinity uptake of tritiated GABA (Somogyi et al., '81).

A drawback of the present intracellular HRP staining of olivary cells is the fact that gap junctions between HRP labeled structures or between an HRP labeled profile and a non-labeled structure can no longer be identified. This could not have been due to the general ultrastructural preservation because many gap junctions were found between two non-labeled dendritic elements. Possibly the HRP reaction product masks the gap junctions since they only occupy a very narrow interneuronal space of about 2 nm (Peters et al., '70; Sotelo et al., '74). It should be noted that HRP probably does not pass through the pores in these gap junctions, because two HRP labeled dendrites or spiny appendages were rarely located in apposition. Also, it was observed that presynaptic profiles never contained HRP reaction product, indicating that, with the used survival times (1 - 16 hours) no significant transsynaptic transport had occurred.

Fig. 9. Electron micrograph (9A) and reconstructions (9B and C) of a glomerulus containing GABAergic terminals (indicated by stars in electron micrograph, and represented by black profiles filled with white dots in reconstructions) and non-GABAergic terminals (not indicated in electron micrograph, and represented by unfilled black profiles in reconstructions), and an HRP labeled spine and several non-labeled spines two of which (1 and 2) are linked by a gap junction (indicated by small arrows in electron micrograph and by long arrows in the reconstruction). Note that in this case the gap junction is rather located between the stalks of the spines than between their spine heads. A non-GABAergic terminal is positioned strategically contacting both dendritic elements which are coupled (in electron micrograph see arrow heads, in the reconstruction the non-GABAergic terminal is largely located behind the spines). In 9B the whole glomerulus is reconstructed including all its spines (white profiles) and terminals. The HRP labeled spine is derived from type II neuron C. Scale bar in 9A = 0.8 μm .



Our results demonstrate the possibility to use cell degeneration as a dendritic marker, thus providing, together with the combination method described above, triple labeling in single ultrathin sections (Fig. 6). These degenerating profiles presumably originated from a single neuron which was damaged by a microelectrode penetration.

INTERNEURONAL RELATIONS.

Apposition of dendrites, spines and/or spine heads of the same HRP labeled olivary neuron was only occasionally observed. It was found in the single section analysis that a single glomerulus may contain up to 6 different spiny profiles of the same neuron. This is in agreement with a previous ultrastructural study of intracellularly injected HRP labeled neurons in the cat MAO (King, '80). Our serial section analysis showed that all these profiles usually belong to the same spine and that glomeruli rarely incorporate more than a single spine from the same HRP labeled neuron. These data strongly suggest that dendritic elements of the same olivary neuron avoid each other and that they occupy their own receptive field both at the dendritic and spiny level. This excludes the possibility that gap junctions do exist between elements of the same olivary neuron.

It was seen in some fortuitous sections that dendrites and spines of one non-labeled olivary cell were adjacent to spines of an HRP labeled neuron at several places. In addition it was found that HRP labeled and degenerating dendrites were at several extra- and intraglomerular locations apposed to each other. Although it is known from Golgi studies and from the ultrastructure of the IO that dendrites of neighbouring cells intertwine with each other, the amount of functional interactions (i.e. the proportion of gap junctions or glomeruli shared by the two cells) between these cells has not yet been determined. According to Sotelo et al. ('74) the dendritic arbors of cells in the IO considerably overlap and the somata of these cells are located in clusters each comprising up to eight neurons (with an average of six). These findings are supported by a study of Benardo and Foster ('86) who, after intracellular

injections of Lucifer Yellow in brainstem slices of the guinea pig, observed dye coupling in aggregates comprising 5 to 6 type II olivary neurons. Our reconstructions showed that the olivary glomeruli contain six (average) to eight (maximum) spines. Since these spines originated from different dendrites, and since different dendrites of the same HRP labeled cell never gave off spines to the same glomerulus, a glomerulus in the MAO may indeed comprise dendritic elements of an average of 6 different cells. Taken together, it seems likely that most of the spines within the glomeruli of a single neuron are derived from cells within a cluster.

However, there is no evidence that dendritic fields of neighbouring clusters are strictly separated from each other. On the contrary, the dendritic field of a cluster may be several times larger than the area occupied by its somata (Sotelo et al., '74; Ruigrok et al., submitted). In addition, there are physiological data which suggest that various clusters of cells may be in contact with each other. E.g. it is possible to induce synchronous activity in large groups of cells in the caudal MAO and DAO by the application of harmaline (de Montigny and Lamarre, '73; Llinas and Volkind, '73; Sjölund et al., '80). Furthermore, Ruigrok et al. ('89) recently noted that in cerebellectomized cats, rebound actionpotentials are more easily triggered as the result of mesodiencephalic stimulation, in many cases; even without a direct (short latency) response, indicating that under these experimental conditions oscillations, started by direct stimulation, may spread electrotonically towards other, not directly stimulated areas. Moreover, there are differences between different mammals, and between the two types of olivary neurons, with respect to the size of the dendritic tree. The average diameter of the dendritic arbor of olivary cells (type II) progressively decreases from opossum (280 μm), to cat (211 μm), macaque (152 μm), and humans (115 μm), (Scheibel and Scheibel, '55; Bowman and King, '73), while the 'packing density' also decreases in the same order (Scheibel and Scheibel, '55). Although these results are not unequivocally

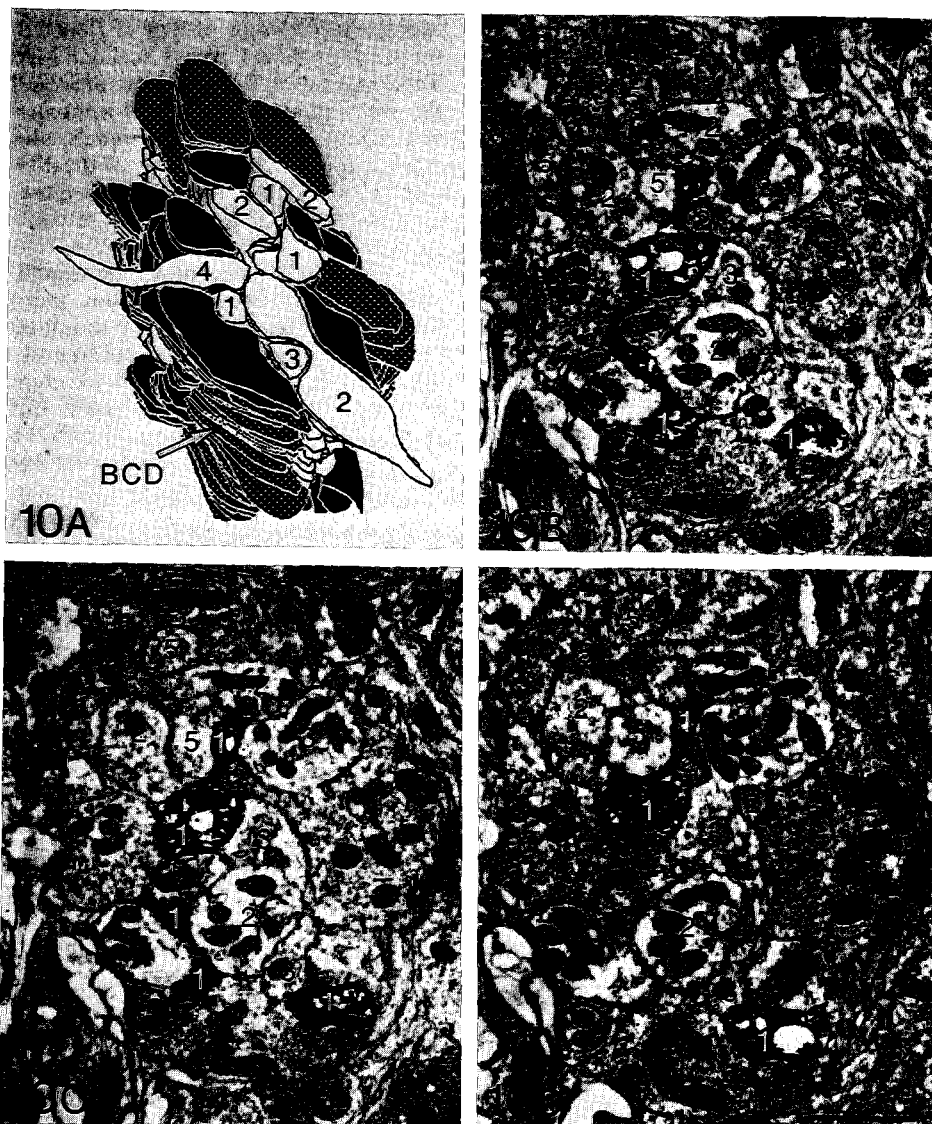


Fig. 10. Electron micrographs (10B, 10C, and 10D) and reconstruction (10A) of a glomerulus containing GABAergic terminals (indicated by black dots in electron micrograph, and represented by black profiles filled with white dots in reconstruction) and non-GABAergic terminals (not indicated in electron micrographs, and represented by unfilled black profiles in reconstruction), and an HRP labeled spine and four non-labeled spines. It is evident that the spines enter the glomerulus from different sides (see for example spine 2 and 4 in Fig. 10A). Note that the different spines intermingle with one another and that they avoid their own brother elements. The HRP labeled spine is derived from type II neuron D. Scale bar in 10D = 1.4 μ m.

interpreted (Foster and Peterson,'86; Ruigrok et al., submitted), they suggest that the overlap between neighbouring cells is higher in lower mammals. With regard to the difference between the neurons of type I and type II, it should be noted that the dendrites of type I neurons radiate away from the soma and occupy a large receptive field with a diameter of approximately 450 μm in cat while those of type II turn back towards the cell body covering a more restricted area with a diameter of about 250 μm (Scheibel and Scheibel,'55; Ruigrok et al. submitted). Therefore, the dendrites and spines of the neurons of type II may indeed remain primarily restricted to the area of their cluster of cells, while the dendritic elements of the neurons of type I intermingle with neurons of a much larger area. In this respect it is interesting to note that the cells of type I are primarily located in the caudal accessory olives (Scheibel and Scheibel,'55; Scheibel et al.,'56; Foster and Peterson,'86), which are the regions most affected by harmaline (de Montigny and Lamarre,'73; Llinas and Volkind,'73; Sjölund et al.,'80).

CAUDAL AND ROSTRAL MAO. In the present study, the type I neurons were selected from the caudal MAO while the type II cells were located in the rostral MAO. Our results indicated that the morphology of these cells also differs at the level of their spines. The average number of HRP labeled spiny profiles which are located within a glomerulus in the plane of a single section is significantly lower for the neurons of type I than for the ones of type II (Table 1). This implies that the anatomical complexity of individual spines of type II is higher than of type I. However, both cell types did not give off more than one spine to a single glomerulus, and the ratio of the number of HRP labeled spines to the total number of spines within individual glomeruli (Table 1) was almost the same for both cell types*. This suggests that the total number of spines in a glomerulus is not different in the caudal and rostral MAO. In addition, it was found in the serial reconstructions that the number of terminals, which innervated individual glomeruli

was similar for cells of type II (located in the rostral MAO) and type I (caudal MAO, see Table 2). Since it was found previously that the rostral part of the MAO contains relatively more glomerular terminals than the more caudally located areas of the MAO (de Zeeuw et al.,'89b), these data suggest that a greater number of glomeruli is present in the rostral MAO.

Although the neuropil of the caudal MAO does probably not differ from the rostral MAO in number of spines or terminals within individual glomeruli, the differences in the complexity of their spines and the total number of glomeruli between these different subdivisions may be related to differences in their response to pathological circumstances. Contralateral cerebellectomy can induce olivary hypertrophy in cats (Verhaart and Voogd,'62; Voogd and Boesten,'76). This phenomenon usually starts in cells of the rostral MAO (Boesten and Voogd,'85). Recent evidence suggests that electrotonic coupling is enhanced between hypertrophic olivary neurons (Ruigrok et al.,'89; de Zeeuw et al.,'89c). Therefore, it can be hypothesized that the high number of glomeruli, the major residence for the gap junctions (Sotelo et al.,'74), favours the development of hypertrophy in neurons of the rostral MAO.

Note. In the quantitative analysis of HRP labeled spiny profiles in single sections it was found that the average ratio between the number of HRP labeled spiny profiles and the total number of spiny profiles within a glomerulus was 0.23 for type I neurons and 0.25 for type II neurons (Table 1), suggesting that in both cases the glomeruli contain spines of 4 different cells. This is less than the average of 6 cells which was found following the serial reconstructions. The underestimation of the results from the single section analysis can be explained by the fact that in this analysis we examined randomly selected glomeruli in which at least one HRP labeled profile was located in the plane of the section, while the glomeruli which contained HRP labeled spines outside the plane of the section were not included in the calculations.*

GABAERGIC AND NON-GABAERGIC INPUT. It has been estimated that about 1/3 of both the GABAergic and non-GABAergic terminals in the rostral MAO are located within glomeruli (de Zeeuw et al., '89b). This calculation was based on the assumption that a glomerulus contained at least three spiny profiles and two terminals. In the present study, it was found in the single section analysis, in which the above definition was used, that 80% of the HRP labeled spines were located within glomeruli, whereas in the serial section analysis of material of the same cells it was observed that most, if not all, of the HRP labeled spines were incorporated in glomeruli. Therefore, the actual proportion of GABAergic and non-GABAergic terminals which are located within glomeruli is higher than 1/3 of the total number.

The GABAergic and non-GABAergic input to neurons of type I and type II is similar. The quantification of randomly selected HRP labeled spines examined in single sections showed that 59% of them were contacted by both GABAergic and non-GABAergic terminals, while the reconstructions of a limited number of spines showed that 100% of these spines and 70% of their spine heads were apposed by both terminals. Together these data allow to conclude that the vast majority of the spines of olivary neurons of both type I and II are innervated by at least one GABAergic and at least one non-GABAergic terminal. These results confirm and extend the findings that single olivary glomeruli in the MAO and PO of the cat receive both a cerebellar and mesodiencephalic input (de Zeeuw et al., in press).

FUNCTIONAL IMPLICATIONS. Physiological studies have indicated that olivary neurons are electrotonically coupled (Llinas et al., '74; Llinas and Yarom, '81a) by gap junctions (Sotelo et al., '74; King, '76; Gwyn et al., '77; Rutherford and Gwyn, '77), which are known to be the morphological correlate of electrotonic coupling (Bennett, '72). This coupling is thought to be dynamic (Bower and Llinas, '83) and may be modulated by a GABAergic input (Sasaki and Llinas, '85).

The electrophysiological properties of olivary neurons are further characterized by their tendency to fire rhythmically (Armstrong et al., '68; Benardo and Foster, '86; Llinas and Yarom, '86). This is probably due to conductances which are distributed differentially over the cell membrane (Llinas and Yarom, '81a,b).

Sofar, no physiological studies have been made on a possible interaction between the GABAergic and non-GABAergic input to the olivary glomerular spines. However, based upon computational studies by Segev and Rall ('88) and Yarom ('89; Yarom and Adan, '88), it was proposed (de Zeeuw et al., in press) that the combined GABAergic cerebellar and excitatory mesodiencephalic terminals regulate the electrotonic coupling between olivary cells and simultaneously their firing frequency, and that these regulating capabilities may be extremely sensitive to the exact timing of both inputs. This would mean that successful inhibition by the GABAergic cerebellar input of mesodiencephalic excitation has a very narrow time resolution. In this respect it is relevant to point out that the GABAergic cerebello-olivary projection is derived from rather small cells, with thin axons (Nelson et al., '84; Ruigrok and Voogd; submitted), whereas larger cerebellar nuclear cells, besides terminating in the thalamus, also provide a projection to mesodiencephalic regions from where the excitatory olivary projections are derived (Ruigrok and Voogd, '88; Ruigrok et al.; submitted). The hypothesis that the spiny appendages of olivary cells may act as timing sensitive instruments was confirmed in the present study by three findings. Firstly, because it was shown that indeed all glomerular spines received both a GABAergic (inhibitory) and non-GABAergic (probably for a major part excitatory) synaptic input. Secondly, because it was found that most of the olivary spines had long and thin stalks which terminated in one or more spine heads. Both morphological features were prerequisites in the model of timing sensitive excitable spines made by Segev and Rall ('88). Thirdly, most, if not all, spines were located within glomeruli, and most spines

were found on secondary or higher order dendrites.

Presently, it is not known whether or not dendritic spines carry excitable channels. However, it is tempting to speculate on their existence for a number of reasons. 1) It has been demonstrated that the high-threshold Calcium conductance is mainly present in a remote place from the soma (Llinas and Yarom,'81); 2) If the spines are not excitable, it would be difficult to understand how they would function since the thin, and frequently very long stalk would represent an enormous resistor; 3) Segev and Rall ('86) indicated that cluster formation (as seen in olivary spines) of excitable spines may enhance their properties and 4) excitable spines are most likely found on distal dendrites to function as current boosters to compensate for the attenuation from the distal dendritic region (Shepherd et al.,'85; Segev and Rall,'88).

Conclusions

It may be concluded that, when physiological, morphological and immunocytochemical identification and serial reconstruction of neurons and their afferents is required, the present ultrastructural combination technique of intracellular HRP labeling with postembedding immunogold labeling offers a useful and reliable method.

The present study provides evidence that the dendritic spines within the olivary glomeruli have a propensity to be located near spines derived from other neurons. The morphology and location of the glomerular spines and their ubiquitous combined GABAergic and non-GABAergic input are in line with the hypothesis that they may serve to modulate the electrotonic coupling of the olivary cells and simultaneously their firing frequency in a timing sensitive way.

c. Intracellular labeling of neurons in the medial accessory olive of the cat: III. Ultrastructure of axon hillock and initial segment, and their GABAergic innervation.

Abstract

The gamma-aminobutyric acid (GABA) synaptic input of identified axons in the cat inferior olive was studied using a combination of intracellular labeling with horseradish peroxidase and postembedding gold-immunocytochemistry. With this technique olivary cells were physiologically identified and light microscopically reconstructed, and the horseradish peroxidase reaction product and the immunogold labeling were subsequently simultaneously visualized for electron microscopical investigation using serial ultra-thin sections.

The axons of cell type I (characterized by dendrites which radiate away from the cell body) originated from the soma whereas those of type II neurons (characterized by dendritic trees which curve back towards the soma) were derived from a primary dendrite. The axons of olivary neurons stand out by the length of their axon hillock (up to 21 μm) and initial segment (up to 40 μm). The hillock contained various spiny appendages which were located within glomeruli together with dendritic spines of other olivary neurons. Axonal spines of type II neurons were more numerous and complex looking than those of type I. The axonal spines, the shaft of the axon hillock, and the transition between the hillock and initial segment were primarily innervated by GABAergic terminals (65%) but non-GABAergic terminals (35%) were present as well. The terminals apposed to the axons of type I contacted mainly the axonal shafts whereas most of the terminals adjacent to the axons of type II established synaptic contacts with the axonal spines. The initial segments were largely devoided of synaptic input. Distally, the initial segment acquired a myelin sheath.

Introduction

Two types of neurons can be distinguished in the inferior olive (IO) of many mammalian species (Scheibel and Scheibel,'55; Bowman and King,'73; Gwyn et al.,'77; Rutherford and Gwyn,'80; Benardo and Foster,'86; Foster and Peterson,'86; Iwahori and Kiyota,'87; Sztejn,'88; Ruigrok et al., submitted). One type (type I) is mainly present in the caudal accessory olives. Its dendrites are relatively long, sparsely branched, running away from the soma and therefore covering a large receptive field. The other type (type II), which is predominantly present in the rostral parts of the accessory olives and principal olive, has dendrites which tend to turn back towards the soma, at times creating spirals (Ramon y Cajal,'09). The extent of the dendritic tree of type II neurons is smaller than of type I neurons. It was demonstrated for the medial accessory olive (MAO) that the dendritic spines of neurons of type II are more complex than those of type I (de Zeeuw et al., submitted). However, the spines of both cell types receive a similar GABAergic and non-GABAergic synaptic input (de Zeeuw et al., submitted). The GABAergic input to the spines is mainly derived from the cerebellar nuclei (Tolbert et al.,'76; Nelson et al.,'84; de Zeeuw et al.,'88 and '89a).

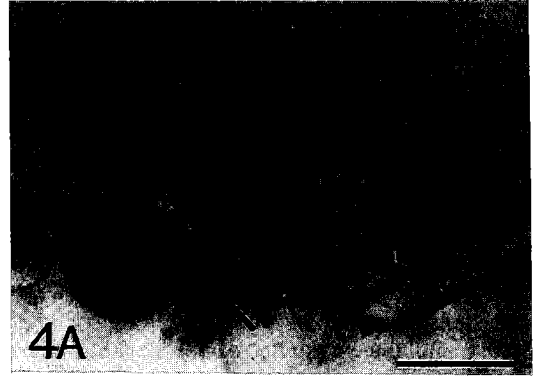
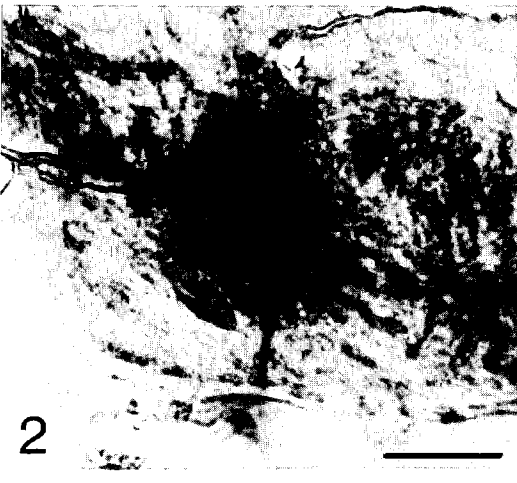
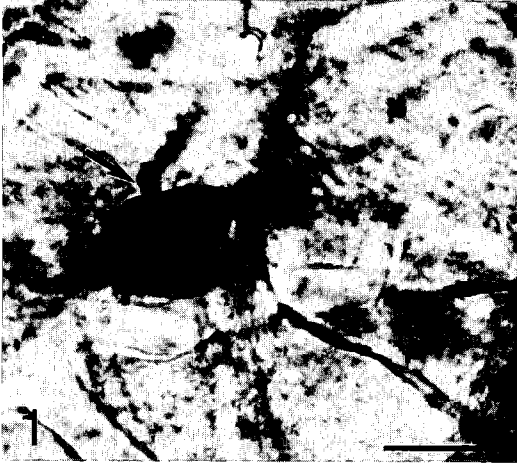
So far, no information is available on the morphology and innervation of the axon hillock and initial segment of olivary cells. The synaptic input to somata of olivary neurons is mainly GABAergic and appears to be derived, at least in part, from a non-cerebellar origin (de Zeeuw et al.,'89a). The morphology and innervation of the axon hillock and initial segment were studied in identified neurons of the MAO by means of a combination of intracellular labeling of horseradish peroxidase (HRP) and postembedding GABA-immunocytochemistry.

Material and methods

Details on the technical procedures are published in both companion papers (Ruigrok et al., submitted; de Zeeuw et al., submitted). Briefly, they consist of the following steps. In pentobarbital anaesthetized cats, HRP was injected intracellularly into electrophysiologically identified inferior olivary cells. Afterwards the cats were perfused transcardially with glutaraldehyde fixative. The brainstem containing the IO was cut transversely on a vibratome (70 μm) and incubated with diaminobenzidine (DAB) according to Graham and Karnovsky ('66). The incubated vibratome sections were rinsed and osmicated in a phosphate buffered glucose solution. Subsequently, all sections were blockstained in uranyl acetate, dehydrated in dimethoxypropane (Muller and Jacks,'75; Truter et al.,'80) and flat embedded in Araldite between teflon coated glass slides (Bishop and King,'82). After curing, the intracellularly labeled neurons were studied with the light microscope (LM), and reconstructed (using a 100x objective and a drawing apparatus attachment). Two type I and two type II cells were selected from the caudal and rostral MAO, respectively, for electron microscopical examination (these cells, which are numbered in the companion paper of Ruigrok et al. as 1868.05, 1863.04, 1887.18 and 1886.15 will be referred to as cell A, B, C, and D, respectively). An important criterion for their selection was that the initial part of the axon was oriented perpendicular to the plane of section (allowing identification of all boutons including all their synapses). Subsequently, the selected cells were photographed at intervals of 5 μm throughout the 70 μm thick embedded tissue sections (Figs 4A to G). The tissue blocks containing the soma and the axon of these neurons were glued on a capsule filled with hardened plastic, cut by a razor blade in an asymmetric pyramid, and then sectioned with a diamond knife on an ultramicrotome (Reichert) in about 1000

serial ultrathin sections mostly with a silver interference colour. The ultrathin sections were mounted on coated nickel slot grids and processed for postembedding GABA-immunocytochemistry (for details, see de Zeeuw et al.,'88). The grids were left overnight in a diluted droplet of GABA-antibody (for specificity tests see Buijs et al.,'87; Seguela et al.,'84) and incubated in goat anti-rabbit IgG labeled with gold particles (diameter 15 nm). Subsequently, the sections were counterstained with uranyl acetate and lead citrate, and examined and photographed in a Philips (300) Electron Microscope (EM).

Figs. 1-4. Light microscopical photographs of olivary cells (cell A, B, C, and D) and their axon hillocks which are intracellularly labeled with HRP. The sections are 70 μm thick, and osmicated in a glucose solution and embedded in araldite. The neurons depicted in Figs 1 and 2 are of type I, while those in Figs 3 and 4 are of type II. In each Figure the axon hillock is indicated by an arrow. In Fig. 2 and 4, it is evident that the hillock arises from the soma and a primary dendrite respectively. Figs 4A-G show the axon focussed at different depths of the same vibratome section. In Fig. 4B it can be seen that several spines are located nearby the hillock. Following electron microscopical examination (see Fig. 9) these spines appeared to originate partly from dendrites and partly from the axon hillock. The initial segment is located between the double arrow heads in Figs 4D and E, and the single arrow heads in Figs 4F and G. After this region one can see the lumpy appearance of the myelinated part of the olivary axon (Fig. 4G). Cell A is obtained from cat 1868 (no. 05), cell B from cat 1863 (no. 04), cell C from cat 1887 (no. 18), and cell D from cat 1886 (no. 15); for LM reconstructions of these cells, see Ruigrok et al., submitted. Scale bar in 1 = 21 μm , in 2 = 29 μm , in 3 and 4 = 25 μm .



Analysis

Guided by the findings in the light microscope the HRP labeled axons of the 4 selected cells could be localized in the ultrathin sections. The axons were followed through the serial sections and photographed. By superimposing all the photomicrographs on tracing paper the axons were reconstructed (Figs 6, 7F, and 9C). The hillock was defined as being located between the base of the axon and the beginning of the dense undercoating of the axolemma, while the initial segment extends from this point up to the disappearance of fascicles of mutually linked microtubuli and the appearance of the myelin sheath (Palay et al., '68; Peters et al., '68). When the myelin sheath was not present in the same embedded vibratome section as the axon hillock it was traced in the next section. The length of the axon hillock and initial segment were measured by counting all the ultrathin transversal sections containing these structures and by multiplying this number with 70 nm (the average thickness of the ultrathin sections according to their silver interference colour (Peachey, '58) and computed from the thickness of the vibratome sections (70 μm) divided by the total number (approximately 1000) of ultrathin sections). For all sections which were not cut sufficiently perpendicular to the axis of the axon we determined the angle and calculated the length of the hillock and/or initial segment according to Pythagoras' theorem.

All GABAergic and non-GABAergic terminals associated with the axon hillock or initial segment were included in the reconstruction. In the analysis a terminal was considered to be GABA-positive if the number of gold particles overlying it was at least 8 times higher than the number of particles over postsynaptic structures (with approximately the same surface area). In addition we determined for each of these terminals whether they established a synaptic contact with the axon and, if so, the type of synapse. Synapses were identified by the presence of a synaptic cleft, a post synaptic density and a cluster of presynaptic vesicles adjacent to the

presynaptic membrane (Gray and Guillery, '66). They were classified as asymmetric (Gray's type I) or symmetric (Gray's type II) synapses, when the width of the synaptic cleft was about 30 nm, or 20 nm, and when the thickness of the postsynaptic density was about 40 nm, or 20 nm, respectively (Gray, '59).

For each axon these morphological features were quantified. The values obtained for each of the 4 axons were averaged and the standard deviations (SD) were calculated (Table 1). A proximal dendrite of one of the four selected neurons was also analysed, reconstructed, and compared with the axon hillock of the same cell (Fig. 7F).

Results

LIGHT MICROSCOPY. The axons of the 4 selected cells were distinguished from dendrites by their long, smooth, unbranched outline. The axons could be traced outside the IO neuropil and, frequently, even to the opposite side of the brainstem. Axon A and B (both cell type I) and axon D (from type II) clearly originated from the soma (Fig. 2) and a primary dendrite (Figs 4A and B), respectively. However, the exact site of origin of the other axon (C) could not be determined unequivocally in the LM. The axon hillock was wide at its base. Its course was either straight or it made an angle just after its appearance (for light microscopical appearance see Figs 1 to 4; for reconstructions see Figs 6, 7F, and 9C), and at the end it became gradually thinner. In some of the light microscopical examinations the hillock was found to give rise to 1 or 2 spiny protrusions (Fig. 4B). Then, after a small bend, a smooth and straight thin shaft could be observed, supposedly corresponding to the initial segment. At its end (i.e. the beginning of the myelin sheath as determined by electron microscopy), the initial segment altered its course and became thicker and more lumpy again. The light microscopical measurements showed that the mean length of the axon hillock was 18 μm and of the initial segment 33 μm (Table 1).

Table 1. Summary of the properties of olivary axons as examined in the electron microscope (the cell types are identified in the light microscope).

	AXON A	AXON B	AXON C	AXON D	$\bar{X} \pm SD$
Cell type	Type I	Type I	Type II	Type II	
Source of axon	Soma	Soma	Dendrite	Dendrite	
Length axon hillock	20 μm	18 μm	21 μm	18 μm	19 \pm 2
Diameter axon hillock	3.1 μm	3.6 μm	2.7 μm	3.5 μm	3.2 \pm 0.4
Length initial segment	33 μm	33 μm	35 μm	40 μm	35 \pm 3
Diameter initial segment	0.9 μm	1.3 μm	1.3 μm	0.8 μm	1.1 \pm 0.3
Total number of axonal spines	1	5	8	7	5 \pm 3
Number of spine heads	1	5	10	18	9 \pm 7
Number of branching axonal spines	0	0	0	3	1 \pm 2

Table 2. Summary of the terminals apposed to the examined olivary axons.

	AXON A	AXON B	AXON C	AXON D	$\bar{X} \pm SD$
Total number of terminals	30	30	23	36	30 \pm 5
GABAergic terminals	20 (67%)	23 (77%)	13 (57%)	21 (58%)	65% \pm 9
On axonal shaft	18 (90%)	15 (65%)	3 (23%)	3 (14%)	48% \pm 36
With synapse on shaft	17 (94%)	13 (87%)	3 (100%)	3 (100%)	95% \pm 6
On axonal spine	2 (10%)	8 (35%)	10 (77%)	18 (86%)	52% \pm 36
With synapse on spine	2 (100%)	8 (100%)	9 (90%)	16 (89%)	95% \pm 6
Non-GABAergic terminals	10 (30%)	7 (23%)	10 (43%)	15 (42%)	35% \pm 10
On axonal shaft	9 (90%)	5 (71%)	2 (20%)	2 (13%)	49% \pm 38
With synapse on shaft	7 (78%)	3 (60%)	0	2 (100%)	60% \pm 43
On axonal spine	1 (10%)	2 (29%)	8 (80%)	13 (87%)	52% \pm 38
With synapse on spine	1 (100%)	2 (100%)	8 (100%)	12 (92%)	98% \pm 4

ELECTRON MICROSCOPY. In contrast to the light microscopical examination, the source of all 4 studied axons was readily identified by examining the serial sections in the EM. The axons of both type I cells were derived from the cell body whereas the axons of both type II cells originated from a proximal dendrite. The diameter of the base of these axons varied from 2.7 μm to 3.6 μm . At

this base of the axon hillock microtubuli funneled into the axon and some of the microtubules assembled into fascicles. The hillock did not contain cisterns of endoplasmic reticulum but in some cases free ribosomes were observed. Most of the shaft of the hillock was covered with astrocytic lamelles but occasionally dendritic shafts were directly apposed to them (Figs 9A and

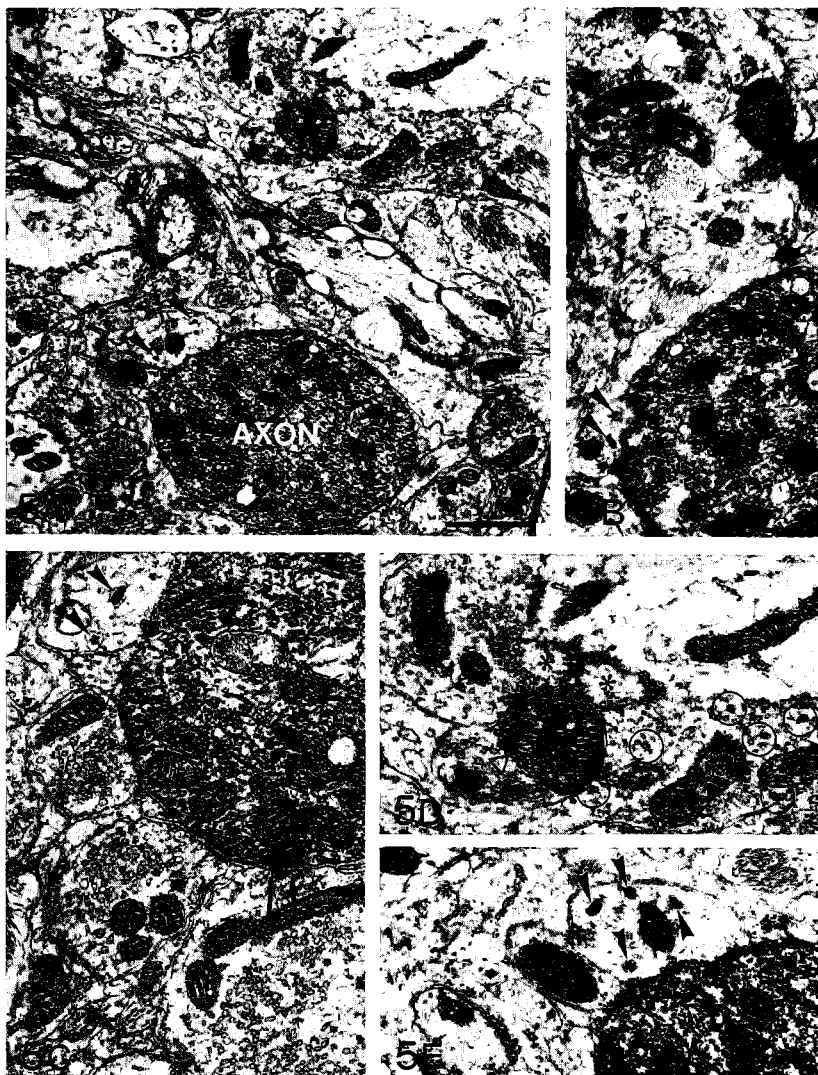


Fig. 5. Electron micrographs of an HRP labeled axon hillock (cell A). The axon gives off a spine (black stars in 5A, B and D), which is located together with spines (asterisks in 5A and D) of another cell in a small glomerulus. Both the axonal shaft and spine are contacted by GABAergic (black gold particles) and non-GABAergic terminals. The GABAergic terminals reveal symmetric synapses (triangles in 5D) while in Fig. 5C it can be seen that a non-GABAergic terminal contacts the axonal shaft with an asymmetric synapse (arrows) showing subsynaptic densities (small arrow heads). The non-GABAergic terminal filled with dense core vesicles (large arrow heads in 5A, B, C, and E) which was apposed to the axonal shaft over a long distance (see asterisk in Fig. 6) did not show a membrane specialization in any of the serial sections. Note that the non-GABAergic terminal in Fig. 5D contains relatively many coated vesicles. Scale bar = 1.8 μ m.

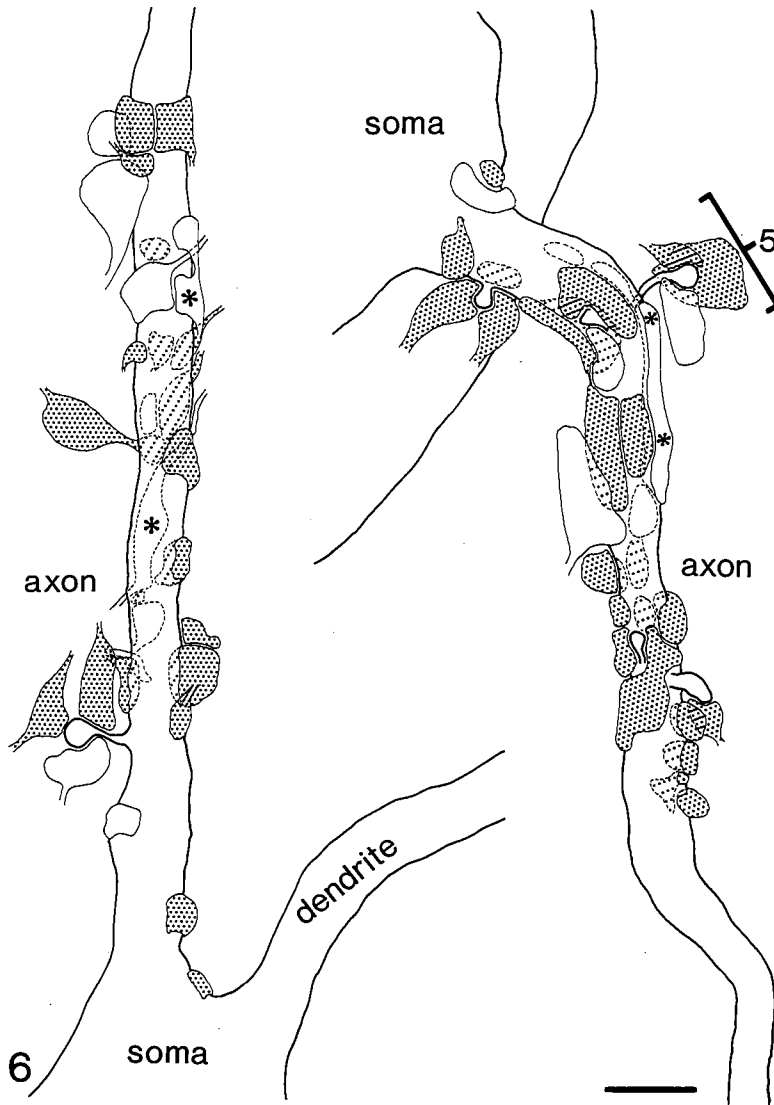


Fig. 6. Reconstructions of the axon hillocks of the two neurons of type I (picture on the right side represents axon hillock of cell A, and the figure on the left side gives a reconstruction of the axon hillock of cell B). Both axons arise from the soma, and receive many GABAergic (profiles filled with black dots) and non-GABAergic (empty profiles) terminals. Hatched profiles indicate structures which are located behind non-shaded structures. Terminals labeled with an asterisk are large granular terminals. In the upper right the axonal part is indicated which is represented in the electron micrographs of Fig. 5. Scale bar = 2.8 μm

B). Each axon hillock gave rise to one or more spines (varying in number from 1 to 8; see Table 1). All axonal HRP labeled spines were located within glomeruli, together with non-labeled spines of other olivary neurons (Figs 5, 7, 8, and 9). In all cases where the non-labeled spines could be traced back to their origin, it was found that they were derived from a dendrite. Morphologically, the axonal spines resembled the dendritic spines (de Zeeuw et al., submitted). The heads of the axonal spines were often filled with multivesicular bodies and large irregular shaped vesicles, and an occasional mitochondrion, but they did not contain microtubules or small presynaptic vesicles. The spines of the axons of type I cells were relatively simple, sometimes they consisted of a spine head which emerged almost directly from the shaft. Spines of cell type II axons were more complex, giving off several spine heads from a single stalk. Some of the axonal spines of one of the type II neurons (axon D) even branched (Fig. 9). From this single axon 18 different spine heads originated. The maximum distance between a spine head and the axonal shaft was approximately 8 μm .

In agreement with the light microscopical observations, the initial segment of the axons was found to be smoother and thinner as compared to the hillock. The beginning of an initial segment was recognized by the appearance of its dense undercoating. Frequently it could be observed that the microtubules within the segments were linked by small cross bands at regular distances of about 25 nm. In this way sometimes a closed chain of tubuli appeared (Fig. 11A). At the end of the initial segments the mean diameter was 1.1 μm . At this point all axons acquired a myeline sheath. The mean diameter of the axon without its myeline sheath was 1.4 μm . The greatest lengths of the axon hillock and initial segment amounted to 21 μm and 40 μm respectively. There were no important differences in the measurements of the two cell types (see Table 1).

TERMINALS ON AXONS. Most of the terminals contacted the axon hillock but some of them were apposed to the proximal part of the initial segment. A total of 119 terminals were observed adjacent to the 4 selected axons. Most of these terminals (65%) were GABAergic (Table 2). The GABAergic terminals established in 95% of the cases symmetric synapses, they contained primarily pleiomorphic vesicles, and they varied in diameter from 0.6 μm to 2.5 μm . GABAergic terminals terminating on the axon were never associated with a subsynaptic cistern containing ribosomes. In this respect they are different from the somatic terminals in the IO (de Zeeuw et al., '89a). Free subsynaptic polyribosomes, which have been associated with GABAergic synapses on axon initial segments in various brain regions (Steward and Ribak, '86), were observed only in 2 cases. The GABAergic terminals contacted both the axonal shafts (48%) and the axonal spines (52%). Of all the GABAergic terminals apposed to the olivary axons, 53% was also adjacent to one or more dendrites and about half of these GABAergic terminals established an axodendritic synapse. Of the non-GABAergic terminals (35%) apposed to the axons, 83% showed a synaptic complex. They were of the same size as the GABAergic terminals but they usually contained round to oval vesicles and their synapses were asymmetric (one of them showed subsynaptic densities as described by Taxi ('61: see Fig. 5C). Four out of the 42 non-GABAergic terminals were filled with dense core vesicles (Figs 5A, B, C, and E; indicated in the reconstructions with asterisks). These terminals were relatively long but they displayed no synaptic specializations in none of the observed serial sections. Like the GABAergic terminals, the non-GABAergic ones showed no preference for the axonal shafts or spines (see Table 1). However, the non-GABAergic boutons apposed to the axons were often (82%) located next to a dendrite and 69% of them were in synaptic contact with these den-

drites. In this respect they did not resemble the GABAergic terminals.

Terminals apposed to axons of cell type I (axon A and B) mostly contacted the axonal shaft and only 21% (\pm 12 SEM) was located next to axonal spines, whereas most terminals (82% \pm 4 SEM) adjacent to the axons of cell type II (axon C and D) were apposed to spines. This difference was significant (Student T-test, $p < 0.005$), (see Fig. 10). More than half of the spines of cell type II (10 out of 15) and only half of the spines of type I (3 out of 6) were contacted by both a GABAergic and non-GABAergic terminal.

AXODENDRITIC TERMINALS. The innervation of the reconstructed proximal dendrite differed from the axon (axon C) of the same cell (type II, Figure 7F). There were relatively few (13) terminals apposed to this dendrite, which was reconstructed over the same length as the axon hillock and which received 23 terminals. Of these 13 terminals 7 were GABAergic. With regard to the morphology, both the GABAergic and non-GABAergic axodendritic terminals resembled the terminals in the olivary neuropil in their general appearance (de Zeeuw et al., '89a). In addition, it was found that the proximal dendrite (3) gave off few spines when compared to the axon hillock (8), therefore, relatively few of the terminals were in synaptic contact with the dendritic spines.

Discussion

MORPHOLOGY OF THE OLIVARY AXON. Characteristic properties of the inferior olivary axons appeared to be the great length of their axon hillock and initial segment, and the existence of spiny appendages at the hillock. The axon hillock and initial segment had an average length of 19 μm and 35 μm , respectively, according to our calculations from the electron micrographs. These data were in good agreement with the light microscopic measurements (18 μm and 33 μm). When the mean length and diameter of the axon hillock (19 μm ; 3.2 μm) and initial segment (35 μm ; 1.1 μm) of cat olivary

cells are compared with other neurons in the central nervous system, it becomes evident that the olivary axon hillock and initial segment are relatively long and thin. The axon hillock of motoneurons in the cat is usually about 11 μm long, with a width of 8 μm at its base (Conradi, '69), while the initial segment of α -motor axons in cats has an average length and diameter of 26 μm and 3.5 μm respectively (Cullheim and Kellerth, '78). The mean length of the axon hillock plus the initial segment of Purkinje cells in humans is 35 μm (Kato and Hirano, '85) and of pyramidal cells in the sensory-motor cortex of the monkey 28 μm (DeFelipe et al., '85). The diameter of the axon hillock and initial segment of a pyramidal cell in the cerebral cortex of the rat is about 3.5 μm and 1.7 μm (Peters et al., '68). The fact that the axon hillock, initial segment, and also the initial myelinated part (1.4 μm) of the olivary axons are relatively thin, is in line with the findings that the climbing fibers are thin (Busch, '61; Szentagothai and Rajkovits, '59) and have a relatively slow mean conduction velocity (4 to 10 m/sec), (Eccles et al., '66ab; Ito et al., '66).

Up to now it was believed that the core of the olivary glomeruli was composed solely of dendritic appendages (Nemecek and Wolff, '69; Sotelo et al., '74; King, '76; Gwyn et al., '77; Rutherford and Gwyn, '80). The present study showed that glomerular spines can also be derived from the axon hillock. Most of the axonal spines are probably incorporated in the glomeruli together with dendritic spines of other olivary cells. However, the axonal spines could not be distinguished from the dendritic spines on morphological grounds. Like the dendritic spines (de Zeeuw et al., submitted), the axonal spines of the neurons of type I are more numerous and more complex than those of type II. These data suggest that the axonal and dendritic spines are not different. Whether this means that the axonal spines are also linked by gap junctions, as it was shown for dendritic spines (Sotelo et al., '74; King, '76; Gwyn et al., '77; Rutherford and Gwyn, '77), could not be decided in the present study. Due to the intracellular injection of HRP, gap junctions could

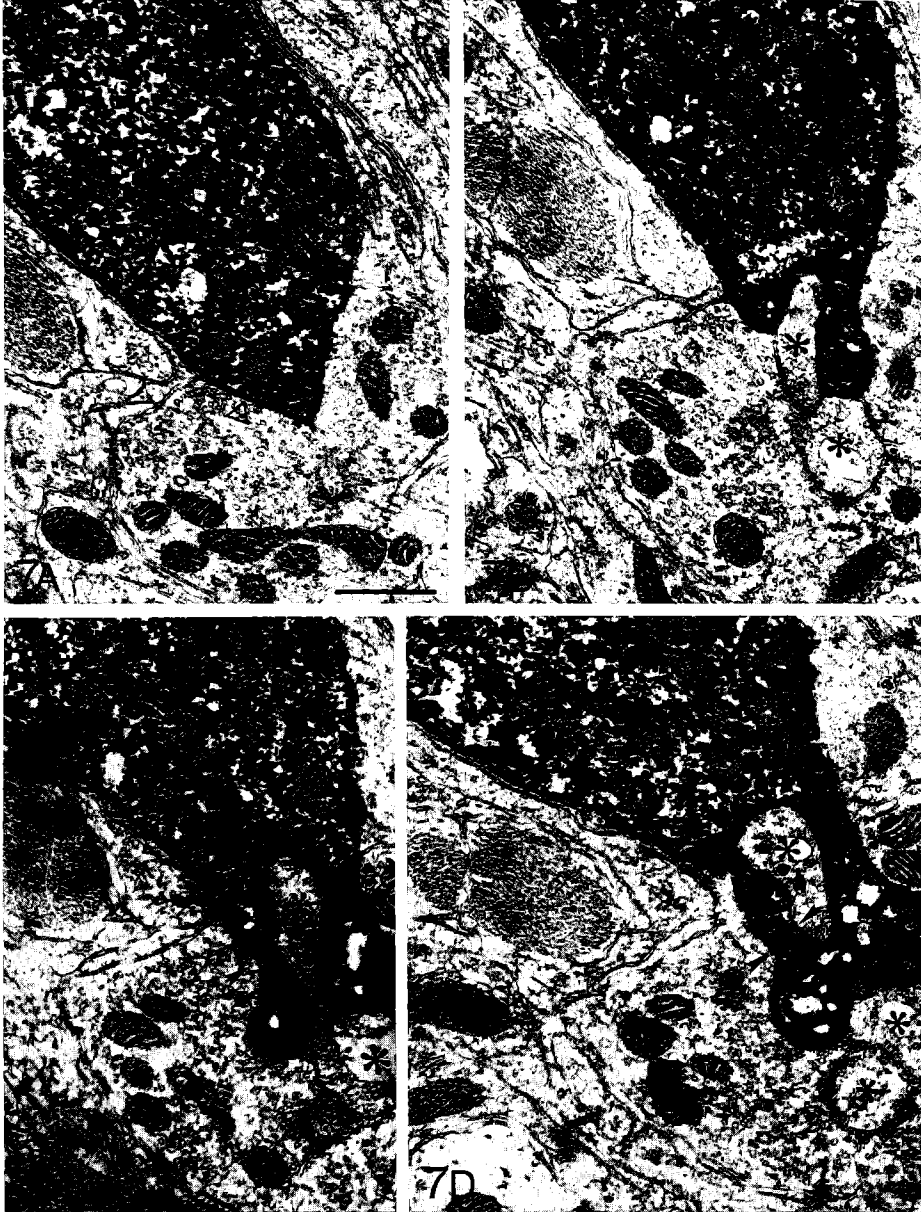
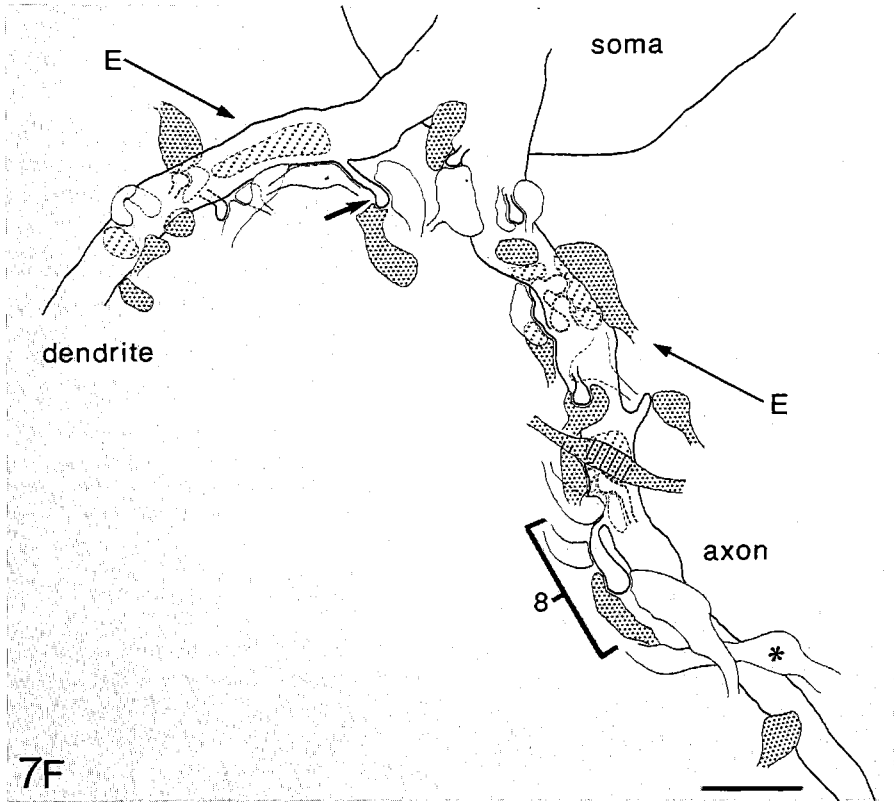
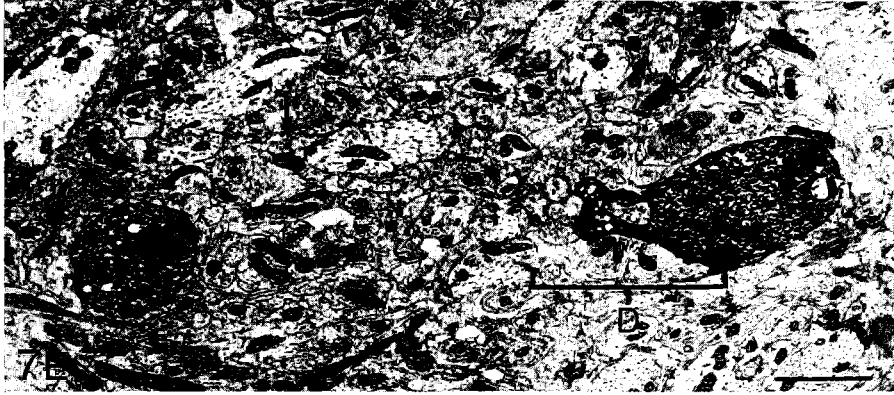


Fig. 7. Electron micrographs (7A to E) and reconstruction (7F) of the axon hillock of type II neuron C. In Fig. 7A to 7D one can see that the axon gives off two spines which are apposed to one another (arrow heads in C and D), and which are both located together with other spines (asterisks) within the same glomerulus. A GABAergic terminal straddles these two axonal spines (symmetric synapse indicated by triangle). Fig. 7E shows the axon as given in Fig. 7D at a lower



magnification, and additionally a nearby located proximal dendrite. Both the axon and the dendrite are represented in the reconstruction. The plane of the section from which Fig. 7E was made is depicted in the reconstruction (large thin arrows in 7F indicated by E's). Note that one (arrow) of the dendritic spines can be observed in the electron micrograph as well as in the reconstruction. For symbols see Fig. 6. Scale bar in 7A = $1.1 \mu\text{m}$, in 7E = $2.7 \mu\text{m}$, and in 7F = $3.3 \mu\text{m}$.

not be identified (see also, de Zeeuw et al., submitted). Nevertheless, since the initial segment is generally believed to be the site of initiation of the axonally conducted action-potential (Fuortes et al., '57; Coombs et al., '57; Eccles, '64), the possible existence of axo-axonal or axo-dendritic gap junctions offers the interesting possibility that electrotonic coupling exists between olivary structures which are directly involved in impulse generation.

Spines originating from an axon hillock or initial segment have only been reported for pyramidal neurons in the sensory-motor cortex of the cat (Bragina, '83) and the monkey (DeFelipe et al., '85). In these cases the spines were never as complex as the olivary axonal spines.

INNERVATION OF THE OLIVARY AXON. This study provides direct evidence for the existence of axo-axonal synaptic contacts in the IO. It was found that axons of cells of the IO receive an average of 30 terminals. These numbers are more or less comparable with those found for the axons of cortical pyramidal cells (DeFelipe et al., '85) and motoneurons (Conradi, '69) in the cat. Of all examined terminals, 65% were GABAergic. A similar percentage was found for the GABAergic innervation of the somata of olivary neurons (de Zeeuw et al., '89a). In this study indirect statistical evidence was found that the GABAergic projection to the olivary somata is not only derived from the cerebellar nuclei but also from a non-cerebellar source. Possible sources for these non-cerebellar GABAergic terminals include the nucleus paragiganto-cellularis and/or the raphe nuclei* (Bishop and Ho, '86; Walberg and Dietrichs, '82; Mugnaini and Oertel, '85; de Zeeuw et al., '89a), or GABAergic neurons from the IO itself (Nelson et al., '88; Walberg and Otterson, '89). However, a non-cerebellar origin of the GABAergic innervation of the olivary axons seems unlikely because: 1) The GABAergic terminals contacting the axon were often apposed to axonal spines located within glomeruli while the vast majority of the somatic GABAergic terminals are directly apposed to the perikaryon (de Zeeuw et al.,

'89a; de Zeeuw et al., submitted). 2) GABAergic large granular terminals were observed next to the soma (de Zeeuw et al., '89a) but not to the axon, whereas the opposite was found for non-GABAergic large granular terminals. 3) The GABAergic terminals adjacent to the perikaryon frequently showed subsynaptic cisterns of endoplasmic reticulum, which were lacking in the axons. The fact that many of the GABAergic axonal terminals were located within glomeruli suggests that they are of a cerebellar origin because statistical analysis showed that most, if not all, GABAergic glomerular terminals are derived from the cerebellum (de Zeeuw et al., '89ab).

Olivary neurons, like for example motoneurons (Conradi, '69), also receive an excitatory input to their somata and axon. The non-GABAergic terminals (35%) apposed to the axon hillock and initial segment of the IO consisted largely of terminals with an excitatory morphology (round to oval vesicles and asymmetric synapses; Uchizono, '65) but non-labeled terminals filled with dense core vesicles were also relatively frequently found (cf. de Zeeuw et al., '89a). Terminals containing these dense core vesicles never displayed any membrane specialization throughout the serial sections. This confirms the idea that they may contain neurotransmitters which can be non-synaptically released (Nieuwenhuys, '85; Zhu et al., '86; Hökfelt et al., '86; Holstege and Kuypers, '87). Morphologically, these non-GABAergic granular terminals resembled serotonergic terminals (Wiklund et al., '81; King et al., '84).

DIFFERENCES BETWEEN CELL TYPE I AND II. The differences between cell type I and II are not readily reflected in their physiological properties (Llinás and Yarom, '81ab; Benardo and Foster, '86;

*Note *. This would be in accordance with a recent study by Andersson et al. ('89) which showed that IO neurons can be inhibited when an area directly rostral to the IO is stimulated. This effect had a much shorter latency than when stimulating the cerebellar nuclei (Andersson et al., '89).*

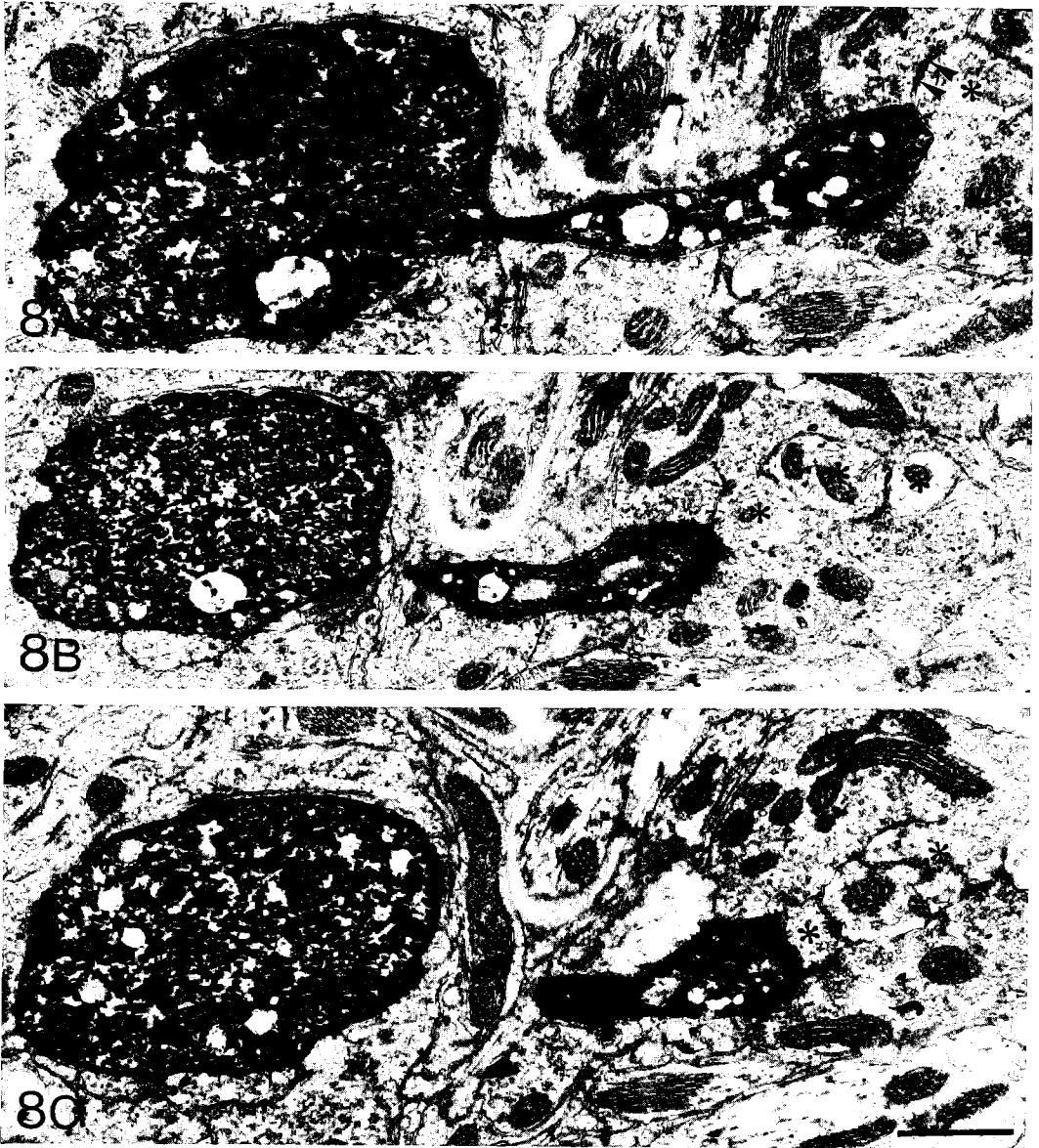


Fig. 8. Electron micrographs of an HRP labeled spine originating from the axon hillock. The spine is innervated by both a GABAergic (black dots) and a non-GABAergic terminal (of which the asymmetric synapse is indicated in Fig. 8A by an arrow head), and it is located together with spines (asterisks) of another cell in a glomerulus. This spine originates from the axon hillock of cell C (position is indicated in Fig. 7F). Scale bar = 1.4 μ m.

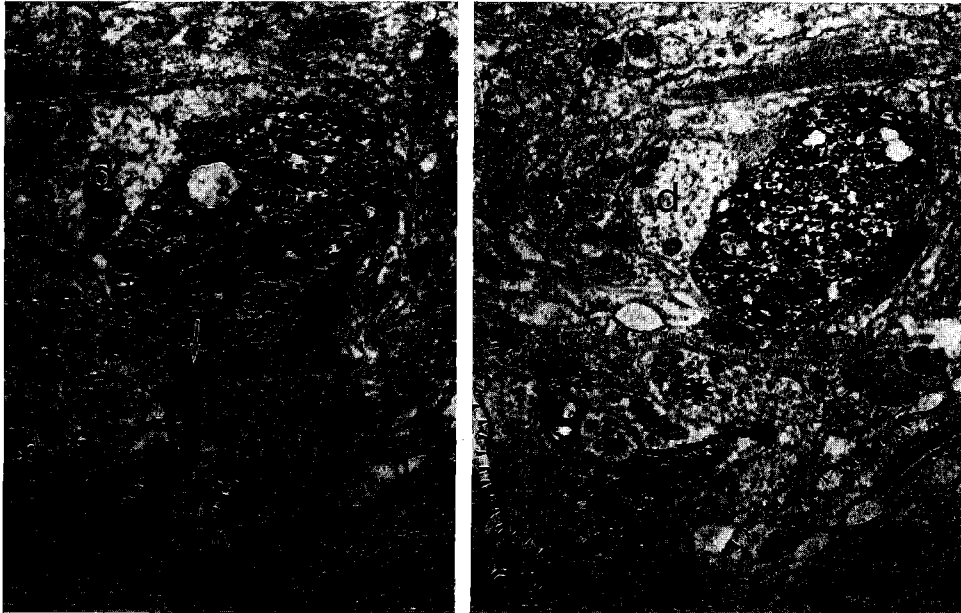
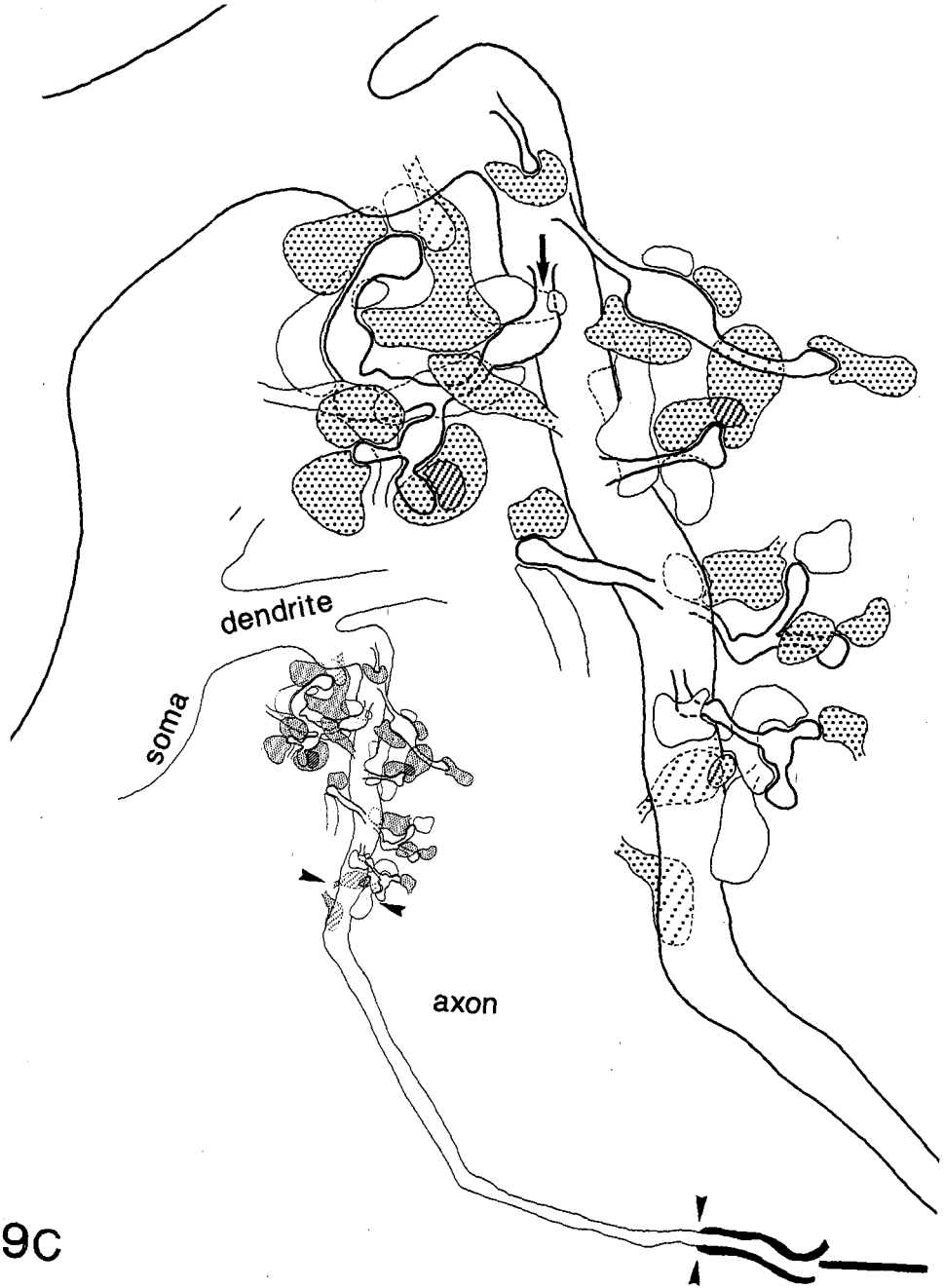


Fig. 9. Electron micrographs (9A and B) and reconstruction (9C) of the axon hillock of the type II neuron D. Figs 9A and B show that the axon gives off a spine (white arrow in A) which enters a glomerulus (surrounded by small arrow heads). The same spine is indicated in C with a black arrow. The GABAergic terminals (stars) contact both the HRP labeled and the non-labeled spines (asterisks). Note that a dendrite (d) is directly apposed to the axonal shaft. The morphology of the axon in the reconstruction clearly corresponds with the light microscopical observations (compare with Figs. 4A to 4G). The axon is derived from a primary dendrite and contains several complex spiny appendages most of which are contacted by both a GABAergic and non-GABAergic terminal (Fig. C). For symbols see Fig. 6. The beginning and end of the initial segment is indicated in the bottom reconstruction by the arrow heads. Scale bar for this reconstruction = 7.1 μm

Ruigrok et al., submitted) but primarily in the morphology of their dendritic trees (Scheibel and Scheibel, '55; Foster and Peterson, '86; Ruigrok et al., submitted) and dendritic spines (de Zeeuw et al., submitted). In the present study of the olivary axons, there were no significant differences between both types of neurons with regard to length and diameter of the axon hillock and the initial segment, and the numbers and proportions of GABAergic and non-GABAergic terminals they received. The axons of type I cells originated from the soma whereas those of type II cells were derived from a primary dendrite. In the present ultrastructural study

only 4 axons were studied but these observations were confirmed in the light microscopical analysis of a larger number ($n = 21$) of intracellularly HRP stained neurons (Ruigrok et al., submitted).

The spines on axons of type II cells were more numerous than in type I cells, moreover they displayed a more complicated morphology. Consequently, the majority (83%) of the terminals on type II axons terminated on axonal spines in glomeruli whereas of the terminals on type I axons only 21% ended upon spines (Figure 10). The finding that the axonal spines of neuron type II were more complex than those of type I is in agreement



with the observations of the dendritic spines of these cells (de Zeeuw et al., submitted).

FUNCTIONAL IMPLICATIONS. The presence of GABAergic terminals (Oertel et al., '81; Freund et al., '83; '85; DeFelipe et al., '85) or of terminals with symmetric synapses and pleiomorphic vesicles (Walberg, '63; Palay et al., '68; Conradi, '69; Muller et al., '84) apposed to somata and/or the axon hillock and initial segment is a commonly known feature of neurons in many regions of the central nervous system. It has been emphasized that these synapses are strategically well positioned to inactivate the cell (Eccles, '64).

However, when we consider the synaptic input and the unusual morphology of the axon hillock of the olivary neurons in relation to their complex electrophysiological properties (Llinás and Yarom, '81a,b; '86; Benardo and Foster, '86; Yarom and Llinás, '87; Yarom and Adan, '88; Yarom, '89), a few more specific suggestions on their function can be made.

Olivary neurons have a tendency to fire rhythmically (Armstrong et al., '68; Benardo and Foster, '86; Llinás and Yarom, '81a; '81b; '86). Llinás and Yarom ('86) demonstrated that the preferred olivary oscillatory firing frequency depends upon the level of participation of the dendritic tree in this proces. When a somatic (initial segment) Na-K actionpotential is triggered, it will antidromically invade the dendritic tree. Whether or not, this may lead to the triggering of a dendritic Calcium spike, depends on the level of active de- c.q. hyperpolarization of the cell membrane. Therefore, as was also proposed for the somatic GABAergic synapses (de Zeeuw et al., '89a), the GABAergic input to the axon hillock may be particularly well suited to reduce the effectiveness of the antidromically invading spike by locally decreasing the membrane resistance. Also, the mere existence of the axonal spines may be important in this proces since a computational study by Pongrácz ('85) demonstrated that spines located in the vicinity of the soma (e.g. axon hillock) may enhance the capabilities of the Na-K spike to invade the dendri-

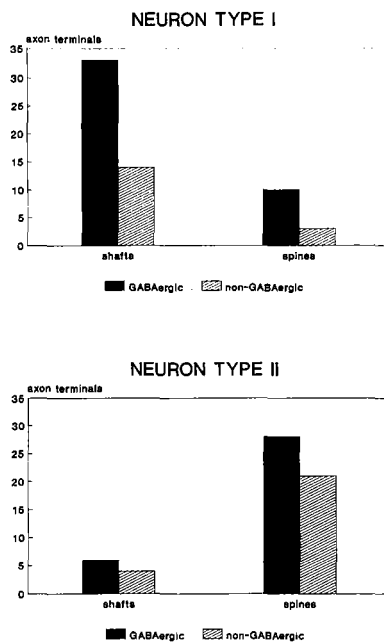


Fig. 10. Graphic representations of the distribution of terminals apposed to the axons of the neurons of type I (Fig. 10A) and type II (Fig. 10B). The axons of both types are primarily innervated by GABAergic terminals. However, most of the terminals on the axons of type I are apposed to the shaft while the majority of the terminals of type II are contacting the axonal spines. For numerical data see Table II.

tic tree, which, in case of the olivary cells, could again influence their preferred oscillatory firing frequency (Llinás and Yarom, '86). If the large granular terminals apposed to the axon hillock indeed contain serotonin, they could counteract the GABAergic synaptic input because it was demonstrated that the administration of serotonin to slices of the guinea pig IO increases the input resistance of olivary cells (Llinás and Yarom, '86).

Finally, without invalidating the above suggestions, it should be stressed that the GABAergic input to the olivary perikarya is partly derived from a non-cerebellar source,

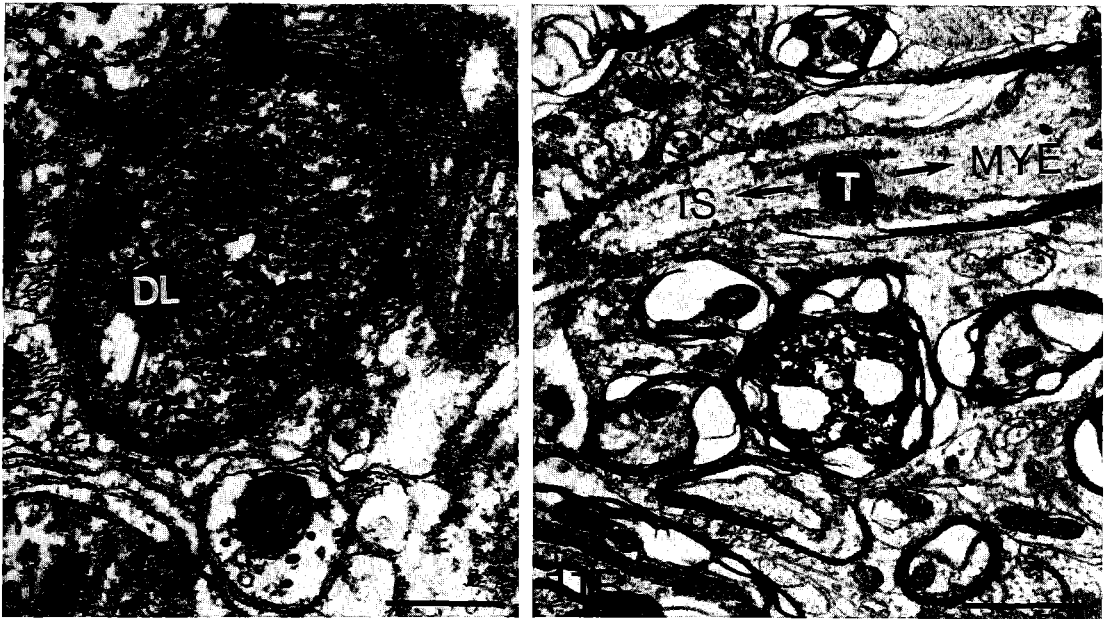


Fig. 11. Electron micrographs of typical axonal structures of olivary neurons. In Fig. 11A one can see an initial segment (of type I neuron A) characterised by its inner dense layer (DL) and fascicles (circle) of microtubuli linked by bars (arrow heads). Fig. 11B shows a myelinated HRP labeled olivary axon (of type II neuron D) at the bottom, and at the top a non-labeled, presumably olivary axon which is coincidentally cut at the transition (T) between its initial segment (IS) and its myelinated part (MYE). Scale bar in A = 0.5 μm , in B = 1.7 μm .

whereas the GABAergic terminals apposed to the axons may be derived from the cerebellar nuclei. This would indicate a different function of the GABAergic inputs to either soma and axon. Recently, it was proposed that the combined GABAergic cerebellar and excitatory mesodiencephalic input to the dendritic spines in the rostral MAO and principal olive may regulate the electrotonic coupling and simultaneously the preferred oscillatory firing frequency of these neurons in a timing sensitive way (de Zeeuw et al., in press). The present results indicate that the axonal spines, since they resemble in many ways the dendritic spines (e.g. they receive a combined inhibitory and excitatory input, have long and thin stalks, and are located within glomeruli), possess all the morpho-

logical prerequisites to function as timing sensitive instruments (Segev and Rall, '88; de Zeeuw et al., submitted).

Conclusions

The axon hillock and initial segment of cells of the IO have a unique morphology with regard to their size and morphology. They give rise to spines which are located within glomeruli, and which are mainly innervated by GABAergic but also by non-GABAergic terminals. The synaptic input to the axon hillock may be involved in inactivating (resetting) the cell, in regulating the oscillatory firing frequency and/or in a timing sensitive operation.

CHAPTER V General discussion

The present study deals with the mesodiencephalic and cerebellar synaptic input to the MAO and PO of the cat. New combinations of ultrastructural techniques were used to identify the origin and neurotransmitter of these afferents at different postsynaptic elements.

Below, the technical aspects, the major morphological results, and the functional implications will be discussed.

a. Technical aspects

Three new ultrastructural combination techniques were used in the present study. These included WGA-HRP anterograde tracing combined with GABA-immunocytochemistry (Chapter II), a combination of anterograde tracing of (3H)leucine and WGA-HRP (Chapter III), and an ultrastructural study combining intracellular labeling of HRP with postembedding GABA-immunocytochemistry (Chapter IV).

WGA-HRP anterograde tracing with GABA-immunocytochemistry. The first combination technique allows a visualization in a single ultrathin section of the neurotransmitter (GABA) in a terminal, which is HRP labeled by anterograde axonal transport from its source. To our knowledge this was the first time that both parameters were determined together within the same terminal profile. It was demonstrated that TMB, which is the most sensitive chromogen (Mesulam,'78), can be used for HRP histochemistry in combination with immunocytochemistry at the ultrastructural level provided that the TMB crystals are stabilized with DAB-cobalt. This stabilization (Lemann et al.,'85) was essential because non-stabilized TMB crystals dissolve during the immuno

staining. In addition, the application of the stabilization had several side effects. Firstly, when a stabilization was used it was possible to perform the TMB incubation at a relatively high pH of about 4.8 (instead of the traditional pH of 3.3) without compromising the final yield of labeling. This difference in pH resulted in a much better preservation of the ultrastructure. Despite the general improvement of the appearance of the neuropil, the sites of the TMB/DAB-Co reaction products showed electron lucent spaces in their center. These holes were also due to the DAB-Co stabilization procedure, since they were not present in non-stabilized tissue (Mesulam,'78; Holstege and Kuypers,'87ab; De Zeeuw et al.,'88ab) and since they also were observed in stabilized material, which was not processed for immunocytochemistry (Lemann et al.,'85). Another advantage was that stabilized vibratome sections could be stained en block in uranyl acetate whereas the unstabilized HRP reaction products were found to disappear in this aqueous solution. This block staining is of particular importance for studies of the IO since it improves the visualization of gap junctions (Sotelo et al.,'74).

The results showed that most, if not all, WGA-HRP labeled terminals from the cerebellum were GABAergic. This high ratio of double-labeled terminals indicated that the GABA-antibody can detect nearly all the GABAergic nucleoolivary terminals, indicating that the sensitivity of the antibody was good. In addition, these experiments provided an estimate for the efficacy of anterograde tracing with WGA-HRP (using the stabilization procedure for HRP histochemistry). Since, about one third of the GABAergic terminals were WGA-HRP

labeled in the experiments with the highest yields and since probably more than 90% of the GABAergic terminals are derived from the cerebellum (Nelson and Mugnaini,'87), it may be concluded that the WGA-HRP anterograde tracing technique as applied to the cerebello-olivary projection, detects about one third of the actual number of terminals.

The WGA-HRP labeled terminals from the mesodiencephalic junction were never found to be GABA-positive. This experiment demonstrated that the WGA-HRP reaction product did not induce false positive GABA-labeling providing an argument that the specificity of the antibody was good as well (for detailed tests about the specificity of the antibody used in these studies see Seguela et al.,'84; Buijs et al.,'87).

An important advantage of this antibody was that it could be applied to osmicated sections. So far only GABA, glutamate (Watson,'88), aspartate, taurine, and glycine (Otterson,'88) can be detected in osmicated tissue using antibodies against conjugates of these small molecules. Thus, when it is required to determine the neurotransmitter of an identified system in well preserved tissue, WGA-HRP anterograde tracing can be combined with gold-immunocytochemistry only of the amino-acids neurotransmitters mentioned above. In the cases of other substances one could try to combine anterograde tracing of (3H)leucine with preembedding immunocytochemistry (see Chapter I, part f). However, this combination technique is more time consuming, since the autoradiographic procedures require long exposure times and complex analytical identification methods (Holstege and Vrensen,'88).

Anterograde tracing of (3H)leucine and WGA-HRP. The second combination technique of (3H)leucine anterograde tracing with WGA-HRP anterograde tracing allows a simultaneous visualization of two afferent systems of a

different origin in a single ultrathin section (Chapter III). Autoradiography and HRP/DAB (Dekker,'81) or WGA-HRP/TMB (Holstege and Kuypers,'87ab) histochemistry were used before at the ultrastructural level for the combination of anterograde tracing with retrograde tracing. However, to our knowledge the present ultrastructural study was the first in which (3H)leucine and WGA-HRP anterograde tracing were combined. In contrast to the combination technique of WGA-HRP anterograde tracing with postembedding immunocytochemistry described above, it appeared that this combination is equally effective whether the WGA-HRP reaction products were stabilized with DAB-cobalt or not. The efficacy of WGA-HRP anterograde tracing was not decreased by the stabilization. This was in agreement with a previous tracing study by Molinari ('87) in which the stabilization and normal WGA-HRP histochemistry were compared for one afferent system in one type of animal.

Other means of anterograde tracing which may be used in combination techniques are anterograde degeneration and anterograde tracing of Phaseolus vulgaris leucoagglutinine (PHA-L), (Chapter I, part f). When anterograde degeneration is used, it should be realized that this method is less sensitive and that it can not be applied to every projection system since lesions will damage passing fiber systems (Dekker,'77). The application of anterograde tracing of PHA-L, which is visualized by immunocytochemical means (Gerfen and Sawchenko,'84; Wouterlood and Groenewegen,'85), seems a more promising method to combine with other anterograde axonal tracers. Although not performed yet, it may be possible to combine anterograde tracing of PHA-L with anterograde tracing of WGA-HRP, since it has been shown in combined immunocytochemical procedures, that two different antigens which are each

visualized initially with a peroxidase reaction, can still be labeled differently in the same section (van den Pol and Gorcs, '86; see also Chapter I, part f). If future studies will show that these two methods of anterograde tracing can indeed be combined, this combination has advantages over the combination of (3H)leucine with WGA-HRP which would require the long exposure times which are an inherent feature of the autoradiographic procedure.

Intracellular labeling of HRP with postembedding GABA-immunocytochemistry. The third ultrastructural technique consists of a combination of intracellular labeling of HRP with postembedding GABA-immunocytochemistry (Chapter IV). This technique allows physiological and lightmicroscopical identification of the injected neuron, and makes it possible to study this cell and its GABAergic afferents at the ultrastructural level. The lightmicroscopic examination of the osmicated material is drastically improved when glucose is added during osmication, resulting in less darkly stained sections. The fact that the use of glucose counteracts the osmication may also explain why it enhances the GABA immunogold staining (de Zeeuw et al., '88a), since osmium is known to have a negative effect on the identification of antigens by antibodies (Priestly, '84). Fortunately, the ultrastructural preservation was not seriously compromised by the use of glucose (see also Holstege and Kuypers, '87b).

It was found that it is preferable to osmicate the tissue sections in a glucose solution, to dehydrate them with dimethoxy propane, and to embed them in araldite even when the tissue only has to be analysed with the light microscope. This way, the morphology of the HRP labeled profiles in the embedded sections was improved with significantly less artifacts compared to the non-osmicated sections dehydrated in ethanol and

nissl stained in cresyl violet.

An additional advantage of this combination technique is the fact that an endless serie of ultrathin sections can be cut from an embedded vibratome section (70 um in the present study) before the postembedding GABA-immunocytochemistry is performed. For this reason, it is possible to reconstruct long structures, like axons (see de Zeeuw et al., b, submitted), of physiologically identified neurons together with their GABAergic input.

To our best knowledge four other ultrastructural techniques combining cellular labeling with GABA-immunocytochemistry have been described. One technique is described in a study in which intracellular HRP labeling was combined with postembedding GABA-immunocytochemistry on semithin sections (thickness of about 1 to 2 um) using the PAP method (Freund et al., '85), while in other studies Golgi impregnation was combined with GABA immunogold labeling (Somogyi et al., '85; Cipolloni and Keller, '89), with glutamic acid decarboxylase (GAD) or GABA-immunocytochemistry using the PAP method (Freund et al., '83; Somogyi et al., '83; Somogyi et al., '85), or with intraneuronal uptake of tritiated GABA (Somogyi et al., '81). However, in these studies it was not possible to make complete reconstructions through long neuronal structures (Freund et al., '83 and '85; Somogyi et al., '83) and/or to combine it with physiological identification of the neurons (Somogyi et al., '81, '83 and '85; Freund et al., '83; Cipolloni and Keller, '89).

A drawback of the intracellular HRP staining of olivary cells is the fact that gap junctions could not be identified between HRP labeled structures or between an HRP labeled profile and a non-labeled structure. The most likely explanation for this failure seemed to be that the HRP reaction product masks the narrow interneuronal space of the

gap junctions. Despite this masking effect, HRP did probably not pass through the gaps in these junctions since HRP labeled spines were rarely located near each other, and no gradient of labeling intensity could be detected.

It was accidentally found that cell degeneration could be used as an additional label for neurons at the ultrastructural level. This provides triple labeling in a single ultrathin section. Neuronal degeneration in this case could be the result of a lesion by the microelectrode penetration of the cell. Further studies will be needed to find out whether this phenomenon is reproducible.

It can be concluded that the three combination techniques used in our studies can provide new important data on the ultrastructure of the CNS. They all have their advantages and their specific restrictions and complications. Therefore, they should be carefully selected and weighed against other available combination techniques (for a review see Table 1, Chapter I, part f).

b. Major results

The present study showed that the bulk of the non-GABAergic and GABAergic innervation of the MAO and PO is derived from the mesodiencephalic junction and the cerebellar nuclei, respectively. Below, the terminals of these afferents will be discussed with regard to their morphology and postsynaptic distribution. In addition, special emphasis will be put on the olivary glomerulus, soma and axon.

b1. Types of terminals.

Based on differences in vesicle shape, three types of GABAergic terminals and three types of non-GABAergic terminals were observed.

The first and most numerous GABAergic terminal contained mainly small pleomorphic vesicles. These terminals

were often WGA-HRP labeled from the ce-rebellar nuclei. They established primarily, but not invariably, symmetric synapses corresponding to Gray's type II. This type of GABAergic terminal was located both in the extra- and intraglomerular neuropil but occasionally they were also adjacent to the olivary somata and axon hillock. These findings were largely in agreement with recent studies of the GABAergic and cerebellar innervation of the rat IO (Sotelo et al., '86; Angaut and Sotelo,'87). However, in previous studies of the IO of the opossum and the cat it was found that cerebellar terminals contained spherical vesicles (King et al.,'76; Mizuno et al.,'80) and exhibited asymmetric synapses (Mizuno et al.,'80). The difference in shape of the vesicles may be due to a different type and osmolarity of the buffer used for the fixative (Valdivia,'71) and/or to a different duration of exposure of the tissue to aldehydes (Paula-Barbosa,'75). These GABAergic terminals occasionally showed single rows of subsynaptic densities. This occurred more regularly in the caudal MAO than in the rostral MAO. In the rostral MAO, the subsynaptic densities were in some cases located in a constriction of a dendrite and interposed between two terminals with clear asymmetric synapses. These structures, which resembled the so-called crest synapse (Milhaud and Pappas,'66ab; Akert et al.,'67), have been described before in the dorsal cap of the rabbit (Mizuno et al.,'74), in the MAO of the monkey (Rutherford and Gwyn,'80), and in the rat (Sotelo et al.,'86).

The second type of GABAergic terminal, which was less frequently observed, contained mainly large oval vesicles. Apart from the shape and size of the vesicles, these terminals resembled the first type. They were infrequently labeled from the cerebellum. Some of these terminals were apposed to perikarya. At this location they frequently showed subsynaptic cisterns, which were most

often present as a single cistern with a few ribosomes. These subsurface somatic structures, which were found previously in the IO of the opossum (Bowman and King, '73), were observed more frequently subsynaptic to GABAergic terminals than to non-GABAergic terminals.

The third terminal, the GABAergic granular type, contained a large number of dense core vesicles, interspersed between clear oval vesicles and tubulovesicular elements. All types of vesicles in these terminals were irregularly shaped. These terminals were often elongated. They rarely exhibited a synapse. None of them was ever found to be WGA-HRP labeled in the cerebellar experiments. This type of terminal, which was not described before in GABAergic studies of the IO, was found primarily in the extraglomerular neuropil and apposed to somata.

The first type of non-GABAergic terminal accounted for about 95% of the non-GABAergic terminals, and it was the only type, which was WGA-HRP labeled from the mesodiencephalic junction. They contained primarily large, round and oval vesicles. Like the cerebellar terminals they usually contained mitochondria and a few dense core vesicles but sometimes they also included some coated vesicles. The vast majority of them formed asymmetric synapses corresponding to Gray's type I. The excitatory morphology of these terminals (Uchizono, '65), was in agreement with the recordings in the IO upon stimulation in the mesodiencephalic junction (part a, Chapter IV). The non-GABAergic terminals dominated both the innervation of the glomerular spines and the shafts of the distal dendrites. These results were in agreement with studies of King et al. ('78) and Cintas et al. ('80), which showed, for opossum and rat respectively, that most of the mesodiencephalic terminals had round vesicles and asymmetric synapses. Furthermore

they confirmed previous studies in monkey (Rutherford and Gwyn, '80), cat (Mizuno et al., '76) and rabbit (Mizuno et al., '74), which found that the majority of randomly selected olivary terminals had round and oval vesicles and asymmetric synapses. In the present study these non-GABAergic terminals were only infrequently found to be located adjacent to an olivary soma. These data agree with the study of the projection from the mesodiencephalic junction in rat by Cintas et al. ('80), and with the general study of the rat IO by Gwyn et al. ('77). However, mesodiencephalic terminals apposed to perikarya, and somatic terminals provided with asymmetric synapses were never observed in the study of the mesodiencephalic projection to the rat IO by King et al. ('78), and in studies of the IO in cat (Walberg, '63) and monkey (Rutherford and Gwyn, '80). When Taxi bodies (Taxi, '61) were observed they were more frequently located subsynaptic to this type of WGA-HRP-labeled and non-labeled, non-GABAergic terminals than to GABAergic terminals. Similar structures have also been observed subsynaptic to asymmetric synapses of round vesicle containing terminals in the IO of the opossum (Bowman and King, '73), and the squirrel monkey (Rutherford and Gwyn, '80). The precise functional significance of these subsynaptic densities, which are primarily associated with excitatory synapses, has not yet been elucidated.

The second type of non-GABAergic terminal, contained a large number of dense core vesicles. This type of non-GABAergic terminals accounted for only a fraction of all the terminals in the IO, but they made up approximately 85% of the total number of large granular terminals. Like the GABAergic large granular terminals, they were never WGA-HRP labeled in the tracing experiments. They were located primarily outside the glomeruli rarely establishing a synaptic contact. These terminals were relatively

often apposed to the axon hillock. In morphology, both the GABAergic and non-GABAergic large granular terminals resembled serotonergic terminals, which are known to be present in the IO (King et al., '84; Wiklund et al., '81).

The third type of non-GABAergic terminal contained only flattened vesicles. It was observed before in the IO of the opossum by Bowman and King ('73). These terminals were never found to be WGA-HRP labeled in the mesodiencephalic experiments. Synaptic contacts were seldomly observed and they were situated mainly outside the glomeruli.

b2. The olivary glomeruli.

Held (1897) introduced the name glomerulus for the protoplasmic islets composed of mossy fiber rosettes interwoven with the claw-like terminals of granule cell dendrites and the terminal branchlets of the Golgi cell axons in the cerebellar cortex. The same glomeruli were also the first complex synaptic arrangements to be identified at the ultrastructural level (Palay, '61; Gray, '61; Kirsche et al., '65). They are characterized by one or more central terminal boutons and a peripheral mantle of dendrites and other axon terminals. Later the name was applied to similar structures in other parts of the central nervous system including the dorsal lateral geniculate nucleus (Szentagothai, '63; Peters and Palay, '66; Famiglietti and Peters, '72), the medial geniculate nucleus (Majorossy and Rethelyi, '68), the lateral vestibular nucleus (Sotelo and Palay, '70), the main sensory trigeminal nucleus (Gobel and Dubner, '69), the pontine nuclei (Mihailoff et al., '88), and various thalamic nuclei (Papas et al., '66; Jones and Powell, '69). An inversion of this organization occurs in the thalamic pulvinar and lateral posterior nuclear group (Majorossy et al., '65), the ventrobasal complex of the thalamus (Ralston and Herman, '69), and the IO (Nemecek and Wolff, '69; Bow-

man and King, '73; Sotelo et al., '74). Although the intrinsic organization of the olivary glomeruli is similar, their center consists of the profiles of numerous spines whereas the glomeruli of the other brain areas contain only a single, large dendritic protuberance or only one or two small dendrites. Thus, the multiple elements of their central core make the olivary glomeruli unique among the synaptic glomeruli described thus far.

SPINES IN GLOMERULI. The present study unraveled several questions with regard to the composition of the spiny center of the olivary glomerulus. Following serial section analysis of HRP labeled olivary neurons in the cat it was found that most, if not all, HRP labeled spines were located within glomeruli. Different spine heads of the same spine were frequently incorporated within the same glomerulus but they could also be located in different glomeruli. However, the glomeruli rarely contained more than a single spine from the same HRP labeled cell. Moreover, when more than one spine head of the same spine was located within a single glomerulus, they were only occasionally located near each other. These data strongly suggested that the dendritic elements of the same olivary neurons avoid each other. As a consequence, gap junctions between elements of the same olivary neuron are excluded. It was found that the glomeruli on average contain spines of six different cells (with a maximum of eight).

Sofar, the olivary glomeruli were presumed to include spines solely of a dendritic origin (Nemecek and Wolff, '69; Bowman and King, '73; Sotelo et al., '74; Gwyn et al., '77; Rutherford and Gwyn, '80). The present study demonstrated that axonal spines are located within glomeruli as well. In the center of these glomeruli, the axonal appendages were apposed to dendritic spines of other olivary cells. The axonal spines could not

be distinguished from the dendritic spines on morphological grounds. It remained unclear though, whether the axonal spines were also linked by gap junctions, as was shown for dendritic spines in cat (Sotelo et al., '74; de Zeeuw et al., '89a), rat (Gwyn et al., '77), monkey (Rutherford and Gwyn, '77), and opossum (King, '76). It will have to be examined whether axo-axonal or axo-dendritic gap junctions indeed do exist, because it offers the interesting possibility that olivary structures directly involved in impulse generation are electrotonically coupled.

BOUTONS IN GLOMERULI. With regard to the innervation of the glomeruli it was estimated in a single section analysis that about one third of both the GABAergic and non-GABAergic terminals in the rostral MAO were located within glomeruli (de Zeeuw et al., '89b). This calculation was based on the assumption that a synaptic complex was a glomerulus when it contained at least three spiny profiles and two terminals. In the reconstructions from intracellularly injected neurons, it was found that most, if not all, of the HRP labeled spines are incorporated in glomeruli. Therefore, the actual proportion of the terminals which are located within glomeruli has to be higher than one third. No calculations were performed to estimate the proportion of all the terminals which are located in the glomeruli, but this figure would amount to about half of the terminals. The ratio of non-GABAergic mesodiencephalic terminals to GABAergic, cerebellar boutons is independent from the actual number of terminals located within glomeruli, since it was found to be the same for the extra- and intraglomerular neuropil (see Figure 3, part c, Chapter II). In both divisions of the neuropil 38% of the terminals were GABAergic.

These conclusions were based on the entire population of glomeruli in the rostral MAO but it was also demon-

strated, by calculations of probabilities, that they are also valid for individual glomeruli: There was no obvious separation or coexistence of the GABAergic and mesodiencephalic terminals in the glomeruli (see part b, Chapter II). It was concluded, therefore, that the innervation of glomeruli in the rostral MAO by the GABAergic-cerebellar and the non-GABAergic-mesodiencephalic afferent systems is random and equal.

Many efforts were taken in the present study, to find out whether the spines in the olivary glomeruli were innervated separately by mesodiencephalic and cerebellar terminals or by both. In the experiments in which anterograde tracing of WGA-HRP was combined with GABA-immunocytochemistry, it was found in the rostral MAO that mesodiencephalic and GABAergic terminals innervate the same glomerular spines and that the same is true for the cerebellar and non-GABAergic terminals. Direct observations of spines in the glomeruli which were innervated by both mesodiencephalic and cerebellar terminals were made in the experiments in which anterograde tracing of WGA-HRP was combined with anterograde tracing of ³H-leucine. This was confirmed and quantitatively extended by serial section analysis of intracellularly labeled neurons where all the dendritic and most of the axonal spines were innervated by both GABAergic and non-GABAergic terminals. Taken together, these data indicate that all olivary spines in the glomeruli of the MAO and PO receive both an excitatory input from the mesodiencephalic junction and an inhibitory input from the cerebellar nuclei. These findings are unusual, since it has been shown for various regions in the central nervous system that the vast majority of dendritic spines are contacted solely by asymmetric synapses (Kemp and Powell, '71; Palay and Chan-Palay, '74; Wilson and Grove, '80; Wilson et al., '83; Muller et al., '84).

GAP JUNCTIONS IN GLOMERULI. Glomerular spines in the IO can be linked by gap junctions. Serial section analysis in the present study showed that these electrical synapses are not necessarily restricted to contacts between two spine heads, but they can also occur between the stalks of two spines.

The glomerular spines linked by gap junctions may be a specific group with respect to their innervation. Quantitative analysis showed that of the terminals strategically located next to both dendritic elements coupled by a gap junction significantly ($p < 0.05$) more terminals were GABAergic (54%) than would be expected from the distribution of GABAergic terminals over the entire neuropil (38%). Significant differences were found only for the strategically located terminals, stressing the importance of the exact location of terminals next to the gap junctions.

About one third of the strategically and non-strategically located GABAergic terminals were double labeled, following injection of WGA-HRP in the cerebellar nuclei. Since the present technique of WGA-HRP tracing may detect at most about one third of the actual number of terminals (see above), this indicates that most if not all GABAergic terminals associated with gap junctions originate from the cerebellum. These findings, which provided the first direct evidence for the cerebellar origin of the GABAergic terminals associated with gap junctions, extended the results of previous ultrastructural studies of the cerebellar (King et al., '76; Angaut and Sotelo, '87) and GAD positive (Sotelo et al., '86) terminals of the IO of the rat. Later, the same double labeling technique was applied to the rat IO and gave similar results (Angaut and Sotelo, '89).

The present study was also the first to show that dendrites of olivary cells which are linked by gap junctions are contacted by non-GABAergic terminals

as well. For the rostral MAO, it was demonstrated that most of them probably originate from the mesodiencephalic junction. It should be noted that, although relatively many GABAergic terminals were located next to gap junctions, still about half of all terminals strategically or non-strategically located next to dendrites coupled by gap junctions, were non-GABAergic.

These data allow the conclusion that electrotonically coupled spines receive more strategically located GABAergic terminals derived from the cerebellum than would be expected from their general distribution over the olivary neuropil, but that the innervation of these spines is not fundamentally different from all other spines.

DIFFERENCES BETWEEN CELL TYPES AND SUBNUCLEI IN THE INFERIOR OLIVE. The morphological differences between cell type I and II are not readily expressed in their physiological properties (Llinas and Yarom, '81ab; Benardo and Foster, '86, Chapter V, part a). These differences mainly involve the morphology of their dendritic tree (Scheibel and Scheibel, '55; Foster and Peterson, '86; Chapter V, part a) and their dendritic and axonal spiny appendages (Chapter V, part b and c). The dendrites of type I radiate away from the soma, while those of type II tend to curl back in the direction of the soma. Following electron microscopical examination of the intracellular injected cells it was found that the glomerular spines of cell type II were more complex than those of type I. This holds both for the dendritic and axonal spines. In addition, the axons of type II neuron mostly originated primarily from a primary dendrite while those of type I neurons emerged from the soma. Type II axons were more amply provided with spines, and, in accordance with this, the majority (83%) of the terminals on these axons terminated on axonal spines in glomeruli, whereas of the terminals on type I axons

only 22% ended upon spines. However, the proportion of GABAergic terminals apposed to dendrites and axons, remained the same for the two types of neurons.

Type I neurons are primarily located in the caudal accessory olives whereas type II neurons are present in each olivary subnucleus and outnumber type I neurons (Scheibel and Scheibel,'55; Scheibel et al.,'56; Foster and Peterson,'86; Chapter V, part a). The serial reconstructions showed that the number of terminals, which innervated individual glomeruli of the type II cells (located in the rostral MAO), was in the same range as the number of terminals innervating glomeruli of type I (caudal MAO). Since it was found previously that the rostral part of the MAO contains relatively more glomerular terminals than the more caudally located areas of the MAO (de Zeeuw et al., '89b), these data suggest that the number of glomeruli is increased in the rostral MAO.

CONSEQUENCES FOR THE DISTRIBUTION OF OLIVARY HYPERTROPHY. Although the neuropil of the caudal MAO probably does not differ from the rostral MAO in the numbers of spines or terminals within individual glomeruli, the differences in the complexity of their spines and the total number of glomeruli between these subnuclei may explain why they respond differently to certain pathological conditions.

Contralateral cerebellectomy can induce olivary hypertrophy in MAO and PO of cats (Verhaart and Voogd,'62; Voogd and Boesten,'76). The enlargements of the cells usually starts in the rostral MAO and only rarely in the caudal MAO (Boesten and Voogd,'85). Recent evidence suggests that electrotonic coupling of hypertrophic neurons is enhanced (Ruigrok et al.,'89; de Zeeuw et al.,'89c). Therefore, it is attractive to hypothesize that the neuropil of the rostral MAO with its complex spines and

its relatively high number of glomeruli (the major residence for the gap junctions; Sotelo et al.,'74), provides better conditions for the development of hypertrophy than the caudal MAO.

Differences in the level of electrotonic coupling may also explain why hypertrophy occurs in the MAO and PO but not in the DAO. In various animal species gap junctions have been observed in the MAO (King,'76; Gwyn et al., '77; Rutherford and Gwyn,'77; de Zeeuw et al.,'89a) and PO (King,'76; Gwyn et al.,'77; Angaut and Sotelo,'87; Angaut and Sotelo,'89; de Zeeuw et al., in press) but also in the DAO (King,'76; Gwyn et al.,'77; Rutherford and Gwyn,'77). However, the glomeruli are most prominent and numerous in the PO and rostral MAO (Gwyn et al.,'77; Chapter IV), while the neuropil of the DAO appears to be dominated by dendritic thickets rather than synaptic clusters (Gwyn et al.,'77; Molinari,'87). These morphological data, which suggest that the electrotonic coupling is more extensive in the rostral MAO and PO than in the DAO, are well in accordance with physiological recordings made in the IO of in vitro guinea pig brain stem slices (Llinás and Yarom,'81a). They found that electrotonically coupled cells were most readily found in the MAO. Moreover, the size of the somatosensory receptive fields in the DAO of the cat are such small, that they don't seem to be blurred by extensive electrotonic coupling (Gellman et al.,'83). Furthermore, the fact that hypertrophy occurs in cat and higher mammals, and not in rat also supports the hypothesis that the level of electrotonic coupling influences the appearance of hypertrophy, because the glomeruli of the rat were found to be smaller than those of the cat (Chapter III).

Differences in the level of electrotonic coupling in the glomeruli between the olivary subnuclei may well be a prerequisite but do not constitute the only

factor responsible for the appearance of olivary hypertrophy. Firstly, because hypertrophy probably only occurs when the cerebellar input to the olive is disrupted (Verhaart and Voogd,'62; Voogd and Boesten,'76; Boesten and Voogd,'85). In this respect it is interesting to note that the DAO is probably the only one of the three main olivary subnuclei which receives an additional GABAergic input from the cuneate nucleus in the hindbrain (Nelson and Mugnaini,'89). This could possibly compensate for the loss of cerebellar GABAergic input to this region and prevent the occurrence of hypertrophy. Secondly, it may be relevant that the MAO and PO receive a strong excitatory input from the mesodiencephalic junction (also in the hypertrophic IO; de Zeeuw et al.,'89c) while the DAO is devoid from such afferents (Onodera,'84). Finally, we have suggestive evidence that hypertrophy only occurs when the cats are allowed to move freely around for at least a few hours a day (unpublished results).

Taken together, the data suggest that the electrotonic coupling between olivary cells will be enhanced when the GABAergic cerebellar input is removed from their dendrites. Locomotion apparently activates the remaining mesodiencephalic input of these neurons, which will then react with an extensive retrograde reaction, involving expansion, distension, and vacuolization of their rough endoplasmic reticulum on transection of their axons.

b3. The innervation of soma and axon of olivary neurons.

Both the somata and axons of olivary cells received an afferent input which consisted for about 65% of GABAergic terminals. This was significantly higher than the proportion of GABAergic terminals selected randomly from the entire neuropil (38%). For both the somata and axons, the proportion of GABAergic terminals would be even higher when

only terminals with synaptic junctions were considered. The findings for somata generally agree with previous studies of the IO in different species, which described that most or all of the terminals contacting the IO somata contained pleomorphic vesicles and established Gray's type II synapses (Walberg,'63; Bowman and King,'73; Gwyn et al.,'77; Rutherford and Gwyn,'80).

The terminals which were in contact with the axon hillock were often apposed to axonal spines located within glomeruli, whereas terminals on somata, which gave rise to only few spines, were directly apposed to the perikaryon. In addition, GABAergic large granular terminals were observed next to the soma but not to the axon, whereas the opposite was true for the non-GABAergic large granular terminals. Moreover, the GABAergic terminals adjacent to the perikaryon frequently showed subsynaptic cisterns of endoplasmic reticulum, while these profiles were not observed in the olivary axons. Therefore, the origin of the GABAergic terminals apposed to the somata and axon hillock does not appear to be the same.

The GABAergic terminals on the olivary axons are not yet studied in combination with anterograde tracing, but the fact that many of them were located on axonal spines within glomeruli suggest that they were of a cerebellar origin because most of the GABAergic terminals within glomeruli are derived from this source (Chapter II).

The origin of the GABAergic input to somata probably is heterogeneous. In experiments combining anterograde tracing of WGA-HRP with postembedding GABA-immunocytochemistry, it was found that the proportion of the GABAergic terminals, which was labeled with WGA-HRP from the cerebellum was significantly lower among the somatic terminals than among the terminals selected randomly from the

entire neuropil. This suggests that, in the cat at least, a relatively small proportion of the GABAergic input to somata is derived from the cerebellum. Cerebellar axosomatic terminals were not observed in previous studies of the IO of the opossum (King et al., '76) and the cat (Mizuno et al., '80), but in the rat they appear to be present (Angaut and Sotelo, '87). The possible existence of a non-cerebellar GABAergic projection to the olivary somata is supported by several studies. First of all, it is evident that there has to be a non-cerebellar source for GABAergic terminals in the IO because Nelson and Mugnaini ('85) showed that total cerebellectomy does not cause a complete depletion of GAD-positive terminals in the rat IO. Secondly, Scheibel and Scheibel ('55) demonstrated in their Golgi studies of the IO of various species the existence of fibers projecting specifically to somata and nearby dendrites. Thirdly, stimulation in the brachium conjunctivum of the cerebello-olivary fibers exerted an inhibition of climbing fiber responses with a relatively long latency while stimulation in an area just rostral from the IO evoked a direct inhibition with a much shorter latency (Anderson et al., '89). This could be explained by the fact that the cerebellar input innervates the dendrites and the spines while the other projection would innervate the somata.

A non-cerebellar GABAergic projection to the somata indeed could be derived from nearby regions. Scheibel and Scheibel ('55) described that the fibers, which innervated primarily the olivary somata, entered the IO from the dorsomedial side and the adjoining reticular formation. It was found in the present study that a minority of the GABAergic terminals could be classified as large granular terminals. Large granular terminals were never, neither in the present nor in a previous study (King et al., '76; Mizuno et al., '80; Angaut and Sotelo, '87), found to originate from the

cerebellum and part of them were apposed to somata. These terminals resembled morphologically serotonergic terminals (Wiklund et al., '81; King et al., '84), possibly indicating a coexistence of GABA and serotonin. This projection probably takes its origine from the nearby located nucleus reticularis paragigantocellularis (NPGC) and/or the nucleus raphe pallidus (NRP), both regions are known for the coexistence of GABA and serotonin (Belin et al., '83; Mugnaini and Oertel, '85; Millhorn et al., '87; Harandi et al., '87) and for their projection to the IO (Walberg and Dietrichs, '82; Bishop and Ho, '86).

Taken together these data suggest that the GABAergic input to the somata of olivary neurons is partly derived from a non-cerebellar source, which may include a combined serotonergic and GABAergic input from the NPGC or NRP, whereas the GABAergic input to the axon hillock would mainly be derived from the cerebellar nuclei.

b4. Conclusions from morphological results.

Based upon direct and indirect morphological evidence obtained in the present study the following model of the neuropil in the MAO and PO of the cat is proposed (see Figure 1). The dendrites and spines of an olivary neuron are apposed to other olivary neurones but never contact other elements of the own cell. The olivary spines are 1) complex structures comprising a long stalk and several spine heads, 2) frequently coupled by gap junctions, 3) always located within glomeruli, and 4) derived from dendrites and sometimes from axons, but rarely from somata. The MAO and PO are mainly innervated by excitatory terminals from nuclei at the mesodiencephalic junction and by GABAergic afferents from the cerebellum. About half of these terminals end upon glomerular spines, while the other half terminates mostly on the

shafts of distal dendrites. Most, if not all, of the dendritic and axonal spines and shafts are innervated by both afferent systems. In addition, there probably exists a non-cerebellar GABAergic input which is directed mainly to the somata, and a serotonergic input which is primarily located within the extraglomerular neuropil. Both latter projections account for only a small proportion of the olivary boutons, and both may be derived from areas in the proximity of the IO.

d. Functional implications

Several morphological features distinguish the neuropil of the IO from other regions of the central nervous system. The shape of their dendritic arbor and the morphology of their dendritic and axonal spines is unusual, the combination of an excitatory and inhibitory input to these spines is remarkable. The total design of the olivary glomeruli, therefore is unique. These morphological characteristics have specific functional implications.

Some of these implications can be deduced from physiological experimental studies of the olivo-cerebellar system and theoretical studies of spines. Several studies of Llinás and colleagues have demonstrated that the degree of synchronization of complex spike activity in cerebellar Purkinje cells can be increased in the medio-lateral direction and to less extent in the rostro-caudal direction by applying GABA antagonists to the IO (Sasaki and Llinás,'85; Lang et al.,'89) or by lesioning the central nuclei of the cerebellum (Llinás, personal communication). This strongly suggests that the cerebellar GABAergic terminals located within the glomeruli next to the gap junctions are involved in the regulation of electrotonic coupling. However, since the present study indicates that the olivary spines receive all both a GABAergic input from the cerebellum and an

excitatory input from the mesodiencephalic junction, other or additional functional implications should be considered as well.

Segev and Rall ('88) showed in a computational study based upon the Hodgkin and Huxley equations of excitable membranes ('52) that the effect of synaptic inhibition can be enhanced in dendritic spines that are contacted by both excitatory and inhibitory synapses, and that this enhanced inhibitory effect can be extremely sensitive to the timing between both types of inputs, with a temporal resolution well below 100 us (see also Diamond et al.,'70; Jack et al.,'75; Koch and Poggio,'83; Segev and Parnas,'83). These properties hold true especially for spines of which the spine heads contain a significant number of voltage-dependent channels. At present, it is not known whether the olivary dendritic spines have such excitable channels. However, since it has been shown that inferior olivary neurons possess a variety of complex and interacting conductances (Llinás and Yarom,'81a, '81b and '86; Yarom and Llinás,'87), some of which may occur solely within the dendrites (high threshold non-inactivating $Ca(2+)$ -channels), it seems an attractive and likely working hypothesis that the spines of olivary dendrites indeed carry excitable channels. Moreover, several morphological features of the olivary neurons support the assumption of excitable channels within their spines: 1) Olivary spines are complex with extremely long and thin spine stalks. These are thought to be favourable assets for excitable spines (high input resistance combined with sufficiently available synaptic current; Segev and Rall,'88). 2) Most olivary spines are located at secondary or tertiary dendrites (part a, Chapter IV). These are the most likely candidates for carrying excitable spines which may function as current boosters to compensate for the attenuation of the potential from distal dendritic regions

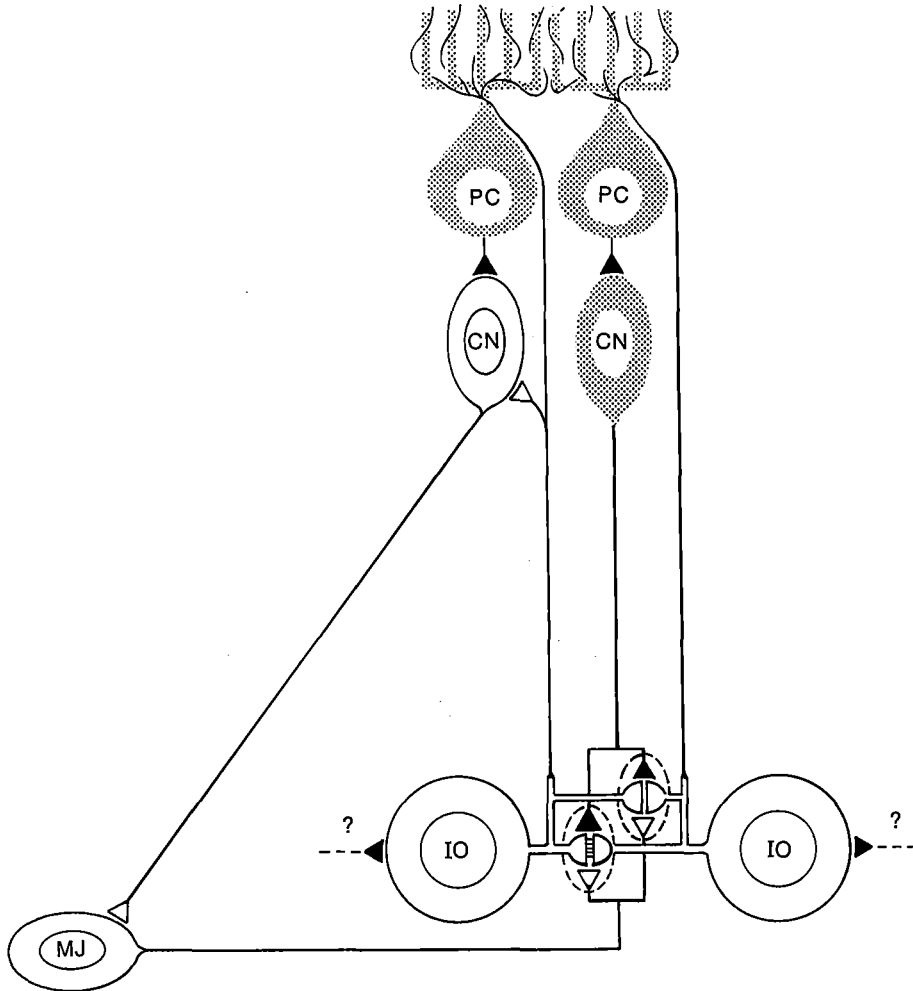


Fig.1. Diagram (see also cover of this thesis) of the neuropil in the medial accessory and principal olive (bottom), and its relation with the cerebellum (top) and the mesodiencephalic junction (left side). The cerebellar cortex contains large Purkinje cells (GABAergic) and central nuclear cells which are innervated by the climbing fibers and the collaterals of the olivo-cerebellar fibers, respectively. The excitatory central nuclear neurons of the cerebellum innervate neurons in the mesodiencephalon, while the excitatory mesodiencephalic cells and the GABAergic central nuclear cells innervate the spines (half circles) of the olivary neurons. Most, if not, all spines, i.e. both the dendritic and axonal spines, and both the spines which are linked by gap junctions (small lines between spines) and those which are not electrotonically coupled, are located within glomeruli (dotted circles) and are innervated by both mesodiencephalic and cerebellar terminals (white and black triangles). The olivary somata receive a GABAergic input from an unknown source (question mark).

(Shepherd et al., '85; Segev and Rall, '88). 3) Olivary spines are coupled by gap junctions within glomeruli. This is in line with the idea that olivary spines contain excitable channels because the properties of excitable spines will be enhanced when they are located in clusters receiving a synchronous synaptic input (Segev and Rall, '86 and '88). Therefore, it is attractive to apply the model of Segev and Rall to the olivary spines. If we do so, this may have two implications. Firstly, it would mean that the inhibitory cerebellar terminals, which contact the same spines as the excitatory mesodiencephalic terminals, are extremely well positioned to block the olivary firing induced by the mesodiencephalic input. Thus, the cerebellar GABAergic input to the olive is not only strategically located with respect to the dendritic spines linked by gap junctions but also with respect to the excitatory (see part a, Chapter IV) mesodiencephalic terminals terminating on the same spine. This implies that the same afferent system is able to uncouple the olivary cells and to reduce their firing frequency, simultaneously. This is in accordance with a recent study by Yarom and Adan ('88) which showed, by connecting an analog simulator with an olivary neuron, that once induced but intrinsically maintained oscillations of electrotonically coupled olivary neurons can be stopped more readily when they are disconnected from each other. A second implication of the model by Segev and Rall is that the excitation of olivary cells can only be stopped when the inhibitory cerebellar terminals are firing within a specific period of time related to the activity of the excitatory mesodiencephalic terminals.

The functional significance of the importance of timing between the cerebellar and mesodiencephalic input might be related to the proposal by Llinás that the IO functions as a "clock" (see part e2, Chapter I). It was postulated by

Llinás ('87 and '89) that olivary cells are involved in the onset of movements, most probably modulating the synchronicity of motoneuronal firing through the effect of their climbing fibers on cerebellar output. When movements need to be performed in a strict time constraint, such as a reaction movement after an unexpected event (Gibson and Gellman, '87) or a response to a visual stimulus (Mano et al., '86 and '89), specific sets of olivary cells are synchronously activated at the onset of the movement (Mano et al. ('89). The activation of the climbing fibers subsequently exert a direct effect on a specific set of Purkinje cells (Llinás, '85; see also part e4, Chapter I) and/or a short lasting enhancement of the simple spike activity in these cells (Bloedel and Zuo, '89), which would indirectly modulate motoractivity through the cerebellar nuclei.

The significance of the proposed timing sensitivity of the olivary spines could be that an external signal reaching the olive through an excitatory system could only be transmitted to the cerebellum, and thus lead to the triggering of a motor response, when it is activated within a specific time interval related to the activity in the GABAergic nucleo-olivary pathway. The timing of events in this pathway may be one of the essential tasks of the cerebellar cortex.

In the case of the rostral MAO and PO (innervating the intermediate and lateral cerebellum) both the GABAergic nucleo-olivary and the excitatory mesodiencephalic input are under control of the cerebellar cortex (see part b, Chapter I). Given the correct timing, this system might be able to react to an external stimulus with a longlasting reverberating activity. Proper timing of the activities in this system would result in well timed movements. This is supported by the observation that patients with lesions of the cerebellum, especially of the lateral part, do not have an accurate timing of motoractivity (Ivry et al., '88).

The timing hypothesis presented above is mainly based on the morphology and innervation of the olivary spines. Since about half of the terminal boutons in the IO are apposed to the dendritic shafts and not to the spines within the glomeruli, it must be explained why it is legitimate to characterize the olivary function by the outstanding properties of the spines. How do the terminals contacting the spines interact with the dendritic terminals? According to the theoretical model presented by Segev and Rall ('88) the threshold conditions for an action potential at the spine head membrane are sensitive to the conductance loading and the distribution of membrane potential along the dendritic tree (a preexisting dendritic depolarization reduces the spine stem current, and lowers the spike threshold voltage in this way), while the dendritic and also the somatic depolarizations themselves can be amplified several times by the synaptic input of the spines. Therefore, it seems clear that the synaptic input to the dendritic tree of the olivary neurons probably does not overrule the input of the spines but rather that the dendritic input, to be effective, largely depends on the activity of the synaptic inputs on the spiny appendages.

Another possibility, which is not mutually exclusive with the one presented above, is that the spines, especially when they are excitable (Segev and Rall, '88), could be instrumental for learning processes within the IO itself. Differences in spine stem resistance (Rall, '74; Rinzel, '82) and/or spine geometry (Purpura, '74; Fifkova and van Harreveld, '77; Desmond and Levy, '81; Crick, '82; Coss and Perkel, '85) seem to be relevant variables for controlling the effectiveness of synaptic inputs. However, many studies of the olivo-cerebellar system indicated that long term changes occur at the Purkinje cell spines (see Chapter I) but evidence for plastic changes associated with learning processes within

the IO are not available at present. Moreover, the presence of a combined excitatory and inhibitory input to the olivary spines is a requirement for a timing sensitive system but may not be essential for a learning device (Segev and Rall, '88).

The GABAergic input to the olivary somata derives its special significance from its origin from a non-cerebellar source and from the apposition of its terminals to the soma without the intermediate somatic spines.

The property of olivary neurons to fire rhythmically is due to specific conductances which are distributed differentially over the cell membrane of the soma and the dendrites (Llinás and Yarom, '81ab). The somatic calcium spike is the main factor responsible for generating sustained membrane oscillations, which form the basis for rhythmic firing in the IO (Llinás and Yarom, '86; Benardo and Foster, '86; Yarom and Adan, '87). The neuronal firing frequency of hyperpolarized cells will be dominated by a de-inactivation of the somatic Calcium conductance and this frequency may be dependent on the level of hyperpolarization. Therefore, the main function of the prominent GABAergic input to the olivary somata, may be to regulate the somatic hyperpolarization level, and in this way, the excitability and the oscillatory firing rate. This would be in line with the findings by Andersson et al. ('89) who showed, as mentioned above, that stimulation in an area just rostral to the IO (the presumed source of the GABAergic terminals apposed to the somata) exerts a more direct inhibitory control of the excitability of the olivary neurons than the cerebellar GABAergic input. The precise source and the function of these presumed non-cerebellar GABAergic fibers still has to be established.

Taken together, the combined cerebellar and mesodiencephalic input to the olivary spines of neurons in the rostral

MAO and PO may regulate the electrotonic coupling between olivary cells and simultaneously their firing frequency, in a timing sensitive manner, and provide, in this way, an instrument for the timing of the onset of motoneuronal firing. The GABAergic input to the olivary somata may have an additional impact upon the excitability of the olivary cells.

e. General conclusions

1) The combination techniques, WGA-HRP anterograde tracing with postembedding GABA-immunocytochemistry, WGA-HRP anterograde tracing with (3H)leucine anterograde tracing, and intracellular labeling of HRP with postembedding GABA-immunocytochemistry can provide new data on the ultrastructure of the CNS.

2) The dendrites and spines of an olivary cell in the MAO are apposed to neuronal elements of other olivary neurons but not to other parts of its own cellmembrane. The olivary spines are mainly derived from dendrites, sometimes from axons, but rarely from somata. Their shape is complex, they are composed of long stalks carrying several spine heads. They are located within glomeruli, and frequently electrotonically coupled to other spines by gap junctions.

3) The MAO and PO are mainly innervated by excitatory afferents from the mesodiencephalic junction and by GABAergic afferents from the cerebellum. About half of the terminals end upon glomerular spines. The other half mostly terminates on the shafts of distal dendrites. All the dendritic and most of the axonal spines and shafts are innervated by both afferent systems.

4) In addition, one can distinguish a non-cerebellar GABAergic input which is directed mainly to the somata of the olivary neurons, and a possible serotonergic input which is primarily located within the extraglomerular neuropil. Both these projections constitute only a fraction of the population of olivary boutons, and both may be derived from areas located nearby the IO.

5) The combined GABAergic cerebellar and excitatory mesodiencephalic input innervating the dendritic and probably also the axonal spines in the MAO and PO may regulate the electrotonic coupling between olivary cells and simultaneously their firing frequency, in a timing sensitive manner, and provide, in this way, an instrument for the timing of a motor response. The GABAergic input to the olivary somata may have an additional impact upon the excitability of the olivary cells.

REFERENCES

- Aas, J.-E., and P. Brodal (1989) Putative inhibitory transmitters in subcortical pathways to the pontine nuclei: GABA and Glycine. *Europ. J. Neurosci. (Suppl.)*2:39-11.
- Airaksinen, M.S., and P. Panula (1988) The histaminergic system in the guinea pig central nervous system: an immunocytochemical mapping study using an antiserum against histamine. *J. Comp. Neurol.* 273:163-186.
- Ajika, K., and T. Hökfelt (1973) Ultrastructural identification of catecholamine neurones in the hypothalamic periventricular-arcuate nucleus median eminence complex with special reference to quantitative aspects. *Brain Res.* 57:97-117.
- Akert, K., K. Pfenninger, and C. Sandri (1967) Crest synapses with subjunctional bodies in the subfornical organ. *Brain Res.* 5:118-121.
- Albert, P., M.D. Munoz, A. Alonso, and F.J. Rubia (1986) Vagal afferents to the inferior olive. *Neurosci. Lett. Suppl.* 26:S261.
- Albus, J.S. (1971) A theory of cerebellar function. *Math. Biosci.* 10:25-61.
- Allen, G.I., N.H. Sabah, and K. Toyama (1972a) Synaptic actions of peripheral nerve impulses upon Deiters' neurones via the climbing fibre afferents. *J. Physiol. London* 226:311-334.
- Allen, G.I., N.H. Sabah, and K. Toyama (1972b) Synaptic actions of peripheral nerve impulses upon Deiters' neurones via the mossy fibre afferents. *J. Physiol. London* 226:335-352.
- Allen, G.I., and N. Tsukahara (1974) Cerebrocerebellar communication system. *Physiol. Rev.* 54:957
- Alley, K., R. Baker, and J.I. Simpson (1975) Afferents to the vestibulo-cerebellum and the origin of the visual climbing fibers in the rabbit. *Brain Res.* 98:582-589.
- Alonso, A., M.J. Blanco, C.L. Paino, and F.J. Rubia (1986) Distribution of neurons in the main cuneate nucleus projecting to the inferior olive in the cat. Evidence that they differ from those directly projecting to the cerebellum. *Neuroscience* 18:671-683.
- Andersson, G. (1984) Mutual inhibition between olivary cell groups projecting to different cerebellar microzones in the cat. *Exp. Brain Res.* 54:293-303.
- Andersson, G., and D.M. Armstrong (1986) Complex spike activity in Purkinje cells in the lateral vermis (b zone) of the cat cerebellum during locomotion. *J. Physiol. (Lond.)* 385:107-134.
- Andersson, G., and D.M. Armstrong (1987) Complex spikes in Purkinje cells in the lateral vermis (b zones) of the cat cerebellum during locomotion. *J. Physiol.* 385:107-134.
- Andersson, G., C.F. Ekerot, O. Oscarsson, and J. Schouenborg (1987b) Convergence of afferent paths to olivo-cerebellar complex. In M. Glickstein, Chr. Yeo, and J. Stein (eds), *Cerebellum and Neuronal Plasticity, Series A: Life Sciences*, vol. 148, p.165-175.
- Andersson, G., and L. Eriksson (1981) Spinal, trigeminal and cortical climbing fibre paths to the lateral vermis of the cerebellar anterior lobe in the cat. *Exp. Brain Res.* 44:71-81.
- Anderson, W.A., and B.A. Flumerfelt (1984) Sensitivity of rat inferior olivary neurons to 3-acetylpyridine. *Brain Res.* 314:285-291.
- Andersson, G., M. Garwicz, and G. Hesslow (1987a) Effect of bicuculline on cerebellar inhibition of the inferior olive. *Neurosci. Suppl.* 22:S631.
- Andersson, G., M. Garwicz, and G. Hesslow (1988) Evidence for a GABA-mediated cerebellar inhibition of the inferior olive in the cat. *Exp. Brain Res.* 72:450-456.
- Andersson, G., M. Garwicz, and G. Hesslow (1989) Cerebello-olivary inhibition mediated by an indirect pathway. *Europ. J. Neurosci. (Suppl.)*2:39.17 pp.133.
- Andersson, G., and G. Hesslow (1986) Evidence for an inhibitory action by cerebellar nuclear cells on the inferior olive. *Neurosci. Lett. Suppl.* 26:S231.
- Andersson, G., and G. Hesslow (1987a) Inferior olive excitability after high frequency climbing fibre activation in the cat. *Exp. Brain Res.* 67:523-532.
- Andersson, G., and G. Hesslow (1987b) Activity of Purkinje cells and interpositus neurones during and after high frequency climbing fibre activation in the cat. *Exp. Brain Res.* 67:533-542.
- Andersson, G., and G. Hesslow (1987c) Cerebellar inhibition of the inferior olive. In M. Glickstein, Chr. Yeo, and J. Stein (eds), *Cerebellum and Neuronal Plasticity, Series A: Life Sciences*, Vol. 148, p. 141-155.
- Andersson, G., and J. Nyquist (1983) Origin and sagittal termination areas of cerebro-cerebellar climbing fibre paths in the cat. *J. Physiol.* 337:257-285.
- Andersson, G., and O. Oscarsson (1978a) Projections to lateral vestibular nucleus from cerebellar climbing fibre zones. *Exp. Brain Res.* 32:549-564.
- Andersson, G., and O. Oscarsson (1978b) Climbing fiber microzones in cerebellar vermis and their projection to different groups of cells in the lateral vestibular nucleus. *Exp. Brain Res.*32:565-579.
- Angaut, P., and C. Sotelo (1987) The dentato-olivary projection in the rat as a presumptive GABAergic link in the olivo-cerebello-olivary loop. An ultrastructural study. *Neurosci. Lett.* 83:227-231.

- Angaut, P., and C. Sotelo (1989) Synaptology of the cerebello-olivary pathway. Double labelling with anterograde axonal tracing and GABA immunocytochemistry in the rat. *Brain Res.* 479:361-365.
- Appelberg, B. (1967) A rubro-olivary pathway. II. Simultaneous action on dynamic fusimotor neurones and the activity of the posterior lobe of the cerebellum. *Exp. Brain Res.* 3:382-390.
- Appelberg, B., and T. Jeneskog (1973) Parallel activation from the cat brain stem of hind limb dynamic fusimotor neurones and climbing fibres to the cerebellar paramedian lobule. *Brain Res.* 58:229-233.
- Appelberg, B., and C. Molander (1967) A rubroolivary pathway. I. Identification of a descending system for control of the dynamic sensitivity of muscle spindles. *Exp. Brain Res.* 3:372-381.
- Araneda, S., R. Magoul, and A. Calas (1986) Transmitter-specific hodology, anatomical use of retrograde flow linked to (3H)-serotonin combined with immunocytochemistry of other mediators. In Satellite Symposium Technical Workshop 10th Annual Meeting of the Europ. Neurosci. Assoc. (Marseille)
- Armstrong, D.M. (1966) Responses in the inferior olive to stimulation of the cerebellar and cerebral cortices in the cat. *J. Physiol. Lond.* 187:553-574.
- Armstrong, D.M. (1967) Cerebro-olivo-cerebellar pathways in the cat (PhD thesis). Australian National Univ.
- Armstrong, D.M. (1974) Functional significance of connections of the inferior olive. *Physiol. Rev.* 54:358-417.
- Armstrong, D.M., and G. Andersson (1987) Climbing fibre activity associated with unperturbed and perturbed step cycles during skilled locomotion in the cat. In M. Glickstein, Chr. Yeo, and J. Stein (eds), *Cerebellum and Neuronal Plasticity, Series A: Life Sciences*, vol. 148, p. 225-249.
- Armstrong, D.M., N.C. Campbell, S.A. Edgley, R.F. Schild, and J.R. Trott (1982) Investigations of the olivocerebellar and spino-olivary pathways. *Exp. Brain Res.* 6:195-232.
- Armstrong, D.M., B. Cogdell, and R.J. Harvey (1973e) Responses of interpositus neurones to nerve stimulation in chloralose anaesthetised cats. *Brain Res.* 55:461-466.
- Armstrong, D.M., J.C. Eccles, R.J. Harvey, and P.B.C. Matthews (1968) Responses in the dorsal accessory olive of the cat to stimulation of hind-limb afferents. *J. Physiol. (Lond.)* 194:125-145.
- Armstrong, D.M., and R.J. Harvey (1968) Cerebellar responses to cerebral cortical stimulation. *J. Physiol. (Lond.)* 196:81-82P.
- Armstrong, D.M., R.J. Harvey, and R.F. Schild (1971a) Climbing fibre pathways from the forelimb to the paramedian lobule of the cerebellum. *Brain Res.* 25:199-202.
- Armstrong, D.M., R.J. Harvey, and R.F. Schild (1971b) Distribution in the anterior lobe of the cerebellum of branches from climbing fibres to the paramedian lobule. *Brain Res.* 25:203-206.
- Armstrong, D.M., R.J. Harvey, and R.F. Schild (1973a) Branching of inferior olivary axons to terminate in different folia lobules or lobes of the cerebellum. *Brain Res.* 54:365-371.
- Armstrong, D.M., R.J. Harvey, and R.F. Schild (1973b) Spino-olivo-cerebellar pathways to the posterior lobe of the cat cerebellum. *Exp. Brain Res.* 18:1-18.
- Armstrong, D.M., R.J. Harvey, and R.F. Schild (1973c) Cerebello-cerebellar responses mediated via climbing fibres. *Exp. Brain Res.* 18:19-39.
- Armstrong, D.M., R.J. Harvey, and R.F. Schild (1973d) The spatial organization of climbing fibre branching in the cat cerebellum. *Exp. Brain Res.* 18:40-58.
- Armstrong, D.M., and J.A. Rawson (1979) Activity pattern of cerebellar cortical neurons and climbing fibre afferents in the awake cat. *J. Physiol. (Lond.)* 289:425-448.
- Armstrong, D.M., and R.F. Schild (1970) A quantitative study of the Purkinje cells in the cerebellum of the albino rat. *J. Comp. Neurol.* 139:449-456.
- Azizi, S.A., G.A. Mihailoff, G.A. Burne, and D.J. Woodward (1981) The pontocerebellar system in the rat: An HRP study. I. Posterior vermis. *J. Comp. Neurol.* 197:543-558.
- Baimbridge, K.G., and J.J. Miller (1982) Immunohistochemical localization of calcium-binding protein in the cerebellum, hippocampal formation and olfactory bulb of the rat. *Brain Res.* 245:223-229.
- Baker, R., W. Precht, and R. Llinás (1972) Mossy and climbing fibre projections of extraocular muscle afferents to the cerebellum. *Brain Res.* 38: 440-445.
- Bardin, J.M., C. Batini, J.M. Billard, C. Buisseret-Delmas, M. Conrath-Verrier, and N. Corvaja (1983) Cerebellar output regulation by the climbing and mossy fibers with and without the inferior olive. *J. Comp. Neurol.* 213:464-477.
- Barmack, N.H. (1979) Immediate and sustained influence of visual olivocerebellar activity on eye movement. In R.E. Talbot, D.R. Humphrey (eds) *Posture and movement: perspective for integrating sensory and motor research on the mammalian nervous system*. Raven Press, New York, pp.123-168.
- Barmack, N.H., and D.T. Hess (1980) Eye movements evoked by microstimulation of dorsal cap of inferior olive in the rabbit. *J. Neurophysiol.* 43:165-181.
- Barmack, N.H., E. Mugnaini, and B.J. Nelson (1989) Vestibularly-evoked activity of single neurons in the beta nucleus of the inferior olive. In: *The Olivocerebellar System in Motor Control*. P. Strata (Ed.). *Exp. Brain Res. Series* 17:313-323.
- Barmack, N.H., and J.I. Simpson (1980) Effects of microlesions of dorsal cap of inferior olive of rabbits on optokinetic and vestibuloocular reflexes. *J. Neurophysiol.* 43:182-206.

- Barmack, N.H., and W.S. Young III (1988) Optokinetic stimulation increases corticotropin releasing factor mRNA in inferior olivary neurons of rabbits. Soc. for Neurosci. Abstr. Annual Meeting Toronto 14:758.
- Barragan, L.A., N. Delhaye-Bouchaud, and P. Laget (1985) Drug-induced activation of the inferior olivary nucleus in young rabbits. Differential effects of harmaline and quipazine. *Neuropharmacology* 24:645-654.
- Batini, C., J.F. Bernard, P.G. Montarolo, and P. Strata (1983) The olivocerebellar pathway exerts a tonic control on the postural activity. *Neurosci. Lett. Suppl.* 14:S20.
- Batini, C., and J.M. Billard (1985) Release of cerebellar inhibition by climbing fiber deafferentation. *Exp. Brain Res.* 57:370-380.
- Beal, M.F., S.M. Gabriel, K.J. Swartz, and U.M. MacGarvey (1988) Distribution of galanin-like immunoreactivity in baboon brain. *Peptides* 9:847-851.
- Beauvillain, J.C., G. Tramu, and J.C. Garaud (1984) Coexistence of substances related to enkephalin and somatostatin in granules of the guinea pig median eminence: demonstration by use of colloidal gold immunocytochemical methods. *Brain Res.* 301:389-393.
- Belin, M.F., D. Nanopoulos, M. Didier, M. Aguera, H. Steinbusch, A. Verhofstad, M. Maitre, and J.F. Pujol (1983) Immunohistochemical evidence for the presence of gamma-aminobutyric acid and serotonin in one nerve cell. A study on the raphe nuclei of the rat using antibodies to glutamate decarboxylase and serotonin. *Brain Res.* 275:329-339.
- Bell, C.C., and R.J. Grimm (1969) Discharge properties of Purkinje cells recorded on single and double microelectrodes. *J. Neurophysiol.* 32:1044-1055.
- Bell, C.C., and T. Kawasaki (1972) Relations among climbing fibre responses of nearby Purkinje cells. *J. Neurophysiol.* 35:155-169.
- Benardo, L.S., and R.E. Foster (1986) Oscillatory behaviour in inferior olive neurons: mechanism, modulation, cell aggregates. *Brain Res. Bull.* 17:773-784.
- Bendayan, M. (1982) Double immunocytochemical labelling applying the protein A-gold technique. *J. Histochem. Cytochem.* 30:81-85.
- Benedetti, F., P.G. Montarolo, P. Strata, and F. Tempia (1983) Inferior olive inactivation decreases the excitability of the intracerebellar and lateral vestibular nuclei in the rat. *J. Physiol.* 340:195-208.
- Bennett, M.V.L. (1972) A comparison of electrically and chemically mediated transmission. In G.D. Pappas and D.P. Purpura (eds), *Structure and Function of Synapses*, New York, Raven, pp.221-256.
- Berkley, K.J., and P.J. Hand (1978) Projections to the inferior olive of the cat. II. Comparisons of input from the gracile, cuneate and the spinal trigeminal nuclei. *J. Comp. Neurol.* 180:253-264.
- Berman, A.L. (1968) *The brainstem of the cat*. Madison, Milwaukee and London: The University of Wisconsin Press.
- Bernard, J.F., C. Buisseret-Delmas, and S. Laplante (1984) Inferior olivary neurons: 3-acetylpyridine effects on glucose consumption, axonal transport, electrical activity and harmaline-induced tremor. *Brain Res.* 322:382-387.
- Bharos, T.B., H.G.J.M. Kuypers, R.N. Lemon, and R.B. Muir (1981) Divergent collaterals from deep cerebellar neurons to thalamus and tectum, and to medulla oblongata and spinal cord: Retrograde fluorescent and electrophysiological studies. *Exp. Brain Res.* 42:399-410.
- Biscoe, T.J., A.W. Duggan, P.M. Headley, and D. Lodge (1973) Rhythmical field potentials induced in the inferior olive complex by iontophoretically applied harmaline and other unrelated alkaloids. *Brit. J. Pharmacol.* 49:174P-175P.
- Bishop, G.A. (1989) Corticotropin releasing factor (CRF) potentiates the actions of aspartate and glutamate in the cat's cerebellum. *Soc. Neurosci. (Abstr.)* 15:164.10.
- Bishop, G.A., and R.H. Ho (1984) Substance P and serotonin immunoreactivity in the rat inferior olive. *Brain Res. Bull.* 12:105-113.
- Bishop, G.A., and R.H. Ho (1986) Cell bodies of origin of serotonin-immunoreactive afferents to the inferior olivary complex of the rat. *Brain Res.* 399:369-373
- Bishop, G.A., and J.S. King (1982) Intracellular horseradish peroxidase injections for tracing neural connections. In M.-M. Mesulam (ed) *Tracing neural connections with horseradish peroxidase*. Chichester: John Wiley and Sons, pp 185-247.
- Bishop, G.A., and J.S. King (1986) Reticulo-olivary circuits: an intracellular HRP study in the rat. *Brain Res.* 371:133-145.
- Bishop, G.A., R.A. McCrea, and S.T. Kitai (1976) A horseradish peroxidase study of the cortico-olivary projection in the cat. *Brain Res.* 116:306-311.
- Björkeland, M., and J. Boivie (1984a) An anatomical study of the projections from the dorsal column nuclei to the midbrain in cat. *Anat. Embryol.* 170:29-43.
- Björkeland, M., and J. Boivie (1984b) The termination of spinomesencephalic fibers in cat. An experimental anatomical study. *Anat. Embryol.* 170:265-277.
- Blanks, R.H., and W. Precht (1983) Responses of units in the rat cerebellar flocculus during optokinetic and vestibular stimulation. *Exp. Brain Res.* 53:1-15.

- Bloedel, J.R., and J. Courville (1981) A review of cerebellar afferent systems. In V.B. Brooks (ed) Handbook of physiology, vol. II. Motor Control. Williams & Wilkins, Baltimore, pp.735-830.
- Bloedel J.R., and T.J. Ebner (1985) Regulation of Purkinje cell responsiveness. In J.R. Bloedel, J. Dichgans, and W. Precht (eds) Cerebellar Functions, Springer-Verlag, Berlin, Heidelberg, New York, Tokyo pp.247-260.
- Bloedel, J.R., and J.S. Lou (1987) The relation between Purkinje cell simple spike responses and the action of the climbing fiber system in unconditioned and conditioned of the forelimb to perturbed locomotion. In: M. Glickstein, C. Yeo, and J. Stein (Eds.), Cerebellum and Plasticity, Nato ASI Series A: Life Sciences, vol. 148:261-276.
- Bloedel, J.R., and W.J. Roberts (1971) Action of climbing fibers in cerebellar cortex of the cat. *J. Neurophysiol.* 34:17-31.
- Bloedel, J.R., and C.C. Zuo (1989) The heterosynaptic action of climbing fibers in the cerebellar cortex. In P. Strata (ed): The Olivocerebellar System in Motor Control. Suppl. Exp. Brain Res. 17:246-264.
- Boesten, A.J.P., and J. Voogd (1975) Projections of the dorsal column nuclei and the spinal cord on the inferior olive in the cat. *J. Comp. Neurol.* 161:215-238.
- Boesten, A.J.P., and J. Voogd (1985) Hypertrophy of neurons in the inferior olive after cerebellar ablations in the cat. *Neurosci. Lett.* 61:49-54.
- Bosler, O., A. Beaudet, and V.M. Pickel (1986) Characterization of chemically defined neurons and their cellular relationships by combined immunocytochemistry and radioautographic localization of transmitter uptake sites. *J. Electron Microsc. Techn.* 4:21-39.
- Bower, J., and R. Llinás (1983) Simultaneous sampling of the responses of multiple, closely adjacent, Purkinje cells responding to climbing fibre activation. *Soc. Neurosci. Abstr.*, 9:607
- Bower, J.M., and Woolston, D.C. (1983) Congruence of spatial organization of tactile projections to granule cell and Purkinje cell layers of cerebellar hemispheres of the albino rat: vertical organization of cerebellar cortex. *J. Neurophysiol.* 49:745-766.
- Bowman, J.P., and C.M. Combs (1969) Cerebellar responsiveness to stimulation of the lingual spindle different fibers in the hypoglossal nerve of the Rhesus monkey. *Exp. Neurol.* 23:537-548.
- Bowman, M.H., and J.S. King (1973) The conformation, cytology and synaptology of the opossum inferior olivary nucleus. *J. Comp. Neurol.* 148:491-524.
- Boylls, C.C. (1978) Prolonged alterations of muscle activity induced in locomoting preamillary cats by microstimulation of the inferior olive. *Brain Res.* 159:445-450.
- Boylls, C.C. (1980) Contributions to locomotor coordinations of an olivo-cerebellar projections to the vermis in the cat: experimental results and theoretical proposals. In J. Courville, C. de Montigny, Y. Lamarre (eds) The inferior olivary nucleus: anatomy and physiology. Raven Press, New York, pp.321-348.
- Bozhilova, A. and W. Ovtsharoff (1979) Synaptic organization of the medial accessory olivary nucleus of the cat. *J. Hirnforsch.* 20:19-28.
- Bragina, T.A. (1983) Ultrastructure of the synapses of the initial axonal segment of the pyramidal neuron. *Arkh. Anat. Gistol. Embriol.* 85:17-24.
- Braitenberg, V., and R.P. Atwood (1958) Morphological observations on the cerebellar cortex. *J. Comp. Neurol.* 109:1-33.
- Brand, S., A.-L. Dahl, and E. Mugnaini (1976) The length of parallel fibers in the cat cerebellar cortex. An experimental light and electron microscopic study. *Exp. Brain Res.* 26:39-58.
- Brodal, A. (1940) Experimentelle Untersuchungen über die olivocerebellare Lokalisation. *Z. ges. Neurol. Psychiat.*, 169:1-153.
- Brodal, P., and A. Brodal (1981) The olivocerebellar projection in the monkey. Experimental studies with the method of retrograde tracing of horseradish peroxidase. *J. Comp. Neurol.* 201:375-393.
- Brodal, P., and A. Brodal (1982) Further observations on the olivocerebellar projection in the monkey. *Exp. Brain Res.* 45:71-83.
- Brodal, A., and K. Kawamura (1980) Olivocerebellar projection: A review. In A. Brodal, W. Hild, J. van Limborgh, R. Ortmann, T.H. Schiebler, G. Töndury and E. Wolff (eds): Advances in Anatomy, Embryology and Cell Biology, Vol. 64. Berlin, Heidelberg, New York: Springer-Verlag, pp.1-140.
- Brodal, A., F. Walberg, and T.H. Blackstad (1950) Termination of spinal afferents to inferior olive in cats. *J. Neurophysiol.* 13:431-454.
- Brooks, V.B., and W.T. Thach (1981) Cerebellar control of posture and movement. In J.M. Brookhart, V.B. Mountcastle (eds) Handbook of physiology, section I: The Nervous System, vol. II: Motor Control. Am. Physiol. Soc. (Bethesda), pp.877-946.
- Brown, A.G. (1981) Organization in the spinal cord: the anatomy and physiology of identified neurones. Berlin, Heidelberg, New York: Springer-Verlag.
- Brown, J.T., V. Chan-Palay and S.L. Palay (1977) A study of afferent input to the inferior olivary complex in the rat by retrograde axonal transport of horseradish peroxidase. *J. Comp. Neurol.* 176:1-22.
- Buchtel, H.A., G. Iosie, G.F. Marchesi, L. Provini, and P. Strata (1972) Analysis of the activity evoked in the cerebellar cortex by stimulation of the visual pathways. *Exp. Brain Res.* 15: 278-288.

- Buck, S.H., C.J. Helke, E. Burcher, C.W. Shults, and T.L. O'Donohue (1986) Pharmacologic characterization and autoradiographic distribution of binding sites for iodinated tachykinins in the rat central nervous system. *Peptides* 7:1109-1120.
- Buisseret-Delmas, C. (1980) An HRP study of the afferents to the inferior olive in cat. *Arch. Ital. Biol.* 118:270-286.
- Buisseret-Delmas, C., C. Batini, C. Compoin, H. Daniel, and D. Menetrey (1987) The GABAergic neurons of the cerebellar nuclei: A comparison of the cerebellar cortex and the bulbar reticular formation. In *The Olivocerebellar System in Motor Control*, Satellite Symposium of the 2nd IBRO World Congress of Neuroscience, Turin, 9-12 August, 1987, pp.42.
- Buisseret-Delmas, C., C. Batini, C. Compoin, H. Daniel, and D. Menetrey (1989) The GABAergic Neurons of the Cerebellar Nuclei: Projection to the Caudal Inferior Olive and to the Bulbar Reticular Formation. In: *The Olivocerebellar System in Motor Control*. P. Strata (Ed.), *Exp. Brain Res. Series* 17:108-111. Springer-Verlag.
- Buijs, R.M., E.H.S. van Vulpen, and M. Geffard (1987) Ultrastructural localization of GABA in the supraoptic nucleus and the neural lobe. *Neuroscience* 20:347-355.
- Busch, H.F.M. (1961) An anatomical analysis of the white matter in the brain stem of the cat. *Van Gorcum and Comp. N.V., Assen.*
- Caceres, A., M.R. Payne, L.I. Binder, and O. Steward (1983) Immunocytochemical localization of actin and microtubule-associated protein MAP2 in dendritic spine. *Proc. natl. Acad. Sci. USA* 80:1738-1740.
- Campbell, N.C., C.-F. Ekerot, and G. Hesslow (1983a) Interaction between responses in Purkinje cell evoked by climbing fibre impulses and parallel fibre volleys in the cat. *J. Physiol. (Lond)* 340:225-238.
- Campbell, N.C., C.-F. Ekerot, G. Hesslow, and O. Oscarsson (1983b) Dendritic plateau potentials evoked in Purkinje cells by parallel fibre volleys in the cat. *J. Physiol. (Lond)* 340:209-223.
- Campbell, N.C., and G. Hesslow (1986) The secondary spikes of climbing fibre responses recorded from Purkinje cell somata in cat cerebellum. *J. Physiol.* 377:207-224.
- Campistron, G., R.M. Buijs, and M. Geffard (1986) Specific antibodies against aspartate and their immunocytochemical application in the rat. *Brain Res.* 365:179-184.
- Carrea, R.M.E., M. Reissig, and F.A. Mettler (1947) The climbing fibres of the simian and feline cerebellum. Experimental inquiry into their origin by lesions of the inferior olive and deep cerebellar nuclei. *J. Comp. Neurol.* 87:321-365.
- Chai, S.Y., M.J. McKinley, and F.A. Mendelsohn (1987) Distribution of angiotensin converting enzyme in sheep hypothalamus and medulla oblongata visualized by in vitro autoradiography. *Clin. Exp. Hypertens.* 9:449-460.
- Christensen, B.N. (1973) Procion brown: An intracellular dye for light and electron microscopy. *Science* 182:1255-1256.
- Cintas, H.M., J.G. Rutherford, and D.G. Gwyn (1980) Some midbrain and mesodiencephalic projections to the inferior olive in the rat. In: *J. Courville, C. de Montigny and Y. Lamarre (Eds.), The Inferior Olivary Nucleus*. Raven Press, New York. 73-96.
- Cipolloni, P.B., and A. Keller (1989) Thalamocortical synapses with identified neurons in monkey primary auditory cortex: a combined Golgi/EM and GABA/peptide immunocytochemistry study. *Brain Res.* 492:347-355.
- Colin, F., J. Manil, and J.C. Desclin (1980) The olivocerebellar system. I. Delayed and slow inhibitory effects: An overlooked salient feature of cerebellar climbing fibers. *Brain Res.* 187:3-27.
- Colonnier, M. (1964) Experimental degeneration in the cerebral cortex. *J. Anat. Lond.* 98:47-53.
- Compoin, C., and C. Buisseret-Delmas (1988) Origin, distribution and organization of the serotonergic innervation in the inferior olivary complex of the rat. *Arch. Ital. Biol.* 126:99-110.
- Conradi, S. (1969) Observations on the ultrastructure of the axon hillock and initial axon segment of lumbosacral motoneurons in the cat. *Acta Physiol. Scand. Suppl.* 332:65-84.
- Conrath-Verrier, M., M. Dietl, M. Arluison, F. Cesselin, S. Bourgoin, and M. Hamon (1983) Localization of Met-enkephalin-like immunoreactivity within pain-related nuclei of cervical spinal cord, brainstem and midbrain in the cat. *Brain Res. Bull.* 11:587-604.
- Coombs, J.S., D.R. Curtis, and J.C. Eccles (1957) The generation of impulses in motoneurons. *J. Physiol.* 139:232-249.
- Coons, A.H. (1958) Fluorescent antibody methods. In *General Cytochemical Methods* (ed. J.F. Danielli) pp. 399-422. Academic Press, New York.
- Coss, R.G., and D.H. Perkel (1985) The function of dendritic spines: a review of theoretical issues. *Behav. Neural Biol.* 44:151-185.
- Cotter, J.R., and L.K. Laemle (1987) Distribution of somatostatin-like immunoreactivity in the brain of the little brown bat (*Myotis lucifugus*). *Am. J. Anat.* 180:289-294.
- Courville, J. (1966) Rubrobulbar fibres to the facial nucleus and the lateral reticular nucleus (nucleus of the lateral funiculus). An experimental study in the cat with silver methods. *Brain Res.* 1:317-337.
- Courville, J., C. DeMontigny, and Y. Lamarre (eds.) (1980) *The inferior olivary nucleus*. Raven Press, New York.
- Crepel, F., J. Dupont, and R. Gardette (1983) Voltage clamp analysis of the effect of excitatory amino acids and derivatives on Purkinje cell dendrites in rat cerebellar slices maintained in vitro. *Brain Res.* 279:311-315.
- Crick, F. (1982) Do dendritic spines twitch? *Trends Neurosci.* 5:44-46.

- Crill, W.E. (1970) Unitary multiple-spiked responses in cat inferior olive nucleus. *J. Neurophysiol.* 33:199-209.
- Cuello, A., J.V. Priestley, and C. Milstein (1982) Immunocyto-chemistry with internally labeled monoclonal antibodies. *Proc. Natl. Acad. Sci. USA* 79:665-669.
- Cuello, A.C., C. Milstein, and G. Galfré (1983) Immunocytochemistry with monoclonal antibodies. In A.C. Cuello (ed) *Immunohistochemistry*, Chichester, John Wiley & Sons. 215-255.
- Cuenod, M., and P. Streit (1983) Neuronal tracing using retrograde migration of labeled transmitter-related compounds. In: A. Björklund, and T. Hökfelt (Eds.), *Handbook of Chemical Neuroanatomy. Methods in Chemical Neuroanatomy.* Elsevier Science Publishers BV, Vol. 1.
- Cuenod, M., K.Q. Do, F. Vollenweider, and P. Streit (1988) cerebellar climbing fibers: Excitatory amino acid and adenosine release. In *Neurobiology of the cerebellar systems: A centenary of Ramon y Cajal's description of the cerebellar circuits.* Barcelona, 19-22 october, pp. 26
- Cuenod, M., E. Audinat, K.Q. Do, P. Grandes, T. Knöpfel, P. Streit, F. Vollenweider, and B.H. Gähwiler (1989) Homocysteic acid as transmitter candidate in rat cerebellar climbing fibers: release, localization and postsynaptic effects. *Europ. J. Neurosci (Suppl)*2:59.1.
- Cullheim, S., and J.O. Kellerth (1978) A morphological study of the axons and recurrent axon collaterals of cat sciatic alpha-motoneurons after intracellular staining with horseradish peroxidase. *J. Comp. Neurol.* 178:537-558.
- Cummings, S., and J.S. King (1988) Coexistence of corticotropin releasing factor and enkephalin in cerebellar afferent systems. *Soc. Neurosci. Abst.* 202.11
- Cummings, S., B. Sharp, and R. Elde (1988) Corticotropin-releasing factor in cerebellar afferent systems: A combined immunohisto- chemistry and retrograde transport study. *J. Neurosci.* 8:543-554.
- DeFelipe, J., S.H.C. Hendry, E.G. Jones, and D. Schmechel (1985) Variability in the terminations of GABAergic Chandelier Cell axons on initial segments of pyramidal cell axons in the monkey sensory-motor cortex. *J. Comp. Neurol.* 231:364-384.
- Dekker, J.J. (1977) Identification of axon terminals and synapses of different fiber systems in the brain. EM autoradiography and EM degeneration techniques compared. Thesis. Bronder-Offset B.V. Rotterdam.
- Dekker, J.J. (1981) Anatomical evidence for direct projections from the cerebellar nucleus interpositus to rubrospinal neurons. A quantitative EM study in the rat combining anterograde and retrograde intra-axonal tracing methods. *Brain Res.* 205:229-244.
- Demer, J.L., and D.A. Robinson (1982) Effects of reversible lesions and stimulation of olivocerebellar system on vestibulo-ocular reflex plasticity. *J. Neurophysiol.* 47:1084-1107.
- De Montigny, C., and Y. Lamarre (1973) Rhythmic activity induced by harmaline in the olivocerebello-bulbar system of the cat. *Brain Res.* 53:81-95.
- De Montis, G., K. Beaumont, F. Javoy-Agid, J. Constandinidis, A. Lowenthal, and K.G. Lloyd (1982) Glycine receptors in the human substantia nigra as defined by [3H]strychnine binding. *J. Neurochem.* 38:718-724.
- Descarries, L., and A. Beaudet (1983) The use of autoradiography for investigating transmitter-specific neurons. In A. Björklund and T. Hökfelt (eds) *Handbook of Chemical Neuroanatomy, Vol.1. Methods in Chemical Neuroanatomy.* Amsterdam, Elsevier, pp.286.
- Desclin, J.C. (1974) Histological evidence supporting the inferior olive as the major source of cerebellar climbing fibers in the rat. *Brain Res.* 77:365-384.
- Desmond, N.L., and W.B. Levy (1981) Ultrastructure and numerical changes in dendritic spines as a consequence of long-term potentiation. *Anat. Rec.* 119:68A-69A.
- de Zeeuw, C.I., J.C. Holstege, F. Calkoen, T.J.H. Ruijgrok, and J. Voogd (1988a) A new combination of WGA-HRP anterograde tracing and GABA-immunocytochemistry applied to afferents of the cat inferior olive at the ultrastructural level. *Brain Res.* 447:369-375.
- de Zeeuw, C.I., J.C. Holstege, T.J.H. Ruijgrok, and J. Voogd (1988b) The GABAergic, the cerebellar and the mesodiencephalic innervation of the rostral medial accessory olive of the cat. A quantitative comparison at the ultrastructural level. *Suppl. Europ. J. Neurosci.* 10.9, pp.25.
- de Zeeuw, C.I., J.C. Holstege, T.J.H. Ruijgrok, and J. Voogd (1989a) An ultrastructural study of the GABAergic, the cerebellar and the mesodiencephalic innervation of the cat medial accessory olive: Anterograde tracing combined with immunocytochemistry. *J. Comp. Neurol.* 284 (1): 12-35.
- de Zeeuw, C.I., J.C. Holstege, T.J.H. Ruijgrok, and J. Voogd (1989b) The GABAergic, cerebellar and mesodiencephalic innervation of the glomeruli in the cat inferior olive. A comparison at the ultrastructural level. In: *The Olivocerebellar System in Motor Control.* Ed. P. Strata. *Suppl. Exp. Brain Res.* 17: 111-117.
- de Zeeuw, C.I., T.J.H. Ruijgrok, J.C. Holstege, M.P.A. Schalekamp, and J. Voogd (1989c) Ultrastructural study of the normal and hypertrophic cat inferior olive. *Soc. Neurosci. (Phoenix)* 15:164.8, pp.405.
- de Zeeuw, C.I., J.C. Holstege, T.J.H. Ruijgrok, and J. Voogd. (1990) Mesodiencephalic and cerebellar terminals end upon the same dendritic spines within the glomeruli of the cat and rat inferior olive: An ultrastructural study using a combination of (3H)leucine and WGA-HRP anterograde tracing. *Neuroscience.* In Press.
- de Zeeuw, C.I., T.J.H. Ruijgrok, J.C. Holstege, H.G. Jansen, and J. Voogd (a). Intracellular labeling of neurons in the medial accessory olive of the cat. II. Ultrastructure of dendritic spines and their GABAergic innervation. Submitted.

- de Zeeuw, C.I., T.J.H. Ruigrok, J.C. Holstege, M.P.A. Schalekamp, and J. Voogd (b). Intracellular labeling of neurons in the medial accessory olive of the cat. III. Ultrastructure of the axon hillock and initial segment and their GABAergic innervation. *J. Comp. Neurol.* Submitted.
- Diamond, J., E.G. Gray, and E.N. Yasargil (1970) The function of dendritic spines: an hypothesis. In P. Anderson and J.K.S. Jansen (eds), *Excitatory Synaptic Mechanisms*. Universitets-forlaget, Oslo, p.213-222.
- Dietl, M.M., A. Probst, and J.M. Palacios (1987) On the distribution of cholecystokinin receptor binding sites in the human brain: an autoradiographic study. *Synapse* 1:169-183.
- Dietrichs, E., and F. Walberg (1985) The cerebellar nucleo-olivary and olivo-cerebellar nuclear projections in cat as studied with anterograde and retrograde transport in the same animal after implantations of crystalline WGA-HRP. II. The fastigial nucleus. *Anat. Embryol.* 173:253-261.
- Dietrichs, E., F. Walberg, and T. Nordby (1985) The cerebellar nucleo-olivary and olivo-cerebellar nuclear projections in the cat as studied with anterograde and retrograde transport in the same animal after implantation of crystalline WGA-HRP. I The dentate nucleus. *Neurosci. Res.* 3:52-70.
- Dietrichs, E., and F. Walberg (1986) The cerebellar nucleo-olivary and olivo-cerebellar nuclear projections in the cat as studied with anterograde and retrograde transport in the same animal after implantation of crystalline WGA-HRP. III The interposed nuclei. *Brain Res.* 373:373-383.
- Doerr-Schott, J., and C.M. Lichte (1984) A double immunostaining procedure using colloidal gold, ferritin, and peroxidase as markers for simultaneous detection of two hypophysial hormones with the electron microscope. *J. Histochem. Cytochem.* 32:1159-1166.
- Donegan, N.H., R.W. Lowery, and R.F. Thompson (1983) Effects of lesioning cerebellar nuclei on conditioned leg-flexion responses. Society for Neuroscience (Boston) Abstract No.100.7.
- Dow, R.S., and G. Moruzzi (1958) *The physiology and pathology of the cerebellum*. Minneapolis, Minn. University of Minnesota Press.
- Duggan, A.W., D. Lodge, P.M. Headley and T.J. Biscoe (1973) Effects of excitants on neurones and cerebellar evoked field potentials in the inferior olivary complex of the rat. *Brain Res.* 64: 397-401.
- Ebbeson, S.O.E.A. (1968) A connection between the dorsal column nuclei and the dorsal accessory olive. *Brain Res.* 8:393-397.
- Ebner, T.J., and J.R. Bloedel (1981a) Role of climbing fiber afferent input in determining responsiveness of Purkinje cells to mossy fiber inputs. *J. Neurophysiol.* 45:962-971.
- Ebner, T.J., and J.R. Bloedel (1981b) Temporal patterning in simple spike discharge of Purkinje cells and its relationship to climbing fiber activity. *J. Neurophysiol.* 45:933-947.
- Ebner, T.J., and J.R. Bloedel (1984) Climbing fiber action on the responsiveness of Purkinje cells to parallel fiber inputs. *Brain Res.* 309:182-186.
- Ebner, T.J., Q.X. Yu, and J.R. Bloedel (1983) Increase in Purkinje cell gain associated with naturally activated climbing fiber input. *J. Neurophysiol.* 50:205-219.
- Eccles, J.C. (1966) The excitatory synaptic action of climbing fibers on the Purkinje cells of the cerebellum. *J. Physiol. (London)* 182:268-296.
- Eccles, J.C., M. Ito, and J. Szentagothai (1967) *The cerebellum as a neuronal machine*. New York: Springer.
- Eccles, J.C., R. Llinás, and K. Sasaki (1966) The excitatory synaptic action of climbing fibers on the Purkinje cells of the cerebellum. *J. Physiol. (Lond.)* 182:268-296.
- Eccles, J.C., L. Provini, P. Strata, and H. Táboriková (1968a) Analysis of electrical potentials evoked in the cerebellar anterior lobe by stimulation of hindlimb and forelimb nerves. *Exp. Brain Res.* 6:171-194.
- Eccles, J.C., L. Provini, P. Strata, and H. Táboriková (1968b) Topographical investigations on the climbing fiber inputs from forelimb and hindlimb afferents to the cerebellar anterior lobe. *Exp. Brain Res.* 6:195-215.
- Eccles, J.C., N.H. Sabah, and H. Táboriková (1971) Responses evoked in neurones of the fastigial nucleus by cutaneous mechano-receptors. *Brain Res.* 35:523-527.
- Eccles, J.C., N.H. Sabah, R.F. Schmidt, and H. Táboriková (1972a) Cutaneous mechano-receptors influencing impulse discharges in cerebellar cortex. III. In Purkinje cells by climbing fiber input. *Exp. Brain Res.* 15:484-497.
- Eccles, J.C., N.H. Sabah, R.F. Schmidt, and H. Táboriková (1972b) Integration by Purkinje cells of mossy and climbing fiber inputs from cutaneous mechanoreceptors. *Exp. Brain Res.* 15:498-520.
- Eccles, J.C., N.H. Sabah, and H. Táboriková (1974a) Excitatory inhibitory responses of neurones of the cerebellar fastigial nucleus. *Exp. Brain Res.* 19:61-77.
- Eccles, J.C., N.H. Sabah, and H. Táboriková (1974b) The pathways responsible for excitation and inhibition of fastigial neurones. *Exp. Brain Res.* 19:78-99.
- Einstein, G. (1988) Intracellular injection of lucifer yellow into cortical neurons in lightly fixed sections and its application to human autopsy material. *J. Neurosci. Methods* 26:95-103.
- Eisenman, L.M., D.D. Sieger, and G.J. Blatt (1983) The olivocerebellar projection to the uvula in the mouse. *J. Comp. Neurol.* 221:53-59.

- Ekerot, C.-F. (1985) Climbing fibre actions of Purkinje cells-Plateau potentials and long-lasting depression of parallel fibre responses. In J.R. Bloedel, J. Dichgans, and W. Precht (eds) *Cerebellar Functions*, Springer-Verlag, Berlin, Heidelberg, New York, Tokyo pp.268-275.
- Ekerot, C.-F., P. Gustafsson, O. Oscarsson, and J. Schouenborg (1985a) Climbing fibres projecting to cerebellar anterior lobe activated by nociceptive C-fibres. *Neurosci. Lett. Suppl.* 22:S28.
- Ekerot, C.-F., P. Gustafsson, O. Oscarsson, and J. Schouenborg (1985b) Noxious stimulation causing tonic and synchronous activity in climbing fibres. *Neurosci. Lett. Suppl.* 22:29.
- Ekerot, C.-F., and M. Kano (1983) Climbing fibre induced depression of Purkinje cell responses to parallel fibre stimulation. *Proc. Int. Union Physiol. Sci. Vol. XV. Sydney*, p. 393.
- Ekerot, C.-F., and M. Kano (1985) Long-term depression of parallel fibre synapses following stimulation of climbing fibres. *Brain Res.* 342:357-360.
- Ekerot, C.-F., and B. Larson (1973) Correlation between sagittal projection zones of climbing and mossy fibre paths in cat cerebellar anterior lobe. *Brain Res.* 64:446-450.
- Ekerot, C.-F., and B. Larson (1980) Termination in overlapping sagittal zones in cerebellar anterior lobe of mossy and climbing fiber paths activated from dorsal funiculus. *Exp. Brain Res.* 38:163-172.
- Ekerot, C.-F., and B. Larson (1982) Branching of olivary axons to innervate pairs of sagittal zones in the cerebellar anterior lobe of the cat. *Exp. Brain Res.* 48:185-198.
- Ekerot, C.-F., B. Larson, and O. Oscarsson (1979) Information carried by the spinocerebellar paths. In: *Reflex Control of Posture and Movement. Progress in Brain Research. Vol. 50.*
- Ekerot, C.-F., and O. Oscarsson (1980) Prolonged dendritic depolarizations evoked in Purkinje cells by climbing fibre impulses. *Brain Res.* 192:272-275.
- Ekerot, C.-F., and O. Oscarsson (1981) Prolonged dendritic depolarizations elicited in Purkinje cell dendrites by climbing fibre impulses in the cat. *J. Physiol. (Lond)* 318:207-221.
- Estable, C. (1923) Notes sur la structure comparative de l'écorce cérébelleuse et dérivés physiologiques possibles. *Trav. Lab. Biol. Univ. Madrid* 21:169-256.
- Faber, D.S., K. Ishikawa, and M.J. Rowe (1971) The responses of cerebellar Purkinje cells to muscle vibration. *Brain Res.* 26:184-187.
- Faber, D.S., and J.T. Murphy (1969) Axonal branching in the climbing fibre pathway in the cerebellum. *Brain Res.* 15:262-267.
- Falck, B., N.A. Hillarp, G. Thieme, and A. Torp (1962) Fluorescence of catecholamines and related compounds condensed with formaldehyde. *J. Histochem. Cytochem.* 10:348-354.
- Famiglietti, E.V., and A. Peters (1972) The synaptic glomerulus and the intrinsic neuron in the dorsal lateral geniculate nucleus of the cat. *J. Comp. Neurol.* 144:285-334.
- Ferin, M., R.A. Grigorian, and P. Strata (1970) Purkinje cell activation by stimulation of the labyrinth. *Pflüger's Arch.* 321:253-258.
- Ferin, M., R.A. Grigorian, and P. Strata (1971) Mossy fibre and climbing fibre activation in the cat cerebellum by stimulation of the labyrinth. *Exp. Brain Res.* 12:1-17.
- Fifkova, E., and A. van Harrevelde (1977) Long-lasting morphological changes in dendritic spines of dentate granular cells following stimulation of the entorhinal area. *J. Neurocytol.* 6:211-230.
- Fink, R.P., and L. Heimer (1967) Two methods for selective silver impregnation of degenerating axons and their synaptic endings in the central nervous system. *Brain Res.* 4, 369-374.
- Flumerfelt, B.A., and A.W. Hryciyshyn (1985) Precerebellar nuclei and red nucleus. In G. Paxinos (Ed.) *The Rat Nervous System*, volume 2, Hindbrain and spinal cord. Academic Press Sydney. Chapter 10:221-250.
- Foix, C., J.A. Chavany, and P. Hillemand (1926) Le syndrome myoclonique de la calotte: étude anatomo-clinique du nystagmus du voile et des myoclonies rythmiques associées, oculaires, faciales, etc. *Dev. Neurol (Paris)* 45:942-956.
- Foote, S.L., and I.C. Choong (1988) Distribution of corticotropin-releasing-factorlike immunoreactivity in brainstem of two monkey species (*Saimiri sciureus* and *Macaca fascicularis*): An immunohistochemical study. *J. Comp. Neurol.* 276:239-264.
- Foster, R.E., and B.E. Peterson (1986) The inferior olivary complex of guinea pig: cytoarchitecture and cellular morphology. *Brain Res. Bull.* 17:785-800.
- Fournet, N., L.M. Garcia-Segura, A.W. Norman, and L. Orci (1986) Selective localization of calcium-binding protein in human brainstem, cerebellum and spinal cord. *Brain Res.* 399:310-316.
- Fox, C.A., A. Andrade, and R.C. Schwyn (1969) Climbing fiber branching in the granular layer. In *Neurobiology of Cerebellar Evolution and Development*, edited by R. Llinás. Am. Med. Assoc. p.603-611.
- Freund, T.F., and M. Antal (1988) GABA-containing neurons in the septum control inhibitory interneurons in the hippocampus. *Nature* 336: 170-173.
- Freund, T.F., K.A.C. Martin, A.D. Smith, and P. Somogyi (1983) Glutamate decarboxylase-immunoreactive terminals of Golgi-impregnated axo-axonal cells and of presumed basket cells in synaptic contact with pyramidal cells of the cat's visual cortex. *J. Comp. Neurol.* 221:263-278.

- Freund, T.F., K.A.C. Martin, P. Somogyi, and D. Whitteridge (1985) Innervation of cat visual areas 17 and 18 by physiologically identified x- and y- type thalamic afferents. II. Identification of postsynaptic targets by GABA immunocytochemistry and Golgi impregnation. *J. Comp. Neurol.* 242:275-291.
- Fujita, Y. (1968) Activity of dendrites of single Purkinje cells and its relationship to so-called inactivation response in rabbit cerebellum. *J. Neurophysiol.* 31:131-141.
- Fukuda, M., T. Yamamoto, and R. Llinás (1987) Simultaneous recordings from Purkinje cells of different folia in the rat cerebellum and their relation to movement. *Soc. Neurosci. Abstr.* 13:603.
- Fuortes, M.G.F., K. Frank, and M.C. Becker (1957) Steps in the production of motoneuron spikes. *J. gen. Physiol.* 40:735-752.
- Fuxe, K. (1965) Evidence for the existence of monoamine neurons in the central nervous system. IV. Distribution of monoamine nerve terminals in the central nervous system. *Acta Physiol Scand* 64: Suppl 247:39-85.
- Geffen, L.B., D.G. Livett, and R.A. Rush (1969) Immunohisto- chemical localization of protein components of catecholamine storage vesicles. *J. Physiol.* 204:593-605.
- Gehlert, D.R., R.C. Speth, D.P. Healy, and J.K. Wamsley (1984) Autoradiographic localization of angiotensin II receptors in the rat brainstem. *Life Sci.* 34:1565-1571.
- Gellman, R., A.R. Gibson, and J.C. Houk (1985) Inferior olivary neurons in the awake cat: detection of contact and passive body displacement. *J. Neurophysiol.* 54:40-60.
- Gellman, R.S., J.C. Houk, and A.R. Gibson (1983) Somatosensory properties of the inferior olive in the cat. *J. Comp. Neurol.* 215:228-243.
- Gerfen, C.R., and P.E. Sawchenko (1984) An anterograde neuroanatomical tracing method that shows the detailed morphology of neurons their axons and terminals: immunohistochemical localization of an axonally transported plant lectin, Phaseolus vulgaris leucoagglutinin (PHA-L). *Brain Res.* 290:219-238.
- Gerrits, N.M. (1988) Afferent control of the cerebellum. An hypothesis to explain the differences in the mediolateral distribution of mossy fibre terminals in the cerebellar cortex. In: *Cerebellum and Neuronal Plasticity*. M. Glickstein, C. Yeo, and J. Stein (Eds.). pp. 83-101. New York and London, Plenum Press.
- Gerrits, N.M. and J. Voogd (1982) The climbing fiber projection to the flocculus and adjacent paraflocculus in the cat. *Neurosci.* 7:2971-2991.
- Gerrits, N.M., and J. Voogd (1987) The projection of the nucleus reticularis tegmenti pontis and adjacent regions of the pontine nuclei to the central cerebellar nuclei in the cat. *J. Comp. Neurol.* 258:52-69.
- Gerrits, N.M., J. Voogd, and I.N. Magras (1985a) Vestibular afferents of the inferior olive and the vestibulo-olivocerebellar climbing fiber pathway to the flocculus in the cat. *Brain Res.* 332:325-336.
- Gerrits, N.M., J. Voogd, and W.S.C. Nas (1985b) Cerebellar and olivary projections of the external and rostral internal cuneate nuclei in the cat. *Exp. Brain Res.* 57:239-255.
- Ghelarducci, B., M. Ito, and N. Yagi (1975) Impulse discharges from the flocculus Purkinje cells of alert rabbits during visual stimulation combined with horizontal head rotation. *Brain Res.* 87:66-72.
- Gibson, G.E. and Blass, J.P. (1985) Oxidative metabolism and acetylcholine synthesis during acetylpyridine treatment. *Neurochem. Res.* 10:453-467.
- Gibson, A.R., and R. Chen (1988) Does stimulation of the inferior olive produce movement? Society for Neuroscience Abstracts. Toronto no.305.2.
- Gibson A.R., and R.S. Gellman (1987) Functional implications of inferior olivary response. In M. Glickstein, Chr. Yeo and J. Stein (eds), *Cerebellum and Neuronal Plasticity*, Series A: Life Sciences, vol. 148:119-141.
- Gilbert, C.D., and T.N. Wiesel (1978) Intracellular staining of physiologically identified cells and afferents in cat visual cortex. *Soc. for Neurosci. Abstracts* 4:1235,
- Gilbert, P.F.C., and W.T. Thach (1977) Purkinje cell activity during motor learning. *Brain Res.* 128:309-328.
- Gillette, R. and B. Pomeranz (1973) Neuron geometry and circuitry via the electron microscope: intracellular staining with osmiophilic polymer. *Science* 182:1256-1258.
- Glantz, S.A. (1981) Primer of biostatistics. R.S. Laufer and T.K. Geno (Eds.). McGraw-Hill Book Company.
- Gobel, S., and R. Dubner (1969) Fine structural studies of the main sensory trigeminal nucleus in the cat and rat. *J. Comp. Neurol.* 137:459-494.
- Goodman, D., and J.A. Kelso (1983) Exploring the functional significance of physiological tremor: a biospectroscopic approach. *Exp. Brain Res.* 49:419-431.
- Gotow, T., and C. Sotelo (1987) Postnatal development of the inferior olivary complex in the rat: IV. Synaptogenesis of GABAergic afferents, analyzed by glutamic acid decarboxylase immunocytochemistry. *J. Comp. Neurol.* 263: 526-552.
- Graf, W., J.I. Simpson, and C.S. Leonard (1988) Spatial organization of visual messages of the rabbit's cerebellar flocculus. II. Complex and simple spike responses of Purkinje cells. *J. Neurophysiol.* 60:2091-121.
- Graham, R.C., and M.J. Karnowsky (1966) The early stages of absorption of injected horse radish peroxidase in the proximal tubules of the mouse kidney. Ultrastructural cytochemistry by a new technique. *J. Histochem. Cytochem.* 14:291-302.
- Granit, R., and C.G. Phillips (1956) Excitatory and inhibitory processes acting upon individual Purkinje cells of the cerebellum in cats. *J. Physiol. (Lond.)* 133:520-547.

- Gray, E.G. (1959) Axo-somatic and axo-dendritic synapses of the cerebral cortex: An electron microscope study. *J. Anat. (London)* 93:420-433.
- Gray, E.G. (1961) Ultra-Structure of synapses of the cerebral cortex and of certain specialisations of neuroglial membranes. In: *Electron Microscopy in Anatomy*. J.D. Boyd, F.R. Johnson, and J.D. Lever (Eds.). London, Arnold, pp.54-73.
- Gray, E.G., and R.W. Guillery (1966) Synaptic morphology in the normal and degenerating nervous system. In *International review of cytology*. Ed. by G.H. Bourne and J.F. Danielli. 19:111-181.
- Gray, E.G., and L. Hamlyn (1962) Electron microscopy of experimental degeneration in the avian optic tectum. *J. Anat. Lond.* 96:309-316.
- Groenewegen, H.J., and J. Voogd (1977) The parasagittal zonation within the olivocerebellar projection. 1. Climbing fiber distribution in the vermis of cat cerebellum. *J. Comp. Neurol.* 174:417-488.
- Groenewegen, H.J., J. Voogd, and S.L. Freedman (1979) The parasagittal zonation within the olivo-cerebellar projection. II. Climbing fiber distribution in the intermediate and hemispheric parts of cat cerebellum. *J. Comp. Neurol.* 183:551-602.
- Guillain, G., and P. Mollaret (1931) Deux cas de myoclonies synchrones et rythmées vélo-pharyngo-oculo-diaphragmatiques. Le problème anatomique et physio-pathologique de ce syndrome. *Rev. Neurol. (Paris)* 2:545-566.
- Gutkind, J.S., M. Kurihara, E. Castren, and J.M. Saavedra (1988) Increased concentration of angiotensin. II. Binding sites in selected brain areas of spontaneously hypertensive rats. *J. Hypertens.* 6:79-84.
- Gwyn, D.G., G.P. Nicholson, and B.A. Flumerfelt (1977) The inferior olivary nucleus of the rat: A light and electron microscopic study. *J. Comp. Neurol.* 174:489-520.
- Gwyn, D.G., J.G. Rutherford, and G.P. Nicholson (1983) An electron microscopic study of the direct spino-olivary projection to the inferior olivary nucleus in the rat. *Neurosci. Lett.* 42: 243-248.
- Hanamori, T., M. Nakashima, and N. Ishiko (1987) Origin of the climbing fibers activated by glossopharyngeal nerve stimulation in the frog. *Neurosci. Lett.* 75:11-16.
- Hanker, J.S., C. Deb, H.L. Wasserkrug, and A.M. Seligman (1966) Staining tissue for light and electron microscopy by bridging metals with multidentate ligands. *Science* 152:1631-1634.
- Hanker, J.S., P.E. Yates, C.B. Metz, and A. Rustioni (1977) A new specific, sensitive and non-carcinogenic reagent for the demonstration of horseradish peroxidase. *Histochem. J.* 9:789-792.
- Harandi, M., M. Aguera, H. Gamrani, M. Didier, M. Maitre, A. Calas, and M.F. Belin (1987) Gamma-aminobutyric acid and 5-hydroxytryptamine interrelationship in the rat nucleus raphe dorsales: Combination of radiographic and immunocytochemical techniques at light and electronmicroscopy levels. *Neuroscience.* 21:237-251.
- Harfstrand, A., K. Fuxe, L.F. Agnati, F. Benfenati, and M. Goldstein (1986) Receptor autoradiographical evidence for high densities of 125I-neuropeptide Y binding sites in the nucleus tractus solitarius of the normal male rat. *Acta Physiol. Scand.* 128:195-200.
- Harrison, P.J., H. Hultborn, E. Jankowska, R. Katz, B. Storai, and D. Zytnicki (1984) Labeling of interneurons by retrograde transsynaptic transport of horseradish peroxidase from motoneurons in rat and cat, *Neurosci. Lett.* 45:15-19.
- Hartmann Von Monakow, K., K. Akert, and H. Künzle (1979) Projections of precentral and premotor cortex to the red nucleus and other midbrain areas in *Macaca fascicularis*. *Exp. Brain Res.* 34:91-106.
- Held, H. (1897) Beiträge zur Structur der Nervenzellen und ihrer Fortsätze. Part II. *Archiv Anat. Physiol. Anat. Abt.* pp.204-293; and Part III. *Archiv Anat. Physiol., Anat. Abt. (Suppl. for 1897)*, pp.273-312.
- Helke, C.J., C.W. Shults, T.N. Chase, and T.L. Donohue (1984) Autoradiographic localization of substance P receptors in rat medulla: effect of vagotomy and nodose ganglionectomy. *Neuroscience* 12:215-223.
- Heritage, A.S., W.E. Stumpf, M. Sar, and L.D. Grant (1981) (3-H)-dihydrotestosterone in catecholamine neurons of rat brain stem: combined localization by autoradiography and formaldehyde-induced fluorescence. *J. Comp. Neurol.* 200:289-307.
- Hesslow, G. (1986) Inhibition of inferior olivary transmission by mesencephalic stimulation in the cat, *Neurosci. Lett.* 63:76-80.
- Hoddevik, G.H., A. Brodal, and F. Walberg (1976) The olivocerebellar projection in the cat studied with the method of retrograde axonal transport of horseradish peroxidase. III. The projection to the vermal visual area. *J. Comp. Neurol.* 169:155-170.
- Hodgkin, A.L., and A.F. Huxley (1952) A quantitative description of membrane current and its application to conduction and excitation in nerve. *J. Physiol. Lond.* 117:500-544.
- Holstege, G., and J. Tan (1988) Projections from the red nucleus and surrounding areas to the brainstem and spinal cord in the cat. An HRP and autoradiographical tracing study. *Beh. Brain Res.* 28:33-57.
- Holstege, J.C. (1987) Brainstem projections to lumbar motoneurons in rat-II An ultrastructural study by means of the anterograde transport of wheat-germ agglutinin coupled to horseradish peroxidase and using the tetramethyl benzidine reaction. *Neuroscience* 21:369-376.
- Holstege, J.C. (1989) Brainstem projections to motoneurons in the lumbar spinal cord. An ultrastructural study in rat. Erasmus University Press, Rotterdam. Thesis.

- Holstege, J.C., and J.J. Dekker (1979) Electron microscopic identification of mammillary body terminals in the rat's AV thalamic nucleus by means of anterograde transport of HRP. A quantitative comparison with the EM degeneration and EM autoradiographic techniques. *Neurosci. Lett.* 11:129-135.
- Holstege, J.C., and H.G.J.M. Kuypers (1987a) Brainstem projections to spinal motoneurons: an update. *Neurosci.* 23:809-821.
- Holstege, J.C., and H.G.J.M. Kuypers (1987b) Brainstem projections to lumbar motoneurons in rat. An ultrastructural study using autoradiography and the combination of autoradiography and horseradishperoxidase. *Neuroscience.* 21:345-367.
- Holstege, J.C., and G.F.J.M. Vrensen (1988) Anterograde tracing in the brain using autoradiography and HRP-histochemistry. A comparison at the ultrastructural level. *J. Microsc.* 150:233-243.
- Hökfelt, T., G. Fried, S. Hansen, V. Holets, J.M. Lundberg, and L. Skirboll (1986) In progress in brain research (eds. van Ree J.M., and Matthysse S.), Vol. 65, pp. 115-137. Elsevier, Amsterdam.
- Horn, A.K.E., and K.P. Hoffman (1987) Combined GABA immunocytochemistry and TMB/HRP histochemistry of pretectal nuclei projecting to the inferior olive in rats, cats, and monkeys. *Brain Res.* 409:135-138.
- Houk, J.C., A.R. Gibson, C.F. Harvey, P.R. Kennedy, and P.L. van Kan (1988) Activity of primate magnocellular red nucleus related to hand and finger movements. *Behav. Brain Res.* 28:201-206.
- Huerta, M.F., T. Hashikawa, M.J. Gayoso, and J.K. Harting (1985) The trigemino-olivary projection in the cat: Contributions of individual subnuclei. *J. Comp. Neurol.* 241:180-190.
- Hunt, S.P., J.S. Kelly, and P.C. Emson (1980) The electron microscopic localisation of methionine enkephalin within the superficial layers (I and II) of the spinal cord. *Neuroscience* 5:1871-1890.
- Hyde, T.M., M. Gibbs, and S.J. Peroutka (1988) Distribution of muscarinic cholinergic receptors in the dorsal vagal complex and other selected nuclei in the human medulla. *Brain Res.* 447:287-292.
- Ishikawa, K., J. Kawaguchi, and M.J. Rowe (1972a) Actions of afferent impulses from muscle receptors on cerebellar Purkinje cells. I. Responses to muscle vibrations. *Exp. Brain Res.* 15:177-193.
- Ishikawa, K., S. Kawaguchi, and M.J. Rowe (1972b) Actions of afferent impulses from muscle receptors on cerebellar Purkinje cells. II. Responses to muscle contraction. Effects mediated via the climbing fibre pathway. *Exp. Brain Res.* 16:104-114.
- Ito, M. (1972) Cerebellar control of the vestibular neurones: Physiology and pharmacology. In: *Progress in Brain Research*, Vol. 37: Basic Aspects of Central Vestibular Mechanisms, edited by A. Brodal and O. Pompeiano, pp.387-390. Elsevier, Amsterdam.
- Ito, M. (1974) Control mechanisms of cerebellar motor system. In: *The Neurosciences, Third Study Program*. Edited by F.O. Schmidt and F.G. Worden, pp.293-303. MIT Press, Massachusetts.
- Ito, M. (1982a) Cerebellar control of the vestibulo-ocular reflex - around the flocculus hypothesis. *Annu. Rev. Neurosci.* 5:275-296.
- Ito, M. (1982b) Experimental verification of Marr-Albus plasticity assumption for the cerebellum. *Acta Biol. Acad. Sci. Hung.* 33:189-199.
- Ito, M. (1984) *The cerebellum and neuronal control*. Raven Press, New York.
- Ito, M., and M. Kano (1982) Long-lasting depression of parallel fiber-Purkinje cell transmission induced by conjunctive stimulation of parallel fibers and climbing fibers in the cerebellar cortex. *Neurosci. Lett.* 33:253-258.
- Ito, M., K. Obata, and R. Ochi (1966) The origin of cerebellar induced inhibition of Deiters' neurones. *Exp. Brain Res.* 2:350-364.
- Ito, M., M. Sakurai, and P. Tongroach (1982) Climbing fibre induced depression of both mossy fibre responsiveness and glutamate sensitivity of cerebellar Purkinje cells. *J. Physiol. (Lond)* 324:113-134.
- Ito, M., and J.I. Simpson (1971) Discharges in Purkinje cell axons during climbing fibre activation. *Brain Res.* 31:215-219.
- Ito, M., and M. Yoshida (1966) The origin of cerebellar-induced inhibition of Deiters' neurones. I. Monosynaptic initiation of the inhibitory postsynaptic potential. *Exp. Brain Res.* 2:330-349.
- Ito, M., M. Yoshida, K. Obata, N. Kawal, and M. Udo (1970) Inhibitory control of intracerebellar nuclei by the Purkinje cell axons. *Exp. Brain Res.* 10:64-80.
- Itoh, K., M. Takada, Y. Yasui, M. Kudo, and N. Mizuno (1983) Direct projections from the anterior pretectal and retrograde wheat germ agglutinin-horseradish peroxidase study in the cat. *Neurosci. Lett. (Suppl.)* 13:S23.
- Ivry, R.B., S.W. Keele, and H.C. Diener (1988) Dissociation of the lateral and medial cerebellum in movement timing and movement execution. *Exp. Brain Res.* 73:167-180.
- Iwahori, N., and E. Kiyota (1987) A Golgi study on the inferior olivary nucleus in the red sting ray, *Dasyatis akajei*. *5(2):*113-125.
- Jack, J.J.B., D. Noble, and R.W. Tsien (1975) *Electric Current Flow in Excitable Cells*. Oxford, UK: Oxford Univ. Press.
- Jansen, J.K.S. (1957) Afferent impulses to the cerebellar hemispheres from the cerebral cortex and certain subcortical nuclei. *Acta Physiol. Scand.* 41, Suppl.143.
- Jansen, J.K.S., and C. Fangel (1961) Observations on cerebro-cerebellar evoked potentials in the cat. *Exp. Neurol.* 3:160-173.

- Jeneskog, T. (1974) A descending pathway to dynamic fusimotor neurones and its possible relation to a climbing fibre system. Umea University Medical Dissertations.
- Jeneskog, T. (1981a) On climbing fibre projections to cerebellar paramedian lobule activated from mesencephalon in the cat. *Brain Res.* 211:135-140.
- Jeneskog, T. (1981b) Identification of a tecto-olivocerebellar path to posterior vermis in the cat. *Brain Res.* 211:141-145.
- Jeneskog, T. (1983) Zonal termination of the tecto-olivocerebellar pathway in the cat. *Exp. Brain Res.* 49:353-362.
- Jeneskog, T. (1987) Termination in posterior and anterior cerebellum of a climbing fibre pathway activated from the nucleus of Darkschewitsch in the cat. *Brain Res.* 412:185-189.
- Johnson, J.L. (1978) The excitant amino acids glutamic and aspartic acid as transmitter candidates in the vertebrate central nervous system. *Progress in Neurobiology.* Vol. 10:155-202.
- Jones, L.S., L.L. Gauger, and J.N. Davis (1985) Anatomy of brain alpha 1-adrenergic receptors: in vitro autoradiography with [¹²⁵I]-heat. *J. Comp. Neurol.* 231:190-208.
- Jones, E.G., and T.P.S. Powell (1969) Connections of the somatic sensory cortex in the rhesus monkey. II. Contralateral cortical connections. *Brain* 92:717-730.
- Kamei, I., S. Shiosaka, E. Senba, H. Takagi, M. Sakanaka, S. Inagaki, K. Takatsuki, K. Nakai, H. Imai, T. Itakura, N. Komai, and M. Tohyama (1981) Comparative anatomy of the distribution of catecholamines within the inferior olivary complex from teleosts to primates. *J. Comp. Neurol.* 202:125-133.
- Kamin, L. (1967) Predictability, surprise, attention, and conditioning. In B.A. Campbell, R.M. Church (eds) Punishment and aversive behavior. Appleton-Century-Crofts, New York, pp.279-296.
- Kano, M., and M. Kato (1987) Quisqualate receptors are specifically involved in cerebellar synaptic plasticity. *Nature* 325:276-279.
- Kano, K., and M. Kato (1988) Mode of induction of long-term depression at parallel fibre-Purkinje cell synapses in rabbit cerebellar cortex. *Neurosci. Res.* 5:544-556.
- Kato, T., and A. Hirano (1985) A Golgi study of the proximal portion of the human Purkinje cell axon. *Acta Neuropathol. (Berl.)* 68:191-195.
- Kato, N., S. Kawaguchi, and H. Miyata (1988) Cerebro-cerebellar projections from the lateral suprasylvian visual area in the cat. *J. Physiol.* 395:473-485.
- Kawamura, S., S. Hattori, S. Higo, and T. Matsuyama (1982) The cerebellar projections to the superior colliculus and pretectum in the cat: An autoradiographic and horseradish peroxidase study. *Neuroscience* 7:1673-1689.
- Kawamura, K., and S. Onodera (1984) Olivary projections from the pretectal lesion in the cat studied with horseradish peroxidase or tritiated amino acid axonal transport. *Arch. Ital. Biol. (in press)*.
- Kemp, J.M., and T.P.S. Powell (1971) The termination of fibers from the cerebral cortex and the thalamus upon dendritic spines in the caudate nucleus: a study with a Golgi method. *Philos. Trans. R. Soc. Lond. B. Biol. Sci.* 262:429-439.
- Kennedy, P.R., H.G. Ross, and V.B. Brooks (1982) Participation of the principal olivary nucleus in neocerebellar motor control. *Exp. Brain Res.* 47:95-104.
- Kievit, J. (1979) Cerebello-thalamische projecties en de afferente verbindingen naar de frontaalschors in de rhesusaap. Thesis. Bronder-offset B.V. Rotterdam.
- Kim, J.H., J.-J. Wang, and T.J. Ebner (1987) Climbing fiber afferent modulation during treadmill locomotion in the cat. *J. Neurophysiol.* 57:787-202.
- Kimura, H., O. Kamoto, and Y. Sakai (1985) Pharmacological evidence for L-aspartate as the neurotransmitter of cerebellar climbing fibres in the guinea pig. *J. Physiol.* 365:103-119.
- King, J.S. (1976) The synaptic cluster (glomerulus) in the inferior olivary nucleus. *J. Comp. Neurol.*, 165:387-400.
- King, J.S. (1980) The synaptic organization of the inferior olivary nucleus. In J. Courville, C. de Montigny and Y. Lamarre (eds), *The Inferior Olivary Nucleus*. New York, Raven Press. pp.1-35.
- King, J.S., J.A. Andrezik, W.M. Falls, and G.F. Martin (1976) The synaptic organization of the cerebello-olivary circuit. *Exp. Brain Res.* 26:159-170.
- King, J.S., G.A. Bishop, S.L. Cummings, and R.H. Ho (1987b) Localization of neuropeptides within the inferior olivary complex of the opossum. In *The Olivocerebellar System in Motor Control, Satellite Symposium of the 2nd IBRO World Congress of Neuroscience, Turin, 9-12 August, 1987*, 13.
- King, J.S., S.L. Cummings, R.H. Ho, J.J. Walker, and G.A. Bishop (1988) Peptides in adult and developing climbing fibers: localization and co-localization. In *Neurobiology of the cerebellar systems: A centenary of Ramon y Cajal's description of the cerebellar circuits*. Barcelona, 19-22 October, 25, pp.62.
- King, J.S., J.E. Hamos, and B.E. Maley (1978) The synaptic terminations of certain midbrain-olivary fibers in the opossum. *J. Comp. Neurol.* 182:185-200.
- King, J.S., R.H. Ho, and G.A. Bishop (1986) Anatomical evidence for enkephaline immunoreactive climbing fibres in the cerebellar cortex of the opossum. *J. Neurocytol.* 15:545-559.
- King, J.S., R.H. Ho, and G.A. Bishop (1987a) The origin and distribution of enkephaline-like immunoreactivity in the opossum's cerebellum. In JS King (ed): *New Concepts in Cerebellar Neurobiology*. New York: Alan R. Liss, Inc, pp. 1-28.

- King, J.S., R.H. Ho, and R.W. Burry (1984) The distribution and synaptic organization of serotonergic elements in the inferior olivary complex of the opossum. *J. Comp. Neurol.* 227:357-368.
- King, J.S., G.F. Martin, and M.H. Bowman (1975) The direct spinal area of the inferior olivary nucleus: An electron microscopic study. *Brain Res.* 22:13-24.
- King, R.B. (1948) The effect of interolivary lesions on muscle tone in the trunk and limb girdles. *J. Comp. Neurol.* 89:207-223.
- Kirsche, W., H. David, E. Winkelman, and I. Marx (1965) Elektronenmikroskopische Untersuchungen an synaptischen Formationen im Cortex cerebelli von *Rattus rattus norvegicus*. *Berkenhoot, Z. Mikroskop. Anat. Forsch.* 72:49-80.
- Kisvárdy, Z.F., A. Cowey, A.D. Smith, A.J. Hodgson, and P. Somogyi (1984) Relationship between GABA immunoreactive neurons and neurons accumulating [3H]-GABA or [3H]d-aspartate in striate cortex of monkey, *Trab. Inst. Cajal Invest. Biol. LXVV:55*.
- Kitahama, K., P.H. Luppi, G. Tramu, J.P. Sastre, C. Buda, and M. Jouvet (1988) Localization of CRF-immunoreactive neurons in the cat medulla oblongata: their presence in the inferior olive. *Cell Tissue Res.* 251:137-143.
- Kitai, S.T., R.A. McCrea, R.J. Preston, and G.A. Bishop (1977) Electrophysiological and horseradish peroxidase studies of precerebellar afferents to the nucleus interpositus anterior. I. Climbing fiber system. *Brain Res.* 122:197-214.
- Koch, C., and T. Poggio (1983) A theoretical analysis of electrical properties of spines. *Proc. R. Soc. Lond. B. Biol. Sci.* 218:455-477.
- Kolb, F.P., and F.J. Rubia (1980) Information about peripheral events conveyed to the cerebellum via the climbing fiber system in the decerebrate cat. *Exp. Brain Res.* 38:363-373.
- Kooy, F.H. (1916) *The Inferior Olive in Vertebrates*. Thesis. Even Bohn, Haarlem.
- Kostopoulos G.K., J.J. Limacher, and J.W. Phillis (1975) Action of various adenine derivatives on cerebellar Purkinje cells. *Brain Res.* 88:162-165.
- Kreuzfuchs, S. (1902) Die Grösse der Oberfläche des Kleinhirns. *Arb. Neurol. Inst. Wiener Univ.* 9:274-278.
- Krnjevic, K., and S. Schwartz (1966) Is gamma-aminobutyric acid an inhibitory neurotransmitter? *Nature (London)*. 211:1372-1374.
- Kuypers, H.G.J.M., and D.G. Lawrence (1967) Cortical projection to the red nucleus and the brain stem in the rhesus monkey. *Brain Res.* 4:151-188.
- Lam, R.L., and J.H. Ogura (1952) An afferent representation of the larynx in the cerebellum. *Laryngoscope* 62:486-495.
- Lamarre Y., and C.E. Chapman (1986) Comparative timing of neuronal discharge in cortical and cerebellar structures during a simple arm movement in the monkey. *Suppl. Exp. Brain Res.* 15:14-27.
- Lang, E.J., M. Chou, I. Sugihara, and R. Llinás. (1989) Intraolivary injection of picrotoxin causes reorganization of complex spike activity. *Society for neuroscience abstracts, Phoenix:* 15:77.5, pp. 179.
- Larson, B., S. Miller, and O. Oscarsson (1969a) Termination and functional organisation of the dorsolateral spino-olivocerebellar path. *J. Physiol. (Lond.)* 203:611-640.
- Larson, B., S. Miller, and O. Oscarsson (1969b) A spinocerebellar climbing fibre path activated by the flexor reflex afferents from all four limbs. *J. Physiol. (Lond.)* 203:641-649.
- Larson, L.I., and T.W. Schwartz (1977) Radioimmunocytochemistry-a novel immunocytochemical principle. *J. Histochem. Cytochem.* 25:1140-1146.
- Latham, A., and D.H. Paul (1971) Spontaneous activity of Purkinje cells and responses to impulses in climbing fibres. *J. Physiol. (Lond.)* 213:135-15
- Latham, A., D.H. Paul, and A.J. Potts (1970) Responses of fastigial nucleus neurones to stimulation of a peripheral nerve. *J. Physiol. (Lond.)* 206:15-16P.
- Lavond, D.G., J.S. Lincoln, D.A. McCormick, R.F. Thompson (1984) Effect of bilateral lesions of the dentate and interpositus cerebellar nuclei on conditioning of heart-rate and nictitating membrane/eyelid responses in the rabbit. *Brain Res.* 305:323-330.
- Leaton, R.N., and Supple, W.F. Jr. (1986) Cerebellar vermis: essential for long-term habituation of the acoustic startle response. *Science* 232:513-515.
- Leight, R., M.J. Rowe, and R.F. Schmidt (1972) Cutaneous convergence on to the climbing fibre input to cerebellar Purkinje cells. *J. Physiol. (Lond.)* 228:601-618.
- Leight, R., M.J. Rowe, and R.F. Schmidt (1973) Cortical and peripheral modification of cerebellar climbing fibre activity arising from cutaneous mechanoreceptors. *J. Physiol. (Lond.)* 228:619-636.
- Lemann, W., C.B. Saper, D.B. Rye, and B.H. Wainer (1985) Stabilization of TMB reactionproduct for electronmicroscopic retrograde and anterograde fiber tracing. *Brain Res. Bull.* 14:277-281.
- Leonard, C.S., and J.I. Simpson (1982) Effects of suspending climbing fiber activity on the discharge patterns of floccular Purkinje cells. *Soc. Neurosci. Abstr.* 8:830.

- Leonard, C.S., J.I. Simpson, W. Graf, M. Linauts, and G.F. Martin (1978) An autoradiographic study of midbrain-diencephalic projections to the inferior olivary nucleus in the opossum (*Didelphis virginiana*). *J. Comp. Neurol.* 179:325-354.
- Leonard, C.S., J.I. Simpson, and W. Graf (1988) Spatial organization of visual messages of the rabbit's cerebellar flocculus. I. Typology of inferior olive neurons of the dorsal cap of Kooy. *J. Neurophysiol.* 60:2073-2090.
- Leranth, C.S., and M. Frotscher (1983) Commissural afferents to the rat hippocampus terminate on VIP-like immunoreactive non-pyramidal neurons. An EM immunocytochemical degenerative study. *Brain Res.* 276:357-361.
- Lieberman, A.R. (1971) The axon reaction: A review of the principal features of perikaryal responses to axon injury. *Int. Rev. Neurobiol.* 14:49-124.
- Liposits, Z., T. Görcs, and K. Trombitás (1985) Ultrastructural analysis of central serotonergic neurons immunolabeled by silver-gold intensified diaminobenzidine chromogen. *J. Histochem. Cytochem.* 33:604-610.
- Liu, C.-J., P. Grandes, C. Matute, M. Cuénod, and P. Streit (1989) Glutamate-like immunoreactivity revealed in rat olfactory bulb, hippocampus and cerebellum by monoclonal antibody and sensitive staining method. *Histochem.* 90:427-445.
- Ljungdahl, A., T. Hökfelt, G. Nilsson, and M. Goldstein. (1978) Distribution of substance P-like immunoreactivity in the central nervous system of the rat. I. Cell bodies and nerve terminals. *Neuroscience* 3:861-943.
- Llinás, R. (1970) Neuronal operations in cerebellar transactions. In: *The Neurosciences, Second Study Program*, edited by F.O. Schmitt. New York, Rockefeller Univ. Press, p.409-426.
- Llinás, R., (1974) *The Physiologist* 17:19
- Llinás, R. (1981) Electrophysiology of the cerebellar networks. In J.M. Brookhart, V.B. Mountcastle (eds) *Handbook of physiology. Sect. 1: The nervous system, vol. II: Motor control.* Am. Physiol. Soc. (Bethesda), pp.831-876.
- Llinás, R. (1982) General discussions: Radial connectivity in the cerebellar cortex: A novel view regarding the functional organization of the molecular layer. In: S.L. Palay, V. Palay (eds), *The Cerebellum-New Vistas*, New York, Springer-Verlag. pp.189-194.
- Llinás, R. (1984) Rebound excitation as the physiological basis for tremor: a biophysical study of the oscillatory properties of mammalian central neurones in vitro. In L.J. Findley and R. Capildeo (Eds) *Movement Disorders: Tremor*. New York: Oxford University Press, pp.165-182.
- Llinás, R. (1985) Functional significance of the basic cerebellar circuit in motor coordination. In J.R. Bloedel, J. Dichgans, and W. Precht (eds) *Cerebellar Functions*, Springer-Verlag, Berlin, Heidelberg, New York, Tokyo pp. 170-186.
- Llinás, R. (1987) Electrophysiology of the olivo - cerebellar system as studied with multiple microelectrode recording. In *The Olivocerebellar System in Motor Control, Satellite Symposium of the 2nd IBRO World Congress of Neuroscience*, Turin, 9-12 August, 1987, 21.
- Llinás, R. (1989) Electrophysiological properties of the olivo-cerebellar system. In P. Strata (Ed.): *The Olivocerebellar System in Motor Control. Suppl. Exp. Brain Res.* 17:201-209.
- Llinás, R., R. Baker, and C. Sotelo (1974) Electrotonic coupling between neurons in the cat inferior olive. *J. Neurophysiol.* 37:560-571
- Llinás, R., and M. Mühlthaler (1988a) An electrophysiological study of the in vitro, perfused brain stem-cerebellum of adult guinea-pig. *J. Physiol.* 404:215-240.
- Llinás, R., and M. Mühlthaler (1988b) Electrophysiology of guinea-pig cerebellar nuclear cells in the in vitro brain stem-cerebellar preparation. *J. Physiol.* 404:241-258.
- Llinás, R., and M. Sugimori (1980) Electrophysiological properties of in vitro Purkinje cell dendrites in mammalian cerebellar slices. *J. Physiol.* 305:197-213.
- Llinás, R., and M. Sugimori (1982) Functional significance of the climbing fiber input to Purkinje cells: An in vitro study in mammalian cerebellar slices. *Exp. Brain Res. Suppl.* 16:402-411.
- Llinás, R., and R.A. Volkind (1973) The olivocerebellar system functional properties as revealed by harmaline induced tremor. *Exp. Brain Res.* 18:69-87.
- Llinás, R., K. Walton, D.E. Hillman, and C. Sotelo (1975) Inferior olive: its role in motor learning. *Science* 190:1230-1231.
- Llinás, R., and Y. Yarom (1981a) Electrophysiology of mammalian inferior olivary neurons in vitro. Different types of voltage-dependent ionic conductances. *J. Physiol. (Lond.)* 315:549-567
- Llinás, R., and Y. Yarom (1981b) Properties and distribution of ionic conductances generating electroresponsiveness of mammalian inferior olivary neurons in vitro. *J. Physiol. (Lond.)* 315:569-584.
- Llinás, R., and Y. Yarom (1986) Oscillatory properties of guinea-pig inferior olivary neurones and their pharmacological modulation: An in vitro study. *J. Physiol.* 376:163-182.
- Loewy, A.D., and H. Burton (1978) Nuclei of the solitary tract: efferent projections to the lower brain stem and spinal cord of the cat. *J. Comp. Neurol.* 181:421-450.
- Lou, J.S., and J.R. Bloedel (1986) The responses of simultaneously recorded Purkinje cells to the perturbations of the step cycle in the walking ferret: a study using a new analytical method - the real-time postsynaptic response (RTPR). *Brain Res.* 365:340-344.

- Luppi, P.H., K. Sakai, K. Kitahama D. Salvetti, and M. Jouvet (1986) Peptidergic afferents to the neural lobe of the cat hypophysis. *Neurosci. Lett. Suppl.* 26:S602.
- Mabuchi, M., and T. Kusama (1966) The cortico-rubral projection in the cat. *Brain Res.* 2:254-273.
- Maekawa, K., and J.I. Simpson (1973) Climbing fibre responses evoked in vestibulocerebellum of rabbit from visual system. *J. Neurophysiol.* 36:649-666.
- Mailleux, P., and J.J. Vanderhaeghen (1988) Transient neurotensin in the human inferior olive during development. *Brain Res.* 456:199-203.
- Majorossy, K., and M. Réthelyi (1968) Synaptic architecture in the medial geniculate body (ventral division). *Exp. Brain Res.* 6:306-323.
- Majorossy, K., M. Réthelyi, and J. Szentagotai, J. (1965) The large glomerular synapse of the pulvinar. *J. Hirnforsch.* 7:415-432.
- Maler, L., S. Jande, and E.M. Lawson (1984) Localization of vitamin D-dependent calcium binding protein in the electrosensory and electromotor system of high frequency gymnotid fish. *Brain Res.* 301:166-170.
- Mano, N. (1970) Changes of simple and complex spike activity of cerebellar Purkinje cells with sleep and waking. *Science* 170:1325-1327.
- Mano, N. (1974) Simple and complex spike activities of the cerebellar P-cell in relation to selective alternate movement in intact monkey. *Brain Res.* 70:381-393.
- Mano, N., I. Kanazawa, and K. Yamamoto (1986) Complex-spike activity of cerebellar Purkinje cells related to wrist tracking movement in monkey. *J. Neurophysiol.* 56:137-158.
- Mano, N., I. Kanazawa, and K. Yamamoto (1989) Voluntary movements and complex-spike discharges of cerebellar Purkinje cells. In P. Strata (Ed.): *The Olivocerebellar System in Motor Control. Suppl. Exp. Brain Res.* 17:265-280
- Mantyh, P.W., T. Gates, C.R. Mantyh, and J.E. Maggio (1989) Autoradiographic localization and characterization of tachykinin receptor binding sites in the rat brain and peripheral tissues. *J. Neurosci.* 9:258-279.
- Marani, E., J. Voogd, and A. Boeke (1977) Acetylcholinesterase staining in subdivisions of the cat's inferior olive. *J. Comp. Neurol.* 174:209-225.
- Maranto, A.R. (1982) Neuronal mapping: a photooxidation reaction makes lucifer yellow useful for electron microscopy. *Science* 217:953-955.
- Marchesi, G.F., and P. Strata (1970) Climbing fibers of cat cerebellum: modulation of activity during sleep. *Brain Res.* 17:145-148.
- Marchesi, G.F., and P. Strata (1971) Mossy and climbing fiber activity during phasic and tonic phenomena of sleep. *Arch. Ges. Physiol.* 323:219-240.
- Marr, D. (1969) A theory of cerebellar cortex. *J. Physiol. (Lond.)* 202:437-470.
- Martin, G.F., J. Culbertson, C. Laxson, M. Linauts, M. Panneton, and I. Ischismadia (1980) Afferent connections of the inferior olivary nucleus with preliminary notes on their development: Studies using the North American Opossum. In J. Courville et al. (Eds.). *The Inferior Olivary Nucleus: Anatomy and Physiology.* Raven Press, New York.
- Martinez, F.E., W.E. Crill, and T.T. Kennedy (1971) Electrogenesis of cerebellar Purkinje cell responses in cats. *J. Neurophysiol.* 34:348-356.
- Matsukawa, K., and M. Udo (1985) Responses of cerebellar Purkinje cells to mechanical perturbations during locomotion of decerebrate cats. *Neurosci. Res.* 2:393-398.
- Matsuyama, K., Y. Ohta, and S. Mori (1988) Ascending and descending projections of the nucleus reticularis gigantocellularis in the cat demonstrated by the anterograde neural tracer, Phaseolus vulgaris leucoagglutinin. *Brain Res.* 460:124-141.
- Matute, C., L. Wiklund, P. Streit, and M. Cuenod (1987) Selective retrograde labeling with D-[3H]-aspartate in the monkey olivocerebellar projection. *Exp. Brain Res.* 66:445-447.
- Maxwell, D.J., R.E. Fyffe, and A.G. Brown (1984) Fine structure of normal and degeneration primary afferent boutons associated with characterized spinocervical tract neurons in the cat. *Neuroscience* 12:151-163.
- Maxwell, D.J., and H.R. Koerber (1986) Fine structure of collateral axons originating from feline spinocervical tract neurons. *Brain Res.* 363:199-203.
- Maxwell, D.J., H.R. Koerber, and B.A. Bannatyne (1985) Light and electron microscopy of contacts between primary afferent fibres and neurones with axons ascending the dorsal columns of the feline spinal cord. *Neuroscience* 16:375-394.
- McCormick, D.A., J.E. Steinmetz, and R.F. Thompson (1985) Lesions of the inferior olivary complex cause extinction of the classically conditioned eyeblink response. *Brain Res.* 359:120-130.
- McCormick, D.A., and R.F. Thompson (1984) Neuronal responses of the rabbit cerebellum during acquisition and performance of a classically conditioned nictitating membrane-eyelid response. *J. Neurosci.* 4:2811-2822.
- McCrea, R.A., and R. Baker (1985a) Anatomical connections of the nucleus prepositus of the cat. *J. Comp. Neurol.* 237:377-407.
- McCrea, R.A., G.A. Bishop, and S.T. Kitai (1977) Electrophysiological and horseradish peroxidase studies of precerebellar afferents to the nucleus interpositus anterior. II. Mossy fiber system. *Brain Res.* 122:215-228.

- McCurdy, M.L., C. Melton, J.C. Houk, and A.R. Gibson (1988) Sensory input to the forelimb inferior olive and its relationship to motor pathways. Society for Neuroscience (Toronto) Abstract No.305.4.
- McElligot, J.G. (1976) Cerebellar neuronal firing patterns in intact and unrestrained cat during walking. In: R.M. Herman, S. Grillner, P.S.G. Stein, and D.G. Stuart (Eds.). Neural control of locomotion. Plenum, New York, p.781.
- Mendelsohn, F.A., R. Quirion, J.M. Saavedra, G. Aguilera, and K.J. Catt (1984) Autoradiographic localization of angiotensin II receptors in rat brain. *Proc. Natl. Acad. Sci. (USA)* 81:1575-1579.
- Menétrey, D. (1985) Protein-gold complex as a retrograde cell tracer: possible applications in both light and electron microscopy after silver intensification. *Neurosci. Lett. Suppl.*22:S83.
- Menétrey, D., and C.L. Lee (1985) Retrograde tracing of neural pathways with a protein gold complex. II. Electron microscopic demonstration of projections and collaterals. *Histochem.* 83:525-530.
- Mesulam, M.M. (1978) Tetramethyl benzidine for horse radish peroxidase neurochemistry: a non-carcinogenic blue reaction-product with superior sensitivity for visualizing neural afferents and efferents. *J. Histochem. Cytochem.* 26:106-117.
- Mesulam, M.M. (1982) Principles of horseradish peroxidase neurochemistry and their applications for tracing neural pathways-axonal transport, enzyme histochemistry and light microscopic analysis. In *Tracing Neural Connections with Horseradish Peroxidase. IBRO Handbook Series, Methods in the Neurosciences.* Chichester, John Wiley, pp.1-151.
- Mihailoff, G.A., R.J. Kosinski, B.G. Border, and H.S. Lee (1988) A review of recent observations concerning the synaptic organization of the basilar pontine nuclei. *J. Electron Microsc. Tech.* 10(3):229-246.
- Milhaud, M., and G.D. Pappas (1966a) Postsynaptic bodies in the habenula and the interpeduncular nuclei in the cat. *J. Cell. Biol.* 30:437-441.
- Milhaud, M., and G.D. Pappas (1966b) The fine structure of neurons and synapses of the habenula of the cat with special reference to subjunctional bodies. *Brain Res.* 3:158-173.
- Miller, S., N. Nezlina, and O. Oscarsson (1969a) Projection and convergence patterns in climbing fibre paths to cerebellar anterior lobe activated from cerebral cortex and spinal cord. *Brain Res.* 14:230-233.
- Miller, S., N. Nezlina, and O. Oscarsson (1969b) Climbing fibre projection to cerebellar anterior lobe activated from structures in midbrain and from spinal cord. *Brain Res.* 14:234-236.
- Miller, S., and Oscarsson, O. (1970) Termination and functional organisation of spino-olivo-cerebellar paths. In: *The Cerebellum in Health and Disease*, edited by W.S. Fields and W.D. Willis. St. Louis, Mo.: Green, p.172-220.
- Millhorn, D.E., T. Hokfelt, K. Seroogy, W. Oertel, A.A.J. Verhofstad, and J.Y. Wu (1987) Immunohistochemical evidence for colocalization of gamma-aminobutyric acid and serotonin in neurons of the ventral medulla oblongata projecting to the spinal cord. *Brain Res.* 410:179-185.
- Mitomo, S. (1942) Eine vergleichend-anatomische Studie über den roten Kern der Raubtiere, mit besonderen Berücksichtigung des innigen Zusammenhanges zwischen diesen Kern und den Nachbarkernen und auf die mediale Haubenbahn. *Kaibougaku Zassi* (in Japanese) 19:212-239.
- Mizuno, N. (1966) An experimental study of the spino-olivary fibres in the rabbit and the cat. *J. Comp. Neurol.* 127:267-292.
- Mizuno, N., A. Konishi, and Y. Nakamura (1976) An electron microscopic study of synaptic terminals of the spino-olivary fibers in the cat. *Brain Res.* 104:303-308.
- Mizuno, N., A. Konishi, K. Itoh, N. Iwahori, and Y. Nakamura (1980) Identification of axon terminals of the cerebello-olivary fibers in the cat: An electron microscope study using the anterograde horseradish peroxidase method. *Neurosci. Lett.* 20:11-14.
- Mizuno, N., K. Mochizuki, C. Akimoto, R. Matsushima, and K. Sasaki (1973) Projections from the parietal cortex to the brain stem nuclei in the cat, with special reference to the parietal cerebro-cerebellar system. *J. Comp. Neurol.* 147:511-522.
- Mizuno, N., Y. Nakamura, and N. Iwahori (1974) An electronmicroscopic study of the dorsal cap of the inferior olive in the rabbit, with special reference to the pretecto-olivary fibers. *Brain Res.* 102:303-308.
- Mlonyeni, M. (1973) The number of Purkinje cells and inferior olivary neurones in the cat. *J.Comp.Neurol.*147:1-9.
- Moatamed, F. (1966) Cell frequencies in the human inferior olivary nuclear complex. *J. Comp. Neurol.* 128:109-116.
- Molinari, H.H. (1987) Ultrastructure of the gracile nucleus projection to the dorsal accessory subdivision of the cat inferior olive. *Exp. brain Res.* 66:175-184.
- Molinari, H.H. (1988) Ultrastructural heterogeneity of spinal terminations in the cat inferior olive. *Neuroscience* 27:425-435.
- Molinari, H.H., and R.N. Sluyters (1987) Somatic afferent termination patterns in the cat inferior olive. *Abstr. Society for Neuroscience, New Orleans.* No. 171.1.
- Molinari, H.H., and K.A. Starr (1988) Somatic afferent termination on spines in the cat medial accessory olive. *Abstr. Society for Neuroscience.* Toronto. No.202.7.
- Monaghan, D.T., and C.W. Cotman (1985) Distribution of N-methyl-D-aspartate-sensitive L-[3H]glutamate-binding sites in rat brain. *J. Neurosci.* 5:2909-2919.
- Montarolo, P.G., M. Palestini, and P. Strata (1981) Effects of inferior olive cooling on the Purkinje cell activity. *Neurosci. Lett. Suppl.* 7:S120.

- Montarolo, P.G., M. Palestini, and P. Strata (1982) The inhibitory effect of the olivocerebellar input to the cerebellar Purkinje cells in the rat. *J. Physiol.* 332:187-202.
- Montgomery J.C. (1980) Dogfish horizontal canal system: Responses of primary afferent, vestibular and cerebellar neurons to rotational stimulation. *Neuroscience* 5:1761-1769.
- Morgan, C. (1972) The use of ferritin-conjugated antibodies in electron microscopy. *Int. Rev. Cytol.* 32:291-326.
- Morris, R.E., and C.B. Saelinger (1982) Combined use of immunoferritin and immunocolloidal gold for the simultaneous demonstration of two antigens by immuno-electron microscopy. *Stain Technol.* 57:225-237.
- Mortimer, J.A. (1973) Temporal sequence of cerebellar Purkinje and nuclear activity in relation to the acoustic startle response. *Brain Res.* 50:457-462.
- Mortimer, J.A. (1975) Cerebellar responses to teleceptive stimuli in alert monkeys. *Brain Res.* 83:369-390.
- Mourre, C., M. Hugues, and M. Lazdunski (1986) Quantitative autoradiographic mapping in rat brain of the receptor of apamin, a polypeptide toxin specific for one class of Ca²⁺-dependent K⁺ channels. *Brain Res.* 382:239-249.
- Mugnaini, E. (1972) The histology and cytology of the cerebellar cortex. In: *The Comparative Anatomy and Histology of the Cerebellum. The Human Cerebellum, Cerebellar Connections, and Cerebellar Cortex*, edited by O. Larsell and J. Jansen, pp.201-264. University of Minnesota Press, Minneapolis.
- Mugnaini, E. (1983) The length of cerebellar parallel fibers in chicken and rhesus monkey. *J. Comp. Neurol.* 220:7-15.
- Mugnaini, E., and B. Nelson (1987) Corticotropin-releasing factor (CRF)-like immunoreactivity in feline inferior olive and climbing fibers. In *The Olivocerebellar System in Motor Control*, Satellite Symposium of the 2nd IBRO World Congress of Neuroscience, Turin, 9-12 August, 1987, 15.
- Mugnaini, E., and B.J. Nelson (1989) Corticotropin-releasing factor (CRF) in the olivocerebellar system and the feline olivary hypertrophy. In *The Olivocerebellar System in Motor Control*. P. Strata (Ed.). *Exp. Brain Res. Series* 17:187-199.
- Mugnaini, E., and W.H. Oertel (1985) An atlas of the distribution of GABAergic neurons and terminals in the rat CNS as revealed by GAD-immunohistochemistry. In A. Bjorklund and T. Hokfelt (eds.). *GABA and Neuropeptides in the CNS, Part 1, The Handbook of Chemical Neuroanatomy*, Vol. 4, Elsevier, Amsterdam, 1985, Chapter 10, pp. 541-543.
- Muller, L.J., A. Patteiselanno, J. Nunes Cardozo and G. Vrensen (1984) Development of synapses of identified pyramidal and multipolar neurons in the visual cortex of rabbits. A combined Golgi-electron microscope study. *Neuroscience* 12:1045-1069.
- Muller, L.J., R.W.H. Verwer, B. Nunes Cardozo, and G. Vrensen (1984) Synaptic characteristics of identified pyramidal and non-pyramidal neurons in the visual cortex of young and adult rabbits. A quantitative Golgi-Electron microscope study. *Neuroscience* 12:1071-1087.
- Muller, L.L., and T.J. Jacks (1975) Rapid chemical dehydration of samples for electron microscopic examinations. *J. Histochem. Cytochem.* 23:107-110.
- Muller, K.J., and U.J. McMahan (1976) The shapes of sensory and motor neurones and the distribution of their synapses in ganglia of the leech: a study using intracellular injection of horseradish peroxidase. *Proc. R. Soc. Lond. B.* 194:481-499.
- Murphy, J.T., and N.H. Sabah (1971) Cerebellar Purkinje cell responses to afferent inputs. I. Climbing fiber activation. *Brain Res.* 25:449-467.
- Murphy, J.T., W.A. Mackay, and F. Johnson (1973) Differences between cerebellar mossy and climbing fibre responses to natural stimulation of forelimb muscle proprioceptors. *Brain Res.* 55:263-289.
- Murphy, M.G., and J.L. O'Leary (1971) Neurological deficit in cats with lesions of the olivocerebellar system. *Arch. Neurol.* 24:145-157.
- Nagai, T., T. Maeda, H. Imai, P.L. McGeer, and E.G. McGeer (1985) Distribution of GABA-T-intensive neurons in the rat hindbrain. *J. Comp. Neurol.* 231:260-269.
- Nakada, H., and Y. Nakai (1985) Electron microscopic examination of the catecholaminergic innervation of neurophysin- or vasopressin-containing neurons in the rat hypothalamus. *Brain Res.* 361:247-257.
- Nakada, H., C.M. Wiczorek, and T.C. Rainbow (1984) Localization and characterization by quantitative autoradiography of [125I]LSD binding sites in rat brain. *Neurosci. Lett.* 49:13-18.
- Nakamura, Y., Y. Kitao, and S. Okoyama (1983) Cortico-Darkschewitsch-olivary projection in the cat: an electron microscope study with the aid of horseradish peroxidase tracing technique. *Brain Res.* 274:140-143.
- Nauta, W.J.H., and P.A. Gyfax (1954) Silver impregnation of degenerating axons in the central nervous system: a modified technique. *Stain Technol.* 29:91-94.
- Nazarali, A.J., J.S. Gutkind, and J.M. Saavedra (1987) Regulation of angiotensin II binding sites in the subfornical organ and other rat brain nuclei after water deprivation. *Cell Mol. Neurobiol.* 7:447-455.
- Nelson, B.J., J.C. Adams, N.H. Barmack, and E. Mugnaini (1989) Comparative study of glutamate decarboxylase immunoreactive boutons in the mammalian inferior olive. *J. Comp. Neurol.* 286:514-539.
- Nelson, B., N.H. Barmack, and E. Mugnaini (1984) A GABAergic cerebello-olivary projection in the rat. *Soc. Neurosci. Abstr.* 10:161.7, pp.539.

- Nelson, B., N.H. Barmack, and E. Mugnaini (1986) GABAergic projection from vestibular nuclei to rat inferior olive. *Soc. Neurosci. Abstr.* 71:15.
- Nelson, B., and E. Mugnaini (1985) Loss of GABAergic nerve terminals in the inferior olive cerebellectomized rats. *Soc. Neurosci. Abstr.* 11:59.8, pp.182.
- Nelson, B., and E. Mugnaini (1987a) GABAergic innervation of the inferior olivary complex and experimental evidence for its origin. In *The Olivocerebellar System in Motor Control, Satellite Symposium of the 2nd IBRO World Congress of Neuroscience, Turin, 9-12 August, 1987*, 9.
- Nelson, B., and E. Mugnaini (1987b) The rat inferior olive as seen with immunostaining for glutamate decarboxylase. *Anat. Embryol.* 179:109-127.
- Nelson, B., and E. Mugnaini (1988) The rat inferior olive as seen with immunostaining for glutamate decarboxylase. *Anat. Embryol.* 179:109-127.
- Nelson, B., E. Mugnaini, J.C. Adams, and N.H. Barmack (1988) GABAergic components of the mammalian IO. *Soc. Neurosci. Abstr.* 202:8.
- Némeček, S., and J. Wolff (1969) Light and electron microscopic evidence of complex synapses (glomeruli) in olivary inferior (cat). *Experientia* 25:634-636.
- Newman, P.P., and D.H. Paul (1969) The projection of splanchnic afferents on the cerebellum of the cat. *J. Physiol. (Lond.)* 202:223-238.
- Nieuwenhuys, R. (1985) *Chemoarchitecture of the brain*. Berlin, Heidelberg, NY, Tokyo, Springer-Verlag.
- Niimi, K., S. Kishi, M. Miki et al. (1963) An experimental study of the course and termination of the projection fibers from cortical areas 4 and 6 in the cat. *Folia Psychiat. Neurol. Jap.* 17:167-216.
- Nunes-Cardozo, B., and J.J.L. van de Want. Ultrastructural organization of the retino-pretectal-olivary pathway. A combined WGA-HRP retrograde / GABA immunohistochemical study. *J. Comp. Neurol.* in press.
- Ochi, R. (1965) Occurrence of post-synaptic potentials in the inferior olive neurones associated with their antidromic excitation. In: *Proc. Intern. Congr. Physiol. Sci.* 23rd, Tokyo, p.401.
- Oertel, W.H., D.E. Schmechel, E. Mugnaini, M.L. Tappaz, and I.J. Kopin (1981) Immunocytochemical localization of glutamate decarboxylase in rat cerebellum with a new antiserum. *Neuroscience.* 6:2715-2735.
- Ogawa, T. (1939) The tractus tegmenti medialis and its connection with the inferior olive in the cat. *J. Comp. Neurol.* 70:181-190.
- Oka, H. (1988) Functional organization of the parvocellular red nucleus in the cat. *Behav. Brain Res.* 28:233-240.
- Onodera, S. (1984) Olivary projections from the mesencephalic structures in the cat studied by means of axonal transport of horseradish peroxidase and tritiated amino acids. *J. Comp. Neurol.* 227:37-49
- Oscarsson, O. (1967) Functional significance of information channels from the spinal cord to the cerebellum. In: *Neurophysiological Bases of Normal and Abnormal Motor Activities*, edited by D.P. Purpura and M.D. Yahr, New York, Raven, p.93-113.
- Oscarsson, O. (1968) Termination and functional organization of the ventral spino-olivocerebellar path. *J. Physiol. (Lond.)* 196:453-478.
- Oscarsson, O. (1969a) Termination and functional organization of the dorsal spino-olivocerebellar path. *J. Physiol. (Lond.)* 200:129-149.
- Oscarsson, O. (1969b) The sagittal organization of the cerebellar anterior lobe as revealed by the projection patterns of the climbing fibre system. In: *Neurobiology of Cerebellar Evolution and Development*, edited by R. Llinás, Chicago: Am. Med. Assoc., p.525-532.
- Oscarsson, O. (1973) Functional organization of spinocerebellar paths. In: *Handbook of Sensory Physiology. II. Somato-Sensory System*, edited by A. Iggo, Berlin: Springer, p.339-380.
- Oscarsson, O. (1979) Functional units of cerebellum: Sagittal zones and microzones. *Trends Neurosci.* 2:143-145.
- Oscarsson, O. (1980) Functional organization of olivary projection to the cerebellar anterior lobe. In J. Courville, C. de Montigny, Y. Lamarre (eds) *The inferior olivary nucleus, anatomy and physiology*. Raven Press, New York, pp.279-289.
- Ottersen, O.P. (1988) Electron microscopic immunocytochemistry of putative amino acid transmitters in the cerebellum. In: *Neurobiology of the cerebellar systems: A centenary of Ramon Y Cajal's description of the cerebellar circuits*. Barcelona (Spain) 19-22 October.
- Palay, S.L. (1961) The electron microscopy of the glomeruli cerebellosi. In: *Cytology of Nervous Tissue, Proceedings of the Anatomical Society of Great Britain and Ireland*. London, Taylor and Francis, pp.82-84.
- Palay, S.L., and V. Chan-Palay (1974) *Cerebellar cortex, cytology and organization*. Springer-Verlag Berlin Heidelberg New York.
- Palay, S.L., C. Sotelo, A. Peters, and P.M. Orkand (1968) The axon hillock and initial segment. *J. Cell Biol.* 38:193-201.
- Palkovits, M., M.J. Brownstein, and W. Vale (1985) Distribution of corticotropin-releasing factor in rat brain. *Fed. Proc.* 44:215-219.
- Palkovits, M., C. Leranth, T. Gorcs, and W.S. Young III (1987) Corticotropin-releasing factor in the olivocerebellar tract of rats: demonstration by light- and electron-microscopic immunohistochemistry and in situ hybridization histochemistry. *Proc. Natl. Acad. Sci. (USA)* 84:3911-3915.

- Palkovits, M., P. Magyar, and J. Szentágothai (1971) Quantitative histological analysis of the cerebellar cortex in the cat. I. Number and arrangement in space of the Purkinje cells. *Brain Res.* 32:1-13.
- Pappas, G.D., E.B. Cohen, and D.P. Purpura (1966) Fine structure of synaptic and non-synaptic neuronal relations in the thalamus of the cat. In: *The Thalamus*, D.P. Purpura and M.D. Yahr (Eds.), New York, Columbia Univer. Press, pp. 47-75.
- Pare, M., and L. Descarries (1985) Serotonin and Substance P coexist in axon terminals of the hyperinnervated inferior olive after intraventricular 5,6-dihydroxytryptamine. *Soc. Neurosci. Abst.* 11:27.6 pp. 88.
- Pare, M., L. Descarries, and L. Wiklund (1987) Innervation and reinnervation of rat inferior olive by neurons containing serotonin and substance-P: An immunohistochemical study after 5,6-dihydroxytryptamine lesioning. *J. neurocytol.* 16:155-167.
- Passouant, P., J. Cadilhac, M. Baldy-Moulinier, and P. Cabanac (1965) Données expérimentales sur l'olive bulbaire. *Rev. Neurol.* 113:489-501.
- Paula-Barbosa, M. (1975) The duration of aldehyde fixation as a "flattening factor" of synaptic vesicles. *Cell. Tissue Res.* 164:63-72.
- Peachey, L.D. (1958) Thin sections. I. A study of section thickness and physical distortion produced during microtomy. *J. Biophysiol. Biochem. Cytol.* 4:233.
- Pelletier, G. (1983) Identification of endings containing dopamine and vasopressin in the rat posterior pituitary by a combination of radioautography and immunocytochemistry at the ultrastructural level. *J. Histochem. Cytochem.* 31:562-564.
- Pelletier, G., and G. Morel (1984) Immunoenzyme techniques at the electron microscopical level. In: *Immunolabelling for Electron Microscopy*. J.M. Polak, and I.M. Varndell (Eds.) Elsevier, Amsterdam-New York-Oxford.
- Pellionisz, A. (1985) Tensorial brain theory in cerebellar modelling. In J.R. Bloedel, J. Dichgans, and W. Precht (eds) *Cerebellar Functions*, Springer-Verlag, Berlin, Heidelberg, New York, Tokyo pp. 201-230.
- Pellionisz A., and R. Llinás (1982) Space-time representation in the brain. The cerebellum as a predictive space-time metric tensor. *Neuroscience* 7:2949-2970.
- Peters, A., and S.L. Palay (1966) The morphology of laminae A and A1 of the dorsal nucleus of the lateral geniculate body of the cat. *J. Anat. (London)* 100:451-486.
- Peters, A., S.L. Palay, and H.F. Webster (1970) *The fine structure of the nervous system*. Hoeber Medical Division, Harper and Row, Publishers, New York, Evanston, and London, pp.156.
- Peters, A., C.C. Proskauer, and I.R. Kaiserman-Abramof (1968) The small pyramidal neuron of the rat cerebral cortex. The axon hillock and initial segment. *J. Cell Biol.* 39:604-619.
- Pettigrew, A.G., F. Crepel, and M. Krupa (1988) Development of ionic conductances in neurons of the inferior olive in the rat: an in vitro study. *Proc. R. Soc. (Lond.)* 234:199-218.
- Pickel, V.M., and A. Beaudet (1984) Combined use of autoradiography and immunocytochemical methods to show synaptic interactions between chemically defined neurons. In J.M. Polak and I.M. Varndell (eds) *Immunolabelling for Electron Microscopy*. Amsterdam, Elsevier, Science Publishers, 259-266.
- Pitman, R.M. C.D. Tweedle, and M.J. Cohen (1972) Branching of central neurons: Intracellular cobalt injection for electron microscopy. *Science* 176:412-414.
- Polak J.M., and I.M. Varndell (eds) (1984) *Immunolabelling for Electron Microscopy*. Amsterdam, Elsevier Science Publishers, pp.370.
- Pongrácz, F. (1985) The function of dendritic spines: A theoretical study. *Neuroscience* 15:933-946.
- Powers, R.E., E.B. DeSouza, L.C. Walker, D.L. Price, W.W. Vale, and W.S. Young III (1987) Corticotropin-releasing factor as a transmitter in the human olivocerebellar pathway. *Brain Res.* 415:347-352.
- Precht, W., J.I. Simpson, and R. Llinás (1976a) Responses of Purkinje cells in rabbit nodulus and uvula to natural vestibular and visual stimuli. *Pflügers Arch.* 367:1-6.
- Precht, W., R. Volkind, and R.H.I. Blanks (1977) Functional organization of the vestibular input to the anterior and posterior cerebellar vermis of cat. *Exp. Brain Res.* 27:143-160.
- Precht, W., R. Volkind, M. Maeda, and M.L. Giretti (1976b) The effects of stimulating the cerebellar nodulus in the cat on the responses of vestibular neurons. *Neuroscience* 1:301-312.
- Priestly, J.V. (1984) Pre-embedding ultrastructural immunocytochemistry: Immunoenzyme techniques. In J.M. Polak and I.M. Varndell (eds), *Immunolabeling for electron microscopy*. Amsterdam, Elsevier Science Publishers, pp.37-53.
- Probst, A., R. Cortes, and J.M. Palacios (1984) Distribution of alpha 2-adrenergic receptors in the human brainstem: an auto- radiographic study using [3H]p-aminoclonidine. *Eur. J. Pharmacol.* 106:477-488.
- Provini, L., S. Redman, and P. Strata (1967) Somatotopic organization of mossy and climbing fibres to the anterior lobe of cerebellum activated by the sensorimotor cortex. *Brain Res.* 6:378-381.
- Provini, L., S. Redman, and P. Strata (1968) Mossy and climbing fiber organization on the anterior lobe of the cerebellum activated by forelimb and hindlimb area of the sensorimotor cortex. *Exp. Brain Res.* 6:216-233.
- Purpura, D. (1974) Dendrite spines dysgenesis and mental retardation. *Science Wash. DC* 186:1126-1128.

- Rall, W. (1974) Dendritic spines, synaptic potency and neuronal plasticity. In: Cellular Mechanisms Subservicing Changes in Neuronal Activity, edited by C.D. Woody, K.A. Brown, T.J. Crow, and J.D. Knispel. Los Angeles, CA: Brain Inform. Service Res. Report, vol. 3: p.13-21.
- Ralston, III, H.J., and M.M. Herman (1969) The fine structure of neurons and synapses in the ventrobasal thalamus of the cat. *Brain Res.* 14:77-97.
- Ramón-Moliner, E. (1962) An attempt at classifying nerve cells on the basis of their dendritic patterns. *J. Comp. Neurol.* 119:211-227.
- Ramón Y Cajal, S. (1909) *Histologie du Système Nerveux de l'Homme et des Vertébrés.* Vol. I, Paris, Maloine.
- Ramón Y Cajal, S. (1911) *Histologie du Système Nerveux de l'Homme et des Vertébrés.* Vol. II, Paris, Maloine.
- Rawson, J.A., and K. Tilokskulchai (1981) Suppression of simple spike discharges of cerebellar Purkinje cells by impulses in climbing fibre afferents. *Neurosci. Lett.* 25:125-130.
- Rawson, J.A., and K. Tilokskulchai (1982) Climbing fibre modification of cerebellar Purkinje cell responses to parallel fibre inputs. *Brain Res.* 237:492-497.
- Rinvik, E., and Walberg, F. (1963) Demonstration of a-somatotopically arranged cortico-rubral projection in the cat. An experimental study with silver methods. *J. Comp. Neurol.* 120:393-407.
- Rinzel, J. (1982) Neuronal plasticity (learning). In: Some Mathematical Questions in Biology-Neurobiology. Lectures on Mathematics in the Life-Sciences. R.M. Miura (Ed.). Providence, RI: Am. Math. Soc. vol. 15: p.7-25.
- Roberts, E. (1974) Gamma-aminobutyric acid and nervous system function. A perspective, *Biochem. Pharmacol.*, 23:2637-2649.
- Robin, J.J. and H. Alcalá (1975) Olivary hypertrophy without palatal myoclonus associated with a metastatic lesion to the pontine tegmentum. *Neurology* 25:771-775.
- Robinson, D.A. (1976) Adaptive gain control of vestibuloocular reflex by the cerebellum. *J. Neurophysiol.* 39:954-969.
- Robinson, F.R. (1987) Vestibular responses in the inferior olive. In M. Glickstein, Chr. Yeo, and J. Stein (eds), *Cerebellum and Neuronal Plasticity, Series A: Life Sciences*, vol. 148, p. 155-165.
- Robinson, F.R., M.O. Fraser, J.R. Hollerman, and D.L. Tomko (1988) Yaw direction neurons in the cat inferior olive. *J. Neurophysiol.* 60: 1739-1752.
- Rogers, A.W. (1979) *Techniques of autoradiography.* Elsevier/North-Holland. pp. 46-50, 290, 403 and 405.
- Rosenbluth, J. (1962) Subsurface cisterns and their relationship to the neuronal plasma membrane. *J. Cell Biol.* 13:405-421.
- Rosina, A., and L. Provini (1983) Somatotopy of climbing fiber branching to the cerebellar cortex in cat. *Brain Res.* 289:45-63.
- Rosina, A., and L. Provini (1985) Brain stem afferents bilaterally branching to the cat cerebellar hemispheres. In J.R. Bloedel, J. Dichgans, and W. Precht (eds) *Cerebellar Functions*, Springer-Verlag, Berlin, Heidelberg, New York, Tokyo pp.326-329.
- Rosina, A., and L. Provini (1987) Spatial distribution of axon collaterals of single inferior olive neurons. *J. Comp. Neurol.* 256:317-328.
- Rossi, F., L. Wiklund, J.J.L. Van der Want, and P. Strata (1989) Short Communication. Climbing fibre plasticity in the cerebellum of the adult rat. *European Journal of neuroscience.* 1:543-547
- Roth, J. (1982) The preparation of protein A-gold complexes with 3 nm and 15 nm gold particles and their use in labelling multiple antigens on ultrathin sections. *Histochem. J.* 14:791-801.
- Roth, J., and M. Binder (1978) Colloidal gold, ferritin and peroxidase as markers for electron microscopic double labeling lectin techniques. *J. Histochem. Cytochem.* 26:163-169.
- Ruda, M.A. (1982) Opiates and pain pathways: demonstration of enkephalin synapses on dorsal horn projection neurons. *Science* 215:1523-1525.
- Ruigrok, T.J.H., C.I. de Zeeuw, and J. Voogd (1988) Morphology of inferior olivary neurons in cat. Intracellular HRP-injections in vivo combined with mesodiencephalic stimulation and anterograde tracing. In *Neurobiology Of The Cerebellar Systems: A Centenary Of Ramon Y Cajal's Description Of The Cerebellar Circuits.* Barcelona, 19-22 October, 37.
- Ruigrok, T.J.H., C.I. de Zeeuw, J. van der Burg, R. Boer, and J. Voogd (1989) Experimental olivary hypertrophy in cat: Comparison of morphological and physiological aspects with normal inferior olive. *Suppl. Europ. J. Neurosci.* 2:39.3, p.129.
- Ruigrok, T.J.H., C.I. de Zeeuw, J. van der Burg, and J. Voogd. Intracellular labeling of neurons in the medial accessory olive of the cat: I. Physiology and lightmicroscopy. *J. Comp. Neurol.* submitted.
- Ruigrok, T.J.H., and J. Voogd (1988) Evidence for cerebello-midbrain-olivary circuits in rat using PHA-L anterograde and gold labeled WGA-BSA retrograde tracing. *Suppl. Europ. J. Neurosci.* 10.3.
- Ruigrok, T.J.H., and J. Voogd. Cerebellar nucleo-olivary projections in rat. An anterograde tracing study with Phaseolus vulgaris-leucoagglutinin (PHA-L). Submitted.
- Rushmer, D.S., W.J. Roberts, and G.K. Augter (1976) Climbing fibre responses of cerebellar Purkinje cells to passive movement of the cat forepaw. *Brain Res.* 106:1-20.
- Rutherford, J.G., and D.G. Gwyn (1977) Gap junctions in the inferior olivary nucleus of the squirrel monkey, *Saimiri sciureus.* *Brain Res.* 128:374-378.

- Rutherford, J.G., and D.G. Gwyn (1980) A light and electron microscopic study of the inferior olivary nucleus of the squirrel monkey, *Saimiri sciureus*. *J. Comp. Neurol.* 189:127-155.
- Rye, D.B., C.B. Saper, and H. Wainer (1984) Stabilization of the tetramethyl benzidine (TMB) reactionproduct. *J. Histochem. Cytochem.* 32:1145-1153.
- Saint-Cyr, J.A. (1983) The projection from the motor cortex to the inferior olive in the cat. An experimental study using axonal transport techniques. *Neuroscience* 10:667-684.
- Saint-Cyr, J.A. (1987) Anatomical organization of cortico-mesencephalo-olivary pathways in the cat as demonstrated by axonal transport techniques. *J. Comp. Neurol* 257:39-59.
- Saint-Cyr, J.A., and J. Courville (1979) Projection from the vestibular nuclei to the inferior olive in the cat. An autoradiographic and horseradish peroxidase study. *Brain Res.* 165:189-200.
- Saint-Cyr, J.A., and J. Courville (1980) Projections from the motor cortex, mid-brain and vestibular nuclei to the inferior olive in the cat. Anatomical organization and functional correlates. In: *The Inferior Olivary Nucleus*, edited by J. Courville, C. de Montigny, and Y. Lamarre, pp. 97-124. Raven Press, New York.
- Saint-Cyr, J.A., and J. Courville (1981) Sources of descending afferents to the inferior olive from the upper brain stem in the cat as revealed by the retrograde transport of horseradish peroxidase. *J. Comp. Neurol.* 198:567-581.
- Saint-Cyr, J.A., and J. Courville (1982) Descending projections to the inferior olive from the mesencephalon and superior colliculus in the cat. *Exp. Brain Res.* 45:333-345.
- Sandell, J.H., and R.H. Masland (1988) Photoconversion of some fluorescent markers to a diaminobenzidine product. *J. Histochem. Cytochem.* 36:555-559.
- Sasaki, K., and R. Llinás (1985) Evidence for dynamic electrotonic coupling in mammalian inferior olive in vivo. *Soc. Neurosci. Abstr.* 11:181
- Sawchenko, P.E. and C.R. Gerfen (1985) Plant lectins and bacterial toxins as tools for tracing neuronal connections. *TINS Sept.* pp.378-384.
- Scheibel, M.E., and A.B. Scheibel (1955) The inferior olive. A Golgi study. *J. Comp. Neurol.* 102:77-132.
- Scheibel, M.E., A.B. Scheibel, F. Walberg, and A. Brodal (1956) Areal distribution of axonal and dendritic patterns in inferior olive. *J. Comp. Neurol.* 106:21-50.
- Schonbach, J., Schonbach C., and Cuenod M. (1971) Rapid phase of axoplasmic flow and synaptic proteins: An electron microscopical autoradiographic study. *J Comp Neurol* 141:485-498
- Schulman, J.A. (1981) Anatomical distribution and physiological effects of enkephalin in rat inferior olive. *Regulatory Peptides* 2:125-137.
- Schulman, J.A., and F.E. Bloom (1981) Golgi cells of the cerebellum are inhibited by inferior olive activity. *Brain Res.* 210:350-355.
- Schwab, M.E., and H. Thoenen (1976) Electron microscopic evidence for a transsynaptic migration of tetanus toxin in spinal cord motoneurons: an autoradiographic and morphometric study. *Brain Res.* 105:213-227.
- Sedgwick, E.M., and T.D. Williams (1967) Responses of single units in the inferior olive to stimulation of the limb nerves peripheral skin receptors cerebellum caudate nucleus and motor cortex. *J. Physiol. (Lond.)* 189:261-280.
- Segev, I., and I. Parnas (1983) Synaptic integration mechanisms: a theoretical and experimental investigation of temporal postsynaptic interactions between excitatory and inhibitory inputs. *Biophysiol. J.* 41:41-50.
- Segev, I., and W. Rall (1986) Excitable dendritic spines clusters: nonlinear synaptic processing. *Soc. Neurosci. Abstr.* 16:726.
- Segev, I., and Rall W. (1988) Computational study of an excitable dendritic spine. *J. Neurophysiol.* 60:499-523.
- Seguela, P., M. Geffard, R. Buijs, and M. Le Moal (1984) Anti-bodies against gamma-aminobutyric acid: Specificity studies and immunocytochemical results. *Proc. Natl. Acad. Sci. USA.*, vol. 81:3888-3892.
- Seiler, N., and A. Lajtha (1987) Functions of GABA in the vertebrate organism. In: D.A. Redburn and A. Schousboe (Eds.), *Neurotrophic activity of GABA during development.* 1-57.
- Sexton, P.M., J.S. McKenzie, R.T. Mason, J.M. Mosely, T.J. Martin, and F.A. Mendelsohn (1986) Localization of binding sites for calcitonin gene-related peptide in rat brain by in vitro autoradiography. *Neuroscience* 19:1235-1245.
- Shepherd, G.M., R.K. Brayton, J.P. Miller, I. Segev, J. Rinzel, and W. Rall (1985) Signal enhancement in distal cortical dendrites by means of interaction between active dendritic spines. *Proc. Natl. Acad. Sci. USA* 82:2192-2195.
- Shigematsu, K., M. Niwa, M. Kurihara, E. Castren, and J.M. Saavedra (1987) Alteration in substance P binding in brain nuclei of spontaneously hypertensive rats. *Am. J. Physiol.* 252:301-306.
- Simpson, J.I., and K.E. Alley (1974) Visual climbing fiber input to rabbit vestibulo-cerebellum: a source of direction-specific information. *Brain Res.* 82:302-308.
- Simpson, J.I., W. Graf, and C.S. Leonard (1981) The coordinate system of visual climbing fibers to the flocculus. In: A. Fuchs, and W. Becker (Eds.) *Progress in oculomotor research.* Elsevier, Amsterdam, pp.475-484.
- Simpson, J.I., W. Graf, and C.S. Leonard (1989) Three-dimensional representation of retinal image movement by climbing fiber activity. In: *The Olivocerebellar System in Motor Control.* P. Strata (Ed.). *Exp. Brain Res. Series* 17:323-338.
- Simpson, J.I., C.S. Leonard, and R.E. Soodak (1988) The accessory optic system of rabbit. II. Spatial organization of direction selectivity. *J. Neurophysiol.* 60:2055-2072.

- Sinclair, J.G., G.F. Lo, and D.P. Harris (1982) Ethanol effects on the olivocerebellar system. *Can. J. Physiol. Pharmacol.* 60:610-614.
- Sinton, C.M., B. Krosser, K.D. Walton, and R.R. Llinás (1987) Blockade of harmaline tremors by alcohols may be mediated by the low threshold calcium channel. *Abstr. Soc. Neurosci. New Orleans.* 69.2
- Sjölund, B., A. Björklund, and L. Wiklund (1977) The indolaminergic innervation of the inferior olive: 2. Relation to harmaline-induced tremor. *Brain Res.* 131:23-37.
- Sjölund, B., L. Wiklund, and A. Björklund (1980) Functional role of serotonergic innervation of inferior olivary cells. In J. Courville, C. de Montigny and Y. Lamarre (eds), *The Inferior Olivary Nucleus*. New York, Raven Press, pp.163-169.
- Skofitsch, G., and D.M. Jacobowitz (1985) Autoradiographic distribution of 125I calcitonin gene-related peptide binding sites in the rat central nervous system. *Peptides* 6:975-986.
- Sladek, J.R., and J.P. Bowman (1975) The distribution of catecholamines within the inferior olivary complex of the cat and rhesus monkey. *J. Comp. Neurol.*, 163:203-214.
- Sladek, J.R., and G.E. Hoffman (1980) Monoaminergic innervation of the mammalian inferior olivary complex. In *The inferior olivary nucleus* (edited by Courville, J., deMontigny, C., and Lamarre, Y.), pp. 145-162. New York: Raven Press.
- Smith, A.M., and D. Bourbonnais (1981) Neuronal activity in cerebellar cortex related to control of prehensile force. *J. Neurophysiol.* 45:286-303.
- Snedecor, G.W., and W.G. Cochran (1980) *Statistical Methods*, 7th edn. Iowa State University Ptness, Ames, Iowa.
- Snider, R.S., and E. Eldred (1951) Electro-anatomical studies on cerebrocerebellar connexions in the cat. *J. Comp. Neurol.* 95:1-16.
- Snider, R.S., and E. Eldred (1952) Cerebro-cerebellar relationships in the monkey. *J. Neurophysiol.* 15:27-40.
- Snow, P.J., A.G. Brown, and P.K. Rose (1976) Tracing axons and axon collaterals of spinal neurons using intracellular injection of horseradish peroxidase. *Science* 191:312-313.
- Soechting, J.F., N.A. Raniish, R. Palmineteri, and C.A. Terzuolo (1976) Changes in a motor pattern following cerebellar and olivary lesions in the squirrel monkey. *Brain Res.* 105:21-44.
- Somogyi, P., T.F. Freund, N. Halasz, and Z.F. Kisvarday (1981) Selectivity of neuronal (3H)-GABA accumulation in the visual cortex as revealed by Golgi staining of the labeled neurons. *Brain Res.* 225:431-437.
- Somogyi, P., T.F. Freund, A.J. Hodgson, J. Somogyi, D. Beroukas, and I.W. Chubb (1985) Identified axo-axonic cells are immunoreactive for GABA in the hippocampus and visual cortex of the cat. *Brain Res.* 332:143-149.
- Somogyi, P., T.F. Freund, J.Y. Wu, A.D. Smith (1983) The section-Golgi impregnation procedure. 2. Immunocytochemical demonstration of glutamate decarboxylase in Golgi-impregnated neurons and in their afferent synaptic boutons in the visual cortex of the cat. *Neuroscience* 9:475-490.
- Somogyi, P., and A.J. Hodgson (1985) Antisera to gamma-aminobutyric acid. III. Demonstration of GABA in Golgi-impregnated neurons and in conventional electron microscopic sections of cat striate cortex. *J. Histochem. Cytochem.* 33:249-257.
- Somogyi, P., A.J. Hodgson, and A.D. Smith (1979) An approach to tracing neuron networks in the cerebral cortex and basal ganglia. Combination of Golgi staining, retrograde transport of horseradish peroxidase and anterograde degeneration of synaptic boutons in the same material. *Neuroscience.* 4(12): 1805-1852.
- Sotelo, C., and R.M. Alvarado-Mallart (1987a) Embryonic and adult neurons interact to allow Purkinje cell replacement in mutant cerebellum. *Nature* 327:421-423.
- Sotelo, C., and R.M. Alvarado-Mallart (1987b) Reconstruction of the defective cerebellar circuitry in adult Purkinje cell degeneration mutant mice by Purkinje cell replacement through transplantation of solid embryonic implants. *Neuroscience* 20:1-22.
- Sotelo, C., T. Gotow, and M. Wassef (1986) Localization of glutamic-acid-decarboxylase-immunoreactive axon terminals in the inferior olive of the rat, with special emphasis on anatomical relations between GABAergic synapses and dendrodendritic gap junctions. *J. Comp. Neurol.* 252:32-50.
- Sotelo, C., R. Llinás, and R. Baker (1974) Structural study of inferior olivary nucleus of the cat: Morphological correlates of electrotonic coupling. *J. Neurophysiol.* 37:541-559
- Sotelo, C., and S.L. Palay (1970) The fine structure of the later vestibular nucleus in the rat. II. Synaptic organization. *Brain Res.* 18:93-115.
- Sousa-Pinto, A., and A. Brodal (1969) Demonstration of a somato-topical pattern in the cortico-olivary projection in the cat. *Exp. Brain Res.* 8:364-386.
- Spence, S.J., and J.A. Saint-Cyr (1988) Comparative topography of projections from the mesodiencephalic junction to the inferior olive, vestibular nuclei, and upper cervical cord in the cat. *J. Comp. Neurol.* 268:357-374.
- Spira, M.E., and M.V.L. Bennett (1972) Synaptic control of electrotonic coupling between neurons. *Brain Res.* 37:294-300.
- Spira, M.E., D.C. Spray, and M.V.L. Bennett (1980) Synaptic organization of expansion motoneurons of Navanax inermis. *Brain Res.* 195:241-269.
- Steinmetz, J.E., D.G. Lavond, and R.F. Thompson (1989) Classical conditioning in rabbits using pontine nucleus stimulation as a conditioned stimulus and inferior olive stimulation as an unconditioned stimulus. *Synapse* 3:225-233.

- Sternberger, L.A., E.J. Donati, J.J. Cuculis, and J.P. Petrali (1965) Indirect immunouranium technique for staining of embedded antigen in electron microscopy. *Exp. Mol. Pathol.* 4:112-125.
- Steward, O., and C.E. Ribak (1986) Polyribosomes associated with synaptic specializations on axon initial segments: localization of protein-synthetic machinery at inhibitory synapses. *J. Neurosci.* 6:3079-3085.
- Stone L.S., and S.G. Lisberger (1986) Detection of tracking errors by visual climbing fiber inputs to monkey cerebellar flocculus during pursuit eye movements. *Neurosci. Lett.* 72:163-168.
- Strata, P. (1985) Inferior olive: functional aspects. In J.R. Bloedel, J. Dichgans, and W. Precht (eds) *Cerebellar Functions*, Springer-Verlag, Berlin, Heidelberg, New York, Tokyo pp. 230-247.
- Strata, P. (1987) Inferior olive and motor control. In M. Glickstein, Chr. Yeo, and J. Stein (eds), *Cerebellum and Neuronal Plasticity, Series A: Life Sciences*, Vol. 148, p. 209-225.
- Strata, P., and P.G. Montarolo (1982) Functional aspects of the inferior olive. *Arch. Ital. Biol.* 120:321-329.
- Strick, P.L., and P. Sterling (1974) Synaptic termination of afferents from the ventrolateral nucleus of the thalamus in the cat motor cortex. A light and electron microscope study. *J. Comp. Neurol.* 153:77-106.
- Stryer, L., (1981) In: W.H. Freeman and Company (Eds.), *Biochemistry*. Second edition, New York.
- Sugimoto, T., N. Mizuno, S. Nomura, and Y. Nakamura (1980) Fastigio-olivary fibers in the cat as revealed by the autoradiographic tracing method. *Brain Res.* 199:443-446.
- Sugimoto, T., N. Mizuno, and K. Uchida (1982) Distribution of cerebellar fiber terminals in the midbrain visuomotor areas: an autoradiographic study in the cat. *Brain Res.* 238:353-370.
- Sumal, K.K., W.W. Blessing, T.H. Joh, D.J. Reis, and V.M. Pickel (1983) Synaptic interaction of vagal afferents and catecholaminergic neurons in the rat nucleus tractus solitarius. *Brain Res.* 277:31-40.
- Swenson, R.S., and A.J. Castro (1982) Plasticity of meso-diencephalic projections to the inferior olive following neonatal hemispherectomy in rats. *Brain Res.* 244:169-172.
- Swenson, R.S., and A.J. Castro (1983) The afferent connections of the inferior olivary complex in rats. An anterograde study using autoradiographic and axonal degeneration techniques. *Neurosci.* 8, 259-275.
- Szentagothai, J. (1963) The structure of the synapse in the lateral geniculate body. *Acta Anat.* 55:166-185.
- Szentagothai, J., and K. Rajkovits (1959) Ueber den Ursprung der Kletterfasern des kleinhirns. *Z. Anat. Entwicklungsgeschichte* 121:130-141.
- Sztejn, S. (1988) Types of neurons in nucleus olivaris inferior of the European bison. *J. Hirnforsch.* 29:353-356.
- Taghert, P.H., M.J. Bastiani, R.K. Ho, and C.S. Goodman (1982) Guidance of pioneer growth cones: filopodial contacts and coupling revealed with an antibody to Lucifer Yellow. *Dev. Biol.* 94:391-399.
- Takeda, T., and K. Maekawa (1989) Olivary branching projections to the flocculus, nodulus and uvula in the rabbit. I. An electrophysiological study. *Exp. Brain Res.* 74:47-62.
- Takeuchi, Y., and Y. Sano (1983) Immunohistochemical demonstration of serotonin-containing nerve fibers in the inferior olivary complex of the rat, cat and monkey. *Cell Tissue Res.* 231:17-28.
- Tank, D.W., M. Sugimori, J.A. Connor, and R.R. Llinás (1988) Spatially resolved calcium dynamics of mammalian Purkinje cells in cerebellar slice. *Science* 242:773-777.
- Tapia, F.J., I.M. Vardell, L. Probert, J. De Mey, and J.M. Polak (1983) Double immunogold staining method for the simultaneous ultrastructural localisation of regulatory peptides. *J. Histochem. Cytochem.* 31:977-981.
- Tatehata, T., S. Shiosaka, A. Wanaka, Z.R. Rao, M. Tohyama (1987) Immunocytochemical localization of the choline acetyltransferase containing neuron system in the rat lower brain stem. *J. Hirnforsch.* 28:707-716.
- Taxi, E. (1961) Etude de l'ultrastructure des zones synaptiques dans les ganglions sympathiques de la Grenouille. *C.R. Acad. Sci. (Paris)* 252:174-176.
- Ten Bruggencate G., R. Teichmann and E. Weller (1972) Neuronal activity in the lateral vestibular nucleus of the cat. III. Inhibitory actions of cerebellar Purkinje cells evoked via mossy and climbing fibre afferents. *Arch. Ges. Physiol.* 337:147-162.
- Thach, W.T. (1967) Somatosensory receptive fields of single units in the cat cerebellar cortex. *J. Neurophysiol.* 30:675-696.
- Thach, W.T. (1968) Discharge of Purkinje and cerebellar nuclear neurons during rapidly alternating arm movements in the monkey. *J. Neurophysiol.* 31:785-797.
- Thach, W.T. (1970) Discharge of cerebellar neurons related to two maintained postures and two prompt movements. II. Purkinje cell output and input. *J. Neurophysiol.* 33:537-547.
- Toggenburger, G., L. Wiklund, H. Henke, and M. Cuenod (1983) Release of endogenous and accumulated exogenous amino acids from slices of normal and climbing fibre-deprived rat cerebellar slices. *J. Neurochem.* 41:1606-1613.
- Tolbert, D. L., L. C. Massopust, M. G. Murphy, and P. A. Young (1976) The anatomical organization of the cerebello-olivary projection in the cat. *J. Comp. Neurol.* 170:525-544.
- Tong, G., L.T. Robertson, and J.F. Brons (1989) Vagal representation by the climbing and mossy fiber systems in the cerebellum of the cat. *Society for Neuroscience (Abstr.)* 15:245.12.
- Trelles, J.O. (1957) L'hypertrophie des neurones olivaires et la signification des olives. *Encéphale* 46:708-717.
- Triller, A., F. Cluzaud, F. Pfeiffer, H. Betz, and H. Korn. (1985) *J. Cell Biol.* 101:683-688.

- Trojanowski, J.Q. (1983) Native and derivatized lectins for in vivo studies of neuronal connectivity and neuronal cell biology. *J. Neurosci. Methods* 9:185-204.
- Truter, E.J., L. Bolt, and E.D.F. Williams (1980) Dimensional stability in tissues dehydrated with 2,2'-dimethoxypropane for electron microscopy. *J. Microsc.* 119:223-240.
- Tsukahara, N., T. Bando, F. Musakami, and Y. Oda (1983) Properties of cerebello-precerebellar reverberating circuits. *Brain Res.* 274:249-259.
- Uchizono, K. (1965) Excitatory and inhibitory synapses in the central nervous system of the cat. *Nature* 207:642-643.
- Udo, M., K. Matsukawa, H. Kamei, K. Minoda, and Y. Oda (1981) Simple and complex spike activities of Purkinje cells during locomotion in the cerebellar vermal zones of decerebrate cats. *Exp. Brain Res.* 41:292-300.
- Uylings, H.B.M., A. Ruiz-Marcos, and J. van Pelt (1986) The metric analysis of three-dimensional dendritic tree patterns: a methodological review. *J. Neurosci. Meth.* 18:127-151.
- Valdivia, O. (1971) Methods of fixation and the morphology of synaptic vesicles. *J. Comp. Neurol.* 142:257-274.
- Van den Dungen, H.J. Groenewegen, H.M., F.J.H. Tilders, and J. Schoemaker (1988) Immunoreactive corticotropin releasing factor in adult and developing rat cerebellum: its presence in climbing and mossy fibres. *J. Chem. Neuroanat.* 1:339-349.
- Van den Pol, A.N. (1985) Silver-intensified gold and peroxidase as dual ultrastructural immunolabels for pre- and postsynaptic neurotransmitters. *Science* 228:332-334.
- Van den Pol, A.N., and T. Gorcs (1986) Synaptic relationships between neurons containing vasopressin, gastrin-releasing peptide, vasoactive intestinal polypeptide, and glutamate decarboxylase immunoreactivity in the suprachiasmatic nucleus: Dual ultrastructural immunocytochemistry with gold-substituted silver peroxidase. *J. Comp. Neurol.* 252:507-521.
- Van der Want, J.J., N.M. Gerrits, and J. Voogd (1987) Autoradiography of mossy fiber terminals in the fastigial nucleus of the cat. *J. Comp. Neurol.* 258:70-80.
- Van der Want H., Guegan M., Wiklund L., and Nunes Cardozo B. (1988) Inferior olivary projections to the deep cerebellar nuclei studied with anterograde PHA-L tracing, quantitative light- and electron microscopy. *Suppl. Europ. J. Neurosci.* 10.2
- Van der Want, J.J.L., L. Wiklund, M. Guegan, T. Ruigrok, and J. Voogd (1989) Anterograde tracing of the rat olivo-cerebellar system with Phaseolus vulgaris leucoagglutinin (PHA-L). Demonstration of climbing fiber collateral innervation of the cerebellar nuclei. *J. Comp. Neurol.* (in press).
- Van der Want, J.J., and J. Voogd (1987) Ultrastructural identification and localization of climbing fiber terminals in the fastigial nucleus of the cat. *J. Comp. Neurol.* 258:81-90.
- Van Gehuchten, A. (1905) *Anatomic du Systeme Nerveux de l'Homme*. Louvain, Libraire Universitaire, A. Uystpruyt-Dieudonne, pp.510-524.
- Van Gilder, J.C., and J.I. O'Leary (1971) Effect of nembutal anaesthesia on Purkinje cell activation in the cat. *Electro-encephalog. Clin. Neurophysiol.* 30: 173-188.
- Van Neerven, J., O. Pompeiano, H. Collewijn, J. Van der Steen (1989) Injections of B-noradrenergic substances in the flocculus of rabbits affect adaptation of the VOR gain. *Exp. Brain Res.* (in press).
- Varndell, I.M., and J.M. Polak (1984) Double immunostaining procedures: Techniques and applications. In: J.M. Polak, and I.M. Varndell (Eds.). *Immunolabelling for Electron Microscopy* Amsterdam, Elsevier Science Publishers, pp.155-177.
- Verhaart, W.J.C., and J. Voogd (1962) Hypertrophy of the inferior olives in the cat. *J. Neuropathol. Exptl. Neurol.* 21:92-104.
- Vincent, S.R., C.H. McIntosh, A.M. Buchan, and J.C. Brown (1985) Central somatostatin systems revealed with monoclonal antibodies. *J. Comp. Neurol.* 238:169-186.
- Vincenzi, L. (1886) Sulla fina Anatomia dell 'uomo. *Estr. della Real. Accad. Medic. di Roma II, 3* (cited in Ramon y Cajal).
- Von Kölliker, A. (1893) *Handbuch der Gewebelehre des Menschen*. 6th edition (cited in Ramon y Cajal).
- Voogd, J. (1964) The cerebellum of the cat: Structure and fiber connections. Doctoral Thesis, Assen: van Gorcum.
- Voogd, J. (1982) The olivocerebellar projection in the cat. In: *The Cerebellum*. New Vistas, edited by S.L. Palay and V. Chan-Palay, *Exp. Brain Res.* (Suppl.)6:134-161. Springer-Verlag, Berlin, Heidelberg, New York.
- Voogd, J., and F. Bigaré (1980) Topographical distribution of olivary and corticonuclear fibers in the cerebellum. A review. In: J. Courville, C. de Montigny and Y. Lamarre (Eds.), *The Inferior Olivary Nucleus*. Raven Press, New York. 207-235.
- Voogd, J., and A.J.P. Boesten (1976) A light- and electron microscopical study of inferior olivary hypertrophy in the cat. *J. Anat. (Lond.)* 122:712-713.
- Voogd, J., and E. Marani. The mammalian cerebellum, morphology and chemoarchitecture. In A. Björklund, T. Hokfelt, and L.W. Swanson (eds.). *The Handbook of Chemical Neuroanatomy*, Elsevier, Amsterdam. in press.
- Waespe, W., and V. Henn (1981) Visual-vestibular interaction in the flocculus of the alert monkey. II. Purkinje cell activity. *Exp. Brain Res.* 43:349-360.
- Walberg, F. (1956) Descending connexions to the inferior olive. *J. Comp. Neurol.* 104:77-173.
- Walberg, F. (1963) An electron microscopic study of the inferior olive of the cat. *J. Comp. Neurol.* 12:1-18.

- Walberg, F. (1964) Further electron microscopical investigations of the inferior olive of the cat. In *Progr. Brain Res. Topics in Basic Neurology*, edited by W. Bargmann and J.P. Schade. Vol. 6, p. 59-75. Amsterdam: Elsevier.
- Walberg, F. (1965) An electronmicroscopic study of terminal degeneration in the inferior olive of the cat. *J. Comp. Neurol.* 125:205-222.
- Walberg, F. (1966) Elongated vesicles in terminal boutons of the central nervous system, a result of aldehyde fixation. *Acta Anat.* 65:224-235.
- Walberg, F. (1974) Descending connections from the mesencephalon to the inferior olive: An experimental study in the cat. *Exp. Brain Res.* 21:145-156.
- Walberg, F. (1982a) Olivary afferents from the brain stem reticular formation. *Exp. Brain Res.* 47:130-136.
- Walberg, F. (1982b) The trigemino-olivary projection in the cat as studied with retrograde transport of horseradish peroxidase. *Exp. Brain Res.* 45: 101-107.
- Walberg, F. (1982c) The origin of olivary afferents from the central grey and its surroundings in the cat. *Anat. Embryol.* 164:139-151.
- Walberg, F., and Dietrichs, E. (1982) Olivary afferents from the raphe nuclei as studied with retrograde transport of horseradish peroxidase. *Anat. Embryol.* 164:85-93.
- Walberg, F., T. Nordby, K.P. Hoffmann, and H. Holländer (1981) Olivary afferents from the pretectal nuclei in the cat. *Anat. Embryol.* 161:291-304.
- Walberg, F., and O.P. Otterson (1989) Demonstration of GABA immunoreactive cells in the inferior olive of baboons (*Papio papio* and *Papio anubis*). *Neurosci. Lett.* 101:149-155.
- Walters, D.E., and Speth, R.C. (1988) Neuronal localization of specific angiotensin II binding sites in the rat inferior olivary nucleus. *J. Neurochem.* 50:812-817.
- Watanabe, E. (1984) Neuronal events correlated with long-term adaptation of the horizontal vestibulo-ocular reflex in the primate flocculus. *Brain Res.* 297:169-174.
- Watson, A.H.D. (1988) Antibodies against GABA and glutamate label neurons with morphologically distinct synaptic vesicles in the locust central nervous system. *Neuroscience* 6:33-44.
- Watson, J.T., E. Adkins-Regan, P. Whiting, J.M. Lindstrom, and T.R. Podleski (1988) Autoradiographic localization of nicotinic acetylcholine receptors in the brain of the zebra finch (*Poephila guttata*). *J. Comp. Neurol.* 274:255-264.
- Weber, J.T., C.D. Partlow, and J.K. Harting (1978) The projection of the superior colliculus upon the inferior olivary complex of the cat: An autoradiographic and horseradish peroxidase study. *Brain Res.* 144:369-377.
- Weber, J.T., H. Xie, L. Meyer, W. Heard, and I-li Chen (1989) On the presence of GABAergic and GABAergic projection neurons within the pretectal complex of the cat. Abstract AAA 102nd Meeting.
- Weiler, R., and Ball, A.K. (1984) Co-localization of neurotensin-like immunoreactivity and 3H-glycine uptake system in sustained amacrine cells of turtle retina. *Nature* 311:759-761.
- Whitworth, R.H., and D.E. Haines (1986) On the question of nomenclature of homologous subdivisions of the inferior olivary complex. *Arch. Ital. Biol.* 124:271-317.
- Wiberg, M., and A. Blomqvist (1984a) The projection to the mesencephalon from the dorsal column nuclei. An anatomical study in the cat. *Brain Res.* 311:225-244.
- Wiberg, M., and A. Blomqvist (1984b) The spinomesencephalic tract in the cat: its cells of origin and termination pattern as demonstrated by the intraaxonal transport method. *Brain Res.* 291:1-18.
- Widén, I. (1955) Cerebellar representation of high threshold afferents in the splanchnic nerve with observations on the cerebellar projection of high threshold somatic afferent fibres. *Acta Physiol. Scand.* 33, Suppl. 117.
- Wiklund, L., A. Björklund, and B. Sjolund (1977) The indolaminergic innervation of the inferior olive. I. Convergence with direct spinal afferents in the areas projecting to the cerebellar anterior lobe. *Brain Res.* 131:1-21.
- Wiklund, L., L. Descarries, and K. Mollgard (1981) Serotonergic axon terminals in the rat dorsal accessory olive: normal ultrastructure and light microscopic demonstration of regeneration after 5,6-dihydroxytryptamine lesioning. *J. Neurocytol.* 10:1009-1027.
- Wiklund, L., G. Toggenburger, and M. Cuenod (1982a) Aspartate: possible neurotransmitter in cerebellar climbing fibers. *Science N.Y.* 216:78-80.
- Wiklund, L., G. Toggenburger, and M. Cuenod (1982b) Selective retrograde labelling of the rat olivocerebellar climbing fiber system with D-(3H)aspartate. *Neuroscience* 13:441-468.
- Wiklund, L., G. Toggenburger, and M. Cuenod (1984) Selective retrograde labelling of the rat olivocerebellar climbing fiber system with D-[3H]aspartate. *Neuroscience* 13:441-468.
- Wiklund, L., J.J.L. Van der Want, M. Guegan, C. Buisseret-Delmas, T.J.H. Ruigrok, and J. Voogd (1988) Evidence for climbing fiber collateral innervation of the deep cerebellar nuclei with PHA-L anterograde tracing in the rat. *Suppl. Europ. J. Neurosci.* 10:1
- Williams, M.A. (1977) Quantitative methods in biology. In *Practical Methods in Electron Microscopy* (ed. Glauert A.M.), Vol 6, pp. 85-173. Elsevier/North-Holland, Amsterdam.
- Willis, T. (1664) *Cerebri anatomae: Cui accessi nervorum descriptio et usus*. Schagen, Amsterdam
- Wilson, C.J., and Grove P.M. (1980) Fine structure and synaptic connection of the common spiny neuron of the rat neostriatum: a study employing intracellular injection of horse radish peroxidase. *J. Comp. Neurol.* 194:599-616.

- Wilson, C.J., Grove P.M., Kitai S.T., and Linder C.I. (1983) Three dimensional structure of dendritic spines in rat neo- striatum. *J. Neurosci.* 3:383-398.
- Wilson, W.C., and Magoun, H.W. (1945) The functional significance of the inferior olive in the cat. *J. Comp. Neurol.* 83:69-77.
- Wouterlood, F.G. (1986) Study of CNS microcircuits by a combination of Phaseolus-vulgaris-leucoagglutinin (PHA-L) tracing, anterograde degeneration and electron microscopy: target neurons of fornix terminals in the septum of the rat. Symposium Marseille, *Neurosci. Lett. Suppl.* S603.
- Wouterlood, F.G., and H.J. Groenewegen (1985) Neuroanatomical tracing by use of Phaseolus vulgaris-leucoagglutinin (PHA-L): electron microscopy of PHA-L-filled neuronal somata, dendrites, axons and axon terminals. *Brain Res.* 326:188-191.
- Yan, Q., and E.M. Johnson, Jr. (1988) An immunohistochemical study of the nerve growth factor receptor in developing rats. *J. Neurosci.* 8:3481-3498.
- Yarom, Y. (1989) Oscillatory behavior of olivary neurons. *Suppl. Exp. Brain Res.* 17:209-221.
- Yarom, Y., and A. Adan (1987) Sinusoidal oscillations of the inferior olivary nucleus produced by interconnecting an analog simulator to an olivary neuron. In the *Olivo-cerebellar System in Motor Control. Satellite Symposium of the 2nd IBRO World Congress of Neuroscience, Turin, 9-12 August, 1987, p.21.*
- Yarom, Y., and A. Adan (1988) Interconnecting an analog simulator with an olivary neuron. *Soc. Neurosci. Abstr.* 14:757.
- Yarom, Y., and R. Llinás (1987) Long-term modifiability of anomalous and delayed rectification in guinea pig inferior olivary neurons. *J. Neurosci.* 7:1166-1177.
- Yeo, C.H., M.J. Hardiman, and M. Glickstein (1984) Discrete lesions of the cerebellar cortex abolish the classically conditioned nictitating membrane response of the rabbit. *Behav. Brain Res.* 13:261-266.
- Yeo, C.H., M.J. Hardiman, and M. Glickstein (1985a) Classical conditioning of the nictitating membrane response of the rabbit. I. Lesions of the cerebellar nuclei. *Exp. Brain Res.* 60:87-98.
- Yeo, C.H., M.J. Hardiman, and M. Glickstein (1985b) Classical conditioning of the nictitating membrane response of the rabbit. II. Lesions of the cerebellar cortex. *Exp. Brain Res.* 60:99-113.
- Yezierski, R.P. (1988) Spinomesencephalic tract: projections from the lumbosacral spinal cord of the rat, cat and monkey. *J. Comp. Neurol.* 267:131-146.
- Young, W.S. III, L. Walker, R. Powers, E. DeSouza, and D. Price (1986) Corticotropin-releasing factor mRNA is expressed in the inferior olives of rodents and primates. *Mol. Brain Res.* 1:189-192.
- Zhu, P.C., A. Thureson-Klein, and R.L. Klein (1986) Exocytosis from large dense cored vesicles outside the active synaptic zones of terminals within the trigeminal subnucleus caudalis: a possible mechanism for neuropeptide release. *Neuroscience* 19:43-54.

SUMMARY

The inferior olive (IO) is the source of the climbing fibres innervating the Purkinje cells of the cerebellum. The function of the IO is characterized by its exceptional synchronizing and electrical properties and by the way in which these properties are influenced by its afferent systems (reviewed in Chapter I). In this thesis the cerebellar and mesodiencephalic innervation of the rostral medial accessory olive (MAO) and principal olive (PO) of the cat are described. Three ultrastructural combination techniques were developed in order to relate the origin of these synaptic inputs to the neurotransmitter they contain (Chapter II), to study the interrelations of the cerebellar and mesodiencephalic system in the IO (Chapter III), and to determine the termination pattern of afferents upon physiologically and morphologically identified olivary cells (Chapter IV).

The technique described in Chapter II is a combination of anterograde transport of wheatgerm agglutinine-conjugated horseradish peroxidase (WGA-HRP) with post-embedding gamma-aminobutyric acid (GABA)-immunocytochemistry. With this technique both the HRP reaction product and the GABA immunogold labeling can be visualized in a single ultrathin section provided that the HRP reaction products are stabilized with diaminobenzidine-cobalt.

In one group of experiments GABA-immunocytochemistry was performed following an injection of WGA-HRP in the central nuclei of the cerebellum and in a second group this method was applied following an injection of WGA-HRP which labeled descending systems from nuclei located at the mesodiencephalic junction. The results indicated that all cerebellar terminals in the MAO and PO contained GABA while all mesodiencephalic terminals appeared to be non-GABAergic. The GABA/WGA-HRP double labeled terminals from the cerebellum generally contained symmetric synapses and pleiomorphic vesicles while the single WGA-HRP labeled terminals originating from the mesodiencephalon showed large round to oval vesicles and asymmetric synapses. In addition two other GABAergic and non-GABAergic type of terminals were observed almost none of which were WGA-HRP labeled in the cerebellar or mesodiencephalic experiments. The GABAergic cerebellar and the non-GABAergic mesodiencephalic terminals in the IO established synaptic contact primarily with dendrites and spines but also with cell bodies. The spines contacted by these terminals were often located in glomeruli and sometimes found to be coupled by gap junctions. The GABAergic input was found to be most prominently present on the cell bodies and close to pairs of dendritic structures coupled by gap junctions. At both neuronal structures the GABAergic input was more extensive than would be expected from the general distribution of GABAergic terminals over the neuropil of the IO. A statistical analysis of the results provided evidence for a separate origin of part of the somatic GABAergic innervation from a non-cerebellar source, whereas the entire GABAergic input to the dendrites linked by gap junctions was found to be derived from the cerebellar nuclei. Despite the strong GABAergic input to the olivary structures mentioned above, the non-GABAergic input predominates the innervation of the extra- and intraglomerular neuropil in the MAO. This non-GABAergic input originates primarily in the mesodiencephalon.

With regard to the glomeruli, the results showed that one third of both the GABAergic cerebellar and the non-GABAergic mesodiencephalic terminals were located within glomeruli. There was no significant difference in this respect between the number of WGA-HRP labeled cerebellar and mesodiencephalic terminals in the

glomeruli and there was no obvious separation or coexistence of GABAergic and mesodiencephalic terminals in these synaptic complexes, indicating that the cerebellar and mesodiencephalic afferent system have a random and equal input to the glomeruli of the cat IO.

In Chapter III a combination technique is presented which allows labeling of two different afferents in a single ultrathin section by combining anterograde transport of tritiated leucine combined with anterograde transport of WGA-HRP in the same animals. This technique was used to study the mesodiencephalic and cerebellar afferents of the MAO and PO in the cat and the rat. It was found that at least one third of the labeled glomeruli contained both mesodiencephalic and cerebellar terminals. In many of these cases the terminals from both afferent systems contacted the same dendritic spines.

Chapter IV describes a study with a technique combining intracellular labeling of neurons with HRP and postembedding GABA-immunocytochemistry. With this technique the olivary cells can be physiologically identified and lightmicroscopically reconstructed (provided that the osmication has been performed in a glucose solution), and the HRP reaction product and the immunogold labeling can be subsequently visualized in the electron microscope in each serial ultrathin section.

The results showed that the structure of dendritic spines of type II olivary neurons (characterized by dendrites turning back towards the soma) were more complex than those of type I (characterized by dendrites running away from the soma). However, the dendritic spines of both cell types were frequently found to have extreme long stalks and their spine heads were in most, if not all, cases located within glomeruli. Different dendrites of the same HRP labeled olivary neuron were never observed to emit spines to the same glomerulus. Following serial reconstruction the spines within individual glomeruli were found to originate on the average from six different cells. The vast majority of the spine heads within the glomeruli were contacted by both a GABAergic and a non-GABAergic terminal.

The axons of type I neurons usually originated from the soma whereas those of type II were mostly derived from a primary dendrite. The morphology of these axons was found to be unusual: The axon hillock and initial segment were both rather long and the hillock was studded with spiny appendages which were located within glomeruli together with the dendritic spines of other olivary neurons. Axonal spines of type II cells were more numerous and more complex than those of type I. These axonal spines and the shaft of the axon hillock were primarily innervated by GABAergic synapses but also by non-GABAergic inputs. All axons acquired a myelin sheath at the end of the initial segment.

The major conclusions from these results obtained with the various combination techniques were that the dendritic and axonal spines in the glomeruli of the IO have a unique morphology, that these spines receive a strong combined GABAergic cerebellar and non-GABAergic mesodiencephalic input, and that the soma receives a prominent GABAergic input, a substantial part of which is probably derived from a non-cerebellar origin. It is proposed in Chapter V that the cerebellar and mesodiencephalic inputs are involved in regulating the electrotonic coupling between olivary neurons in a timing sensitive way, while the GABAergic input to the soma may be an additional instrument in modulating the firing frequency.

SAMENVATTING

De oliva inferior (IO) is de oorsprong van de klimvezels die de Purkinjecellen van het cerebellum innervieren. De functie van de IO wordt gekarakteriseerd door zijn bijzondere synchroniserende en electrofysiologische eigenschappen en de manier waarop deze eigenschappen beïnvloed worden door de afferente systemen van de olijf (zie Hoofdstuk I). In dit proefschrift worden de cerebellaire en mesodiencefale innervatie van de rostrale mediale bijolijf (MAO) en de hoofdolijf (PO) van de kat beschreven. Drie nieuwe ultrastructurele combinatietechnieken werden ontwikkeld: de eerste maakt het mogelijk om tegelijkertijd de oorsprong en de neurotransmitter in eindigingen te kunnen bepalen (Hoofdstuk II), met de tweede methode kan de ruimtelijke verdeling van de cerebellaire en mesodiencefale input met elkaar worden vergeleken (Hoofdstuk III), en met de derde methode kunnen de afferente verbindingen van fysiologisch en morfologisch geïdentificeerde olijfcellen worden onderzocht (Hoofdstuk IV).

De techniek zoals beschreven in Hoofdstuk II bestaat uit een combinatie van anterograad transport van mierikswortel peroxidase gebonden aan agglutinine (WGA-HRP) en postembedding gamma-aminobutyrienzuur (GABA)-immunocytochemie. Met deze techniek kunnen zowel het reactieproduct van het WGA-HRP als de immunogoud-labeling van het GABA gevisualiseerd worden in een enkele ultradunne coupe. Dit kan alleen als het HRP reactie product gestabiliseerd is met diamino-benzidine-cobalt.

In één groep van experimenten werd GABA-immunocytochemie uitgevoerd na een injectie van WGA-HRP in de centrale kernen van het cerebellum en in een tweede groep na een injectie van WGA-HRP in het mesodiencefalon. De resultaten gaven aan dat alle cerebellaire eindigingen in de MAO en PO GABA bevatten, terwijl alle mesodiencefale eindigingen niet-GABAerg bleken te zijn. De GABA/WGA-HRP dubbel gelabelde eindigingen van het cerebellum waren in het algemeen voorzien van symmetrische synapsen en zij bevatten pleiomorfe synaptische blaasjes terwijl de uitsluitend met WGA-HRP gelabelde, mesodiencefale eindigingen grote, ronde tot ovale blaasjes bevatten en voorzien waren van asymmetrische synapsen. Daarnaast werden nog twee andere typen GABAerge en niet-GABAerge eindigingen waargenomen, waarvan er vrijwel geen met WGA-HRP gelabeld kon worden na injecties in het cerebellum of de mesodiencefale overgang. De GABAerge eindigingen uit het cerebellum en de niet-GABAerge eindigingen uit het mesodiencefalon in de IO maakten voornamelijk synaptisch contact met dendrieten en spines, maar in enkele gevallen ook met cellichamen. De spines die door deze afferente systemen geïnnerveerd werden waren vaak gelokaliseerd in glomeruli en soms bleek dat ze onderling verbonden waren door gap junctions. De GABAerge input was vooral prominent aanwezig op de cellichamen en bij dendrietparen die gekoppeld waren door gap-junctions. Voor beide neuronale structuren gold dat de GABAerge input sterker was dan verwacht kon worden op grond van de algemene verdeling van GABAerge eindigingen over de neuropil van de olijf. Statistische analyse van de resultaten toonde aan dat een gedeelte van de GABAerge innervatie van de cellichamen afkomstig is van buiten het cerebellum, terwijl de GABAerge input voor de dendrieten, die gekoppeld zijn door gap-junctions, afkomstig is van de cerebellaire kernen.

Ondanks de sterke GABAerge input naar bovengenoemde structuren bleek dat de niet-GABAerge input toch overheerst in het extra- en intraglomerulaire neuropil.

Deze niet-GABAerge input komt waarschijnlijk voor het grootste gedeelte uit het mesodiencefalon.

Met betrekking tot de innervatie van de glomeruli werd gevonden dat ongeveer een derde van de cerebellaire en de mesodiencefale eindigingen gelokaliseerd waren in glomeruli. Er bestond geen significant verschil tussen het aantal WGA-HRP gelabelde cerebellaire and mesodiencefale eindigingen in de glomeruli. Een scheiding of coëxistentie van GABAerge en mesodiencefale eindigingen in deze synaptische complexen kon niet worden vastgesteld.

In Hoofdstuk III wordt een techniek beschreven waarin anterograad transport van getitiseerd leucine wordt gecombineerd met anterograad transport van WGA-HRP. Deze techniek maakt het mogelijk dat twee verschillende afferente systemen gelabeld worden in een enkele ultradunne coupe, en werd gebruikt om de mesodiencefale en cerebellaire afferenten in de MAO en PO bij de kat en de rat te bestuderen. Er werd gevonden dat op zijn minst een derde van de gelabelde glomeruli zowel geïnnerveerd werd door mesodiencefale als door cerebellaire eindigingen. In veel van deze gevallen maakten beide afferente systemen contact met dezelfde spines.

Hoofdstuk IV beschrijft een studie die uitgevoerd is met een combinatie-techniek van intracellulaire labeling van zenuwcellen met HRP met postembedding GABA-immunocytochemie. Met deze techniek kunnen olijfcellen fysiologisch geïdentificeerd en licht microscopisch gereconstrueerd worden (indien de osmificatie is gebeurd in een glucose oplossing), en kan het HRP reactieproduct in de cel en de immunogoud-labeling van de GABAerge eindigingen gelijktijdig zichtbaar worden gemaakt onder de elektronen microscoop, in iedere ultradunne serie-coupe.

De resultaten toonden aan dat de spines van de dendrieten van type II cellen (gekaracteriseerd door dendrieten die terugkrullen naar het cellichaam toe) doorgaans complexer gebouwd waren dan die van type I (gekaracteriseerd door dendrieten die weg lopen van het soma). De spines van beide typen cellen bleken voorzien te zijn van extreem lange steeltjes, en hun kopjes waren in de meeste, zo niet alle, gevallen gelokaliseerd in glomeruli. Verschillende dendrieten van dezelfde met HRP gelabelde cel gaven nooit spines af aan dezelfde glomerulus. Na reconstructie van serie-coupees bleek dat een enkele glomerulus gemiddeld zes spines bevat, afkomstig van gemiddeld zes verschillende neuronen. De overgrote meerderheid van de spines werd zowel door een GABAerge als een niet-GABAerge eindiging geïnnerveerd.

De axonen van de olijf type I cellen stammen meestal af van het soma, terwijl die van type II doorgaans aan een primaire dendriet ontspringen. De structuur van deze axonen vertoonde een aantal bijzonderheden: de axonheuvel en het initiële segment bleken beiden lang te zijn en de axonheuvel gaf bovendien oorsprong aan een aantal spines. Deze axonale spines maken tezamen met spines afkomstig van dendriten van andere neuronen deel uit van glomeruli. De axonale spines van cell type II waren groter in aantal en complexer van vorm dan die afkomstig van type I cellen. De axonale spines en de schacht van het axon werden voornamelijk geïnnerveerd door GABAerge eindigingen maar ook door niet GABAerge eindigingen. Alle axonen kregen een meergeschede aan het einde van het initiële segment.

De belangrijkste resultaten die werden verkregen met de drie combinatie-technieken zijn: de unieke morfologie van de spines van de dendrieten en axonen van de olijfcellen, de gecombineerde GABAerge cerebellaire en excitatoire mesodiencefale innervatie van deze spines, en dat de GABAerge innervatie van het cellichaam waarschijnlijk voor een belangrijk gedeelte van niet-cerebellaire oorsprong is. In Hoofdstuk V wordt de hypothese naar voren gebracht dat de cerebellaire en mesodi-

encefale innervatie van de spines de electrotonische koppeling van olijfcellen reguleert, dat deze regulatie afhankelijk is van de timing van de activiteit in beide systemen, en dat de GABAerge innervatie van het cellichaam een modulerende invloed heeft op de oscillatie en de vuurfrequentie van olijfcellen.

DANKWOORD

Dit proefschrift is tot stand gekomen door de hulp en inzet van velen. Ik ben hen daarvoor zeer erkentelijk. Een aantal van hen wil ik in het bijzonder bedanken.

Op de allereerste plaats mijn Pia, die zich vrije dagen, avonden, nachten, weekeindes en vakanties ontzegd heeft om mij de gelegenheid te geven dit boekje te schrijven.

Mijn promotor Prof. Dr. Jan Voogd, wiens eigen wetenschappelijke werk bij mij groot respect afdwingt en die voor mij een ideale baas was. Hij heeft mij vaak op het juiste moment gestimuleerd of afgeremd, hij heeft mij goede adviezen gegeven en tegelijkertijd heeft hij me nooit de vrijheid ontnomen dat te doen waar ik zelf belangstelling voor had. Bovendien heeft hij mij in de gelegenheid gesteld om zowel nationaal als internationaal naar buiten te treden.

Mijn co-promotor Dr. Joan Holstege, die mij vrijwel alle belangrijke electronen-microscopische technieken van de neuroanatomie heeft bijgebracht. Verder wil ik hem in het bijzonder bedanken voor het feit dat hij mij op het "gouden" spoor van de anterograde tracing en de immunocytochemie gezet heeft, en dat hij mij goed geholpen heeft bij het schrijven van de artikelen.

Mijn andere dagelijkse begeleider Dr. Tom Ruigrok, die de basis gelegd heeft voor de inhoudelijke kant van dit proefschrift, door mij in te wijden in de anatomische verbindingen van het olivo-cerebellaire systeem en door eindeloos met mij te discussieren over de electrofysiologische eigenschappen van dit netwerk.

Harry Jansen, die er voor gezorgd heeft dat onze elektronen microscoop iedere dag weer werkte, en die door zijn enorme expertise in het serie snijden en met zijn hulp bij het drie dimensionaal analyseren van de coupes in de computer een essentiële bijdrage aan mijn proefschrift geleverd heeft.

Dr. Greet Schalekamp voor haar enthousiasme en samenwerking bij de immunocytochemische vraagstukken.

Prof. Dr. E. Mugnaini who gave me the opportunity to benefit from his world famous immunocytochemical and italian culinary recipies.

Dr. Ruud Buijs van het Nederlands Instituut voor Hersen-onderzoek, die het voor deze studie essentiële GABA antilichaam geproduceerd heeft.

Renee Hartsteen, die voor mij duizenden mooie ultradunne coupe's gesneden heeft.

Ing. Flo Calkoen, Corry Bijker-Biemond, Diety van Goor, en Ing. Colinda Bongers die het overgrote gedeelte van de GABA-immunocytochemie hebben uitgevoerd.

Edith Klink voor haar enorme hulp bij het typen van het manuscript.

Rob Boer voor zijn uitstekende technische assistentie en het uittekenen van intracellulair gelabelde neuronen.

Henny Klink, Erika Goedknegt, Els de Jong voor hun algemene technische assistentie.

Hans van den Burg die mij nooit "teleur kon stelen" als ik hem iets vroeg.

Eddie Dalm voor zijn assistentie bij de chirurgie.

Paula van Alphen voor haar assistentie bij de fotografie.

Prof. R. van Strik voor zijn advies bij de statistische analyse.

En verder Drs. Joep Tan, Drs. Pierre Wentzel, Dr. Nico Gerrits, Dr. Moshe Godschalk, Dr. Somes Sanyal en Dr. Gert Holstege voor hun prettige aanwezigheid en hun bereidheid om te helpen.

Een speciale plaats verdient het Remmert Adriaan Laan Fonds dat mij een grote financiële bijdrage verstrekt heeft voor de drukkosten van dit proefschrift.

Mijn paranymfen, Paul Wester, Saskia Schouten en Willibrord Crijnen, die mij vanaf respectievelijk de lagere school-, middelbare school- en universiteitstijd, alledrie op hun eigen directe of indirecte wijze hebben gestimuleerd om fundamenteel onderzoek te doen.

Last but not least, eindig ik daar waar ik begonnen ben, bij mijn familie: allereerst, mijn geliefde zonen, Ward, Samuel en Zev die er iedere ochtend weer op effectieve wijze voor zorgden dat ik niet in mijn bed bleef liggen, en dat ik met mijn benen in het dagelijkse leven bleef staan.

Vader Norbert en Daphne die mij altijd gestimuleerd hebben in mijn wetenschappelijke werk. Vader Norbert was een van de weinigen die mij niet voor gek verklaarde als ik zondags avonds nog naar het lab ging. Daarmee gaf hij mij het gevoel ten volle achter mijn wetenschappelijke ambities te staan. Daphne zou ik in het bijzonder willen bedanken voor de "voituristische" wijze waarop zij mij heeft aangemoedigd om het proefschrift zo snel mogelijk af te maken.

Schoonmama en Omo, die mijn onderzoek met enthousiasme gevolgd hebben. Zij hebben mij, buiten al hun morele steun, in de gelegenheid gesteld om veel van het schrijfwerk thuis te verrichten. Hierbij zou ik ook oom Freek, de broer van mijn schoonmoeder, willen bedanken voor zijn financiële support.

Mijn allergrootste dank gaat uit naar mijn vader en mijn moeder die zich vanaf mijn geboorte ingezet hebben voor mijn ontwikkeling en die mij daarvoor alle ruimte en vrijheid gegeven hebben. Ook tijdens de afgelopen vier jaren is de algehele steun van mijn ouders onontbeerlijk geweest. Mijn dank zal blijven.

CURRICULUM VITAE

De schrijver van dit proefschrift werd op 30 november 1960 te Gouda geboren. Hij bezocht het Theresia Lyceum in Tilburg en legde in 1979 het eindexamen Gymnasium B met goed gevolg af. Een jaar later begon hij de studie geneeskunde aan de Medische Faculteit van de Universiteit Van Amsterdam, waar hij in 1985 het doctoraal behaalde (oud curriculum). Tijdens de medische studie vervulde hij twee jaar een kandidaats-assistentschap op de afdeling Neurofysiologie (Prof. Dr. P.E. Voorhoeve). Voor zijn doctoraal scriptie heeft hij onderzoek verricht over topologische analyse van dendrietbomen op het Nederlands Instituut Voor Hersenonderzoek (Dr. R. Verwer en Dr. H.B.M. Uylings). Vanaf 1986 was hij werkzaam als assistent in opleiding op de afdeling Neuroanatomie (Prof. Dr. J. Voogd) aan de Erasmus Universiteit van Rotterdam waar hij ultrastructureel onderzoek deed naar de verbindingen van de oliva inferior met behulp van drie nieuwe anatomische combinatietechnieken. De resultaten hiervan zijn beschreven in het proefschrift. Thans loopt hij co-schappen aan de Erasmus Universiteit van Rotterdam, waarna hij in 1991 zijn artsexamen verwacht af te leggen.

LIST OF PUBLICATIONS

1. de Zeeuw, C.I., J.C. Holstege, F. Calkoen, T.J.H. Ruigrok, J. Voogd (1988). A new combination of WGA-HRP anterograde tracing and GABA-immunocytochemistry applied to afferents of the cat inferior olive at the ultrastructural level. *Brain Res.* 447:369-375.
2. de Zeeuw, C.I., J.C. Holstege, T.J.H. Ruigrok, J. Voogd (1989). The cerebellar, mesodiencephalic and GABAergic innervation of the glomeruli in the cat inferior olive. A comparison at the ultrastructural level. *Suppl. Exp. Brain Res.* 17:111-117.
3. de Zeeuw, C.I., J.C. Holstege, T.J.H. Ruigrok, J. Voogd (1989). Ultrastructural study of the GABAergic, cerebellar, and mesodiencephalic innervation of the medial accessory olive in the cat: Anterograde tracing combined with immunocytochemistry. *J. Comp. Neurol.* 284(1):12-35.
4. de Zeeuw, C.I., J.C. Holstege, T.J.H. Ruigrok, and J. Voogd. Cerebellar and mesodiencephalic terminals terminate upon the same dendritic spines within the glomeruli of the cat and rat inferior olive. An ultrastructural study combining anterograde tracing of (3H)leucine and WGA-HRP. *Neuroscience* (in press).
5. Ruigrok, T.J.H. C.I. de Zeeuw, J. van den Burg, and J. Voogd. Intracellular labeling of neurons in the medial accessory olive of the cat: I. Physiology and light microscopy. *J. Comp. Neurol.*, submitted.
6. de Zeeuw, C.I., T.J.H. Ruigrok, J.C. Holstege, H.G. Jansen, and J. Voogd. Intracellular labeling of neurons in the medial accessory olive of the cat:
II. Ultrastructure of dendritic spines and their GABAergic innervation. *J. Comp. Neurol.*, submitted.
7. de Zeeuw, C.I., T.J.H. Ruigrok, J.C. Holstege, M.P.A. Schalekamp, and J. Voogd. Intracellular labeling of neurons in the medial accessory olive of the cat:
III. Ultrastructure of axon hillock and initial segment and their GABAergic innervation. *J. Comp. Neurol.* submitted.

LIST OF ABSTRACTS

1. de Zeeuw, C.I., J.C. Holstege, F. Calkoen, T.J.H. Ruigrok, J. Voogd (1987). An ultrastructural study of the cerebellar GABA-ergic innervation of the inferior olive in the cat using a new combination of anterograde tracing and immunocytochemistry. In *The Olivocerebellar System in Motor Control, Satellite Symposium of the 2nd IBRO World Congress of Neuroscience, Turin, 9-12 August, 1987*, 10.
2. de Zeeuw C.I., J.C. Holstege, T.J.H. Ruigrok and J. Voogd (1988). The GABAergic, the cerebellar and the mesodiencephalic innervation of the rostral medial accessory olive of the cat. A quantitative comparison at the ultrastructural level. *Suppl. Europ. J. Neurosci.* 10:9
3. de Zeeuw C.I., J.C. Holstege, T.J.H. Ruigrok and J. Voogd (1988). A comparison of the GABAergic, the cerebellar and the mesodiencephalic innervation of the rostral medial accessory olive in the cat. A quantitative ultrastructural study combining anterograde tracing with immunocytochemistry. In *Neurobiology Of The Cerebellar Systems: A Centenary Of Ramon Y Cajal's Description Of The Cerebellar Circuits. Barcelona, 19-22 October*, 18.
4. de Zeeuw, C.I., T.J.H. Ruigrok, J.C. Holstege, M.P.A Schalekamp, J. Voogd (1989). Ultrastructural study of the normal and hypertrophic cat inferior olive. *Society for Neuroscience (Phoenix)* 15:164.8, pp. 405.
5. Ruigrok T.J.H., J. Voogd and C.I. de Zeeuw (1986). Demonstration of the modular organization of the olivo-cerebellar connections in the rat using PHA-L as an anterograde tracer. *Neurosc. Lett. Suppl.* S258.
6. Ruigrok T.J.H., C.I. de Zeeuw and J. Voogd (1988). Morphology of inferior olivary neurons in cat. Intracellular HRP-injections in vivo combined with mesodiencephalic stimulation and anterograde tracing. In *Neurobiology Of The Cerebellar Systems: A Centenary Of Ramon Y Cajal's Description Of The Cerebellar Circuits. Barcelona, 19-22 October*, 37.
7. Ruigrok T.J.H., C.I. de Zeeuw, J. van der Burg, R. Boer and J. Voogd (1989). Experimental olivary hypertrophy in cat: Comparison of morphological and physiological aspects with normal inferior olive. *Suppl. Europ. J. Neurosci.* 2: 39.3, pp. 129.

OLIVA
VOILA

